Studies on the expression and function of Epstein-Barr virus encoded microRNAs in Burkitt lymphoma

by

Richard Benjamin Couture Amoroso

A thesis submitted to the University of Birmingham
for the degree of DOCTOR OF PHILOSOPHY

School of Cancer Sciences
College of Medical and Dental Sciences
The University of Birmingham
September 2012

ABSTRACT

Epstein-Barr virus (EBV) encodes at least 40 microRNAs (miRNAs), an important class of negative regulators that control gene expression through posttranscriptional mechanisms. However the contribution of these EBV-encoded miRNAs to the pathogenesis of virus-associated lymphomas remains poorly understood. Using newly-developed PCR assays, we first quantified the levels of viral BHRF1 and BART miRNAs in a range of EBV-positive cell lines. We show for the first time that all three BHRF1 miRNAs are abundantly expressed in Wp-restricted Burkitt lymphoma (BL) cells, but not Latency I BL cells lacking detectable Cp- or Wp-initiated EBNA transcripts. In contrast to some earlier reports, we also detected robust expression of BART miRNAs in B cell lines, although there was wide variation between individual miRNAs in a given cell. Analysis of BHRF1 and BART transcription, both in latent and lytic infection, suggested that maturation may be a key step in regulating steady-state miRNA levels. We also successfully generated lentiviral systems to express the BHRF1 miRNAs and developed reporter constructs to measure BHRF1 miRNA-dependent repression *in vivo*. While attempts to identify BHRF1 miRNA-induced changes on the BL transcriptome were inconclusive, our data suggest that the BHRF1 miRNAs are insufficient to affect BL cell growth and cell survival.

DEDICATION

I dedicate this thesis to my grandfather, Ignatius Christopher Amoroso 1924-2012.

ACKNOWLEDGEMENTS

I would like to thank my supervisors Professor Martin Rowe and Dr. Andrew Bell for their excellent supervision, support and time throughout this PhD. I would also like to thank all members of the B cell and Rowe groups, past and present, for their continuous guidance, tutelage and the more than occasional reagent. I am also very grateful for support received from Dr. Wenbin Wei in the interpretation of the array data. At this point I should also like to give thanks to the support received from friends and family alike. In particular I would like to thank my girlfriend, Rachael, whose loving support and enduring patience have rightfully earned her the nick name “Saint Rach” within the group. Finally I would like to give my sincerest gratitude to Cancer Research UK; without their generous funding this project would never have taken place.

Contents

Contents

List of Illustrations

List of Tables

List of Abbreviations

ACV: **Acyclovir**

ADAR: **Adenosine deaminase associated RNA**

Ago: **Argonaute protein**

AIDS-BL: **AIDS associated BL**

AMO: **Anti-miRNA oligonucleotide**

BARTs: **BamHI A rightward transcripts**

β2M : **Beta-2-micoglobulin**

Bcl-2: **B cell lymphoma 2**

BCR: **B cell receptor**

BL: **Burkitt lymphoma**

Bp: **Base pair**

cDNA: **Complementary DNA**

CDK: **Cyclin dependent kinase**

C. elegans: **Caenorhabditisis elegans**

CTL: **CD8+ cytotoxic T lymphocyte**

CXCL11: **Chemokine (C-X-C motif) ligand 11**

DNA: **Deoxyribonucleic acid**

Dox: **Doxycycline**

eBL **endemic BL**

EBV: **Epstein-Barr virus**

FACS: **Fluorescence-activated cell sorter**

FCS: **Foetal calf serum**

GAPDH: **Glyceraldehyde-3-phosphate dehydrogenase**

GC: **Germinal centre**

GFP: **Green fluorescent protein**

GP: **Glycoprotein**

HL: **Hodgkin lymphoma**

HRS: **Hodgkin-Reed Sternberg cells**

IFN: **Interferon**

Ig: **Immunoglobulin**

IL: **Interleukin**

IM: **Infectious mononucleosis**

IR: **Internal Repeats**

IRES: **Internal ribosome entry site**

Kbp: **Kilobase pair**

KSHV: **Karposi's sarcoma-associated herpesvirus**

LCL: **Lymphoblastoid cell line**

LCV: **Lymphocryptovirus**

LMP: **Latent membrane protein**

LNA: **Locked nucleic acid**

MICB: **Histocompatibility complex class I related chain B**

miRNA: **Micro-RNA**

NK cell: **Natural killer cell**

NPC: **Nasopharyngeal carcinoma**

NT: **Nucleotide**

ORF: **Open reading frame**

PBS: **Phosphate buffer saline**

PCR: **Polymerase chain reaction**

PI: **Propidium iodide**

PTLD: **Post-transplant lymphoproliferative disorder**

PUMA: **P53 up-regulated modulator of apoptosis**

QPCR: **Quantitative polymerase chain reaction**

Rb: **Retinoblastoma protein**

miRISC **MiRNA-induced silencing complex**

RLC: **RISC loading complex**

RNA: **Ribonucleic acid**

RPM: **Revolutions per minute**

RT: **Reverse transcription**

sBL: **Sporadic BL**

SDS: **Sodium dodecyl sulphate**

SV40: **Simian virus 40**

tEBNA-LP: **Truncated EBNA-LP**

Tet: **Tetracycline**

TetR: **Tetracycline repressor protein**

TNF: **Tumour necrosis factor**

TR: **Terminal repeat**

TRBP **HIV trans-activating response RNA-binding protein**

UTR: **Un-translated region**

v-snoRNA: **Viral small nucleolar RNA**

WT: **Wild-type**

1. Introduction

1.1 Discovery of microRNAs

MicroRNAs (miRNAs) are a species of small, 20-22 nucleotide (nt) regulatory RNA capable of controlling over a third of human genes (1). They have been implicated in numerous pathways including differentiation, apoptosis, cellular proliferation and human diseases such as cancer. Here we discuss the identification of the first two miRNAs and how it was discovered that these molecules were part of a large group of highly conserved regulatory molecules.

The products of two genes involved in the timing of *Caenorhabditis elegans* larval development, *lin-4* and *let-7*, were the first molecules to be classified as miRNAs (2-6). Rather than encoding a protein, both genes transcribe a 22 nt RNA predicted to be derived from a longer stem-loop precursor. The *lin-4* product was complementary to multiple areas of the *lin-14* gene product 3′ un-translated region (UTR) previously shown to be important in the negative regulation of lin-14 by lin-4 (2, 7, 8). An analogous situation was observed for let-7 and the lin-41 3′ UTR (9). Thus lin-4 and let-7 were proposed to post-transcriptionally regulate lin-14 and lin-41 respectively by binding their 3′ UTR targets and preventing translation.

Considering that a *let-7* gene homolog exists in other organisms such as humans and *Drosophila melanogaster* (10), a broad search was conducted for similar RNA species in other animals. Initially over 100 candidate genes were found (30 in humans, 20 in fruit fly and 60 in worms) (4-6), many of which were remarkably conserved among different species. These small RNAs formed a unique class of molecule termed miRNAs and were found to be

increasingly abundant across mammals, flies, fish, worms and many other species (11-21). Currently there are 21,264 published miRNA sequences which are collectively stored in the miRNA database miRBase (22, 23).

1.2 Biogenesis of miRNAs

The mechanisms through which mature miRNAs are generated have been investigated in great detail. Briefly, we know that miRNAs are transcribed in the nucleus as part of a large precursor transcript called a pri-miRNA. They are then processed to their mature form in two stages; once in the nucleus by Drosha and again in the cytoplasm by Dicer. An overview of these steps is outlined in Fig. 1.1, taken from Bushati and Cohen (24). In this section we will discuss each step of the miRNA biogenesis pathway.

MiRNA genes are found in all areas of the human genome except the chromosome Y (25-27). They commonly form large polycistronic miRNA gene clusters within intergenic regions of the genome. They also locate to protein coding regions of the genome, where they are primarily embedded within introns. Primary miRNA-containing transcripts (pri-miRNA) are transcribed by polymerase II (pol II) (28) and contain structural features associated with mRNA, such as 5′ caps and poly A tails (29).

Pri-miRNAs are processed in the nucleus by a multi-protein micro-processing complex which includes Drosha (class 2 ribonuclease III) and DGCR8 (DiGeorge syndrome critical region gene 8) (30). Drosha asymmetrically cleaves the pri-miRNA into a 60-100 nt transcript with 2 unpaired 3′ nucleotides and a 5′ phosphate group (31, 32); this transcript is termed the pre-miRNA. DCGR8 in turn serves both to guide Drosha to the pri-miRNA and specify the site of

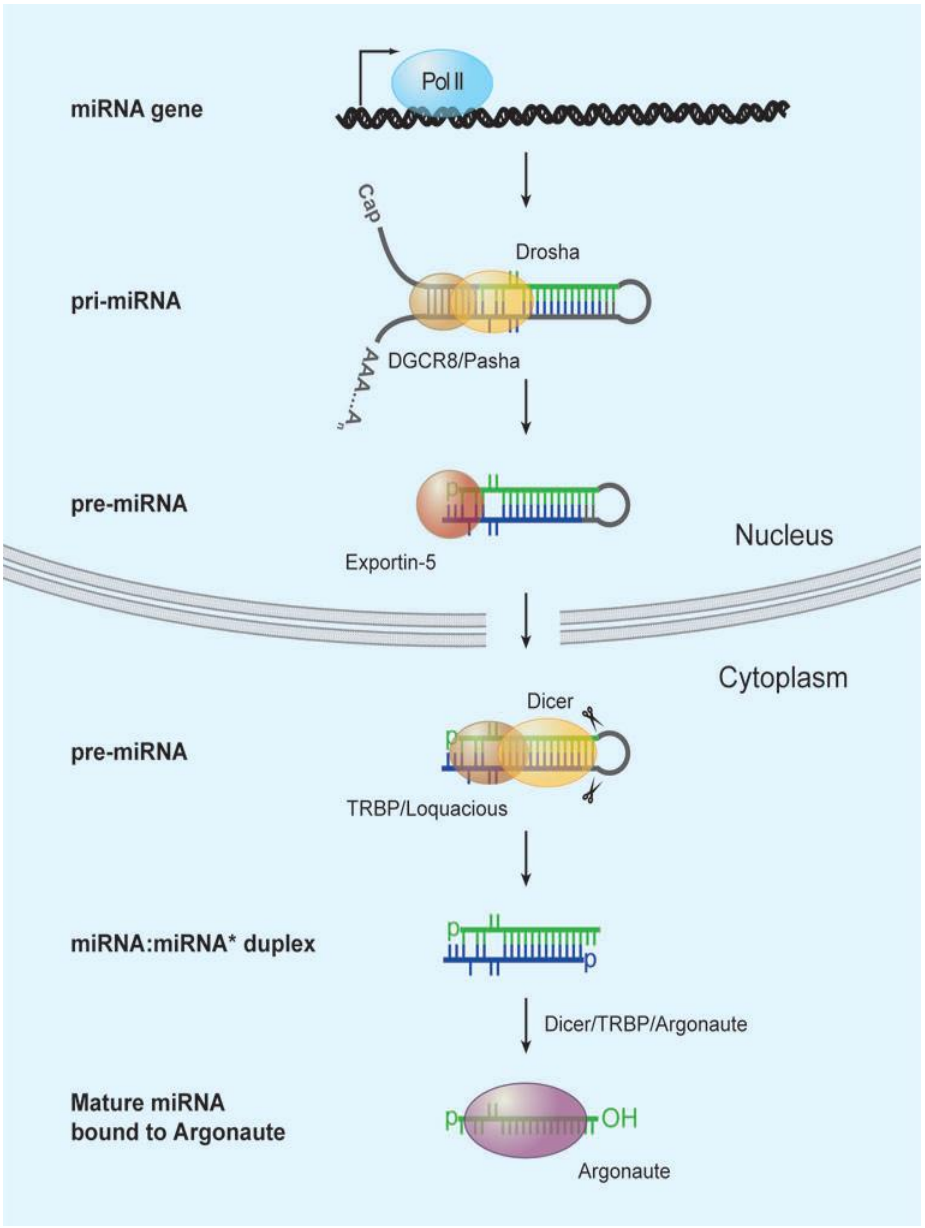

Fig. 1.1. Simplified schematic of the miRNA biogenesis pathway (image taken from Bushati and Cohen) (24). MiRNAs are transcribed in the nucleus as part of a long precursor (pri-miRNA). They are processed by Drosha in the nucleus to a shorter intermediate (pre-miRNA) and exported to the cytoplasm. They are then processed in the cytoplam by Dicer to a mature miRNA duplex. One strand is selected as the guide and loaded into an Argonaute protein as part of miRISC.

cleavage (31). Some miRNA genes within protein coding regions of the genome can be processed in a Drosha-independent manner termed the mirtron pathway (33, 34). In this case the lariat released by the mRNA splicing machinery directly folds into a pre-miRNA thus bypassing the need for Drosha. This can only occur when the 5′ and 3′ ends of the lariat possess a suitable level of complementarity or "hairpin potential". Examples of mammalian miRNAs processed in this manner include miR-877 and miR-1224 (35).

Subsequent transport of the pre-miRNAs across the nuclear membrane is mediated by nuclear receptor Exportin-5 (36, 37). Exportin-5 recognizes pre-miRNAs via their size, structure, and unpaired 3′ end (38, 39). Once Exportin-5 has bound a pre-microRNA target, it associates with RAN-GTP and nucleoporin and subsequently crosses the nuclear membrane (40). Release of the pre-miRNA in the cytoplasm is triggered by the catalytic conversion of RAN-GTP to RAN-GDP (41).

Pre-miRNAs are processed to mature miRNAs by Dicer (class 3 type III ribonuclease) (42, 43). Dicer has a number of functional domains. The double stranded RNA (dsRNA) binding domain and the PAZ domain recognize the pre-miRNA stem and 3′ overhang respectively, while the catalytic RNAse domain cleaves the pre-miRNA to a double stranded miRNA duplex (44, 45). Finally unwinding of the double stranded duplex might be mediated by the Dicer helicase domain (46-48).

Single stranded mature miRNAs need to be loaded into an Argonaute (Ago) protein-containing silencing complex termed miRISC before they can regulate gene expression. This step occurs in tandem with Dicer maturation and is mediated by the RISC loading complex (RLC), which consists of Dicer, TRBP (HIV trans-activating response RNA-binding protein) and an Ago protein (48-51). Usually only one strand of a miRNA duplex, termed the guide, is

loaded into miRISC (52, 53). Its selection depends on the relative thermodynamic properties of the four base pairs at its 5′ terminus. If these base pairs bind less stably on one strand as compared to the other then it will be chosen as the guide. Recent evidence has suggested a role for the helicase domain of Dicer in thermodynamic sampling of the miRNA duplex (54). The precise fate of the unloaded strand, termed the passenger, is a matter of debate (55-57). However in the absence of strand bias, both strands may be loaded into miRISC (4, 16), in which case the passenger is denoted with a * (22).

Ago proteins are one of the key catalytic components of miRISC while the guide strand miRNA acts in target recognition. In humans miRNAs can be loaded into Ago1 through Ago4, although only Ago2 possesses the ability to directly cleave target RNA (57-59). The consequences of this will be discussed in section 1.4.

1.3 Regulation of miRNA synthesis

Because miRNAs regulate over a third of human genes it is important that their biogenesis is carefully controlled (1). Thus miRNA production is tightly regulated at the levels of transcription, processing and miRISC formation. The current section will discuss some of the mechanisms through which the cell regulates miRNA biogenesis.

The transcription of pri-miRNAs is influenced in part by the nature and location of their promoters (60, 61). Intergenic miRNAs, such as miR-210, have their own transcriptional unit (61). Intronic miRNAs depend in part on host gene transcription (17, 26, 62), although many, such as the miR-17 cluster, are additionally regulated by their own internal promoters (60).

MiRNA promoters can be influenced by cellular transcription factors, for instance p53 and c-myc activate the miR-34 and miR-17 clusters, respectively (63-67).

Processing of the pri-miRNA is regulated via proteins which interact with the micro-processor complex and/or the pri-miRNA to stimulate or repress maturation (68, 69). Four of these proteins, SMAD, p53, ADAR and KSRP have been illustrated in Fig. 1.2 (adapted from Treiber *et al*) and will be discussed in more detail (70). The TNF-β responsive SMAD protein family binds a subset of miRNAs that contain R-SMAD binding elements (R-SBE) in their stems, such as miR-21 and miR-199a, and also interact with RNA helicase p68 (71, 72). These interactions both help tether the pri-miRNA to the micro-processing complex and enhance Drosha cleavage. P53 can promote processing of a group of growth-suppressive miRNAs (i.e. pri-miR-145 and pri-miR-16-1) as part of the DNA damage response (73). While the precise mechanism is unclear, it involves an association with RNA helicase p68 and is distinct from p53 mediated transcriptional regulation. KSRP (KH-type splicing regulatory protein) binds to terminal loop G-rich sequences present in certain pri-miRNAs, such as pri-miR-let-7a and pri-miR-21, and promotes both Drosha and Dicer mediated maturation (74). KSRP activity is enhanced in an ATM-dependent manner thus providing another link between the DNA damage response and miRNA biogenesis (75). Finally the editing of certain pri-miRNAs, i.e. pri-miR-142, by ADAR deaminases, which converts adenosine to inosine, may occur. This results in impaired Drosha processing and eventual degradation by the ribonuclease Tudor-SN, which specifically recognizes inosine containing dsRNA (76).

The mechanisms regulating pre-miRNA nuclear export are not understood. The observation that some pre-miRNAs (pre-miR-31, pre-miR-105 and pre-miR-128a) are selectively retained in the nucleus suggests the existence of some form of regulation (77). Furthermore mutations

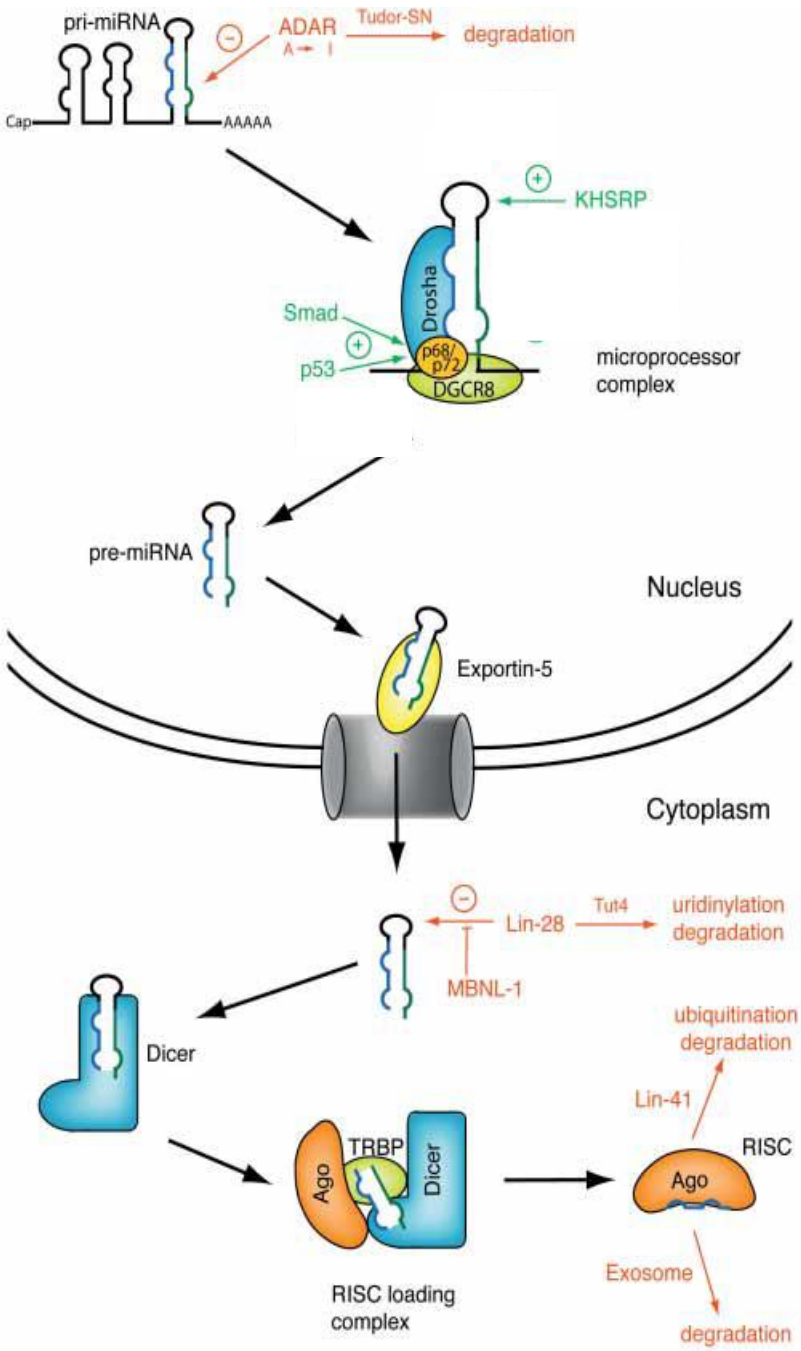

Fig. 1.2. The processing and function of miRNAs is carefully regulated (image adapted from Treiber *et al*) (70). Mechanisms illustrated in green increase miRNA processing and function. Similarly mechanisms illustrated in red antagonize miRNA processing and function.

in exportin-5 are typically observed in cancer and lead to a global block on export and consequent decrease in mature miRNA levels (78).

The processing of pre-miRNAs by Dicer in the cytoplasm is also subject to regulation. The auto-regulatory feedback loop established between the human lin-28 and the let-7 miRNA family serves as a well characterized example (Fig. 1.2). Lin-28 binds to the conserved GGAG loop sequences on pre-miR-let-7 to prevent processing by Dicer, whilst both mature let-7 and miR-125 in turn suppress lin-28 (79, 80). Lin-28 mediated inhibition involves recruitment of TUT4 (terminal uridyl transferase 4) which adds a poly-U tail to the pre-miR-let7 3′ end; this serves both to impair Dicer processing and mediate pre-miRNA degradation (81-84). In humans lin-28 is highly expressed in undifferentiated human embryonic stem cells (ESC) and helps maintain an undifferentiated phenotype (83, 85, 86) while let-7 mediates terminal differentiation (3, 10, 87). Thus the balance of lin-28 and let-7 in part control ESC fate. Incidentally over expression of human lin-28 promotes tumour growth (88) which is likely in part due to over expression of let-7 oncogene targets Ras, HMGA2 and c-myc (89-92).

The accumulation of fully processed mature miRNAs is influenced by their relative stability. For instance while many miRNAs exhibit half lives well beyond 8 hours, some have relatively short half lives i.e. miR-382 (93). Conversely the stability of some miRNAs can be increased through binding certain proteins (94). Furthermore miRNA turnover is generally accelerated in certain cell types e.g. in neuronal cells (95). Non-miRNA components of miRISC can also be targeted, e.g. in stem cells lin-41 impairs miRISC formation by causing Ago protein degradation (Fig. 1.2) (96).

1.4 Regulation of target genes by miRNAs

As discussed towards the end of section 1.2, mature miRNAs are loaded into the miRISC complex. In this complex the miRNA confers target specificity while Ago mediates target suppression (97). The current section will initially discuss the nature of the miRNA interaction with target mRNA. Thereafter we will focus on four proposed mechanisms by which miRISC is believed to suppress mRNA: endonucleolytic cleavage, inhibition of translation initiation, inhibition of translation elongation and mRNA destabilization.

Conventionally miRNAs bind sites in the 3′ UTR of mRNA. Some miRNAs bind the open reading frame (ORF) or 5′ UTR of their target; just how effective these sites are remains unclear (98-100). The degree of complementarity seen in an miRNA-mRNA interaction is somewhat species dependent. Plant miRNAs usually bind their target perfectly, whilst in mammals the interaction is usually characterized by a number of bulges and mismatches (101-103). In both cases, miRNA function is highly dependent on perfect binding of the target to nucleotides 2 through 7 on the 5′ end of the miRNA; this region is called the miRNA seed and is considered to be the most important factor in determining target specificity (102). At times, binding of this region alone may be sufficient for miRNA function; similarly bulges or mismatches in this region, especially a G:U wobble, greatly impair miRNA function (104, 105).

The 3′ UTR sequences surrounding the miRNA binding site can also impact on miRNA function; a proximity of the miRNA binding site to AU rich regions correlates with site efficacy whilst being near to other miRNA binding sites allows for a cooperative target repression (98). Binding sites for miRNAs broadly fall into three groups termed canonical, marginal and atypical (104, 106). Canonical sites include perfect binding of the miRNA seed

as well as an additional match at position 1 or 8. Marginal sites only include binding of 6 miRNA nucleotides which includes all or most of the seed. Atypical sights are seed mismatched but compensate through additional binding of the miRNA 3′ end.

Understanding how miRNAs bind has led to the development of miRNA target prediction programs including Targetscan (102, 107), TargetscanS (1)**,** PicTar (108), MiRanda (109, 110), Microcosm targets (22), PITA Top (111), EIMMo (112) and Diana-microT (113, 114)**.** The number and types of criteria used by these programs to define targets varies. All look for moderate or strong seed binding as well as cross-species conservation. Other variables include thermodynamic stability of miRNA-mRNA base-pairing, the proximity of the miRNA binding site to AU rich regions in the target 3′ UTR, and the degree to which miRISC can access the target. While undoubtedly helpful, target prediction programs have their shortcomings. Target predictions generated by a given program show limited overlap with those produced by a different program (114). This is in part due to different programs using different criteria. Even when the same criteria are used, different programs may have defined the constraints of said criteria in a slightly different way. For instance TargetscanS sets cross-species conservation at a minimum of 5 species while MiRanda only requires conservation among rodents and humans. Importantly computer predictions do not necessarily validate experimentally (115). Those that do validate are being added to a specialist data base, TarBase (115, 116).

While miRNAs are responsible for tethering the miRISC complex to target mRNA, Ago proteins are responsible for target repression. Depleting Ago proteins from cultured mammalian and insect cells inhibits the ability of miRNAs to regulate their target genes (117, 118). Furthermore unloaded Ago protein can repress gene expression when artificially

tethered to the 3′ UTR of a reporter mRNA (119). There are four species conserved Ago proteins in humans consisting of Ago1 though Ago4 (120-122). They share three domains termed PAZ, MID and PIWI; the function of these domains in the context of miRNAs is only partially understood (123-125). The PAZ interacts with the 3′ end of mature miRNAs (124) while there is some evidence to suggest the MID domain binds both the 5′ phosphate of mature miRNAs and the 5′ m7G cap of mRNA (126, 127). The PIWI domain mediates endonucleolytic cleavage of mRNA targeted by siRNAs and miRNAs; note that in humans this may only occur in the context of Ago2 (58, 59, 128). The ability of Ago proteins to mediate target repression appears to depend on binding to the GW182 protein. Preventing the interaction between Ago and GW182 has been shown both *in vivo* and *in vitro* to impair miRNA mediated gene silencing (118, 129-133).

Even today the precise mechanisms by which miRNAs mediate target repression remain somewhat unclear and several models have been suggested (Fig. 1.3)(134). As touched upon earlier, miRNAs can direct the cleavage of their target mRNAs in an Ago2 dependent manner (Fig. 1.3A); an example of this in animals is cleavage of HOXB8 directed by miR-196 (135). This mechanism is dependent both on endonucleolytic activity specific to Ago2, and on the miRNA being perfectly complementary to its target (58, 136). However miRNAs are not preferentially loaded into Ago2 over Ago1, Ago3 and Ago4 (58) and in contrast to plant miRNAs, the vast majority of animal miRNAs form mismatches with their target; this creates a bulge in the miRNA-target duplex which interferes with Ago2 mediated cleavage (97). Nonetheless an early study in human cells has suggested that some siRNAs can direct cleavage of imperfectly bound targets (137). Therefore we can not be entirely sure just how important Ago2 endonuclease activity is in mammalian miRNA mediated gene silencing.

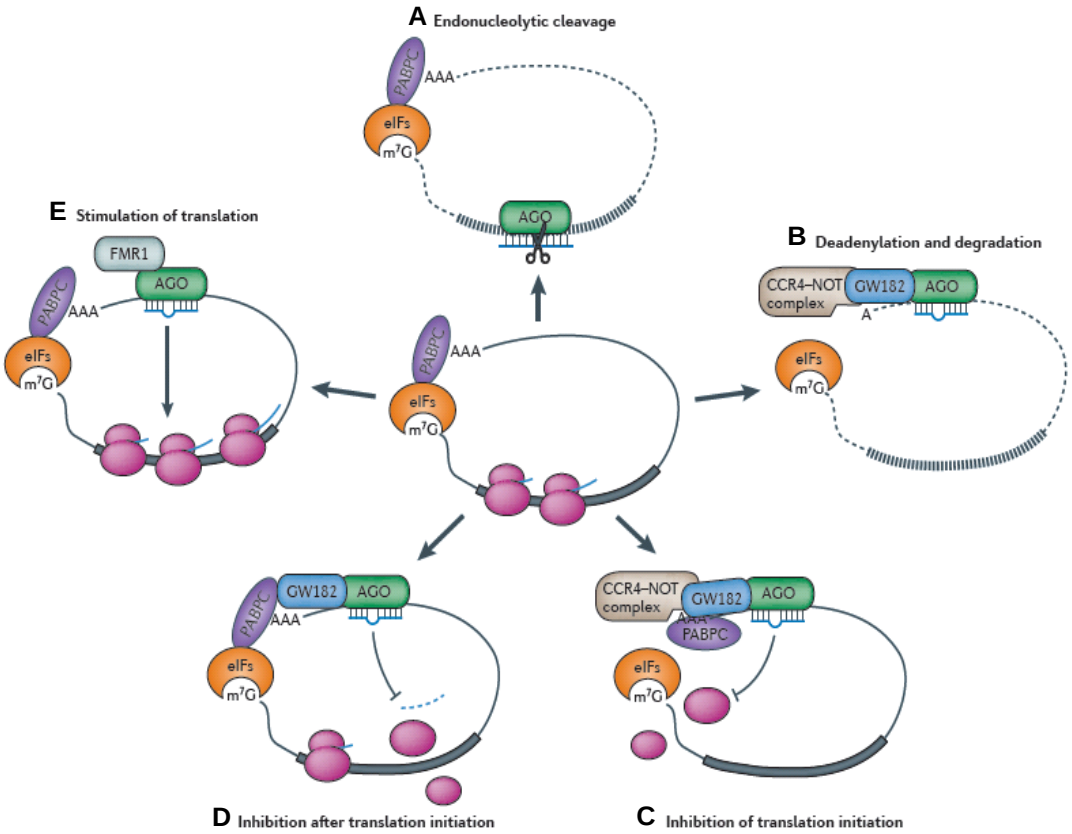

Fig. 1.3. Multiple models have been proposed for the regulation of target genes by miRNAs (image taken from Pasquinelli) (134). Eukaryotic initiation factors, eIFs, (orange) bind the 5′ m7G cap and associate with the poly-A binding protein, PABPC (purple); this results in circularization of a mRNA species which is needed to stimulate translation. **(A)** Perfectly complementary interactions between miRNAs and their targets favours Ago2 mediated endonucleolytic cleavage of target mRNA. **(B)** Imperfect pairing of an miRNA to the 3′ UTR of its target may lead to miRISC mediated recruitment of the CCR4-NOT complex, which causes deadenylation of the target mRNA; this triggers the dissociation of the PABPC and eventual degradation of the target mRNA. **(C)** Imperfect pairing of an miRNA to the 3′ UTR of its target may lead to the inhibition of translation initiation. The precise mechanisms remain unclear but may involve preventing mRNA circularization or blocking assembly of the 80S ribosome. **(D)** Steps after translation initiation may be targeted by miRNAs. Proposed mechanisms involve encouraging ribosomal drop-off and degradation of nascent peptide. **(E)** Positive regulation of translation by miRNAs has been documented. For instance miR-369 binds to TNF-α mRNA and recruits Ago2 and FMR1 to stimulate translation.

Most animal miRNAs are believed to impair various stages of translation and/or decrease mRNA stability. A number of studies have documented the ability of animal miRNAs to reduce the levels of mRNA targets, even when mismatches and bulges are present in the duplex (118, 138-140). Examples include lin-4/miR-125 mediated destabilization of lin-28 in nematodes/humans (138, 140). This mechanism appears to involves initial destabilization of mRNA targets followed by degradation (Fig. 1.3B) (118, 130, 141-145). Briefly miRISC associated protein GW182 recruits the CCR4-CAF1-NOT and PAN2-PAN3 complexes, which mediate deadenylation of the mRNA target. This in turn leads to the dissociation of the poly-A binding protein (PABP) and de-capping of the target by the DCP1:DCP2 complex. This renders the target mRNA susceptible to cellular exonucleases such as the 5′-3′ exonuclease Xrn1 and 3′-5′ exosome complexes. Most proteins involved in this pathway locate to processing bodies (P bodies), suggesting that these structures could be sites where miRISC targeted mRNAs are stored and/or degraded (146-150). Ribosome profiling of human and mouse cells recently demonstrated that as much as 84% of miRNA induced protein changes could be explained by reductions in mRNA levels (151).

Several lines of evidence suggest that miRNAs can inhibit translation initiation; furthermore this mechanism appears dependent on the target mRNA having a functional 5′ m7G cap (Fig. 1.3C). Substitution of the 5′ m7G cap with a non-functional analog ablates miRNA mediated repression while mRNA generated from an internal ribosome entry site (IRES) is not subject to miRNA regulation (152, 153). The latter point can be convincingly demonstrated with a single reporter expressing firefly and *Renilla reniformis* luciferase in a 5′ m7G cap dependent and independent manner respectively (153). One mechanism by which this might occur is through binding of Ago or GW182 to the 5′ m7G cap structure (127, 154). This would serve to prevent the assembly of the initiation complex (eIF4) and circularization of the mRNA

target; note that both these events are necessary in order for efficient translation to take place. Whether or not Ago or GW182 are capable of interacting with the 5′ m7G cap remains controversial (126, 127, 129, 155, 156). Another possibility is that miRISC might recruit the ribosome anti-association factor, eIF6, which in turn impairs assembly of the 80S ribosome (157, 158). Interestingly the CCR4-CAF1-NOT deadenylase complex has been implicated in the inhibition of translational initiation by a mechanism which seemingly does not involve target deadenylation. Mutational studies of this complex in *Xenopus laevis* oocytes revealed that CAF1 lacking deadenylase activity could inhibit reporter mRNAs providing they had a functional 5′ m7G cap structure (159). In contrast repression by deadenylation did not require a functional 5′ m7G cap.

It has also been suggested that miRNAs can inhibit translation elongation (Fig. 1.3D). This mechanism was first indicated by the *C. elegans* lin-4 mediated repression of lin-14 and lin-28; target mRNAs were associated with polysomes indicating translation initiation had already occurred (160, 161). Using human cells, artificial miRNAs and a mRNA reporter system, it has since been shown that repression of translation can occur at the post-initiation step (162). This is evidenced by the observation that IRES translated mammalian mRNA can be targeted by miRNAs and that repressed mRNAs are associated with active polysomes. Proposed mechanisms to address these observations include premature ribosomal drop-off during elongation (162), as well as degradation of nascent peptide by unknown mechanisms (163).

While most miRNAs are believed to antagonize their target, some have the opposite effect of stabilizing their target (Fig. 1.3E). For instance miR-369 targets AU-rich repeats in TNF-α mRNA under conditions of serum starvation (164). It then recruits Ago2 and FMR1 to

mediate translational activation as opposed to repression. Another miRNA, miR-328, binds hnRNP E2 in a seed independent manner and consequently relieves E2 mediated repression of certain targets such as CEBPA (165).

1.5 miRNAs in normal cells

In the current section we will provide a discussion on the roles of miRNAs in the context of normal cells, with an emphasis on cellular pathways such as differentiation, apoptosis and cell growth.

A number of studies on Dicer mutant animals highlighted the *in vivo* importance of miRNAs. *C.elegans* and *D. melanogaster* Dicer mutants are both sterile and develop small ovaries and ruptured vulva respectively (43, 166, 167). Dicer negative zebra fish and mice in turn all die at varying stages of embryonic development (168, 169). Some of the earliest studies on miRNAs highlighted a role for these molecules in regulating developmental processes. Lin-4 and let-7 miRNAs control stem cell fate during *C. elegans* development by repression of lin-14, lin-28, lin-41 and hbl-1 during the appropriate larval stage (2, 3, 8, 9, 170-172). This ensures that transcription factor lin-29 accumulates at the right time and at the right quantities, to mediate terminal differentiation and transition towards the adult developmental stage (173, 174). The Lin-4 and Let-7 miRNAs and their targets were found to be highly conserved and implicated in the development of mice (175, 176), zebra fish (177), fruit flies (178, 179) and humans (180).

MiRNAs are now well established as mediators of embryonic stem cell (ESC) fate. Some miRNAs act to antagonize ESC maintenance. During differentiation miR-145 silences

transcription factors (Oct4, Sox2, Klf4) required to maintain the non-committal phenotype of ESC (181). The let-7 family in turn were shown to down-regulate other targets required for stem cell maintenance such as c-myc (182). Other miRNAs function in deciding into which cell type an ESC develops. The muscle-specific miRNA miR-1 silences an ESC-associated Notch ligand (Dll-1) to promote differentiation towards cardiomyocytes (183, 184). The brain-specific miRNA, miR-9, represses stathmin to promote proliferation and suppresses migration in human neural progenitor cells (hNPCs) (185). Finally miR-34a, miR-100 and miR-137 target a number of genes needed to maintain an undifferentiated ESC phenotype such as SIRT-1 and SMARCA5 (186).

MiRNAs are also heavily involved in apoptosis (programmed cell death) (187). As reviewed by Ola *et al.* apoptosis can occur via the intrinsic or the extrinsic pathway (Fig. 1.4) (188). The intrinsic pathway is regulated by Bcl-2 family member proteins (Fig. 1.4B). Normally anti-apoptotic Bcl-2 members (i.e. Bcl-2, Bcl-XL etc) bind and maintain Bak and Bax in an inactive state. Stimuli such as metabolic or genomic stress cause the pro-apoptotic Bcl-2 members (i.e. Bim, Puma, Bid etc) to bind and inactivate the anti-apoptotic members. This releases Bak and Bax and allows them to trigger pore formation in the mitochondrial membrane which in turn results in the release of pro-apoptotic proteins. One of these proteins, cytochrome c, interacts with the apoptotic protease-activating factor (Apaf1) and dATP to form the apoptosome and activates a series of caspases which ultimately cause cell death.

MiRNAs target a number of Bcl-2 family members. For instance both miR-15a and miR-16 target anti-apoptotic Bcl-2 which leads to apoptosis in a chronic lymphocytic leukaemia (CLL) cell line model (189). miR-34a targets Bcl-2 directly in neuroblastoma cell line models (190) and indirectly up-regulates pro-apoptotic PUMA via SIRT1 (191). Both miR-221 and

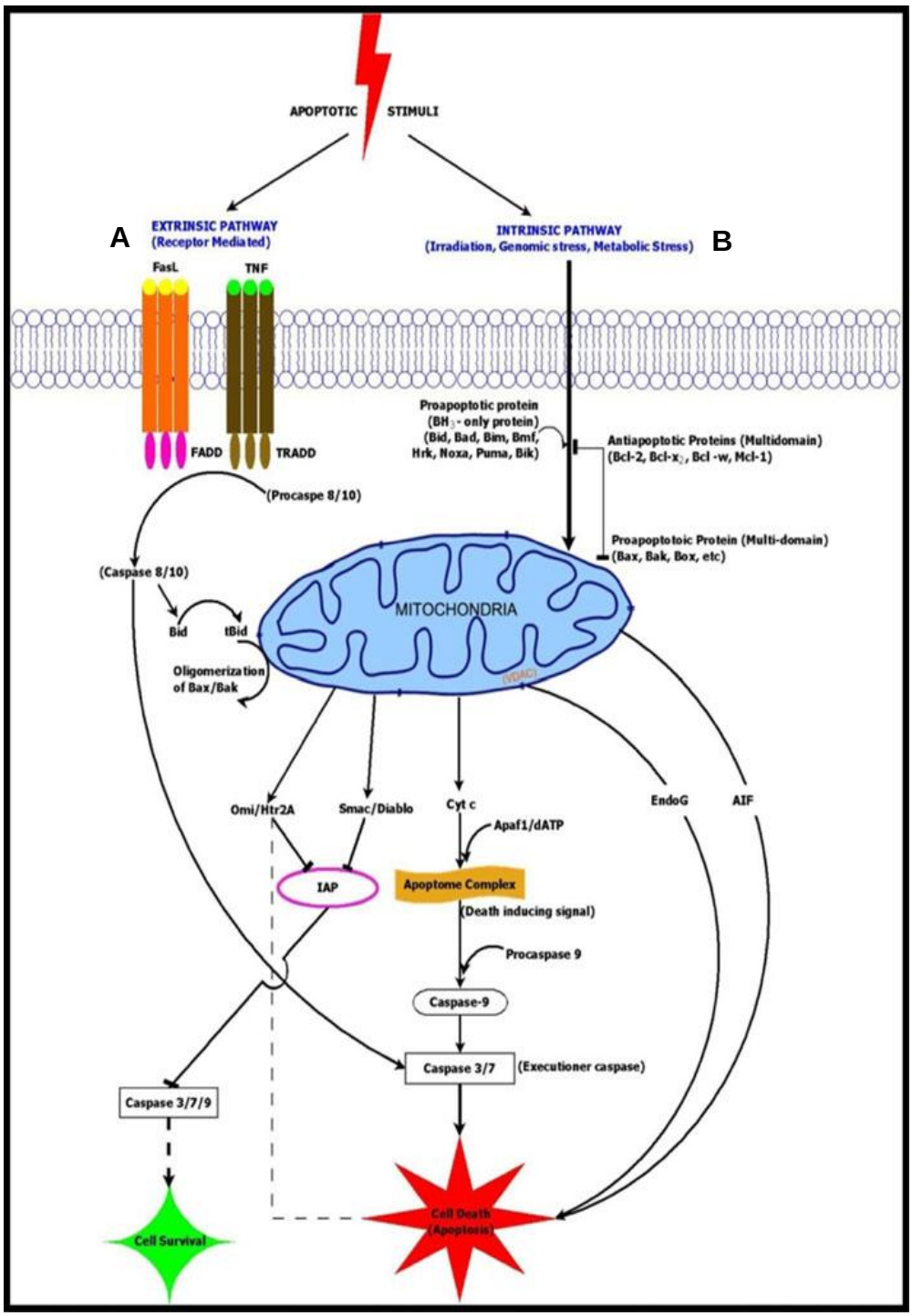

Fig. 1.4. Apoptosis occurs through the extrinsic **(A)** and intrinsic **(B)** pathways (see text for detail). Image taken from Ola *et al* (188).

miR-222 in turn directly target PUMA to promote cell survival in glioma cells (192). The miR-17-92 family, which has essential roles in B cell development, cooperates with the miR-106b-25 family to down-regulate the pro-apoptotic protein Bim (193). Formation of the apoptosome is also regulated by miRNAs. Pro-apoptotic miR-1 targets anti-apoptotic proteins HSP60 and HSP70 which function to prevent Bax-mediated pore formation pro-caspase 9 recruitment respectively (194-196). Anti-apoptotic miR-133 targets caspase 9 which is needed for downstream activation of caspases 3 and 7 (188, 196). Both miR-1 and miR-133 serve to regulate apoptosis in cardiomyocytes (196).

The extrinsic pathway is regulated via cell-cell signalling and is triggered by binding of ligands to the Fas and TNF-α receptors (Fig. 1.4A) (188). Thereafter both receptors become activated and recruit their respective death domain proteins FADD and TRADD; this in turn activates the death-inducing signalling complex (DISC). Downstream signalling continues via caspases and results, as before, in cell death. Examples of miRNAs which target this pathway include miR-21 and miR-182 which target Fas ligand and FADD respectively (197, 198).

MiRNAs are also involved in regulating cellular proliferation (Fig. 1.5). As reviewed by Bueno and Malumbres, before resting cells (G0 phase) can re-enter the cell cycle, they must inactivate the retinoblastoma protein (pRB) and synthesize machinery required for DNA replication (S phase) and mitosis (M phase) (199). This process begins with transcription of D-type cyclins which activate cyclin dependent kinases 4 and 6 (CDK4/6). CDK-mediated inactivation of pRB triggers E2F release and consequent transcription of E2F regulated genes. This commits the cell to undergo DNA replication. Entry into the M phase requires CDK1 and CDK2 which are activated by A or B type cyclins. Additional kinases such as Polo-like kinase 1 (PLK1) or Aurora regulate events during mitosis. Each phase of the cell cycle is

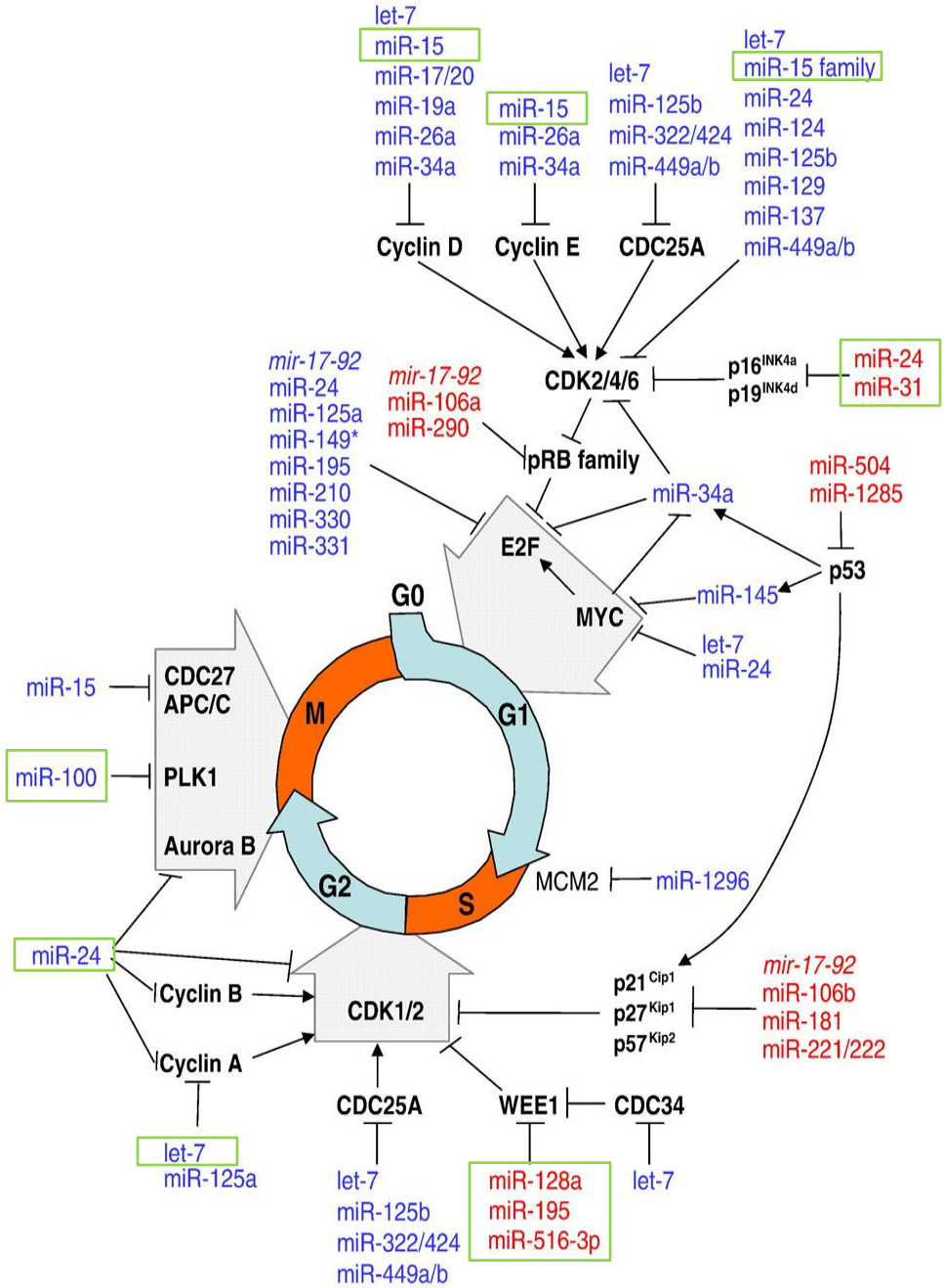

Fig. 1.5. Multiple stages of the cell cycle are subject to miRNA regulation (image adapted from Bueno and Malumbres) (199). Proliferation can be favoured (red) or antagonized (blue) by cellular miRNAs. Individual miRNAs and miRNA clusters are shown in normal text and italics respectively. All miRNAs illustrated in green boxes are discussed in the text. Note that most of the interactions listed have only been validated by luciferase assay.

controlled by checkpoints which arrest or delay cell division in the event of DNA damage or mitotic abnormalities. Such stimuli trigger the activation of anti-proliferative CDK inhibitors such as members of the INK4 and Cip/Kip family.

The relationship between miRNAs and the cell cycle is very complex (Fig. 1.5) and generally involves the G1 to S phase transition (199). Most miRNAs exert an anti-proliferative effect, which may be achieved by targeting cyclins and members of the CDK family. For instance CDK1, CDK2, CDK6, cyclin D1, cyclin D3 and cyclin E1 are all targeted by miR-15a and miR-16 (200-203). On the other hand miRNAs may exert a proliferative effect by targeting CDK inhibitors. For instance both miR-24 and miR-31 target p16INK4a, an inhibitor of CDK4 and CDK6 (204, 205).

Some miRNAs regulate cell cycle events after DNA replication. The anti-proliferative miR-125b, miR-24 and let-7 mediate repression of cyclin A and cyclin B, which in turn prevents CDK1 activation and G2/M progression (206-208). Conversely the proliferative miR-195, miR-128 and miR-516-3p target WEE1, an inhibitor of the cyclinB-CDK1 complex (209, 210). There is little evidence for miRNA mediated regulation during mitosis although PLK1 might be a miR-100 target (211).

1.6 microRNAs in cancer cells

Considering the broad range of biological pathways in which miRNAs are involved, it is not difficult to see how their deregulation could contribute to human disease. In the current section, we shall discuss the concept of oncomiRs, i.e. miRNAs which act as oncogenes or

tumour suppressors. Thereafter we will consider the mechanisms by which miRNA deregulation takes place in the context of human disease.

Two early investigations used different methods to characterize expression of over 200 human miRNAs in a broad range of cancers i.e. solid tumours, lymphomas etc (212, 213). Both studies found that miRNAs were extensively deregulated in cancer compared to normal tissue. These findings were supported by a number of further studies, reviewed by Wang and Lee (214), which showed that certain miRNAs are consistently over expressed (miR-21, miR-155, miR-222 etc.) while others are consistently under expressed in cancer (miR-143, miR-145, let-7 etc.). Additionally different tumours as well as tumour subtypes may be distinguished based on their miRNA signature (212, 213, 215).

When deregulation of a given miRNA promotes tumour progression it is referred to as an oncomiR. Such miRNAs may act as oncogenes or tumour suppressors. For example miR-155 is an oncogenic oncomiR, frequently over expressed in B cell lymphoma (213, 216, 217); it causes lymphoproliferative disease in mouse models when over expressed from a B cell specific transgene (218). Another oncogenic oncomiR, miR-21, encourages disease progression in colorectal and lung cancer by targeting suppressors such as PDCD4 and TPM1 (214, 219-222).

The let-7 family of miRNAs serve as examples of tumour suppressor oncomiRs (89, 90, 92, 223-227) as their expression impairs growth of a number of tumours e.g. colorectal and lung cancer cells, presumably by targeting oncogenes such as RAS and HMGA2. MiR-34a is another tumour suppressor oncomiR which mediates an anti-proliferative and/or pro-apoptotic state in neuroblastoma and brain tumours (190, 228), presumably by repression of c-myc, bcl-2 and c-Met. The respective roles of let-7 and miR-34a in differentiation, apoptosis and

proliferation were discussed in section 1.5. A database (miR2Disease) has been set up in order to accumulate information on the importance of miRNA deregulation in human disease (229).

There are a number of mechanisms through which miRNAs can be deregulated. MiRNA transcription for instance can be regulated by transcription factors such as c-myc or p53. C-myc is over expressed in a number of tumours (230) while p53 is frequently inactivated by mutations (231). For instance p53 usually activates the tumour suppressive miR-34a cluster (63-65), while c-myc activates the human oncogenic miR-17-92 cluster (66, 67). Additionally miRNA transcription may be affected by aberrant DNA methylation i.e. inactivation of miR-124 and miR-34a in colon and prostate cancer respectively (232, 233). MiRNA transcription in cancer cells is often affected by chromosomal rearrangements and aberrations. One study demonstrated that, out of 283 miRNA coding genes, 85.8%, 37.1% and 72.8% had altered copy number in melanoma, ovarian and breast cancer, respectively (223, 234). Interestingly 41 of those genes were similarly altered in all three cancers investigated. Gene amplification of the 17q23 region housing oncogenic oncomiR miR-21 in neuroblastoma (235) and deletion of the 13q14 region housing anti-proliferative/pro-apoptotic miR15a and miR-16-1 miRNAs in chronic lymphocytic leukaemia CLL (189, 200-203, 236) are just some examples.

MiRNA deregulation may also be mediated by aberrant expression of the miRNA processing machinery. Altered Drosha expression is observed in many cancers (237-239). Interestingly high Drosha levels indicates poor disease outcome in esophageal squamous cell carcinoma (ESS) while the opposite is true in ovarian cancer (237, 239). As previously mentioned defects in exportin-5 can lead to retention of pre-miRNAs (77). Exportin-5 has been described as a potential tumour suppressor in a subset of stomach and colon cancer (78). Deregulation of Dicer has also been described in a range of cancers (237, 240-242) with under expression

prognostic of poor disease outcome in lung and ovarian cancer (237, 242). Many components of the nuclear and cytoplasmic miRNA processing machinery, including Drosha and Dicer, can be regulated by tumour suppressors such p53, p63 and p73 (243).

Finally, point mutations either in the miRNA or the 3′ UTR target can interfere with the miRISC silencing pathway. For instance a single G:C change in pre-miR146 reduces mature miR-146a production; this results in an increased risk of developing some types of thyroid and brain cancers whilst reducing the risk of prostate cancer (244-246). Conversely translocation of the normal HMGA 3′ UTR prevents let-7 mediated repression (91). High expression of HMGA2 contributes to disease progression in lung cancer and dually serves a prognostic marker for survival (224, 247, 248).

1.7 Introduction to Epstein - Barr virus (EBV)

Epstein–Barr virus (EBV), a widespread human gammaherpesvirus, is a potent transforming agent of resting B-lymphocytes and is aetiologically linked to several malignancies of lymphoid and epithelial cell origin including Burkitt lymphoma (BL) and nasopharyngeal carcinoma (NPC) (249). EBV was the first virus found to encode its own set of miRNAs (250). This raises questions as to their roles in the virus life cycle as well as how they might contribute to virus mediated oncogenesis. In the next few sections we will cover a few basics of EBV biology including how the virus was discovered and classified (section 1.7), how the viral genome is organized (section 1.8) and the tissue tropism of the virus (section 1.9).

1.7.1 A historical perspective

The path to discovering EBV began in 1958 in Kampala (Uganda) where surgeon Dennis Burkitt investigated a sarcoma affecting the jaws of children (251). The tumour (eventually named Burkitt lymphoma) (252) mapped almost exclusively to equatorial Africa (251) and appeared dependent on climatic factors like rainfall and temperature (253). Therefore it was proposed that transmission of the tumour could occur through a climate dependent vector, thereby opening the possibility of a viral role in disease development (253).

In 1964 Michael Epstein, Bert Achong and Yvonne Barr (London) used electron microscopy to demonstrate the presence of herpes-virus like particles in continuous cell lines grown from BL biopsies (254); a series of collaborations with Werner and Gertrude Henle (Philadelphia) subsequently led to its classification as a novel herpes virus in 1965 (255). Over the next decade EBV research greatly expanded. Newly developed immunofluorescence assays revealed the virus was restricted neither to BL nor equatorial Africa; it was ubiquitous, infecting 90% people by adulthood (256). It was in fact the mosquito transmitted *Plasmodium falciparum* parasite, another co-factor in BL development, which was geographically restricted and climate dependent (257, 258). In the general population, EBV was identified as the causative agent of infectious mononucleosis (259, 260). Its potential to act as a cancer causing agent was demonstrated both *in vitro* and *in vivo*. Lethally irradiated BL cells induced growth transformation in peripheral leukocytes (261), while cell free virus induced lymphomas in immune-suppressed primates (262). Nowadays EBV is an established member of human oncogenic (cancer causing) viruses.

1.7.2 A scientific classification

EBV is formally referred to as human herpesvirus 4 (HHV4) and belongs to the family *Herpesviridae* within the order *Herpesvirales* (263). The *Herpesviridae* family contains primate herpesviruses, 8 of which are associated with humans, and comprises the *alpha-*, *beta-* and *gammaherpesvirinae* subfamilies. EBV is a gammaherpesvirus and the type species of the Lymphocryptovirus (LCV) genus. LCVs are mainly considered B lymphotrophic and, with the exception of EBV, exclusively infect non-human primates.

1.8 Structure and genome of EBV

The EBV particle measures ~180 nm in diameter and is surrounded by a glycoprotein (gp)-rich envelope (264). It contains a protein tegument, a capsid with 162 capsomers, and a protein-DNA core organized in the form of a torus (255, 265). The genome itself consists of a linear double stranded DNA (dsDNA) genome roughly 175 kilobase pairs (kbp) in length (266).

EBV was the first herpesvirus to have its genome fully sequenced; this was achieved with fragments generated by *Bam*HI and *Eco*RI digestion of the B95-8 strain (267-269). Genes were named according to the *Bam*HI fragment (denoted A-Z and a-e in descending order of size) in which they start i.e. BRLF1 is the first leftward reading frame starting in *Bam*HI fragment R. A representative map of the B95-8 genome can be seen in Fig. 1.6 taken from Kalla and Hammerschmidt (270). Presently there are five available complete or partial genomes sequences (B95-8, AG876, GD1, GD2 and HKNPC1) (267, 271-274).

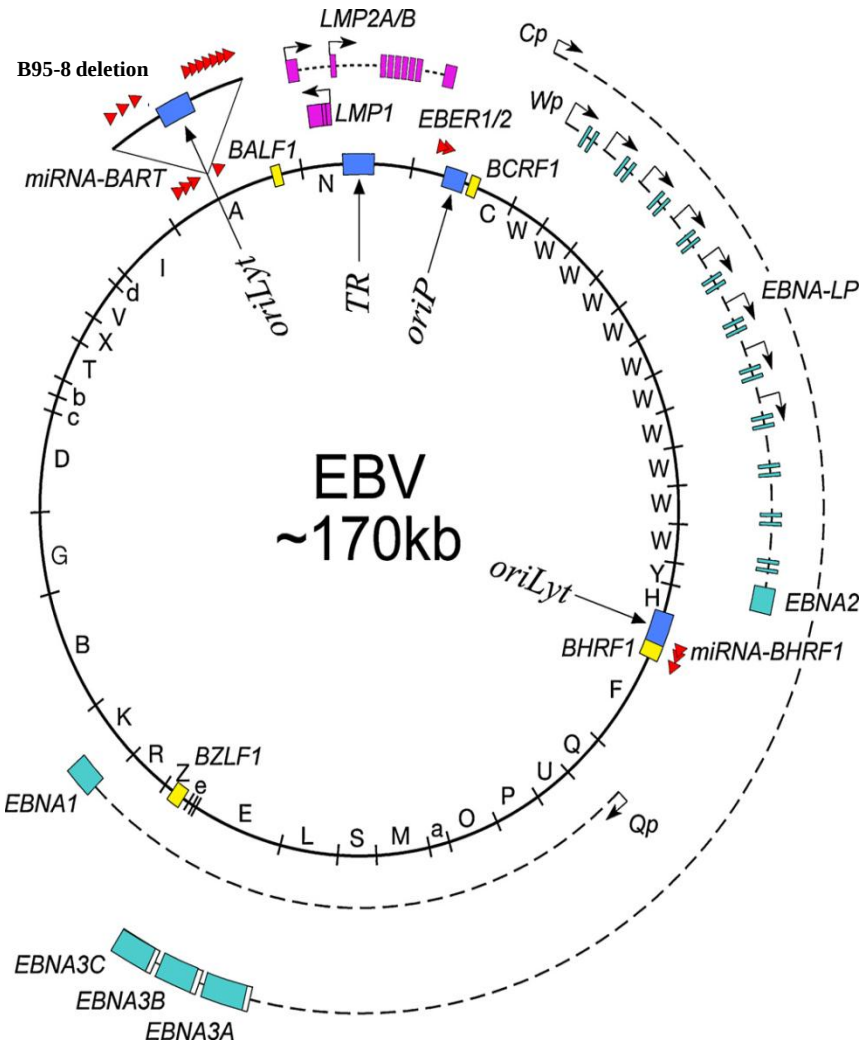

Fig. 1.6. Schematic of the B95-8 prototype strain of EBV (image taken from Hammerschmidt and Kalla) (270). The viral genome is divided into multiple BamHI fragments (A-Z, a-e). The origin of plasmid replication (oriP), the origin of lytic replication (oriLyt), and the terminal repeats (TR) are illustrated with blue boxes. The12kb deletion fragment deleted in the B95-8 strain but present in all field strains of EBV is illustrated in the top left inset. Also shown are the EBV latent genes (turquoise and purple boxes), the C, W, Q and LMP promoters (black arrows) and the viral non-coding RNAs (red arrows). Lytic genes expressed shortly after de novo infection of resting B cells with EBV are illustrated with yellow boxes.

All EBV strains share a near identical genome organization. EBV has ~100 open reading frames (ORFs), with most of the genome's coding capacity being shared between two unique domains: a short 9000 bp (US or U1) and a long 150000 bp (UL) sequence (267, 275-279). Most of these genes are in turn dedicated to productive cycle infection (267). EBV also has a large number of reiterated direct repeat sequences interspersed throughout the genome. The major internal repeat (IR1), which consists of multiple copies of a 3.1 kbp sequence, separates the US from the UL domain (268, 280, 281); the latter domain is further subdivided into four regions (U2-U5) by additional IRs (282, 283). The ends of the genome are flanked by the terminal repeats (TR), multiple copies of a 500 base pair (bp) sequences (284, 285).

Generally the EBV genome is highly conserved. The majority of documented strain associated sequence variation occurs in the EBNA2 and EBNA3 genes; the amino acid identity of EBNA2, 3A, 3B and 3C genes differs for the two major EBV subtypes – Type I and Type II – by 45%, 16%, 20% and 28% respectively (286-288). Both subtypes may be further subdivided into many strains based on the number of repeats within their latent genes (289, 290). Additional polymorphisms within the EBNA and LMP genes have been identified some of which correlate with defined geographical locations, suggesting evolutionary drift in separate populations (291-294).

1.9 Tissue tropism of EBV

EBV predominantly infects B lymphocytes by targeting and binding of the C3d complement receptor, CD21, which is expressed on B cells of all developmental stages except terminally differentiated plasma cells (295-299). CD21 is the primary EBV receptor on B cells. Binding is mediated via the viral gp350 protein which bears two short regions of homology with the

natural CD21 ligand, C3dg (299-301). Subsequently EBV binds a co-receptor on B cells, MHCII, via the viral gp42 protein; this triggers fusion and entry (302-304). Generally infection of B cells results in latent infection although productive infection can occur in a small number of infected cells (305).

EBV also appears capable of infecting a range of CD21 negative cell types including epithelial (306), natural killer (NK) (307) and T cells (308) as evidenced by direct association of EBV with malignancies deriving from these cell lineages. Epithelial cells can be infected *in vitro* via a process termed transfer infection, in which B cell – bound EBV is "transferred" to an epithelial cell via cell to cell contact (309, 310); like B cells, they are also capable of supporting productive infection (311, 312). While some 30% to 40% of T lymphocytes do express low levels of CD21 (ten times lower than B cells) (313) CD21 negative T lymphocytes are still capable of binding EBV via an uncharacterized receptor (314). The natural role of epithelial, T and NK cells in of the viral life cycle remains unclear.

1.10 *In vitro* infection, transformation and immortalization of B cells

The ability of EBV to act as a cancer causing agent was initially demonstrated during *in vitro* infection (261). Specifically, lethally irradiated BL cells induced growth transformation in peripheral leukocytes. The current section will outline the events that take place between *de novo* infection of cultured resting B cells and the outgrowth of an immortalized cell line.

The expression of the full latent gene repertoire is interchangeably termed Latency III or the growth transforming program (Fig. 1.7) (315). Cells infected with EBV *in vitro* express the full range of EBV gene products discussed previously, including 6 nuclear antigens (EBNA-

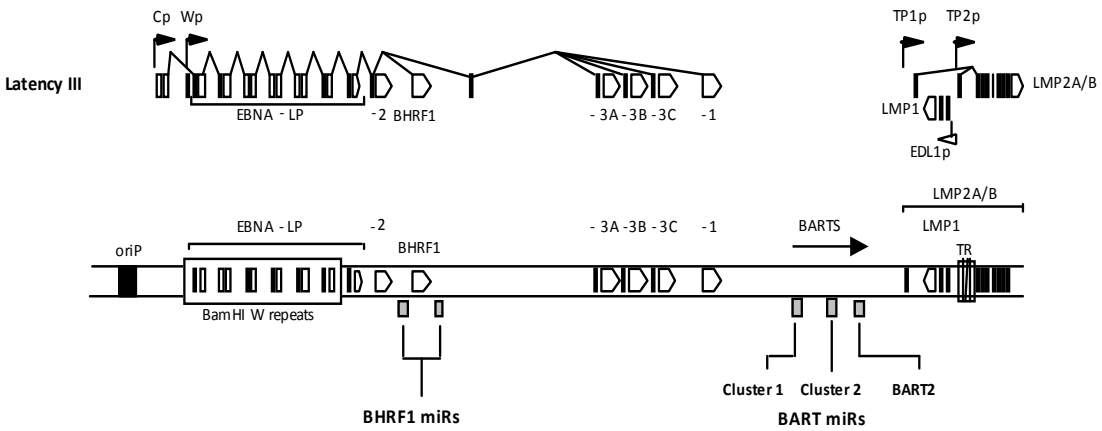

Fig. 1.7. The growth transforming program of LCLs. The location of viral promoters and splice structures of viral transcripts are shown relative to a linear representation of the EBV genome. Growth transformed LCLs express all six EBNAs and BHRF1, predominantly from highly spliced transcripts initiated at the BamHI C promoter (Cp), along with the LMPs which are transcribed from separate promoters in the BamHI N region. Epstein-Barr virus-encoded small RNAs (EBERs) and BamHI A rightward transcripts (BARTs) are expressed from their own respective promoters. Also shown are the positions of the BHRF1 and BART miRNAs, latent origin of replication (oriP) and the terminal repeat region (TR). Note that the growth transforming program is interchangeable referred to as Latency III (Lat III).

LP, EBNA1, EBNA2, EBNA3A, EBNA3B and EBNA3C) driven by promoters C and W (316-319), 3 membrane proteins (LMP1, LMP2A and LMP2B), the EBER and BART RNA species, and a viral Bcl-2 homolog (BHRF1) (320). Also expressed are two groups of viral miRNAs located in the BHRF1 and BART region of the genome termed the BHRF1 and BART miRNAs respectively (250). These molecules will be discussed in more detail throughout later sections (section 1.14.9).

Once inside a B cell the linear EBV genome circularizes via the terminal repeats; episomes appear roughly 16-20 hours post infection (284, 321). This is a key event in transformation and immortalization as it allows the genome to persist in infected B cells. Note that multiple copies of the circular EBV genome can be found per latently infected cell (322). Viral transcription initiates much earlier however and follows a set sequence. Initially the W promoter (Wp) generates large RNA polymerase II driven transcripts which give rise to the EBNA-LP and EBNA2 proteins (detectable at 12h-24 hours) (323-327). Note that that different EBV strains possess a variable number of W repeats and consequently multiple copies of Wp (319, 328). Nonetheless a minimum of 5 copies of Wp are required for optimal transformation (328).

EBNA2 transactivates the C promoter (Cp); at this point levels of Wp transcription start to decrease whilst Cp becomes predominantly responsible for EBNA gene transcription (24h-48h post-infection) (325, 329-332). Cp transcripts are differentially spliced and capable of generating the complete set of EBNA proteins (EBNA1, EBNA2, EBNA3A, EBNA3B, EBNA3C and EBNA-LP). EBNA2 further activates the latent membrane protein (LMP) promoters; LMP1 and LMP2 transcripts are both readily detectable by 5 days post-infection (325). A number of non-coding RNAs are also expressed from their respective promoters

early after primary infection. The BART RNAs are readily detectable by 24h whilst the EBER RNAs (EBER1 and EBER2) can be detected after 3 days (325). Finally a Bcl-2 homolog, BHRF1, is also expressed at low levels in transformed B cells (320).

EBV has innate growth transforming and immortalization properties. *De novo* infection of resting B cells induces unlimited proliferation (261, 333) and ultimately gives rise to the outgrowth of an immortal cell line termed lymphoblastoid cell line (LCL). The process of transformation is B cell specific (334). It begins early post-infection and is characterized by a number of morphological changes i.e. increases in cell size, irregular shaping and clumping (261, 333). Cell cycle entry and progression occurs as a result of cellular changes including the stimulation (cyclin D2, cyclin E, cdk1, cdk2, cdk4, cdk6) and inactivation (pRb, p107) of specific cell cycle regulatory proteins (335-337). EBV is believed to drive and maintain proliferation by mimicking antigen driven B cell activation with T cell help in the absence of T cell signalling or the B cell receptor (338). In agreement with this, a number of genes and cell surface molecules involved in signalling and growth regulation are collectively up regulated. These include growth factors IL-5 (339), IL6 (340), and IL-10 (341, 342) as well as receptors such as CD21, CD23 (343-345), CCR7 (346, 347), and the TNF-α receptor (348). A number of adhesion molecules and proteins involved in cytokine formation are also stimulated (346, 349).

Transformation requires several EBV proteins. EBNA2, LMP1 and EBNA3C are absolutely essential for transformation (350, 351). EBNA-LP, EBNA3A and EBNA1 are also very important; EBNA-LP deleted mutants have reduced transformation efficiencies (352), EBNA3A deleted LCLs are severely growth impaired and sensitised to apoptosis (353) whilst

EBNA1 is needed to maintain the viral genome in proliferating cells (354). The precise functions of the various EBV gene products are discussed elsewhere (section 1.14).

EBV transformed lymphoblastoid cells require additional mutations to achieve immortalization, key to which is telomerase activation (355-358). Non-immortalized LCLs have negligible telomerase activity (359, 360), thus telomere shortening occurs with each cell division until a critical length is reached (typically by 180 passages). At this point cells undergo crisis and only those which have managed to stabilize their telomeres (via telomerase activation) survive. These cells grow out to form an immortalized population characterized by chromosomal aberrations (361). As they become more tumour-like, immortalized LCLs gain the ability to form colonies on agarose and grow in nude mice (362). Other changes are associated with immortalization and tumourigenesis including mutations in p53 (362) and an altered responses to cytotoxic drugs (363). The processes of transformation and immortalization (within context of the LCL model of infection) are important as they have not only provided us with insight into the biology of the Epstein-Barr virus but also clues as to the mechanisms underlining EBV tumourigenesis.

1.11 *In vivo* infection of B cells

EBV is usually contracted during childhood where it causes an asymptomatic infection. Some 50% of EBV infections contracted during adolescence or later result in infectious mononucleosis (IM), a self limiting lymphoproliferative disease (260, 364). The virus is transmitted by saliva and enters the body through the lymphoepithelium lining the oral cavity (365). EBV is believed to initially infect and replicate in tonsillar B lymphocytes (305, 366, 367). It is unclear if and to what extent epithelial cells are involved during the natural biology

of EBV. Evidence suggests that epithelial cells are not infected during primary infection but instead might serve as sites of viral amplification and subsequent shedding in healthy EBV carriers (368-371). Nonetheless primary EBV infection results both in shedding of new virus into the oral cavity and the latent colonization of the host B cell pool.

Primary EBV infection elicits a potent CD8+ cytotoxic T lymphocyte (CTL) response, which both controls the infection and causes the symptoms of IM (372, 373). EBV is not cleared entirely however and may be isolated as infectious virus in throat washings and in latently infected B cells (374, 375). On that note EBV is able to persist within memory B cells where it expresses a very restricted form of latency termed the latency program (Lat 0) where only non-coding RNA species are expressed i.e. the EBERs, BARTs and in theory the BART miRNAs (376, 377).

The mechanism by which EBV gains access to the memory pool is controversial. One widely accepted model is that EBV colonizes naïve B cells and then mirrors antigen driven B cell maturation, allowing for germinal centre (GC) transit in the absence of external stimuli (377). The GC model can be seen in Fig. 1.8A taken from Young and Rickinson (378). EBV primarily infects resting naïve B cells. Subsequently it expresses the full range of latent antigens (Lat III), which causes the naïve B cells to become activated B blasts. Activated B blasts travel to the follicles whereupon EBV gene expression is down regulated to a Hodgkin's lymphoma-like (Lat II) antigen profile termed the default program (379, 380). Two viral antigens, LMP1 and LMP2, are sufficient to allow for GC formation and differentiation of the activated B blast to a memory B cell. LMP1 functions as a constitutively active CD40 receptor thus activating proliferation and survival (381, 382) while LMP2 is capable of providing BCR-like survival signals (383, 384). The LMPs will be discussed in more detail

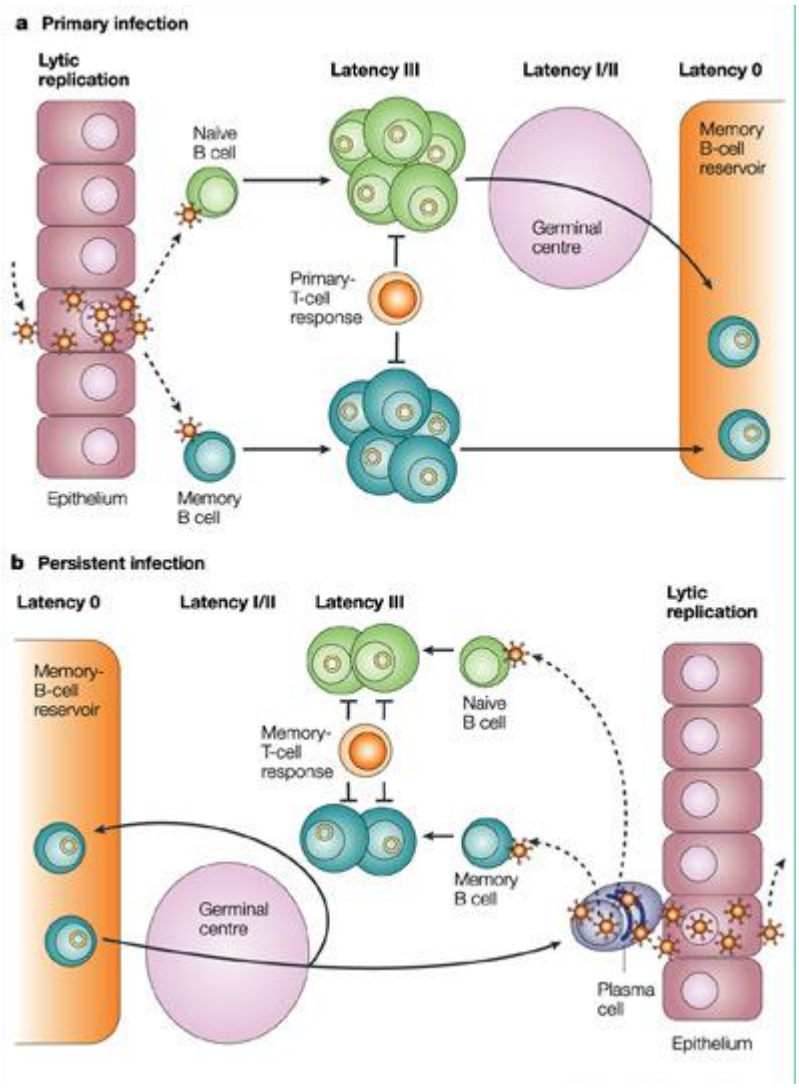

Fig. 1.8. *In vivo* infection and persistence of EBV (image taken from Young and Rickinson) (378). **(A)** Two possible mechanisms through which EBV gains access to the memory B cell reservoir. In the Germinal centre (GC) model EBV infects naïve B cells and mirrors antigen driven differentiation of naïve B cells to memory B cells. In the direct infection model EBV infects pre-existing memory B cells **(B)** Summary of EBV persistence. EBV persists latently in memory B cells until antigen stimulation drives them to differentiate into plasma cells. Plasma cells migrate to the mucosal epithelium and release infectious virus into the saliva.

later (section 1.14.5). In circulating memory B cells viral antigen expression is further suppressed to Lat 0, consequently avoiding immune detection (377). Note that EBNA1 is occasionally expressed to allow for maintenance of the viral genome during cell division (385).

Another possible mechanism is the direct infection of memory B cells in the absence of GC transit (379, 386). This model is supported by a number of observations. Firstly X-linked lymphoproliferative (XLP) patients can be latently infected with EBV; note that XLP patients can not form fully functional germinal centres (387). Secondly EBV is detectable in the non-isotype-switched memory B cells (IgD+ CD27+) of immunocompetent IM patients and persistently infected individuals (388); note this particular B cell subset is believed to arise in a GC-independent manner (389-391). Finally EBV-infected B cells in IM tonsils do not localize to the germinal centre but to extrafollicular areas instead (305, 379, 392). Such B cells lack GC markers such as CD10 and CD77 (388); it is true that they are positive for CD38, also a GC marker, however this may be a consequence of growth activation rather than GC transit (388).

EBV reactivation from latently infected memory B cells *in vivo* is thought to be triggered by antigen driven differentiation of the memory B cell to an antibody secreting plasma B cell (393, 394). Plasma cells naturally migrate to the mucosal surface where infectious virus is released into the tonsils (395-397). As discussed earlier epithelial cells may play a role in amplifying the amount of virus released into the saliva (368, 369). The reactivation process can be seen in Fig. 1.8B taken from Young and Rickinson (378).

1.12 EBV productive infection

Previously we have discussed the establishment of latency both *in vitro* and *in vivo*; in both scenarios a Lat III program of latent gene expression can be observed. The majority of the EBV coding capacity is dedicated to productive infection (267, 270) which may be divided into immediate early, early and late genes. The switch to productive infection depends on two immediate early transcription factor genes, BZLF1 and BRLF1 (398, 399). These transcription factors are responsible for early gene induction; BZLF1 and BRLF1 can auto- and cross- stimulate one another in order to amplify their activities (400-404). BZLF1 is a viral AP-1 homolog (405) that interacts with targets containing Z-response elements (ZRE) (406, 407). Early genes include machinery necessary for DNA replication such as the viral polymerase BALF5 (408-410). By comparison late cycle genes primarily include structural proteins required for virus assembly (408-410).

Productive infection within *in vitro* cultured B cell lines can be triggered through mechanisms such as phorbol ester treatment and immunoglobulin cross linking (411-415). One thing to note however is that significant productive infection does not occur in *de novo* infected cultured B cells, even though BZLF1 is expressed in the majority of cells within the first few hours post-infection (416). BZLF1 expression has been suggested in these circumstances to promote the proliferation of resting B cells. The failure to produce viral progeny is linked to the fact that *de novo* infecting viral genomes are unmethylated; a number of key downstream targets of BZLF1 require promoter methylation in order to be efficiently activated by BZLF1 (417, 418). Production of infectious virus *in vivo* occurs in B cells of the oropharynx, possibly during primary infection or viral reactivation (366, 367, 393, 419); it has been suggested that the source of infectious virus are terminal differentiating plasma B cells (393, 394).

The EBV genome is exponentially amplified by rolling circle replication and expresses an extensive number of genes (267, 408). Consequently EBV has developed a number of mechanisms to subvert immune surveillance. For instance the non-structural late protein BCRF1 acts as a viral IL-10 homolog (vIL-10) (420); BCRF1 may provide pro-survival signals (420-424) and/or interfere with T cell mediated immune surveillance (425-428). Furthermore a number of other gene products such as BILF1, BGLF5 and BNLF2a may also interfere with viral targeting by T cells (429-431). Two early genes, BHRF1 and BALF1, are bcl-2 homologs which have previously been shown to inhibit apoptosis in culture (320, 432). These may further assist in the survival of cells infected with actively replicating EBV.

1.13 EBV-associated B cell lymphomas

EBV is aetiologically linked to a number of malignancies of lymphoid and epithelial cell origin; these include Burkitt lymphoma (BL), Hodgkin lymphoma (HL), post-transplant lymphoproliferative disease (PTLD), nasopharyngeal carcinoma (NPC) and a range of T cell and NK lymphomas (249). In the current section we will discuss a selection of malignancies specific to B cells. We will focus first on a number of proliferative diseases found in immune compromised individuals; thereafter we will focus on Hodgkin and Burkitt lymphoma.

1.13.1 Proliferative disease in immune compromised hosts

The *in vivo* oncogenic properties of EBV are clearly evidenced by a collection of lymphoproliferative diseases in the immune suppressed or compromised. One such disease is post-transplant lymphoproliferative disease (PTLD). It affects patients who are receiving

immune suppression to prevent graft vs. host disease of transplanted tissue. As reviewed by Nalesnik, PTLD occurs in at least 1.4% of transplants although the precise rate depends on factors such as the type of tissue and level of immune suppression received (433). For instance heart transplants (2%-10%) carries a higher risk of PTLD than renal transplants (1%) (433). Rarely (less than 2%) PTLD may also occur in human stem cell transplant (HSCT) patients; note that such patients would have had their own immune system ablated as part of the medical procedure (434-436). PTLD lesions have been described as early, polymorphic and monomorphic (437). The relationship between EBV infection and PTLD is well established (433). Patients with high EBV loads or those undergoing primary EBV infection are at greatest risk (438, 439). PTLD lesions in turn are almost always EBV positive (437). It is believed that PTLD lesions derive from germinal centre (GC) or post-GC B cells; the majority of EBV positive B cells in a PTLD lesion carry mutated Ig gene rearrangements (440). Several lines of evidence point to a loss of the virus-specific CD8+ cytotoxic T cell (CTL) response as the reason for PTLD formation. PTLD lesions display a latency III pattern of EBV gene expression, consistent with EBV infection in the absence of immune surveillance (441-443). Furthermore PTLD lesions are devoid of activated T cell infiltrate (444). Additionally the risk of PTLD throughout bone marrow transplantation rises from 1% to nearly 24% upon ablation of EBV specific T cells from donor marrow (445). Finally PTLD can be reversed via a reduction of immune suppressive therapy; recovery coincides with the appearance of virus specific CD8+ CTLs (446-448).

Another example of an EBV associated lymphoproliferative disease is AIDS-associated lymphoma. As reviewed by Gaidano *et al.* HIV infected individuals have a higher risk of developing a range of B cell lymphomas, especially during end stage disease (449, 450). EBV association with tumour cells varies between 30% and 100% depending on the nature of

lymphoma involved. One of the more prevalent types of AIDS-lymphoma presents with PTLD-like lesion (451). Tumour cells within these lesions seem to derive from memory B cells, are characterized by a Lat III pattern of gene expression and also appear to result from a loss of virus specific T cell monitoring (450, 452-455).

1.13.2 Hodgkin lymphoma

Hodgkin lymphoma (HL) is a common form of lymphoma in the West with 3 cases per 100000 each year (456). It is an unusual disease in that more than 98% of the total tumour mass consists of non-malignant infiltrate, which in turn surrounds a minor population of malignant mononuclear Hodgkin cells and multinuclear Reed-Sternberg cells (H-RS) (457). HL is subdivided into classical HL (cHL) and lymphocyte predominant HL (lp-HL) groups (457). While EBV association in the latter subtype is rare, it is associated with ~35% of cHL in the west and more than 60% of cases in developing countries (458).

Differences in the onset and peaks of childhood and adult HL between western and developing countries mirror IM prevalence thus suggesting a possible role for EBV in HL progression (459, 460). Several pieces of evidence favoured this hypothesis. Firstly a history of IM increased the risk of developing HL three fold (459). Secondly monoclonal EBV genomes were not only detected in tumour biopsies (southern blotting, terminal repeat assays), but specifically located to H-RS cells (*in situ* hybridization) (461-463). Ultimately every H-RS cell of a given tumour was found to carry the exact same EBV genome (464).

EBV gene expression in HL is more restricted than latency III. Antibody staining at the single cell level only revealed the presence of EBNA1 (465), LMP1 (466, 467) and LMP2A (392)

while transcriptional analysis also demonstrated the presence of EBER and BART RNA (468). This pattern of latent antigen expression is termed latency II. H-RS cells were found to derive from somatically hypermutated germinal centre B cells with nonsense Ig gene rearrangements (469-472). Such cells would normally undergo apoptosis but are rescued by two EBV latent antigens termed LMP1 and LMP2. The functions of LMP gene products were briefly discussed in section 1.11 and will be discussed in more detail later (section 1.14.5).

1.13.3 Burkitt lymphoma

Burkitt lymphoma (BL) is a tumour derived from germinal centre B cells which can be separated into three groups: endemic, sporadic and AIDS-associated (473). Endemic BL (eBL) predominantly presents as a mass of the jaw and is the BL group originally described by Dennis Burkitt (251-253, 257). It maps almost exclusively to equatorial Africa and Papua New Guinea and is nearly always EBV associated, suggesting a role for the virus in the disease process (473, 474). Sporadic BL (sBL) presents mainly as an abdominal mass and is ~15% EBV associated (475-477). In contrast to eBL it occurs worldwide, albeit with a much lower incidence (475, 476). AIDS associated BL (AIDS-BL) usually occurs in otherwise healthy HIV carriers and is around 40% EBV associated (450, 477-479). Due to HIV prevalence it is the most common form of BL.

All three groups of BL (eBL, sBL and AIDS-BL) share characteristic gene rearrangements between the c-myc region of chromosome 8 and the immunoglobulin genes (477, 480, 481). For most BL (~80%) this involves a translocation with the heavy chain genes on chromosome 14, but can also involve the lambda or kappa genes on chromosomes 22 and 2 respectively. In all three, over expression of c-myc by the immunoglobulin locus (480-483) leads to aberrant

cell growth and proliferation (484-489). It also triggers a heightened sensitivity to apoptosis (490, 491).

Each tumour cell in EBV positive BL is monoclonal in origin; thus EBV precedes and could be responsible for clonal expansion in BL (254, 492). Studies on the contribution of EBV to the disease progression of BL have investigated a number of latent antigens (493). EBNA1 is the only latent antigen expressed in conventional EBV positive BL and is expressed from promoter Q (Fig 1.9) (494, 495); note that the W, C and LMP promoters are silent in this tumour (496-498). Additionally both the EBER and BART RNA species are expressed (473, 499). This form of latency is termed latency I and it is even more restricted than latency II seen in HL. The observation that EBV positive BL cells are more resistant to apoptosis than spontaneous EBV loss counterparts suggests that EBV might provide survival signals to tumour cells (500). On that note EBNA1 has been shown to destabilize p53 by targeting HAUSP (501). It is unclear how relevant this is as p53 is frequently mutated in BL cell lines; nonetheless there is evidence to suggest such mutations may be less frequent *in vivo* (502, 503). EBERs may also contribute to BL as they have been implicated in driving tumour growth and resisting IFN-α mediated apoptosis (500, 504-508).

Around ~15% of EBV associated BL tumours display a more extensive pattern of antigen expression where promoter W drives expression of EBNA1, EBNA3A, -3B, -3C, BHRF1 and a truncated form of EBNA-LP (t-EBNALP) from an EBNA2 deleted genome (Fig. 1.9) (320, 509, 510); note that these tumours also carry a silent wild type genome. This particular type of BL is termed Wp-restricted BL (Wp-BL) and is more resistant to apoptosis than its latency I BL counter part (510). A number of reports have investigated the contributions of BHRF1, t-EBNA-LP and the EBNA3s to the Wp-BL survival phenotype (320, 511, 512). Briefly,

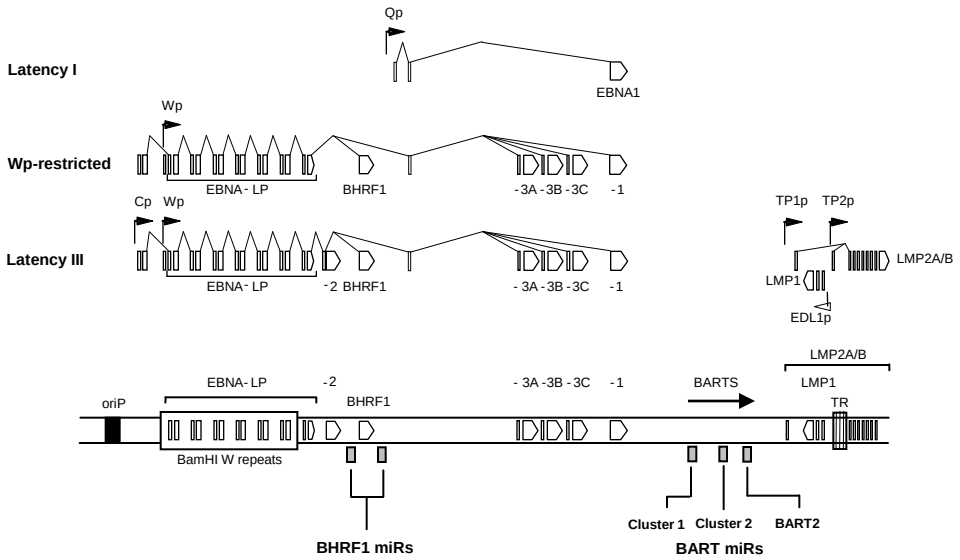

Fig. 1.9. Patterns of latent gene expression in BL cell lines and LCLs. The location of viral promoters and splice structures of viral transcripts are shown relative to a linear representation of the EBV genome. Conventional Latency I BLs express a single latent antigen EBNA1 transcribed from a viral promoter in the BamHI Q region(Qp). Wp-restricted BLs are characterised by the presence of an EBNA2-deleted EBV genome; these BLs express EBNAs 1, -3A, -3B, -3C and –LP, along with BHRF1, all transcribed from the Latency III BamHI W promoter (Wp), but in the absence of EBNA2 and the latent membrane proteins (LMPs). Latency III BL lines and growth transformed LCLs express all six EBNAs and BHRF1, predominantly from transcripts initiated at the BamHI C promoter (Cp), along with the LMPs which are transcribed from separate promoters in the BamHI N region. EBERs (not shown) and BamHI A rightward transcripts (BARTs) are present in all three forms of latency. Also shown are the positions of the BHRF1 and BART miRNAs, latent origin of replication (oriP) and the terminal repeat region (TR).

BHRF1 acts as an anti-apoptotic Bcl-2 homolog (320, 513), while t-EBNA-LP antagonizes caspase-mediated apoptosis via inactivation of protein phosphatase 2A (PP2A) (512). EBNA3A and 3C in turn can down regulate pro-apoptotic Bim and members of the anti-proliferative INK4 family (353, 511, 514). As such EBV may act to counter the sensitisation to apoptosis caused by c-myc deregulation.

1.14 Functions of EBV Latent Gene Products

In sections 1.10 and 1.11 we described the full repertoire of latent gene expression found in transforming B cells both *in vitro* and *in vivo*. In the following sections we will cover in detail the functions of each of these latent gene products and how they contribute towards the viral life cycle.

1.14.1 EBNA1

EBNA1 is a DNA binding protein with essential roles in replication and maintenance of the EBV episome in infected cells (385). It is encoded within the *Bam*HI-K region of the genome and can be transcribed from four different promoters: the C and W promoters in the LCL model (515), the Q promoter in classical Burkitt lymphoma (516) and the F promoter during productive infection (517-519).

EBNA1 directly binds three areas of the viral genome: the dyad symmetry (DS) and the family of repeats (FR), which together form the plasmid origin of replication (oriP), as well as a more distal area located in *Bam*HI-Q (385, 520-524). The DS contains 4 EBNA1 binding sites; it is the site of replication initiation and functions as an EBNA1-dependent replicator

(525-527). FR contains a variable number of EBNA1 binding sites (20 in B95-8) and functions to prevent EBV loss from actively dividing cells by attaching them to the human chromosome (528, 529). EBNA1 is the only viral protein able to associate with the human chromosome (530), which it does via a cellular binding partner EBP2 (EBNA1-binding protein) (531-533). Note that EBNA1contains an AT-hook domain which might allow for EBP2 independent binding (534).

Deletion studies have revealed that genome maintenance is the key essential function of EBNA1 (535). EBNA1 deleted virus can only transform resting B cells if the entire viral genome integrates into the human chromosome. Other functions of EBNA1 involve acting as a transcriptional enhancer or repressor. By binding oriP, EBNA1 can enhance the C and LMP1 promoters (520, 536). Similarly by interacting with the EBNA1 binding site in the *Bam*HI-Q region of the genome EBNA1 can negatively regulate its own expression during Latency I (518, 519, 537, 538). EBNA1 is also capable of binding to and affecting the promoters of many cellular genes; the nature of genes affected appears to be tissue specific (539, 540). Furthermore EBNA1 appears to have a mechanism for avoiding immune detection by CD8+ T cells. This is mediated by a glycine-alanine repeat in its N-terminus which can (a) negatively regulate the efficiency of EBNA1 translation and (b) interfere with EBNA1 degradation by cellular proteosomes (541, 542). Both activities would reduce the amount of EBNA1 derived epitopes available for antigen presentation. Finally EBNA1 might inhibit apoptosis and promote G1-S cell cycle progression (500, 543) by sequestering HAUSP/USP7 (501), a deubiquitylating enzyme involved in protecting p53 from MDM2-mediated degradation.

1.14.2 EBNA2

The EBNA2 gene is located in the *Bam*HI-Y region of the genome and encodes a 487 amino acid protein with an 84kDa molecular weight. (544, 545). It is a viral transcriptional activator protein which acts on a number of viral and cellular promoters (499). Its importance in transformation was demonstrated through reconstitution experiments on an EBNA2 deleted virus (P3HR-1) lacking immortalizing properties (544-546). Indeed the differences in transforming efficiencies observed between EBV type 1 vs. type 2 virus (547) are attributed to changes in their EBNA2 genes; these changes predominantly map to the EBNA2 C-terminus (548, 549).

EBNA2 contains three regions crucial to transformation and immortalization: domains either side of an N-terminal proline repeat motif which facilitate homodimer formation and transcription factor recruitment (550, 551); an acidic 14 amino acid C-terminal region which functions as a trans-activation domain (552); an RBP-Jκ interaction domain which facilitates DNA contact (553-555). Other functionally important regions include the Arg-Gly repeat and C-terminal Lys-Arg-ProArg motifs which both serve as nuclear localization signals (NLS) (556) as well as the large central region which mediates self-association (557). In essence EBNA2 contains a number of features common to cellular transcription factors.

The transforming properties of EBNA2 are directly tied to its ability to potently activate transcription (552) of genes involved in proliferation. The RBP-Jκ interaction domain allows EBNA2 to bind DNA indirectly via the adaptor protein RBP-Jκ (553-555, 558, 559). RBP-Jκ is a ubiquitously expressed and highly conserved cellular DNA-binding protein (560, 561) and forms part of the Notch signalling pathway (562). In non-proliferating cells RBP-Jκ interferes with gene expression as part of a co-repressor complex (SMRT/N-CoR, CIR,

SKIP, Sin3A, SAP30 and HDAC1) (563). In proliferating cells, activated Notch receptor binds RBP-Jκ and displaces the co-repressor complex (564, 565), enabling RBPJ-κ to participate in gene activation (566, 567). The RBP-Jκ interaction domain allows EBNA2 to interact with RBP-Jκ in a similar way to Notch (568, 569), essentially making EBNA2 a functional equivalent to a constitutively active Notch receptor. This is further evidenced by the observation that activated Notch can transiently substitute for EBNA2 in driving proliferation (570).

The C-terminal activation domain of EBNA2 is functionally equivalent to herpes simplex antigen VP16 (556, 571) and allows for similar interactions with cellular transcription factors such as TFIIB, TFIIH, TFIIE and p100 (572-574). EBNA2 also interacts with transcriptional co-activators p300, CBP and PCAF (575) as well as hSNF5/INI1 (576), suggesting the mechanism underlying EBNA2 function involves both histone acetyltransferase (HAT) activity and chromatin restructuring. Three viral (LMP1, LMP2A and C promoters) (577-579) and numerous cellular promoters (including CD21, CD23, CD25, C-FGR, c-myc) (499, 580) have EBNA2 response elements and are thus subject to its regulation.

An additional function of EBNA2, separate from its role in trans-activation, is to counter apoptosis via an interaction with nuclear protein Nur77 (581). Nur77 functions as a transcription factor in the nucleus but as a cytochrome c release signal in the cytoplasm (582, 583). EBNA2 prevents the latter function by retaining Nur77 in the nucleus (581).

1.14.3 EBNA3A/3B/3C

The EBNA3 proteins (EBNA3A, 3B and 3C) were originally discovered by western blotting using rheumatoid arthritis patient sera (584-588). They are encoded by three separate genes arranged in tandem within the *Bam*HI-E region of the genome. EBNA3A, 3B and 3C mRNAs are all processed from the same transcript, but may differentially accumulate due to alternate splicing of the primary transcript (316-318, 589).

EBNA3A, 3B and 3C proteins are highly stable proteins of 944, 937 and 992 amino acids in length, respectively, and are remarkably similar in amino acid sequence (590-593). EBNA3 proteins all have short hydrophilic N-termini, a region extensively conserved between all three EBNA3 proteins (homology domain), and C-termini rich in proline residues and repeat motifs. Thus it is unsurprising that they share a degree of functional homology. EBNA3 proteins can all sequester RBP-Jκ via specific binding sites in their homology domains (594-596). This suggests they function to negatively regulate the trans-activating functions of EBNA2. Indeed EBNA3A has been found to antagonize the expression of EBNA2 stimulated genes i.e. CD21, CD23 and c-myc (597). Similarly EBNA3C represses both the LMP1 and C promoters in an RBP-Jκ dependent manner (593, 598). There is also evidence that EBNA3A and EBNA3C can function as transcriptional activators (594, 599). EBNA3C might enhance LMP1 expression under certain conditions (594, 600, 601), while EBNA3A helps activate the Aryl hydrocarbon receptor (AhR), a transcription factor involved in cell proliferation (602, 603).

The ability of the EBNA3 proteins to act as transcriptional repressors and activators appears to be indispensible for growth transformation. EBNA3C deleted recombinant virus can not immortalize resting B cells and withdrawal of conditionally expressed EBNA3C from

proliferating blasts results in growth arrest (351, 604). EBNA3A is not essential as previously thought but does appear to provide important functions in cell growth and survival (351, 353, 605).

One way by which EBNA3 proteins maintain the proliferating phenotype is through interference with cell cycle checkpoints. EBNA3A and 3C can both down regulate members of the anti-proliferative INK4 family such as p16 (353, 604) thus favouring cell cycle progression. Additionally all three EBNA3 proteins are each capable of bypassing the G2/M checkpoint, possibly by inactivating the checkpoint kinase chk2 (606). Finally EBNA3C can antagonize the formation of pRb-E2F1 complexes thus freeing transcription factor E2F1 (607, 608), as well as stabilize c-myc to ensure continued expression c-myc stimulated genes (609).

EBNA3 proteins have also been shown to modulate the levels of proteins involved in cell death. EBNA3B can cause the up regulation of anti-apoptotic protein bcl-2 when expressed in the EBV negative BL line DG75 (610). Likewise EBNA3A and EBNA3C cooperate in the epigenetic silencing and CpG methylation of pro-apoptotic protein Bim (514). This may prove a novel means by which EBV infection can influence cellular gene expression even after their viral expression is silenced (as would be the case *in vivo*).

EBNA3 may additionally function to modulate the host immune response *in vivo*. Recently it was demonstrated by array analysis that EBNA3C regulates as many as 169 genes, many of which were involved in migration, adhesion and chemotaxis (611). In particular CXCL10 and CXCL11 were shown to be down regulated. Both function to attract CXCR3 expressing cells i.e. NK and T lymphocytes to sights of inflammation; the migration of CXCR3 expressing cells was revealed to be impaired in a number of EBNA3C expressing B cell lines (611).

Remarkably a recent report suggests that up to 1000 cellular genes may be regulated by one or more of the EBNA3 proteins (612).

1.14.4 EBNA-LP

EBNA-LP is expressed together with EBNA2 early post-infection (8-12 hours) and predominantly serves as a co-activator for EBNA2 mediated trans-activation (499). The N-terminus component is located in the W repeat region with each repeat containing two exons (W1W2) which together encode a 66 amino acid sequence. The C-terminus consists of a single stretch of 45 unique amino acids derived from two exons (Y1Y2) in the long unique region of the genome (316, 317, 613, 614). EBNA-LP size is affected by a number of factors (615). Each W repeat contains a functional W promoter capable of initiating EBNA-LP; thus W promoter initiated EBNA-LP varies in size according to the number of W repeats in the viral genome and the specific W promoter used to initiate transcription (319, 499, 616). In addition to this both C and W promoter initiated EBNA-LP are subject to alternate splicing which involves the differential skipping of the W1W2 exons (499, 617).

Evolutionarily conserved regions in the repeat region appear to be necessary for EBNALP mediated co-activation; consequently there is a link between EBNA-LP size and function (618, 619). EBNALP activity is regulated by phosphorylation (620) with serine 35 in the W2 exon being especially important. Serine to alanine substitutions resulted in a reduced induction of EBNA2 trans-activated LMP1 in an Akata cell line model (620). EBNA-LP trans-activating functions are important in the formation of an LCL, since a mutant virus lacking the two C-terminal exons is severely impaired for immortalization (352, 545).

EBNA-LP also appears to be involved in cell cycle regulation. This is suggested by the observation that EBNA-LP phosphorylation is cell cycle dependent (621). EBNA-LP and EBNA2 can cooperate in promoting cell cycle progression by inducing cyclin D2 (622). EBNA-LP also forms stable complexes with p53 and MDM2 which appears to result in the functional inactivation of p53 (623, 624). The inability of p53 to induce p21, a CDK inhibitor, may contribute to cell cycle progression.

As mentioned in section 1.13.3, a truncated form of EBNA-LP (t-EBNA-LP) is produced in Wp-restricted Burkitt lymphoma (Wp-BL); specifically, t-EBNALP lacks the terminal Y1Y2 exons. EBNA-LP can not function as a co-activator in these tumour cells due to an EBNA2 deletion in the active viral genome (512, 625). The role of t-EBNA-LP in Wp-BL may be to antagonize caspase-mediated apoptosis by inactivating protein phosphatise 2A (PP2A) thus acting as a pro-survival factor (512).

1.14.5 LMP1 and LMP2

LMP1 and LMP2 are integral membrane proteins encoded in the *Bam*HI-N region of the genome, adjacent to the terminal repeats. LMP1 is transcribed from three promoters: an EBNA2 activated latency III promoter (626), a STAT regulated latency II promoter (627) and a designated late lytic promoter encoding truncated LMP1 (628). LMP1 consists of three functional domains: a cytoplasmic N terminus which anchors LMP1 to the plasma membrane (629, 630), a trans-membrane region which mediates self-aggregation (631-633) and a cytoplasmic C-terminus which engages in cell signalling via three activation domains termed CTAR1-3 (634, 635). CTAR1 is responsible for initiating cell proliferation while CTAR2 is necessary for immortalization.

LMP1 is essential to *in vitro* transformation of B cells (350, 636) and is sufficient to mediate a range of tumour-associated cellular changes (637-641). The LMP1 C-terminus essentially mimics a constitutively active tumour necrosis factor receptor capable of providing CD40 signalling in B cells (381, 382) and as such engages the NFκB, AP-1, JAK/STAT and PI-PLC-PKC pathways (642, 643). LMP1 can promote cell cycle progression (644) via an NFκB dependent up-regulation of cyclin-D1 (645) and an AP-1 dependent inhibition of INK4 family member p16 (646). It can also promote immortalization by regulating human telomerase reverse transcriptase (hTERT) in an NFκB, AP-1 and c-myc dependent manner (647-650). LMP1 can protect against apoptosis by increasing levels of Survivin, an inhibitor of apoptosis protein (IAP), in an NFκB, AP-1 and c-myc dependent manner (651-653). A broader range of LMP1 functions is reviewed by Dawson *et al* (652).

The LMP2 gene encodes two products, LMP2A and LMP2B, neither of which are essential to transformation (654-662). The role of LMP2A in EBV associated malignancies has been studied using LCL and transgenic mice models (383, 659, 660, 663-667). The N-terminal domain of LMP2A was found to engage in BCR associated signalling pathways (668) and has previously been shown to promote the survival of BCR negative mouse and human B cells (383, 669, 670). The survival phenotype is in part mediated by NF-κB dependent increases in Survivin (671, 672) and Bcl-2, as well as NF-κB or Ras dependent increases in Bcl-XL (669, 673, 674). An additional function of LMP2A appears to be maintenance of viral latency in the presence of reactivation stimuli i.e. CD19 cross-linking. LMP2A mediates these effects by engaging with src family tyrosine kinases (663, 664). The functions of LMP2B have not been fully elucidated. It cannot engage in BCR signalling as it lacks the N-terminal domain of LMP2A (654, 656, 657, 661). Two possible roles for LMP2B may be to negatively regulate LMP2A activity (675-677), and to promote turnover of interferon receptors (678).

1.14.6 BHRF1 and BALF1

The intrinsic or mitochondrial apoptosis pathway is controlled by a number of pro- and anti-apoptotic Bcl-2 family members (see Fig. 1.4) (188). EBV encodes two Bcl-2 homologs termed BHRF1 and BALF1. While predominantly productive cycle antigens (267, 679), both have been identified as latency associated in LCL and tumour cell lines (320, 680). BHRF1 is the main viral Bcl-2 homolog and is considered an important contributor to the survival advantage of Wp-BL over latency I BL (320, 681). Despite similarities to Bcl-2, BHRF1 does not appear to associate with Bax or Bak (682, 683). BHRF1 has however been shown to protect from apoptosis by sequestering the pro-apoptotic protein Bim (684). Much less is known about the function of BALF1. Viral transformation can take place in the presence of individual BHRF1 or BALF1 deletions but not if both are deleted (513, 685, 686), suggesting a degree of redundancy between both proteins. Nonetheless studies on the roles of BALF1 in cell survival were conflicting (680, 687, 688). A recent study has however demonstrated the ability of BALF1 to promote tumour formation in nude mice as well as protect from apoptosis in culture (432).

1.14.7 EBERS

EBER1 and EBER2 are highly conserved small non-polyadenylated RNA species encoded in the *Bam*HI-C region of the EBV genome (267, 689, 690). They are 167 and 172 nucleotides long respectively and are separated by 161 base pairs. EBER RNAs are transcribed from separate promoters containing both polymerase II and III associated elements (691). EBER1 and EBER2 share 54% sequence homology and even greater similarities in secondary

structures, which is characterized by extensive base-pairing and stem-loop formation (692, 693).

EBERS are predominantly nuclear (694-696) though conflicting literature suggests they also locate to the cytoplasm (697-699). EBERS are expressed across a wide range of EBV-associated malignancies (700-703) and often constitute the most abundant transcripts (704). They appear to be latency associated as their expression is diminished during productive infection (705). Other factors influencing EBER expression are EBV load (704), cell background (706) and differential turnover; EBER1 is more stable than EBER2 thus accumulates to 10-fold higher steady state levels (707, 708).

EBERS are believed to modulate cell immunity and apoptosis. They can hold the double stranded RNA (dsRNA) regulated protein kinase (PKR) in an inactive state (709, 710) as well as up-regulate anti-apoptotic protein Bcl-2 (504). Both these actions counteract an antiviral INF-α signalling cascade which would ultimately result in cell death. Gene expression studies using a range of EBV loss BL, EBV negative BL and epithelial cell lines confirm a protection from IFN-α mediated apoptosis in the presence of EBERS (500, 505, 507, 508).

EBERS have also been implicated in stimulating cell growth. When expressed in EBV loss or EBV negative BL they confer both an ability to grow in soft agar as well as form tumours in SCID mice (504, 506, 508). These effects may be mediated by IL-10 which is produced in response to EBER interactions with RIG-I (711). RIG-I is another dsRNA responsive protein which forms an upstream component of the same IFN-α signalling cascade involving PKR. The presence of IL-10 correlates with EBER positivity in BL cells and both can stimulate cell growth (712). Different growth promoting cytokines are stimulated in different cell types i.e. IL-9 in T cell lines or IGF-I in NPC and GC (713-715).

Finally there have been reports that EBERS support growth transformation (716). Specifically EBER2 appears to mediate this effect in an IL-6 dependent manner. The literature concerning EBER function remains conflicting and contains a number of inconsistencies. For instance there is evidence to suggest that EBER mediated cell survival in BL may PKR independent (717). The involvement Bcl-2 is also questionable as it is not expressed in most BL (718).

1.14.8 BARTS

BART transcripts are encoded within the *Bam*HI-A region of the genome. Originally discovered in a nude mouse NPC line (719, 720), they are known to be expressed in all forms of EBV infection both *in vitro* and *in vivo* (719-726). BARTS are a diverse group of heavily spliced RNA species (4kb to 8kb in size), with a common 3′ sequence and poly-A signal (719, 720, 727, 728). They are predominantly generated from promoter P1 but may be generated by P2. P1 and P2 are regulated by different cellular factors and respond differently to alternate cell backgrounds (729). They are dispensable for transformation; indeed most of the BART region is deleted in the transforming B95-8 prototype strain (267).

BART transcripts give rise to a number of open reading frames (BARF0, RK-BARF0, A73 and RPMS1) which can be translated *in vitro* (721, 727, 728, 730-734). A number of studies using artificially translated proteins have revealed regulatory roles for RPMS1 and RK-BARF0 in stimulating and antagonizing Notch signalling respectively (724, 730, 731). A73 on the other hand binds the RACK1 adaptor protein with unknown consequences (731, 735). The relevance of these interactions is questionable as there is little evidence to suggest the BART proteins are natural expressed in latently infected cells (721, 735-737). More recently

the BART transcripts have been shown to encode a large number of miRNAs (BART miRNAs) (250, 738-741) as well as a small nucleolar RNA (v-snoRNA1) (742), both of which could be important in the virus life cycle.

1.14.9 MicroRNAs

EBV encodes at least 40 miRNAs; three are generated from the UTRs either side of the BHRF1 ORF (miR-BHRF1s), while the rest locate to the intronic regions of the BART transcripts (miR-BARTs) (250, 738-741). All three BHRF1 miRNAs are generated during the growth transforming program, likely from the C and W promoters (250, 738, 743-745). During productive infection, two of three BHRF1 miRNAs (miR-BHRF1-2 and miRBHRF1-3) are expressed from the BHRF1 promoter (BHRF1p) (744, 746, 747); miRBHRF1-1 overlaps the BHRF1p and thus is not included in the transcript. BART miRNAs are expressed from the BART promoters in all forms of EBV infection, although steady state levels are especially high in EBV positive NPC tumours and epithelial cell lines (250, 738, 739, 741, 743, 745, 748, 749).

EBV miRNAs are highly conserved among EBV strains and therefore probably mediate important functions in the viral life cycle (738). BHRF1 miRNAs are believed to assist in transformation, cell cycle progression and in resisting apoptosis throughout early EBV infection (750, 751). However neither deleting the BHRF1 miRNAs nor most of the BART miRNAs can prevent LCL formation (267, 750, 751). Cellular BHRF1 miRNA targets may include tumour suppressor p53 (miR-BHRF1-1) and T cell attracting chemokine CXCL11 (miR-BHRF1-3) (752, 753). Cellular BART miRNA targets may include Dicer (miR-BART6-5p) and MICB (miR-BART2-5p), which function in miRNA processing and NK cell

immunity respectively, TOMM22 (miR-BART16) and IPO7 (miR-BART3), which function in protein transport across the mitochondrial and nuclear membrane, respectively, as well as the pro-apoptotic Bcl-2 family members PUMA (miR-BART5) and Bim (miR-BART 1, 3, 9, 11 and 12) (754-758). Viral BART miRNA targets may include BALF5 (miR-BART2), LMP1 (miR-BART 1-5p, 16-5p and 17-5p; miR-BART9) and LMP2A (miR-BART22) (759-762). Thus EBV miRNAs appear to have roles in apoptosis, proliferation, immune evasion and viral gene expression.

The contributions of the EBV miRNAs towards oncogenesis and the viral life cycle remain largely unknown. For instance there are currently no confirmed target genes for the majority of EBV miRNAs. Furthermore it is very likely that individual EBV miRNAs possess more than just one target (754, 755, 759, 760, 763, 764). Finally the literature concerning predicted or validated EBV miRNA targets is conflicting. Different groups can not necessarily validate the same targets (755, 760, 763); likewise there is little overlap between published targetomes (758, 763-765).

1.15 Aims and objectives

We wanted to perform our own investigation into the function of EBV encoded miRNAs, in order to better understand how they contribute towards oncogenesis and the viral life cycle. To do this we first needed a good understanding of when and under what circumstances EBV miRNAs are expressed. Studies released prior to the present work largely relied on Northern blotting, arrays or cloning for detection (250, 738, 744, 745, 748, 749). Unfortunately such methods require large amounts of RNA, have limited sensitivity and only provide qualitative data. Thus the first goal of this thesis was to quantitatively assess viral miRNA expression in

different types of EBV infection. The second goal of this thesis was to establish if and how EBV miRNAs contribute to the oncogenesis of Burkitt lymphoma.

In results chapter I there are three aims. Firstly we will validate a commercial quantitative PCR (QPCR) system for the detection and quantification of EBV miRNAs. Secondly we will use these QPCR assays to characterize EBV miRNA expression in a range of different latently infected BL cell lines and LCLs. Thirdly we will investigate a number of factors determining EBV miRNA steady state levels, such as differential turnover rates and levels of BHRF1 and BART gene transcription.

In results chapter II we continued our study on viral miRNA expression by focusing on two further types of EBV infection. Our first aim was to investigate viral miRNA expression during the early events of EBV mediated B cell transformation. Thus we infected resting B lymphocytes *de novo* with a strain of virus (2089) similar to the B95-8 prototype. Our second aim was to focus on viral miRNA expression following the induction of EBV replication. This was investigated using the AKBM cell system in which EBV-positive Akata-BL cells are stably transfected with a GFP reporter gene under the control of the EBV lytic cycle BMRF1 promoter; these cells enter lytic cycle following Ig cross linking and can be identified by GFP expression.

In results chapter III we had two broad aims. Our first aim was to establish a methodology with which we could study the functions of the BHRF1 miRNAs. In order to achieve our first aim we undertook two complementary approaches. In the first we attempted to knock down the BHRF1 miRNAs in Wp BL lines using antisense oligonucleotide inhibitors. In the second we attempted to express the BHRF1 miRNAs in a panel of EBV negative and Lat I BL lines using a lentivirus. Our second aim was to perform three different investigations into the

function of the BHRF1 miRNAs. First we assessed the effects of the BHRF1 miRNAs on the transcriptome of a BL cell line using array analysis. Secondly we investigated the effects of the BHRF1 miRNAs on cell growth. Thirdly we determined the effects of the BHRF1 miRNAs on cell death by (a) measuring cell viability in the presence of apoptosis inducing drugs and (b) using western blot to look for changes in the protein levels of individual Bcl-2 family members.

2. Materials and Methods

2.1 Cell culture

2.1.1 Lymphoid and epithelial cell lines

Most cell lines used in this study were derived from BL tumour cells. EBV-positive BL lines included Latency I Dante-BL, Sav-BL, Ezema-BL, Akata-BL, Kem-BL, Chep-BL and MutuI-BL cl.59 (291, 766); the group III BL lines MutuIII-BL and GlorIII-BL which have drifted in culture to a Latency III form of infection; the Wp-restricted BL lines Oku-BL, Sal-BL and Ava-BL (625); and Latency I and Wp-restricted sublines derived from Awia-BL (767). EBV-negative BL lines include DG75, BL41, BL30, Ramos-BL and two EBV genome loss BL clones isolated by single cell seeding of MutuI-BL cl.59 and Akata-BL (kindly provided by Dr Gemma Kelly and Leah Fitzsimmons). BJAB is an EBV-negative B lymphoma cell line. Jurkat is an EBV negative T leukaemia cell line (768).

In addition a range of virus transformed LCLs were also used in this work. LCLs carrying natural EBV isolates included IM51.1, IM81.1, IM83.1 and IM93.1 and were established by spontaneous transformation of peripheral blood derived B cells from EBV-infected infectious mononucleosis patients (769), while EH LCL1 and EH LCL2 were generated by *in vitro* infection of EBV-naïve B cells with the recombinant 2089 EBV genome (770).

The following reference cell lines served as standards for quantifying EBV and/or human transcripts: X50/7 LCL (771), CD+Oku LCL (625), the spontaneously permissive Sal tr-LCL (containing 2% BZLF1 positive cells), the EBV-positive nasopharyngeal cell line C666-1 and the EBV-negative NK leukaemia cell line NKL (772). AKBM is a derivative of Akata-BL stably transfected with GFP reporter plasmid under the control of the early BMRF1 promoter

(773). Standard HEK293 cells were used in the production of infectious EBV while the 293FT cell line was used to package lentivirus stocks (Invitrogen).

2.1.2 Maintenance of lymphoid and epithelial cell lines

B cell lines and standard HEK293 cells were maintained in exponential growth in RPMI/10% selected foetal calf serum (FCS) (Biosera) supplemented with 2 mM L-glutamine (Life Technologies) and penicillin/streptomycin (Sigma). Oku-BL, Sal-BL, Ava-BL, and Awia-BL clones (k and m) were maintained in B cell medium supplemented with 1mM sodium pyruvate (Sigma), 50 mM alpha-thioglycerol (Sigma) and 20 nM bathocupronine disulfonic acid (Sigma). 293FT cells were maintained in B cell medium supplemented with heat inactivated FCS (56°C for 1 hour) and 200µg/ml G418 (Life Technologies) if required. Suspension cells were cultured in 25cm^2 flasks and adherent cells in 100mm plates; all cells were grown at standard incubator conditions (37°C, 5% CO2). Where indicated, RNA transcription was inhibited by the addition of 5µg/ml Actinomycin D (Sigma) to the cell culture medium and cells harvested for analysis at the indicated time points.

2.1.3 Cryopreservation and recovery of lymphoid and epithelial cell lines

Between five and ten million cells were taken at log phase (suspension cells) or 80%-90% confluence (adherent cells), spun down by centrifugation for 5 minutes at 450 x g and resuspended in ~0.75 ml RPMI/40% FCS supplemented with 2 mM L-glutamine (Life Technologies) and 10% dimethylsulphoxide (DMSO). Cells were transferred to a cryovial and placed in a freezing container surrounded by a propan-2-ol soaked sponge (Mr Frosty). The freezing container was stored overnight at -80°C to allow for a controlled cooling rate of -

1°C/minute. Cryovials were subsequently removed and transferred to the vapour stage of liquid nitrogen (-180°C) for long term storage.

Upon removal from liquid nitrogen, cells were thawed quickly at 37°C in a water bath and added drop wise to 15 ml of suitable pre-warmed media in order to minimize exposure to DMSO. Cells were spun down by centrifugation for 5 minutes at 1400 rpm using a Heraeus 8155 rotor, resuspended in 10 ml suitable media and transferred either to a 25cm^2 flask (suspension cells) or a 100mm plate (adherent cells).

2.2 Reactivation of EBV in AKBM cells and isolation of cells in lytic cycle

Viral reactivation in AKBM cells was induced by crosslinking surface immunoglobulin (Ig) with 100 µg/ml goat anti-human IgG antibody (Cappel) as described (773). Cells were transferred into fresh medium, plated out at 0.5 x 10^6 cells per ml in a 24 well plate and harvested at each indicated time point. To monitor induction of virus lytic cycle, an aliquot of cells was assayed by flow cytometry, either directly for GFP expression or after staining with the BZLF1-specific mAb BZ.1, as described (773). Where indicated, induced AKBM cultures were sorted into GFP-positive (lytic) and GFP-negative (latent) populations using a MoFlo cell sorter (Dako).

To monitor the changes in EBV viral load in induced AKBM cultures, genomic DNA was extracted using the GenElute Mammalian Genomic DNA kit (Sigma). EBV genome load was then determined by QPCR using primer/probe combinations to amplify EBV DNA polymerase (BALF5) and cellular beta 2-microglobulin sequences, as described (774). Where indicated, EBV genome replication was inhibited by the addition of 200 µg/ml acycloguanosine (Sigma) to the culture medium.

2.3 Primary infection of B Cells

2.3.1 Production of recombinant EBV (2089) from 293 cells

In preparation for the production of recombinant 2089 EBV (770), 293 producer cells carrying the 2089 BAC were split into each well of a 6 well plate and grown to 70% confluence. Cells were transfected with plasmids encoding the BALF4 and BZLF1 gene products (0.5 μg each per well) (770, 775) using Lipofectamine (Invitrogen) in Opti-MEM® reduced serum media (Invitrogen) according to manufacturer's instructions. Cells were then placed in a 37°C incubator for 3 hours, topped up with an additional 1 ml of B cell medium per well, and returned to the incubator for a further 72 hours. Virus containing supernatant was subsequently harvested, debris removed by centrifugation for 5 minutes at 2000 rpm using a Heraeus 8155 rotor and the supernatant subjected to filter sterilization using a 0.45 μm filter. Aliquots of supernatant were frozen at -80°C until required.

2.3.2 Quantifying recombinant EBV (2089) titre

Virus titre quantification was determined using Q-PCR. Briefly, virus containing supernatant was mixed with an equal volume of lysis buffer (10mM Tris-HCL pH 8.8, 1.5mM $MgCl_2$, 50mM KCl:, 100mg/ml proteinase K (Roche) and 0.1% v/v Triton X-100) and incubated for 1 hour at 55°C followed by 10 minutes at 99°C. Real time PCR amplification of the BALF5 gene was performed as in section 2.2, using 5 μl supernatant as input.

2.3.3 Isolation of human primary B cells from whole blood

Lymphocyte enriched buffy coats (NHS Blood and Transplant, Birmingham) were mixed 1:1 with PBS and gently layered over 15ml warmed Lymphoprep solution (Axis Shield) in a 50 ml tube. Tubes were spun for 30 minutes at 1800 rpm using a Heraeus 8155 rotor (without brake to avoid disturbing the interface). Note that peripheral blood mononuclear cells (PBMCs) form a layer at the interface between the upper plasma and lower Lymphoprep solution. PBMCs were isolated and washed three times in 50 ml PBS for 10 minutes at 1600 rpm, 1200 rpm and 1000 rpm, respectively, using a Heraeus 8155 rotor and then resuspended in cold RPMI/1% FCS. A total B cell estimate was made using the assumption that the B cell population accounts for 5% of total PBMCs. B cells were subsequently isolated from PBMCs using magnetic CD19 pan B Dynabeads® and CD19 pan B DETACHaBEAD® (Invitrogen) according to manufacturer's instructions. B cells were used immediately for *in vitro* infection experiments described below.

2.3.4 Infection of human B cells with recombinant EBV (2089)

Primary B cells were exposed to preparations of recombinant 2089 EBV at a multiplicity of infection (moi) of 100 using published methods (326). Briefly, isolated B cells were centrifuged for 5 minutes at 328 x g and resuspended in virus supernatant at the correct moi. After incubating the B cells and virus supernatant together for 2 hours at 37°C, the virus supernatant was removed via centrifugation at 5 minutes at 1200 rpm using a Heraeus 8155 rotor. The infected B cells were resuspended at 2 x 10^6 cells/ml in fresh B cell medium, seeded in a 24 well plate and harvested at the indicated time points.

2.4 Quantitative RT-PCR analysis of viral and cellular transcripts

2.4.1 RNA extraction

RNA samples used for RT-PCR analysis of viral and cellular transcripts were prepared as follows. Approximately 1-3 x 10^6 cells were harvested and washed once in PBS. Total RNA was subsequently prepared using the Nucleospin RNA Isolation kit (Machery-Nagel) according to manufacturer's instructions. All RNA samples were eluted in 50-60 µl of nuclease free water (Ambion), quantified using a Nanodrop spectrophotometer (Thermo Scientific) and where possible diluted to 100 ng/µl. RNA samples were either used directly or stored at -80°C.

Since the majority of QPCR primer/probe combinations used in this study were designed to span across exon-exon splice junctions, residual contaminating DNA was unlikely to yield a false positive signal. However for assays which amplified within a single exon, an additional DNAse I treatment was performed on a 1µg aliquot of RNA using DNA-free™ (Ambion) according to manufacturer's instructions.

2.4.2 Reverse transcription

For the detection of EBV transcripts, RNA was reverse transcribed using a mixture of previously described gene-specific cDNA primers (320, 769) or new cDNA primers described later (section 2.4.3). Five hundred nanogram total RNA was denatured at 90°C for 5 minutes and added to a reaction mix containing 5u AMV-RT (Roche), 1 x AMV reverse transcriptase reaction buffer, 1 µM each cDNA primer, 200 µM each of dATP, dTTP, dCTP and dGTP (Roche) and nuclease free water in a total volume of 20 µl. The reaction incubated for 1 hour at 42°C and then 5 minutes at 90°C.

For the detection of cellular transcripts, 500 ng total RNA was reverse transcribed using the qScriptTM cDNA supermix (Quanta Biosciences), according to manufacturer's instructions. The reaction mix was incubated as above, albeit with an initial 5 minutes incubation at room temperature (RT) to allow for optimal primer annealing. After completion of the cDNA reaction, all reaction mixes were made up to 100 µl with nuclease free water and stored at -20°C.

2.4.3 QPCR

Relative levels of Qp-, Cp- and Wp-initiated transcripts, BARTs (exon 6-7 splice junction), lytic and latent BHRF1 transcripts and immediate early BZLF1 transcripts were determined by QPCR using published primers and Taqman probes (320, 769). In addition, three new assays were designed to detect novel viral transcripts. The first assay detected both latent and lytic BHRF1 transcripts using the following primers and probe: cDNA primer 5'-TCTTGCTGCTAGCT-3', forward primer 5'-CCCTCTTAATTACATTTGTGCCAGAT-3', reverse primer 5'-TCCCGTATACACAGGGCTAACAGT-3', probe 5'-Fam TAGAGCAAGATGGCCTATTCAACAAGGGAGA Tamra-3'. Two further assays were also designed to detect alternatively spliced BART transcripts, either by amplifying across the exon 2-3 splice junction in conventional BART mRNAs (BART 2-3) or across the exon 1-3 splice junction in the variant lacking exon 2 (BART 1-3). These assays used the following primers and probes: common cDNA primer 5'-TCTAAAGTCATACGCCC-3' (exon 3), BART 2-3 forward primer 5'-TCCACTTTGTGTTACAGGTCCG-3' (exon 2-3 junction), BART 1-3 forward primer 5'-CTCTTCATGTGAGGTCCGGC-3' (exon 1-3 junction),

common reverse primer 5'-TGTGTCCGGTAAACGCCATA-3' (exon 3) and BART probe 5'-Fam CCACGGAGACTCGGACGTAGCCCTT Tamra-3' (exon 3).

Relative levels of cellular transcripts (MYC, Drosha, Dicer, ADAM18, DSCR8, ASZ1, HSPA4L, GRM5, CELF2, CRYBG3, FCRL2, IQSEC2, ITGA5, MAN1B1, MIPEP, MMP14, OCA2 and TDRD7) were determined by QPCR using commercially available Taqman gene expression assays (Applied Biosystems); further details are shown in Table 2.1.

Relative quantification of gene expression was performed using an Applied Biosystems 7500 Sequence Detection System using the following conditions: 95°C for 10 minutes, followed by 40 cycles of 95°C for 15 seconds and 60°C for 60 seconds. Each PCR run included duplicate test cDNA samples and serial cDNA dilutions prepared from a suitable reference line (Akata-BL, Qp; X50/7, Wp; CD+Oku LCL, Cp and latent BHRF1; Sal tr-LCL, BZLF1 and lytic BHRF1; C666.1, BARTs) which were used to construct relative standard curves. EBV gene expression data was normalised either to cellular glyceraldehyde-3-phosphate dehydrogenase (GAPDH) or phosphoglycerate kinase (PGK) expression, both quantified using commercially available assays (Applied Biosystems). Normalised data were expressed relative to the appropriate reference line which was assigned an arbitrary value of one. Note that in the case of lytic transcripts, the data were further adjusted such that the final values were expressed relative to a culture containing 100% BZLF1-positive cells.

2.5 Quantitative PCR analysis of EBV miRNAs

All EBV miRNA sequences were obtained from the Sanger miRNA database version 12 (http://microRNA.sanger.ac.uk/) (22). Real time PCR assays to quantify EBV miRNAs were based on the stem-loop RT primer method described by Chen et al. (776). Stem-loop RT

Human Transcripts		EBV miRNAs	
GENE	Assay ID	GENE	Assay ID
ADAM18	Hs00907027_m1	ebv-miR-bhrf1-1	007757
ASZ1	Hs00369973_m1	ebv-miR-bhrf1-2	197239_mat
CELF2	Hs00272516_m1	ebv-miR-bhrf1-3	197221_mat
CRYBG3	Hs00400616_m1	ebv-miR-BART3	004578_mat
DSCR8	Hs00741223_m1	ebv-miR-BART4	005623
FCRL2	Hs00229156_m1	ebv-miR-BART1-3P	464048_mat
GRM5	Hs00168275_m1	ebv-miR-BART15	005699
HSPA4L	Hs00204675_m1		
IQSEC2	Hs00390333_m1		
ITGA5	Hs01547673_m1		
MAN1B1	Hs00359915_m1		
MIPEP	Hs00969246_m1		
MMP14	Hs01037009_g1		
OCA2	Hs01562046_m1		
TDRD7	Hs00380424_m1		
DICER1	Hs00229023_m1		
RNASEN	Hs00203008_m1		
MYC	Hs00153408_m1		
Hu GAPDH	NM_002046.3		
Hu PGK1	NM_000291.2		
Hu β2M	NM_004048.2		
RNU48	001006		

Table 2.1. Commercially available TaqMan (Applied Biosystems) assays used for measuring human transcripts and EBV miRNAs

primers and primer/probe combinations for each target miRNA were either designed using the Custom Taqman Small RNA Assay service (miR-BART5, miR-BART7, miR-BART22, miR-BART13, miR-BART2-5p) or obtained commercially (miR-BHRF1-1, miR-BHRF1-2, miR-BHRF1-3, miR-BART3, miR-BART4, miR-BART1-3p, miR-BART15) (Applied Biosystems); further details are shown in Table 2.1.

For miRNA analysis, RNA was prepared using the mirVana miRNA Isolation Kit (Applied Biosystems) according to the manufacturer's instructions. Input RNA (10 ng) was reverse transcribed in a 20 µl reaction volume containing up to 7 RT stem-loop primers using the TaqMan MicroRNA Reverse Transcription Kit (Applied Biosystems).

QPCR reactions (20 µl) were performed using an Applied Biosystems 7500 Sequence Detection System. In each PCR, duplicate aliquots of each test cDNA were run alongside serial cDNA dilutions prepared from a suitable reference line (X50/7, miR-BHRF1 miRNAs; C666.1, miR-BART miRNAs) which were used initially to construct relative calibration curves.

To convert from relative to absolute quantitation, target miRNAs were obtained as synthetic oligonucleotides (Eurogentec), pooled and reverse transcribed as above. Aliquots of cDNA corresponding to 10^8 to 10^2 miRNA copies were then subjected to PCR amplification and the data used to generate calibration curves from which the absolute number of EBV miRNA molecules in reference X50-7 and C666.1 cells could be determined. Expression data was normalised to RNU48 as a loading control (Applied Biosystems).

2.6 Western blotting

2.6.1 Protein quantification

Approximately 5-10 x106 cells were spun down and washed twice in phosphate buffered saline (PBS). Pellets were maintained on ice, lysed in 50 µl 9M Urea buffer (9M Urea, 5mM EDTA, 5mM EGTA, 1% DTT, 2-4% CHAPS) and sonicated for 15- 20 seconds. Aliquots of lysates were diluted 5-fold with Urea buffer, vortexed, and 5 µl was loaded, in duplicate, onto a 96 well plate. BSA standards of 5, 2, 1, 0.5, 0.2 and 0.1 mg/ml were also vortexed and loaded in duplicate.

Total protein concentrations were determined using BioRad DC protein assay reagents A and B added in a 1:4 ratio, as per manufacturer's instructions. The reaction plate was incubated for 15 minutes at room temperature and the resulting colour change analysed using a 96 well plate reader set at 630nm wavelength. The protein concentration was then determined using line of best fit generated from the standards. All protein samples were subsequently diluted to 2mg/ml in Gel Sample Buffer (0.4M sodium 2-mercaptoethanesulfonate (MESNA), 125mM Tris-HCL pH 6.8, 20% v/v glycerol, 4% v/v SDS and 0.004% v/v bromophenol blue). Diluted samples were boiled for 10 minutes to denature protein and then stored at -20°C.

2.6.2 Protein electrophoresis and membrane transfer

Protein electrophoresis was performed using the Novex XCell SureLock mini cell system (Invitrogen) and NuPAGE 4-12% Bis-Tris gels (Invitrogen). The system was set up as per manufacturer's instructions with 1x NuPAGE MES SDS running buffer (Invitrogen) prepared in distilled water. Protein samples were defrosted and resolubilised for 5 minutes at 80°C.

Twenty µg of protein sample was loaded per well, with one well being used for 10 µl SeeBlue Plus2 Prestained standard (Invitrogen). Samples were electrophoresed at 100 V, 250 mA for 90 minutes. When the run had completed, the apparatus was disassembled and the Bis-Tris gel was placed into an XCell II blot module (Invitrogen) with a PVDF membrane pre-soaked in 100% methanol and then equilibrated with transfer buffer (0.192M Glycine (Sigma), 2.5mM Tris-Base (Fisher Chemicals), 20% Methanol). Protein transfer was performed as per manufacturer's instructions at 30 V for 100 minutes.

2.6.3 Membrane blocking, antibody binding and detection

After transfer, the PVDF membrane was removed from the blotting module and washed in PBS with 0.1% Tween-20 (PBS-T). The membrane was then blocked in 5% dried milk diluted with PBS-T for 1 hour with gentle agitation on a rocking platform. Primary antibodies were diluted in 5% dried milk and incubated with the membrane for 2 hours at room temperature or overnight at 4°C with gentle agitation. After antibody binding, the antibody was removed and the membrane was washed with seven times with PBS-T over a period of 20 minutes. The membrane was then incubated for 1 hour at room temperature with a specific secondary antibody conjugated to Horseradish Peroxidise (Sigma) diluted in 5% milk. After incubation with the secondary antibody, the membrane was washed as above; view Table 2.2 for a full list of primary and secondary antibodies.

Protein visualisation was carried out using an ECL western blotting kit (GE Healthcare) according to the manufacturer's instructions. Finally the membrane was placed inside a film cassette with a sheet of CL Xposure X-ray film (Thermo Scientific), exposed for between 30 seconds and 20 minutes, and then developed using a Kodak X OMAT 1000 film processor.

Protein	1° Antibody	Species	Working Dil.	2° Antibody	Working Dil.
Bak	N-20; Santa-Cruz	Goat	1/200	HRP donkey anti-goat (Sigma)	1/5000
Bax	N-20; Santa-Cruz	Rabbit	1/100	HRP goat anti-rabbit (Sigma)	1/2000
Bcl-2	C-2; Santa-Cruz	Mouse	1/200	HRP goat anti-mouse (Sigma)	1/1000
Bcl-6	D-8; Santa-Cruz	Mouse	1/200	HRP goat anti-mouse (Sigma)	1/1000
Bcl-XL	7B2.5; Santa-Cruz	Mouse	1/200	HRP goat anti-mouse (Sigma)	1/1000
Bid	BID #2002; Cell Signaling	Rabbit	1/500	HRP goat anti-rabbit (Sigma)	1/2000
Bim	Bim # 2819; Cell Signalling	Rabbit	1/500	HRP goat anti-rabbit (Sigma)	1/2000
Mcl-1	22; Santa-Cruz	Mouse	1/200	HRP goat anti-mouse (Sigma)	1/1000
Noxa	FL-54; Santa-Cruz	Rabbit	1/200	HRP goat anti-rabbit (Sigma)	1/2000
PUMA	D-20; Santa-Cruz	Goat	1/200	HRP donkey anti-goat (Sigma)	1/5000
BHRF1	5B11; In House	Mouse	1/50	HRP goat anti-mouse (Sigma)	1/1000
EBNA1	EBNA1; In House	Human	1/1000	AP-anti-human IgG (Biorad)	1/10000
EBNA2	PE2; (443)	Mouse	1/50	HRP goat anti-mouse (Sigma)	1/1000
LMP1	CS1-4; (558)	Mouse	1/50	HRP goat anti-mouse (Sigma)	1/1000
β-Actin	β-Actin; Sigma	Mouse	1/10000	HRP goat anti-mouse (Sigma)	1/1000
Calregulin	Calregulin; Santa-Cruz	Goat	1μg/ml	HRP donkey anti-goat (Sigma)	1/5000

Table 2.2. Antibodies used in western blotting

2.7 Sequencing of BHRF1 miRNAs

Genomic BHRF1 sequences spanning all three BHRF1 miRNAs were PCR amplified using the primers 5′-GGACTTGGGGTGATTTTCTATGT-3′ and 5′-CCCACACTCACCTCAGTTATTTC-3′ under the following conditions; 94°C for 5 mins, 35 cycles of 94°C for 60s, 56°C for 60s and 72°C for 2 mins, and a final extension of 72°C for 10 mins. The 1600bp product was then gel purified and sequenced using an automated Applied Biosystems 3730 (Functional Genomics and Proteomics Services, School of Biosciences, University of Birmingham).

BHRF1 miRNA sequences were aligned to the prototype B95-8 sequence (RefSeq NC_007605.1) using BioEdit sequence alignment editor (http://www.mbio.ncsu.edu/BioEdit/bioedit.html). The pre-miRNA secondary structure prediction through free energy minimisation was calculated using the software programs Mfold (http://mfold.rna.albany.edu/) (777) and RNAfold (http://rna.tbi.univie.ac.at/cgi-bin/RNAfold.cgi) (778, 779).

2.8 Construction of plasmid vectors

2.8.1 Preparation of cloning inserts

DNA oligonucleotide sequences representing individual BHRF1 miRNA binding sites were cloned into pMIR-REPORT^{TM} as described in section 5.2. Individual binding sites (see Fig. 5.1) were custom ordered as two separate single stranded sequences (Alta Bioscience Ltd). Annealing of the two single stranded sequences was achieved in a reaction mix containing 2

μg of each oligonucleotide and 1 x SuRE/Cut Buffer A (buffer) in a final reaction volume of 50 μl. The reaction mix was heated 90°C for 3 minutes in a heating block and subsequently left to cool slowly over several hours.

Lentiviral vectors for the stable expression of the BHRF1 miRNAs were cloned as described in section 5.4. Genomic BHRF1 sequences spanning miR-BHRF1-2 and miR-BHRF1-3 were PCR amplified using the primers 5′-AAAGGATCCTTTAACCAAACAGTGGTCGTGAG-3′ and 5′-AAAGAATTCTTAATTAATCCCAAAACCTACTACCCCATT-3′. Genomic BHRF1 sequences spanning miR-BHRF1-1 were PCR amplified using the primers 5′-AAAGGATCCCCATGAGCCCCGCCTTTA-3′ and 5′-AAAAGATCTGGCTAAACCTAATCCCCAACCTTT-3′. Both fragments were amplified under the following conditions; 94°C for 5 mins, 35 cycles of 94°C for 60s, 56°C for 60s and 72°C for 1 mins, and a final extension of 72°C for 10 mins.

2.8.2 Restriction digestion

PCR-amplified or vector-derived inserts and recipient plasmid vector DNA were digested with the appropriate restriction enzymes following the manufacturer's guidelines (standard enzymes from Promega and Roche, or Fast Digest enzymes from Fermentas). Typically 1μg plasmid DNA was digested in a 20 μl reaction volume with 1μl (10 units) restriction enzyme and 1 x concentration of the appropriate restriction enzyme buffer. Digests were performed at 37°C for 30-60 minutes (FD enzymes) or 3 hours (standard enzymes). After digestion, recipient plasmid vector DNA was treated twice with 1 unit Calf Alkaline Phophatase (Roche) for 30 minutes at 37°C to remove 5′ terminal phosphate groups; this prevents religation and circularization of vector DNA, unless the vector is ligated to a suitable DNA insert (digested

PCR product or released vector-derived insert) possessing 5′ phosphate groups. Note that when inserting annealed oligonucleotides lacking 5′ phosphate groups, vector capping was not performed on recipient plasmid vector DNA.

2.8.3 Agarose gel electrophoresis

Plasmid derived DNA insert fragments were separated and purified from their backbone vector fragments using agarose gel electrophoresis. Agarose gels were prepared using 0.8-1.0% agarose (Eurogentec) resuspended in 1x TBE (88.9mM Tris-Base, 2.49mM EDTA and 88.9mM Boric Acid in distilled water). Agarose suspensions were heated to 100°C until the slurry had fully dissolved and then poured into a casting chamber and allowed to set. Digested DNA products were mixed with 6x gel loading dye (0.25% w/v xylene cyanol, 0.25% w/v bromophenol blue, 30% v/v glycerol) and loaded into each well, with one well being used for loading a DNA size marker (1kb Plus DNA Ladder, Invitrogen). The samples were electrophoresed at 80-100 V for 1-2 hours in a horizontal Flowgen tank containing 1x TBE.

When the run was complete, the agarose gel was soaked for 20 minutes in a bath of distilled water containing 1-5 µl 10mg/ml ethidium bromide (Fisher Scientific) and the DNA visualised under UV light. The appropriately sized inserts were excised manually using a scalpel and subsequently recovered using the QIAquick Gel Extraction kit (Qiagen) as per manufacturer's instructions.

2.8.4 Purification of vector and insert DNA.

In some cases it was not necessary to isolate DNA fragments using gel electrophoresis but instead vector DNA, insert DNA or PCR products were simply purified using a High Pure PCR product purification kit (Roche) as per manufacturer's instructions.

In other cases, DNA products were extracted using organic solvents. Briefly, the sample was increased to a volume of 200µl with DEPC treated nuclease free water (Ambion), mixed with an equal volume of phenol: chloroform: isoamyl alcohol (25:24:1 pH8.0, Sigma) and then vortexed for 15 seconds. After centrifugation at 16000 x g for 2 minutes, the upper layer containing DNA was removed to a fresh tube. The DNA was precipitated by the addition of 2.5 volumes of 100% ethanol and 1/10 volumes of 3M Sodium Acetate pH 5.2 and stored at -20°C overnight. The next day, the sample was centrifuged at 16000 x g for 15 minutes at 4°C, the DNA pellet washed in cold 70% ethanol and allowed to dry at room temperature. In some cases, 0.5 µg glycogen (Roche) was added during the precipitation in order to help visualize the location of the DNA pellet. Finally the DNA pellet was resuspended in DEPC treated water and the DNA concentration was determined using a NanoDrop.

2.8.5 Ligation of inserts into recipient plasmid vectors

The quantity of vector and insert DNA used in each ligation reaction was determined using the following calculation: ((ng of vector × kb size of insert) / kb size of vector) x molar ratio of insert:vector = ng of insert. Ligation reactions were performed using the Rapid Ligation kit (Roche) in a 10 µl reaction volume containing the appropriate ratio of vector and insert fragments, 1 x ligation buffer and 1 unit T4 DNA ligase. The ligation mix was incubated for 2-3 hours at room temperature or overnight at 4°C. Note that annealed oligonucleotide

sequences and purified PCR amplification products were added to cut vector DNA at a 5 x molar surplus.

2.8.6 Bacterial transformation of plasmid DNA

Ligated DNA products were transformed into chemically competent E.coli using standard methods. For most purposes, DH5α cells were used as the host strain. However Stabl3 cells (Invitrogen) were used for cloning of lentivirus plasmids to reduce the frequency of unwanted homologous recombination events between the long terminal repeat regions.

Aliquots of chemically competent DH5α or Stabl3 cells were defrosted slowly on ice. Approximately 100 µl competent cells were subsequently added to each DNA sample, gently mixed and incubated on ice for 30 minutes. In all cases, a no DNA negative control was used and in the case of ligation reactions, an unligated vector sample was included to control for inefficient digestion and/or contamination of ligation reagents. Samples were then heat shocked at 42°C for 90 seconds and returned to ice for a further 2 minutes. Finally 1 ml of sterile LB (25g/L, Fisher Scientific) was added and cells incubated for a further 1 hour at 37°C on a shaker.

Before plating out, the cells were concentrated by centrifugation at 16000 x g for 60 seconds, the supernatant discarded and the cells resuspended in the residual LB liquid. The cells were then aseptically spread onto the surface of a 100mm LB agar plate containing 100 µg/ml ampicillin (Roche). Agar plates were incubated at 37°C overnight to allow the growth of transformants.

2.8.7 Growth of bacterial cultures

To screen for the presence of the desired recombinants, individual colonies were used to inoculate 3ml LB (containing 100 μg/ml ampicillin) and grown overnight at 37°C in a shaking incubator. Plasmid DNA was extracted from these small scale cultures using a QIAprep Spin Miniprep kit (Qiagen), according to the manufacturer's instructions. Recombinant plasmids were digested with suitable restriction enzymes and then screened by gel electrophoresis for the presence of the correct sized insert (see section 2.8.3). Where appropriate, plasmid constructs were confirmed by DNA sequencing using appropriate primers.

Large scale plasmid preparations were made by transforming the desired plasmid DNA constructs into DH5α or Stabl3 cells, inoculating single colonies into 400ml LB (containing 100 μg/ml ampicillin) and shaking the cultures at 37°C overnight. Plasmid DNA was extracted using a Qiagen Plasmid Maxi kit, as per manufacturer's instructions. The concentration of plasmid DNA was determined using a NanoDrop spectrophotometer.

2.9 Generation of BL lines stably transduced with lentiviral vectors

2.9.1 Preparation of lentivirus stocks

293FT virus producer cells were split 1:3 with fresh medium without G418 in 100mm plates (see section 2.1.2). The next day, the cells were monitored until they had reached a confluence of 70-90%. Subsequently the medium was replaced again with fresh medium lacking G418 and the cells transfected with 2μg envelope plasmid (pMD2G), 6μg packaging plasmid (psPax2) and 4μg of the appropriate lentiviral vector using Lipofectamine (Invitrogen) in Opti-MEM® reduced serum media (Gibco). Briefly, all three plasmids were added to 1.5 ml

Opti-MEM® while 26µl Lipofectamine was added to a separate aliquot of 1.5 ml Opti-MEM®. After 5 minutes incubation at room temperature, the two mixes were combined and left for a further 20 minutes. Subsequently the combined transfection mix was added to the 293FT cells and left overnight at 37°C, 5% CO2. Thereafter the 293FT cells were given a fresh change of 293FT medium without G418. At this point the cells will not have undergone any morphological changes.

After 48-72 hours the virus supernatant was harvested into a 50 ml tube and centrifuged for 5 minutes at 1200 rpm using a Heraeus 8155 rotor to remove cellular debris; note the presence of virus is indicated by the formation of numerous budding vesicles. The supernatant was subsequently filtered using a 0.45 µm filter and the virus stored at -80°C, or concentrated and used in downstream applications. Virus supernatant was concentrated at 19500 rpm for 2 hours at 16°C using a Beckman SW40 rotor. After removing most of the medium, the virus pellet was resuspended in ~1 ml residual liquid. Concentrated virus stocks were used immediately to infect target cells or stored overnight at 4°C.

2.9.2 Spin infection of BL lines with lentiviral vectors

Approximately 1 x 10^5 BL cells in 100 µl B cell medium was mixed with 1 ml of concentrated virus in a 1.5 ml microfuge tube and supplemented with polybrene (1 µl per ml). The virus:cell mix was incubated for 30 minutes at 37°C, transferred to a 15 ml tube and spun for 2 hours at 2200 rpm using a Heraeus 8155 rotor (28-30°C). At this point, most of the supernatant was removed and the cell pellet resuspended in the residual medium. The cells were subsequently mixed with 1 ml pre-warmed B cell medium and transferred to one well of a 48-well plate. The efficiency of lentivirus transduction was assessed by GFP expression at

one and two weeks post-transduction using an Accuri C6 flow cytometer (BD Biosciences). Transduced BL cells were sorted on the basis of GFP expression using a MoFlo cell sorter (Dako).

2.10 Electroporation of BL lines

One day prior to transfection, cultures were split 1:3 in fresh medium to ensure the cells were actively growing. Cells were washed once in PBS and resuspended in Opti-MEM® reduced serum media (Gibco) at 16-20 x 10^6 cells per ml. In parallel, electroporation cuvettes were prepared with appropriate amounts of DNA to be transfected. 0.5 ml of Opti-MEM®/cell mix was added to each cuvette (8-10 x 10^6 cells), and each sample was electroporated at 270V and 950μF using a BioRad Gene Pulser II Electroporation system. The contents of each cuvette were then quickly transferred to 7ml pre-warmed medium in one well of a 6 well plate and placed in an incubator at 37°C, 5% CO2.

All reporter and control plasmids (pMIR-REPORT™ Luciferase, pMIR-REPORT™ β-Gal and pRL SV40 Renilla) were used at 4 μg per transfection. FTGW and FTGW derived BHRF1 miRNA expression vectors were used at 16 μg per transfection. Anti-miRNA oligonucleotides were added, where indicated, at concentrations shown in Chapter 5.3; note that these concentrations were relative to the volume of cells in the cuvette, not the final volume in the 6 well plates.

2.11 Measuring the activity of reporter constructs

Firefly luciferase and *Renilla* luciferase activities were measured using the Dual-Luciferase® Reporter Assay System (Promega). Briefly transfected BL cells were harvested 24 hours post-transfection, washed twice in PBS and the cell pellets kept on ice. Cells were lysed by the addition of 1x passive lysis buffer, incubated on ice for 15 minutes and then centrifuged to remove cell debris.

Luciferase activities were measured using an ORION L Microplate Luminometer (Berthold Detection Systems) with a preset programme optimised for Dual Luciferase Assays. Replicate 20 µl aliquots of each lysate were transferred to a 96-well plate which was then loaded into the luminometer. Firefly luciferase activity was measured following the addition of 100 µl Luciferase Assay Reagent II (LAR II) to each sample. The Stop & Glo® reagent was then added in order to both quench the firefly luciferase reaction and initiate the measurements of *Renilla* luciferase activity.

In some experiments, pMIR-REPORT^{TM} β-Gal was used instead of pRL SV40 *Renilla* to normalise for transfection efficiency. In these cases, cells were lysed by the addition of 0.5 ml lysis solution (10 ml 1M Hepes pH 8, 2 ml 100mM $MgCl_2$, 0.5 ml 1M DTT and 2 ml Triton X-100 made to 100 ml using distilled water) and incubated for 15 minutes on ice. Firefly luciferase activity was determined using a Sirius single tube luminometer (Berthold Detection Systems). Briefly 100 µl luciferase assay reagent (LAR) was added manually to 100 µl of cell lysate, the sample placed inside the luminometer and the data collected for 10 seconds. To prepare LAR, 2.5 ml 1M glycylglycine, 5 ml 100mM $MgCl_2$, 20 µl 500mM EDTA, 50.8 mg DTT, 27.8 mg ATP and 21.3 mg co-enzyme A were diluted to 100 ml with distilled water; immediately prior to use, 250 µl luciferin stock was added to 5 ml LAR. In parallel, β-Gal

activity was measured on a separate aliquot of lysate using the Galacto-Light Plus™ System (Applied Biosystems) according to manufacturer's instructions. Following heat inactivation of the cell lysate at 50°C for 1 hour, a 20 µl aliquot was manually added to 200 µl β-gal substrate (Galacton-Plus substrate diluted 1:100 in reaction buffer diluent) and incubated for 1 hour at room temperature. β-gal activity was then measured for 1 second following addition of 300 µl Accelerator-II on a Sirius single tube luminometer.

2.12 Cell growth assays

Approximately 2 x 10^6 lentivirus transduced BL cells were plated out in a 24 well plate and either induced with 1µg/ml doxycycline (Sigma Aldrich) or left untreated. Cell viability was tested at 48 hours using Trypan blue. Briefly a 10µl aliquot of cells was mixed 1:1 with 0.4% trypan blue (Sigma Aldrich), the stained cells were loaded into a dual chamber counting slide and the cell number and percentage viability measured using a TC10 automated cell counter (BioRad). A threshold of 80% viability for Akata BL derived lines and 70% viability for BL41 lines was used.

Cell lines were then diluted in fresh B cell medium to a final concentration of 2 x 10^5 cells/ml and 0.5 ml (1 x 10^5) cells plated out, in triplicate, into a 48 well plate. To each well was then added 0.5 ml B cell medium containing (a) no drug or (b) 1µg/ml doxycycline. Cultures were then incubated at 37°C, 5% CO2 and harvested daily over the next 72 hours. The total number of live cells was determined by measuring GFP. Readings were collected from each well in FL1 using an Accuri C6 Flow Cytometer (BD Bioscience) from a minimum of 10000 cells. Data was expressed as fold change in live cell count relative to the number of cells at day 0.

2.13 Apoptosis assays

Approximately 2 x 10^6 lentivirus transduced BL cells were plated out in a 24 well plate and either induced with 1μg/ml doxycycline or left untreated. Cell viability was tested at 48 hours using Trypan blue as before (section 2.12). A threshold of 80% viability for Akata BL derived lines and 70% viability for BL41 and BL30 lines was used. Cell lines were then diluted in fresh B cell medium to a final concentration of 3 x 10^5 cells/ml and 100 μl (3 x 10^4) cells plated out, in triplicate, into a flat bottomed 96 well plate. To each well was then added 100μl B cell medium containing (a) no drugs, (b) 1μg/ml doxycycline only, (c) the appropriate concentration of ionomycin only or (d) 1μg/ml doxycycline and the appropriate concentration of ionomycin (Sigma). The final concentration of ionomycin was 2μg/ml for Akata, 0.5μg/ml for BL41 and 1μg/ml for BL30 derived lines. Cultures were then incubated at 37°C, 5% CO2 for 48 hours (Akata and BL41) or 72 hours (BL30) before analysis.

Live and dead cells were distinguished following staining with Syto 17 (which stains live cells) and propidium iodide (which is membrane impermeable and stains late apoptotic or dead cells). Initially Syto17 (Invitrogen) was added to each well at a final concentration of 50nM and incubated at 37°C for 1 hour. The plate was then put on ice and propidium iodide (PI, Invitrogen) added to each well at a final concentration of 0.5 ng per ml. Single and unstained samples for Syto17 and PI were also included for the purpose of colour compensation.

Readings were collected from each well using an Accuri C6 Flow Cytometer from a minimum of 10000 cells. Syto17 is detected in FL4, while PI is detected in FL3. Live cells can be described as Syto17 positive, PI negative; early apoptotic cells as Syto17 negative, PI negative; and late apoptotic or dead cells as Syto17 negative, PI positive. The following

equation was used to calculate the amount of induced cell death as a result of ionomycin treatment: (Total number of dead cells in ionomycin treated sample – mean of total number of dead cells in untreated sample) / mean number of live cells in untreated sample.

2.14 Affymetrix gene expression arrays

RNA samples for the Affymetrix microarray analysis were prepared from approximately 5-10 x 10^6 lentiviral transduced cells. After harvesting, cells were washed once in PBS. Total RNA was prepared using TRIzol® reagent (Ambion) according to manufacturer's instructions. RNA quality was confirmed by a 2100 Bioanalyzer (Agilent Technologies) and all samples were found to have RNA integrity numbers (RIN) between 9.8 and 9.9. Note that RIN is measured on a scale of 1 (heavily degraded) to 10 (intact RNA).

Whole transcript profiling was performed by Sim Sihota (Affymetrix Microarray Facility, School of Cancer Sciences, University of Birmingham). Briefly biotinylated RNA was fragmented and hybridised to Affymetrix Human Gene ST1.0 Gene Chip according to the Affymetrix protocol. After washing and staining using an Affymetrix FS450 fluidics station, arrays were scanned using a GeneChip 3000 7G scanner. Probe level quantile normalisation and robust multi-array analysis on the raw CEL files were performed by Dr. Wenbin Wei using the AltAnalyze software package (http://www.altanalyze.org/) (780). Differentially expressed probe sets were identified using Limma analysis. The p-value cut off was set to 0.01 and the fold change cut off to 1.5.

3. Quantitative study of EBV encoded miRNAs in BL cell lines

3.1 Introduction

In earlier sections (1.5, 1.6) we discussed both the broad range of cellular pathways in which miRNAs participate and the potential roles of miRNA deregulation in tumour development. The observation that EBV encodes a set of highly conserved viral miRNAs suggests that they are (a) important to the virus life cycle and (b) likely contribute to the pathogenesis of EBV associated malignancies (738). At the start of our study however only a handful of potential EBV miRNA targets had been validated (CXCL11, LMP1 and BALF5) (753, 759, 760) thus their functions remained largely unknown. By studying the BL cell line model, we aimed to establish if and how virally encoded miRNAs contribute to the oncogenic potential of EBV.

Before we could study the function of the EBV miRNAs, we needed to gain an understanding of when and to what degree they are expressed. Studies published prior to the present work have provided us with some insight into EBV miRNA expression in EBV positive cell lines (250, 738, 740, 744, 745, 748) and primary tumour material (749).

Most of the 40 known EBV miRNAs were collectively discovered by Pfeffer (250), Grundhoff (740) and Cai (738) along with their respective colleagues. These groups used methods such as cloning/sequencing (250, 738) or software prediction (740) to identify candidate miRNAs which were confirmed either by array (740) or northern blotting (250, 738, 740). Cai and co-workers analyzed a larger selection of EBV positive cell lines by northern blot than the other two groups; consequently they were able to draw a number of interesting conclusions (738). The BHRF1 miRNAs were generated during the growth transforming program, specifically in cell lines expressing Cp and Wp initiated transcripts.

The BART miRNAs in turn were detected in all forms of EBV infection and their expression correlated with BART transcription; levels of both were notably elevated in epithelial cell lines. Cai and co-workers also performed the first investigation into EBV miRNA expression during lytic replication. They noticed that at 48h post induction the levels of all 4 BART miRNAs tested, as well as miR-BHRF1-2, were increased. Levels of miR-BHRF1-1 in contrast remained unchanged; this was somewhat predicted as miRBHRF1-1 overlaps the lytic BHRF1p and thus is not included in the transcript (744, 746, 747).

Other studies by Cameron *et al* and Xing and Kieff gave broadly comparable results using northern blots (744) and arrays (745), respectively, to measure EBV miRNA expression. However Xing and Kieff made two interesting observations regarding EBV miRNA expression during lytic cycle which conflicted somewhat with data from Cai and co-workers (738, 744). First, Xing and Kieff could not detect an increase in the levels of the 2 BART miRNAs tested following induction of lytic replication; second, miR-BHRF1-1 levels did increase, but only after 48h, and appeared to correlate with the expression of Lat III latent antigens. Note that these two studies shared just one BART miRNA in common and used entirely different cell backgrounds (738, 744).

Two additional northern blot studies have provided further insights into BART miRNA expression. Kim *et al.* demonstrated that BART miRNAs, but not BHRF1 miRNAs, could be detected in gastric carcinoma cell lines, animal models and patient tumour samples (749). Not only was this study the first to look at EBV miRNA expression in tissue samples, but it suggested that observations made in cell lines can be representative of the tumour from which they derived. Finally Edwards *et al.* extended the observation that the BART miRNAs correlate with BART transcription (748). They noticed that a particular BART exon splice variant (direct joining of exons 1 and 3) favoured BART miRNA accumulation. Furthermore,

they included an extensive panel of BART miRNAs in their study and so were able to convincingly demonstrate that individual BART miRNAs accumulate to different levels within the same cell line.

Thus in summary we know that all three BHRF1 miRNAs are expressed from C and W promoter initiated transcripts during latency III, while miR-BHRF1-2 and 1-3 are expressed from the lytic BHRF1 promoter during productive infection. BART miRNAs in turn are expressed in all forms of EBV infection, and are preferably expressed in epithelial cell lines and NPC tumour cells as compared to cells of lymphoid origin (250, 738, 740, 744, 745, 748, 749).

Unfortunately these studies largely relied on northern blotting, arrays or cloning for detection. Such methods unfortunately require large amounts of RNA, have limited sensitivity and only provide qualitative data. In contrast we wanted to develop a methodology which was sensitive, specific and capable quantifying absolute EBV miRNA copy numbers.

Thus in the first part of our study we aim to address these issues by validating a commercial quantitative PCR (QPCR) system for the detection and quantification of EBV miRNAs. Thereafter we confirm and extend the previous literature by characterizing EBV miRNA expression in a range of different BL cell lines and LCLs. Finally we investigate a number of factors determining EBV miRNA steady state levels, such as differential turnover rates and levels of BHRF1 and BART gene transcription.

3.2 Validating QPCR assays for the detection of EBV miRNAs

Our QPCR assays were based on the stem-loop reverse transcriptase (RT) method described by Chen *et al* (776). Stem-loop RT primers are more efficient and possess greater target specificity than conventional RT primers. They also exclusively bind the mature form of a target miRNA. Furthermore stem-loop RT primers unfold during reverse transcription to produce a template sequence much longer than the mature miRNA target. This enables the generation of cDNA large enough to accommodate the full primer-probe set required for QPCR amplification. In a series of preliminary experiments, we validated both the specificity and sensitivity of a panel of QPCR assays designed to quantify selected EBV miRNAs. These included all three miRNAs derived from the BHRF1 region (miR-BHRF1-1, 1-2 and 1-3), five miRNAs from BART cluster 1 (miR-BART3, 4, 1-3p, 15 and 5), three miRNAs from BART cluster 2 (miR-BART7, 22 and 13) and miR-BART2-5p.

Although it is recommended that each miRNA is reverse transcribed using its specific RT primer in a separate reaction, we first tested if it was possible to reverse transcribe several miRNAs at once by pooling several RT primers in a single reaction. Therefore in initial experiments we optimised a multiplex cDNA synthesis method incorporating up to 7 miRNA-specific RT primers; this would enable us to assay several miRNAs from the same cDNA pool. Representative amplification plots for miR-BHRF1-1 and miR-BART3 produced from this multiplex method are shown in Fig. 3.1A, alongside data from cDNA made in a single reaction. Multiplex cDNA synthesis resulted only in a small (2 cycles or less) reduction in the sensitivity of QPCR detection, as compared to singleplex cDNA synthesis.

Using cDNA prepared by this multiplex protocol, we then carried out a series of control experiments. First we used RNA from eight EBV-negative cell lines to test the specificity of

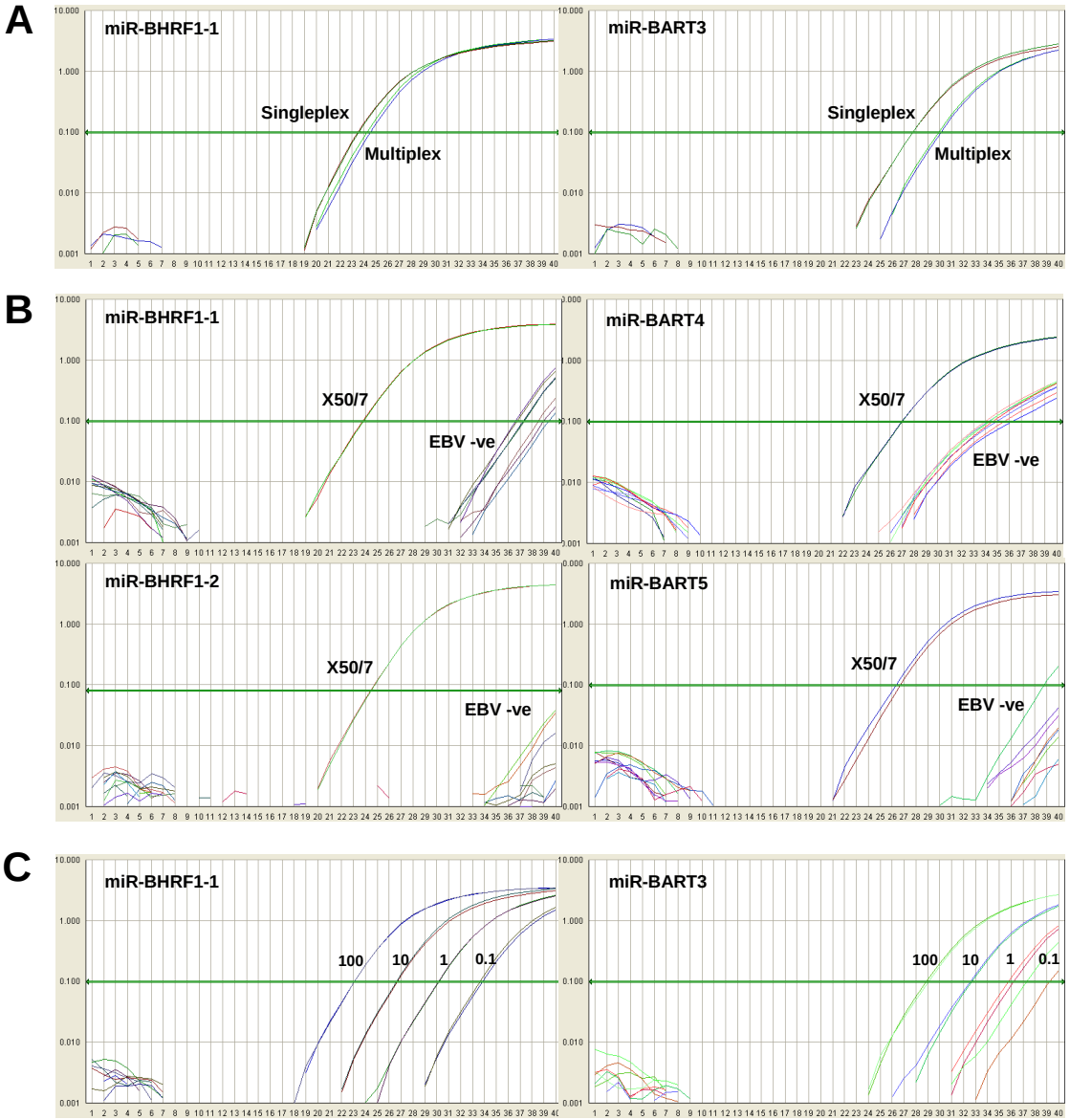

Fig. 3.1. (A) Optimization of a multiplex cDNA synthesis method. cDNA was generated from a suitable reference line using either one (singleplex) or a pool of seven (multiplex) miRNA-specific RT primers. Shown are PCR amplification plots for miR-BHRF1-1 and miR-BART3. **(B)** Specificity of QPCR assays to detect EBV miRNAs. Four EBV negative BLs (DG75, BJAB, BL41 and Ramos), EBV loss clones derived from two Latency I BLs (Mutu 59 and Akata), an EBV negative T cell and NK cell line (Jurkat and NKL respectively) and an EBV positive LCL (X50/7) were used to test the specificity of each QPCR assay. Shown are representative PCR amplification plots for miR-BHRF1-1, miR-BHRF1-2, miR-BART4 and miR-BART5. **(C)** Sensitivity of QPCR assays to detect EBV miRNAs in cell mixtures containing serial dilutions of an EBV-positive LCL (100 – 0.1 cells) in an EBV-negative cell background. Shown are PCR amplification plots for miR-BHRF1-1 and miR-BART3

our assays. Data from representative amplification plots for miR-BHRF1-1, miR-BHRF1-2, miR-BART4 and miR-BART5 are shown in Fig. 3.1B. We found that all but three assays gave a negative PCR result; the exceptions were miR-BHRF1-1, miR-BART3 and miR-BART4 which occasionally yielded extremely weak signals (Fig. 3.1B; also see Fig. 3.13B-D later). Second, we used our assays to detect EBV miRNAs in cell mixtures containing serial dilutions of an EBV-positive LCL (100 – 0.1 cells) in an EBV-negative (BJAB) cell background. Amplification plots for miR-BHRF1-1 and miR-BART3 are shown in Fig. 3.1C. All assays tested reproducibly and detected a single EBV-infected cell.

Finally, the absolute sensitivity of each assay was determined by using cDNA prepared from serial dilutions of a pool of synthetic oligonucleotides containing all 12 target miRNAs. Data from representative amplification plots for 10-fold serial dilutions (10^8 copies – 10^1 copies) of miR-BHRF1-1 and miR-BART3 are shown in Fig. 3.2., while standard curves for all 12 assays are shown in Fig. 3.3. All assays demonstrated an excellent correlation between cycle threshold (Ct) values and RNA input over at least a 5-log range, and had a lower detection limit of between 100-1000 miRNA copies.

3.3 Defining EBV latent gene expression in a panel of EBV positive B cell lines

Having validated our QPCR assays we proceeded to characterize EBV miRNA expression in a panel of B cell lines with different patterns of latency. Our test lines included eight conventional Latency I BL lines (Lat I BL), five Wp-restricted BL lines (Wp BL), two Latency III BL lines (Lat III BL) and seven virus-transformed LCLs. These latency programs are summarized again in Fig. 3.4. While most if not all our cell lines had been previously

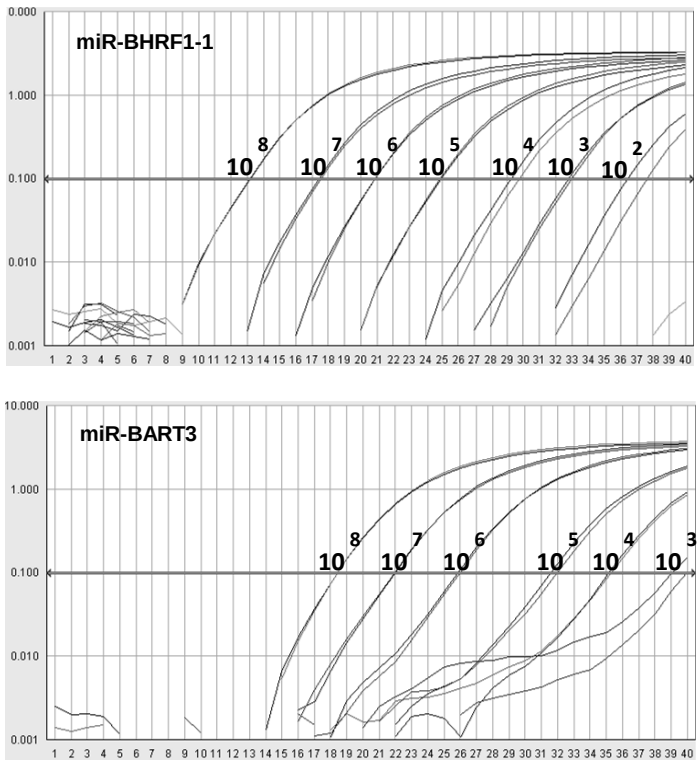

Fig. 3.2. Sensitivity of QPCR assays to detect EBV miRNAs. cDNA samples containing known numbers of synthetic miRNAs (10^8 – 10^2 copies) were used to test the absolute sensitivity of each QPCR assay. Shown are representative PCR amplification plots for miR-BHRF1-1 and miR-BART3.

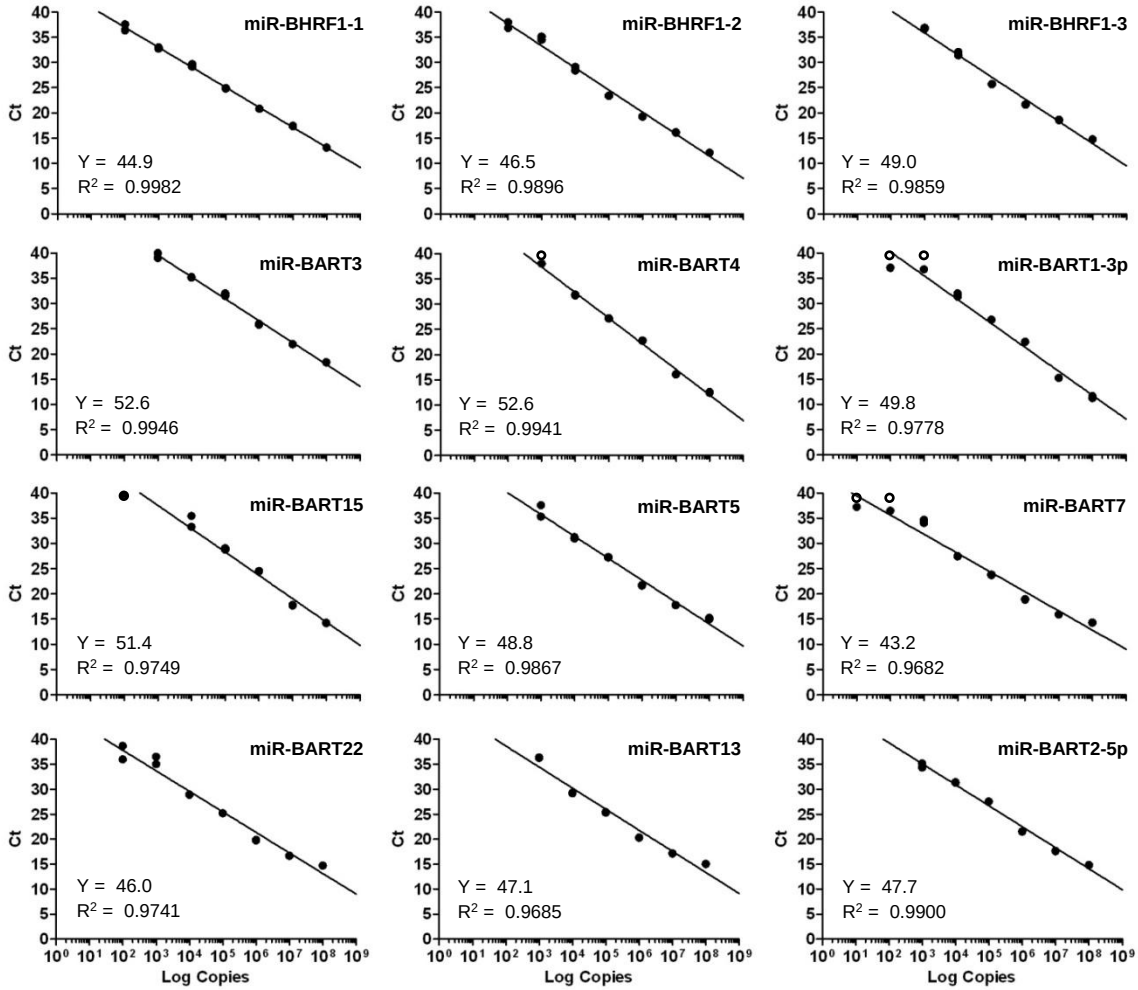

Fig. 3.3. Sensitivity of QPCR assays to detect EBV miRNAs. Standard curves obtained for all 12 miRNAs obtained by plotting the cycle threshold (Ct) values against log input RNA copy number. Open circles indicate absence of a detectable signal (Ct=40).

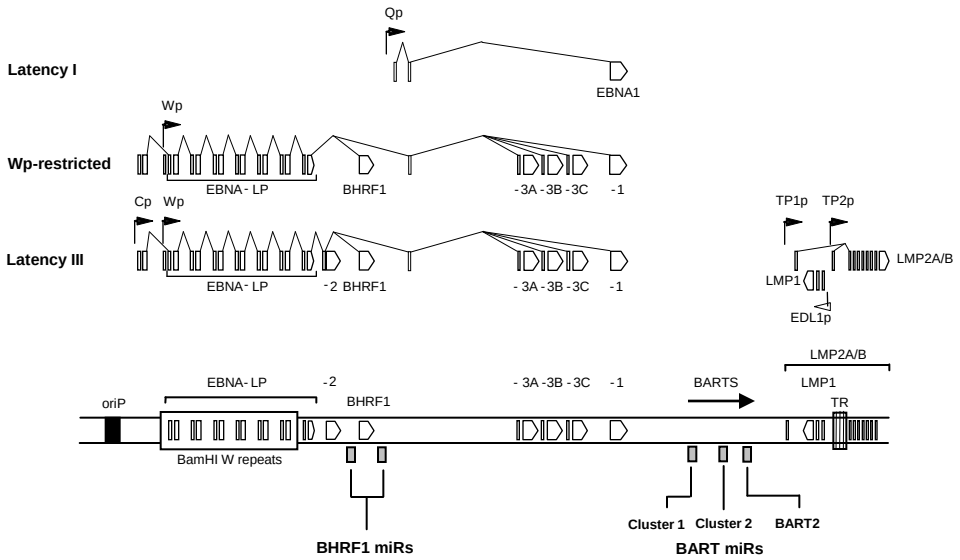

Fig. 3.4. Patterns of latent gene expression in BL cell lines and LCLs. The location of viral promoters and splice structures of viral transcripts are shown relative to a linear representation of the EBV genome. Conventional Latency I BLs express a single latent antigen EBNA1 transcribed from a viral promoter in the BamHI Q region(Qp). Wp-restricted BLs are characterised by the presence of an EBNA2-deleted EBV genome; these BLs express EBNAs 1, -3A, -3B, -3C and –LP, along with BHRF1, all transcribed from the Latency III BamHI W promoter (Wp), but in the absence of EBNA2 and the latent membrane proteins (LMPs). Latency III BL lines and growth transformed LCLs express all six EBNAs and BHRF1, predominantly from transcripts initiated at the BamHI C promoter (Cp), along with the LMPs which are transcribed from separate promoters in the BamHI N region. EBERs (not shown) and BamHI A rightward transcripts (BARTs) are present in all three forms of latency. Also shown are the positions of the BHRF1 and BART miRNAs, latent origin of replication (oriP) and the terminal repeat region (TR).

characterized, it was necessary to ensure they had not drifted towards an unexpected pattern of latency, as is occasionally seen in BL cell lines (781).

3.3.1 Assessing latent promoter usage

Conventionally latency is defined by latent promoter usage. Thus we first verified that our test lines showed the expected pattern of latent viral promoter usage by quantifying levels of Qp-, Cp- and Wp-initiated EBNA transcripts by QPCR using established assays (Fig. 3.5) (769). As expected the Lat I BL lines exclusively used Qp with only trace or undetectable levels of Cp/Wp activity. In contrast, the Wp BL lines were distinguished by high levels of Wp activity, usually in the absence of the other latent promoters. Lat III BLs and LCLs in turn showed variable levels of both Cp and Wp usage, with the exception of X50/7 which lacks Cp sequences (771). Note that Chep-BL was originally defined as a Lat I BL line (781) but appeared to have drifted to Lat III during passage *in vitro*. Finally, all test cell lines were tightly latent since immediate early BZLF1 transcripts were either undetectable or present at very low levels, equivalent to less than 1% BZLF1 positive cells (see Fig. 3.8A later).

3.3.2 Expression of latent proteins

As an additional confirmation of latency we probed for EBNA1, EBNA2, BHRF1 and LMP1 expression in the same lines by western blot (Fig. 3.6). Protein expression correlated broadly with latent viral promoter usage as expected. Thus EBNA1 alone was detected in Lat I BL lines. Both EBNA1 and BHRF1 were detected in Wp BL lines, although BHRF1 protein levels in Awia-BL sub-clones (k, m) were barely detectable. Finally Lat III BL lines and LCLs expressed EBNA1, EBNA2 and variable levels of LMP1; BHRF1 could only be

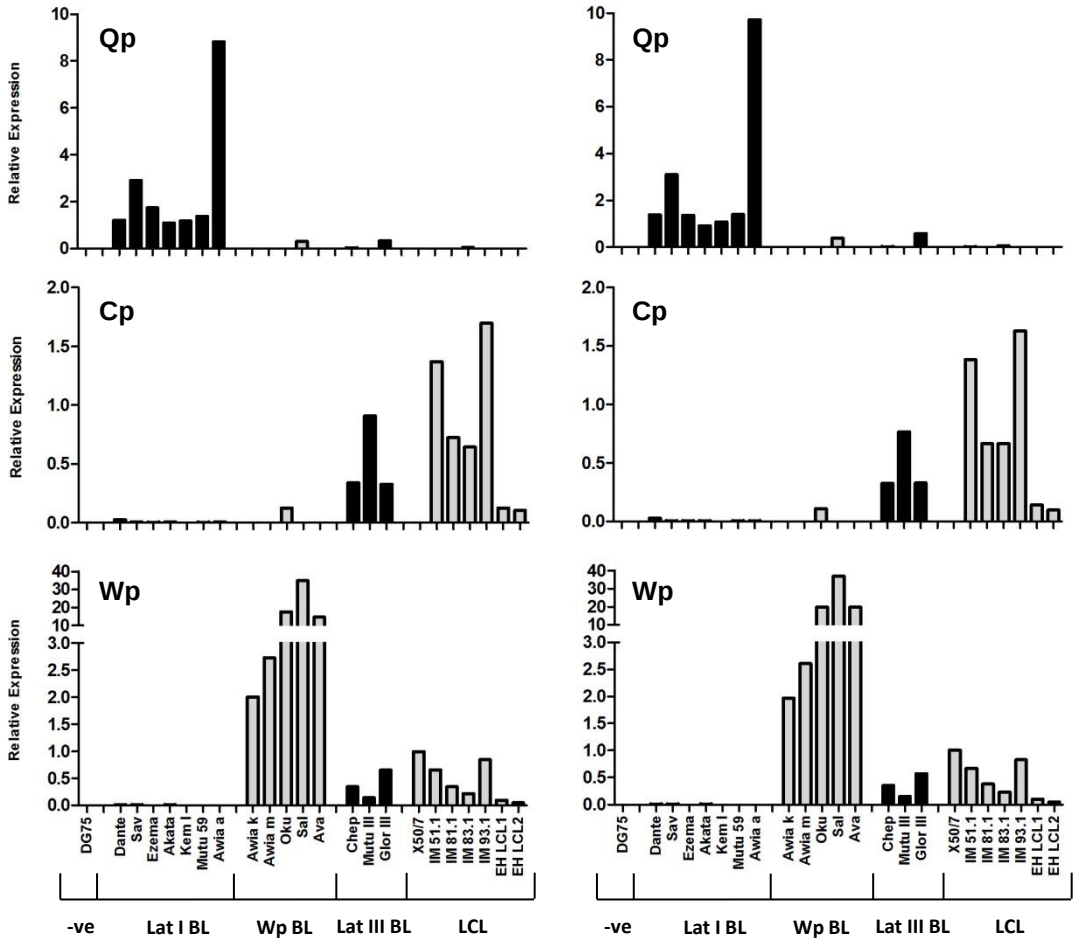

Fig. 3.5. Expression of latent transcripts in EBV-positive B cell lines. Latency I-associated Qp transcripts and Latency III-associated Cp- and Wp-initiated transcripts were quantified by QPCR in seven Latency I BLs (Dante, Sav, Ezema, Akata, Kem and Awia cl. a), five Wp-restricted BLs (Awia cl. k and m, Oku, Sal and Ava), three Latency III BLs (Chep, Mutu III and Glor III) and seven LCLs (X50-7, IM51, -81, -83, -93, EH LCL1 and EH LCL2); DG75 was included as a negative control. Data were normalised to cellular PGK levels and expressed relative to a suitable positive reference line which was assigned an arbitrary value of one. Shown in separate panels are two replicate assay measurements obtained from a single preparation of RNA.

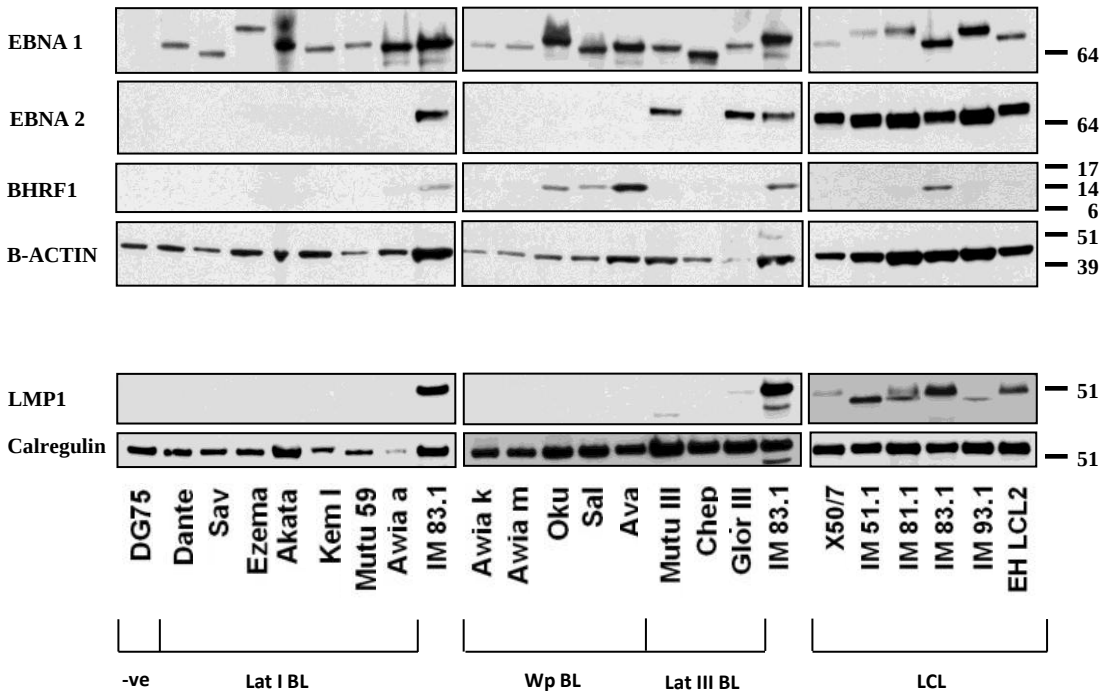

Fig. 3.6. Expression of latent proteins in EBV-positive B cell lines. EBNA1, -2, BHRF1 and LMP1 protein was detected by western blot in the same cell lines shown in Fig. 4. DG75 was included as a negative control. Detection of either β-Actin or Calregulin was performed as a loading control. Molecular weight markers and sizes in kDa are provided on the side of each gel.

detected in one LCL (IM 81.1). Surprisingly Chep-BL expressed EBNA1 in the absence of EBNA2 and LMP1, despite the presence of Cp/Wp initiated EBNA transcription (Fig. 3.5). Due to these contradictory results, we removed Chep-BL from further studies.

3.4 Investigating BHRF1 miRNA expression in EBV positive B cell lines

At this point we have successfully validated our QPCR assays and confirmed the latency pattern of our B cell lines. Thus in the next series of experiments we launched an investigation into the expression of the BHRF1 miRNAs in the same lines. According to earlier reports the BHRF1 miRNAs are processed from the introns of large Cp and Wp initiated EBNA transcripts (738, 744), though they could in theory be processed from the 5′ and 3′ UTRs of latent BHRF1 transcripts (Fig. 3.7A). To further investigate these possibilities, we determined both the copy numbers of all three BHRF1 miRNAs in our test lines and the levels of BHRF1 transcription to determine how well it correlates with BHRF1 miRNA expression.

3.4.1 Correlating BHRF1 miRNA expression and BHRF1 transcription

BHRF1 transcripts were measured using two different primer/probe combinations, one designed to specifically amplify Cp/Wp-initiated latent BHRF1 transcripts and the other designed to detect total (lytic and latent) BHRF1 transcripts. As shown by the data in Fig. 3.8A, the BHRF1 expression profiles were comparable using both assays, and correlated with the presence of Cp and/or Wp promoter activity (Fig. 3.5). Consistent with the very low BZLF1 signals, negligible levels of lytic BHRF1 transcripts were observed in these test lines (data not shown), thus excluding the possibility that a small population of productively infected cells were making a significant contribution to the total levels of BHRF1 transcripts.

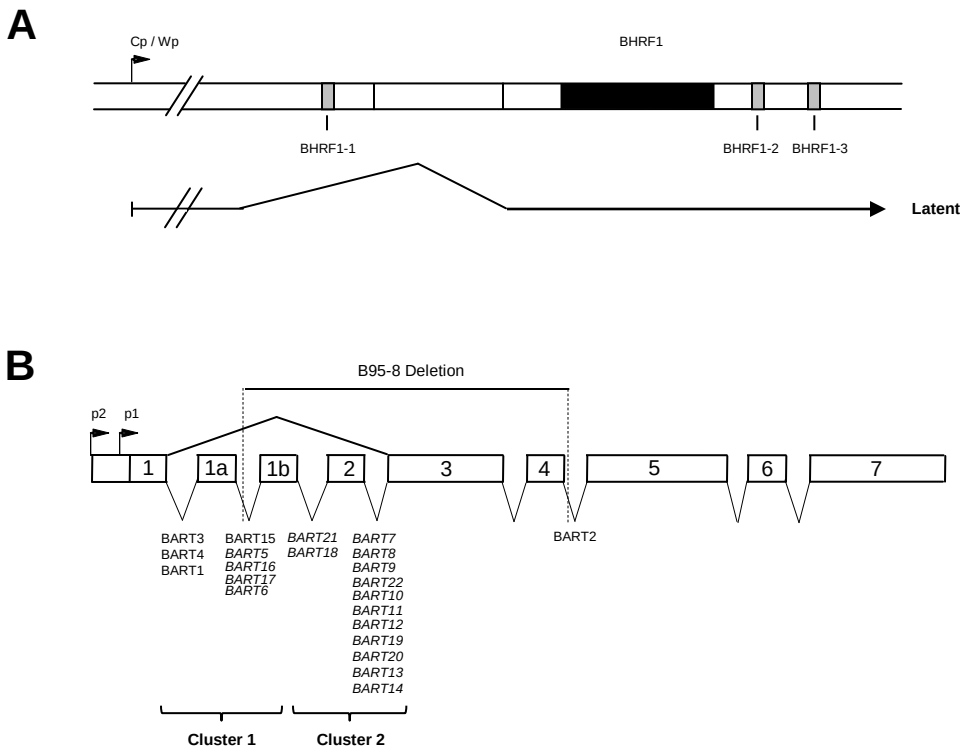

Fig. 3.7. Detailed structure of EBV transcripts and miRNAs. **(A)** BHRF1 transcripts and location of BHRF1-derived miRNAs. All three BHRF1 miRNAs may be generated during latency either by processing of an intron present within the Cp/Wp initiated primary EBNA transcript or by processing of the 5′ and 3′ untranslated regions within latent BHRF1 transcripts with the W2-Y1-Y2-BHRF1 structure. **(B)** Detailed structure of the highly spliced BARTs and location of the BART-derived miRNAs (adapted from Edwards et al.) (748). The BART miRNAs form two clusters within the BART introns, with the exception of mirBART2 which lies further downstream. The prototype B95-8 EBV strain carries a 12kb deletion in this region which removes several cluster 1 miRNAs and all cluster 2 miRNAs (shown in italics).

Fig. 3.8. Expression of BHRF1 transcripts and BHRF1 miRNAs in EBV-positive B cell lines. **(A)** Total BHRF1 transcripts, Cp/Wp-initiated latent BHRF1 transcripts and immediate early BZLF1 transcripts were quantified by QPCR in the same cell lines as shown in Fig. 3.5. BHRF1 values are expressed relative to a reference LCL, while BZLF1 values are expressed relative to a spontaneous LCL and adjusted so that a value of one is equivalent to 100% positive cells. **(B)** Expression of BHRF1 miRNAs in the same cell lines determined by QPCR. Data were normalised to RNU48 expression and expressed as absolute copy numbers per pg total RNA. Shown in separate panels are two replicate assay measurements obtained from a single preparation of RNA. Note that Sal-BL is deleted for miR-BHRF1-1, as indicated by the † symbol.

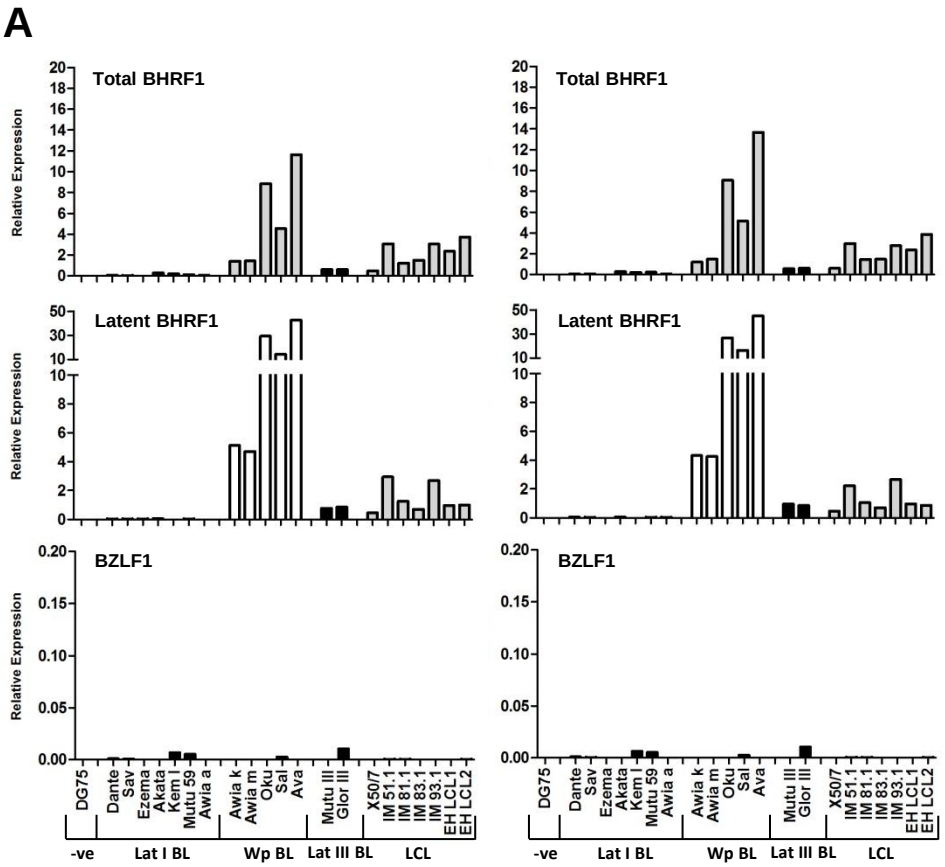
A
Total BHRF1
Latent BHRF1
BZLF1
Relative Expression
DG75
Dante
Sav
Ezema
Akata
Kem I
Mutu 59
Awia a
Awia k
Awia m
Oku
Sal
Ava
Mutu III
Glor III
X50/7
IM 51.1
IM 81.1
IM 83.1
IM 93.1
EH LCL1
EH LCL2
-ve
Lat I BL
Wp BL
Lat III BL
LCL

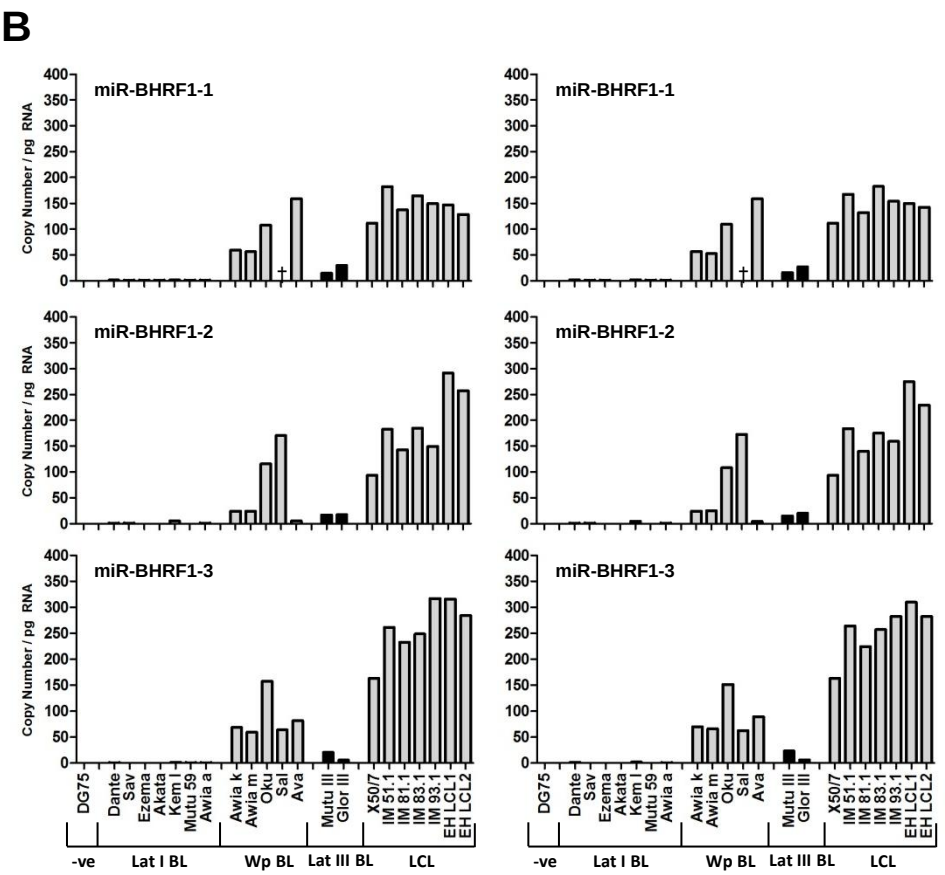
B
miR-BHRF1-1
miR-BHRF1-2
miR-BHRF1-3
Copy Number / pg RNA
DG75
Dante
Sav
Ezema
Akata
Kem I
Mutu 59
Awia a
Awia k
Awia m
Oku
Sal
Ava
Mutu III
Glor III
X50/7
IM 51.1
IM 81.1
IM 83.1
IM 93.1
EH LCL1
EH LCL2
-ve
Lat I BL
Wp BL
Lat III BL
LCL

We then went on to measure the levels of BHRF1 miRNAs in the same panel of cell lines using our newly-developed QPCR assays. The data (Fig 3.8B) show that BHRF1 miRNA expression varied widely, ranging from 0-5 copies per pg RNA in Lat I BL lines to more than 300 copies per pg RNA in Lat III LCLs. Interestingly levels of the BHRF1 miRNAs in the LCLs were at least as high as in the Wp BL lines, despite the latter having much higher levels of BHRF1 transcripts. In most cases, we noted that all three BHRF1 miRNAs were co-ordinately expressed within a cell line, with no more than 3-fold variation in absolute values between individual miRNAs. One exception was Sal-BL, which expressed abundant levels of mir-BHRF1-2 and mir-BHRF1-3 but is known to be deleted for miR-BHRF1-1 (625). Another exception was Ava-BL, where levels of miR-BHRF1-2 were unusually low compared to the other BHRF1 miRNAs.

To determine if BHRF1 transcription correlates with the BHRF1 miRNA expression, we plotted the entire latent BHRF1 data set against that of miR-BHRF1-1, miR-BHRF1-2 or miR-BHRF1-3 and performed linear regression analysis (Fig. 3.9). Cell lines expressing latent BHRF1 also expressed the BHRF1 miRNAs and vice versa. Nonetheless linear regression analysis revealed a startling lack of correlation between the two data sets, with R^2 values falling below 0.1 for each comparison.

3.4.2 BHRF1 miRNA sequence variation

Previous studies have revealed that sequence changes can interfere with miRNA processing (743, 748); such changes could in theory also affect the efficiency of the PCR reaction. Therefore we considered the possibility that EBV strain polymorphisms might account for some of the variation in BHRF1 miRNA levels. To this end, we determined the sequence of

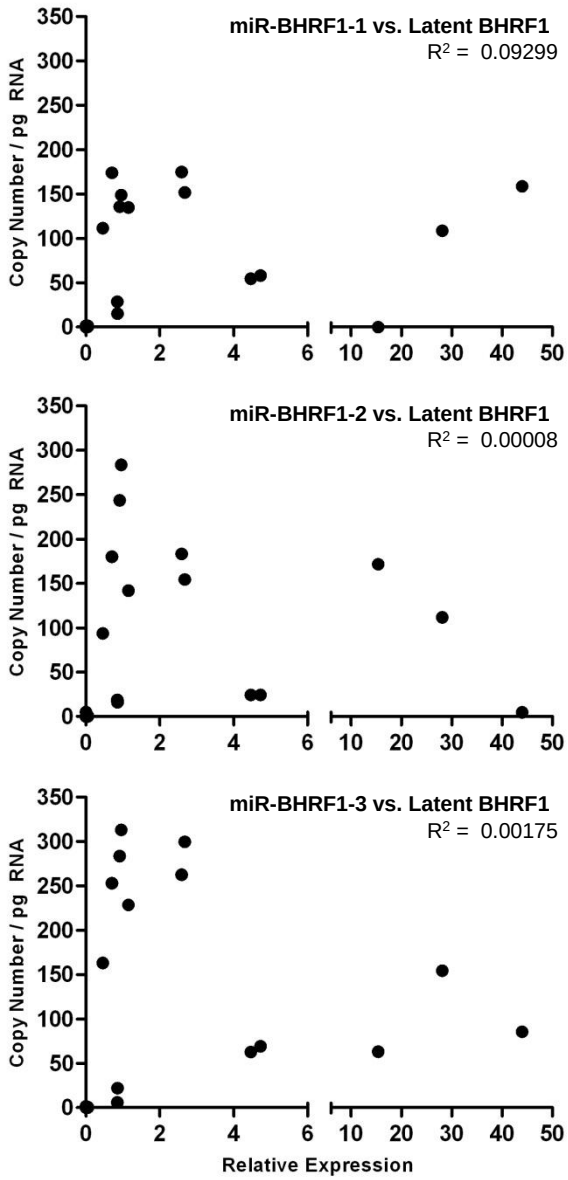

Fig. 3.9. Correlating levels of BHRF1 transcripts and BHRF1 miRNAs in EBV-positive B cell lines. Collective data from Fig. 3.8. were redrawn to plot each BHRF1 miRNA individually against latent BHRF1. Each point on the graph represents data from a single cell line. Linear regression analysis was performed to calculate R squared values.

the BHRF1 pre-miRNAs in 12 EBV isolates and compared the sequences with the published B95-8 genome; the number and position of any sequence changes are summarised in Fig. 3.10 through Fig. 3.12. We also calculated the minimum free energy ΔG associated with each polymorphic variant separately using both Mfold (777) and RNAfold (778, 779). While each program calculated different absolute ΔG values per pre-miRNA sequence, the differences in free energy between a given test sequence and the B95-8 sequence were near identical for both programs.

Overall miR-BHRF1-1 and miR-BHRF1-2 sequences were highly conserved in the BL lines tested. In two cases (Kem-BL and Sav-BL), we found a single change in the mature miR-BHRF1-1 miRNA; however the effect of this mutation on pre-miRNA processing or PCR detection is unclear as the BHRF1 region is not transcribed in these Latency I lines (Fig. 3.10). One cell line, Ava-BL, contained a single polymorphism in the mature miR-BHRF1-2 sequence which disrupts a G-C base pair in the stem-loop (Fig. 3.11). This G to A substitution is predicted to significantly destabilise the pre-miRNA hairpin loop structure and therefore may account for the low levels of miR-BHRF1-2 detected in this cell line (Fig. 3.8B). Finally, five cell lines contained six common nucleotide changes in the miR-BHRF1-3 pre-miRNA (Fig. 3.12). Surprisingly these changes only marginally affected the minimum free energy structure of the BHRF1-3 pre-miRNA, and are therefore unlikely to affect folding or processing of this pre-miRNA.

3.5 Investigating BART miRNA expression in EBV positive B cell lines

The majority of EBV miRNAs form two intronic clusters within the BART region of the genome. The BART transcripts are expressed from two promoters and are reportedly found in

A

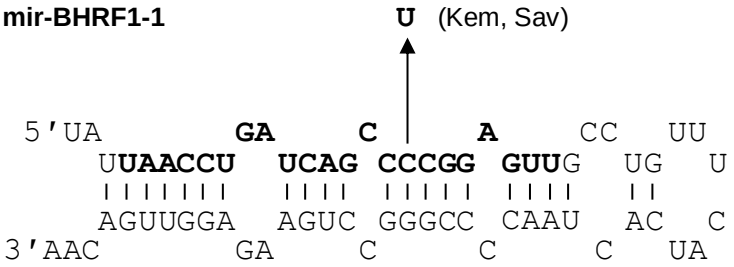

B

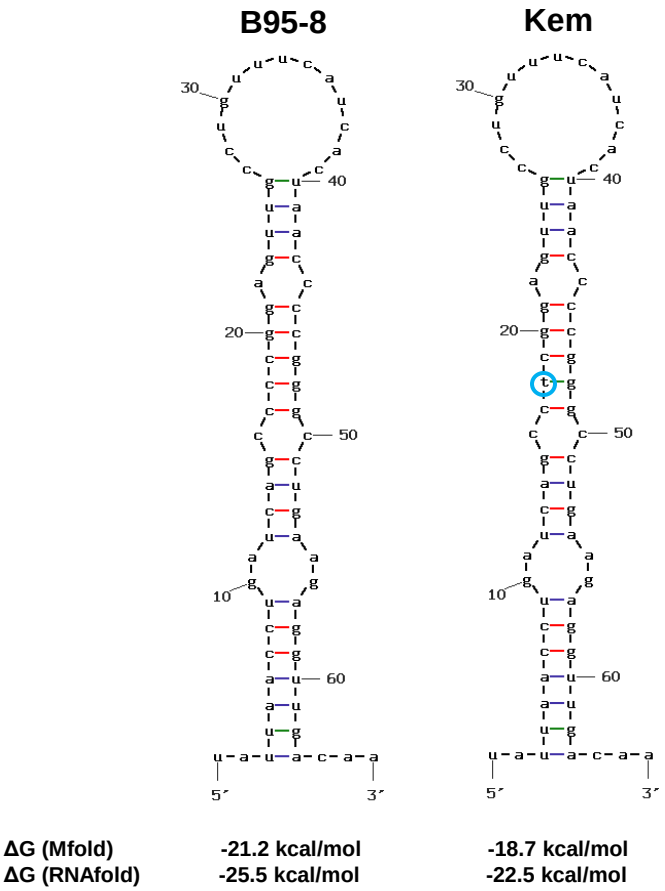

Fig. 3.10. Sequence variation in miR-BHRF1-1. **(A)** The prototype B95-8 sequence of the pre-miRNA is shown with the mature miRNA indicated in bold text. Sequence changes are marked by the arrows with the cell line indicated in brackets. **(B)** Structures of the folded B95-8 and Kem pre-miRNAs were predicted using Mfold. Minimum free energy ΔG was determined separately with Mfold and RNAfold.

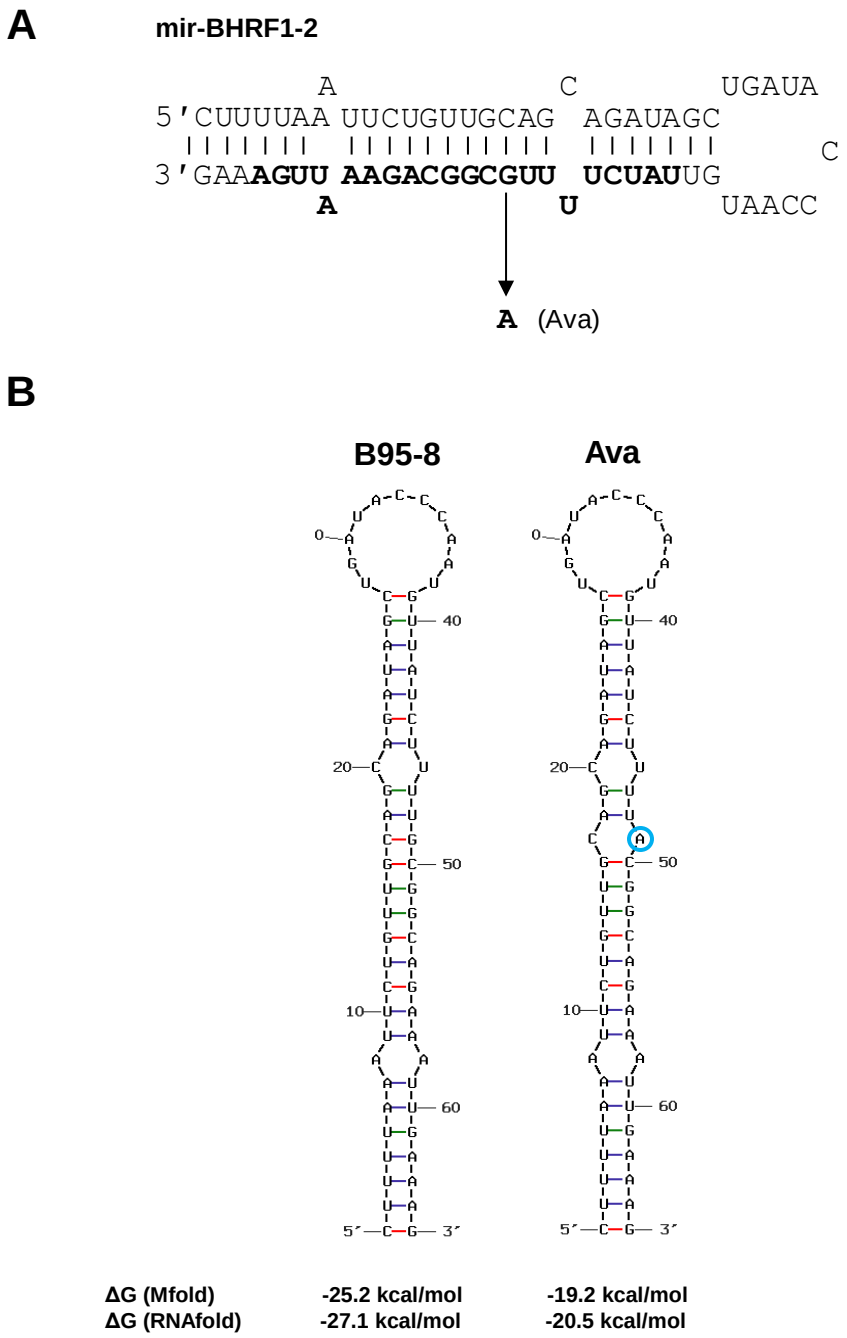

Fig. 3.11. Sequence variation in miR-BHRF1-2. **(A)** The prototype B95-8 sequence of the pre-miRNA is shown with the mature miRNA indicated in bold text. Sequence changes are marked by the arrows with the cell line indicated in brackets. **(B)** Structures of the folded B95-8 and Ava pre-miRNAs were predicted using Mfold. Minimum free energy ΔG was determined separately with Mfold and RNAfold.

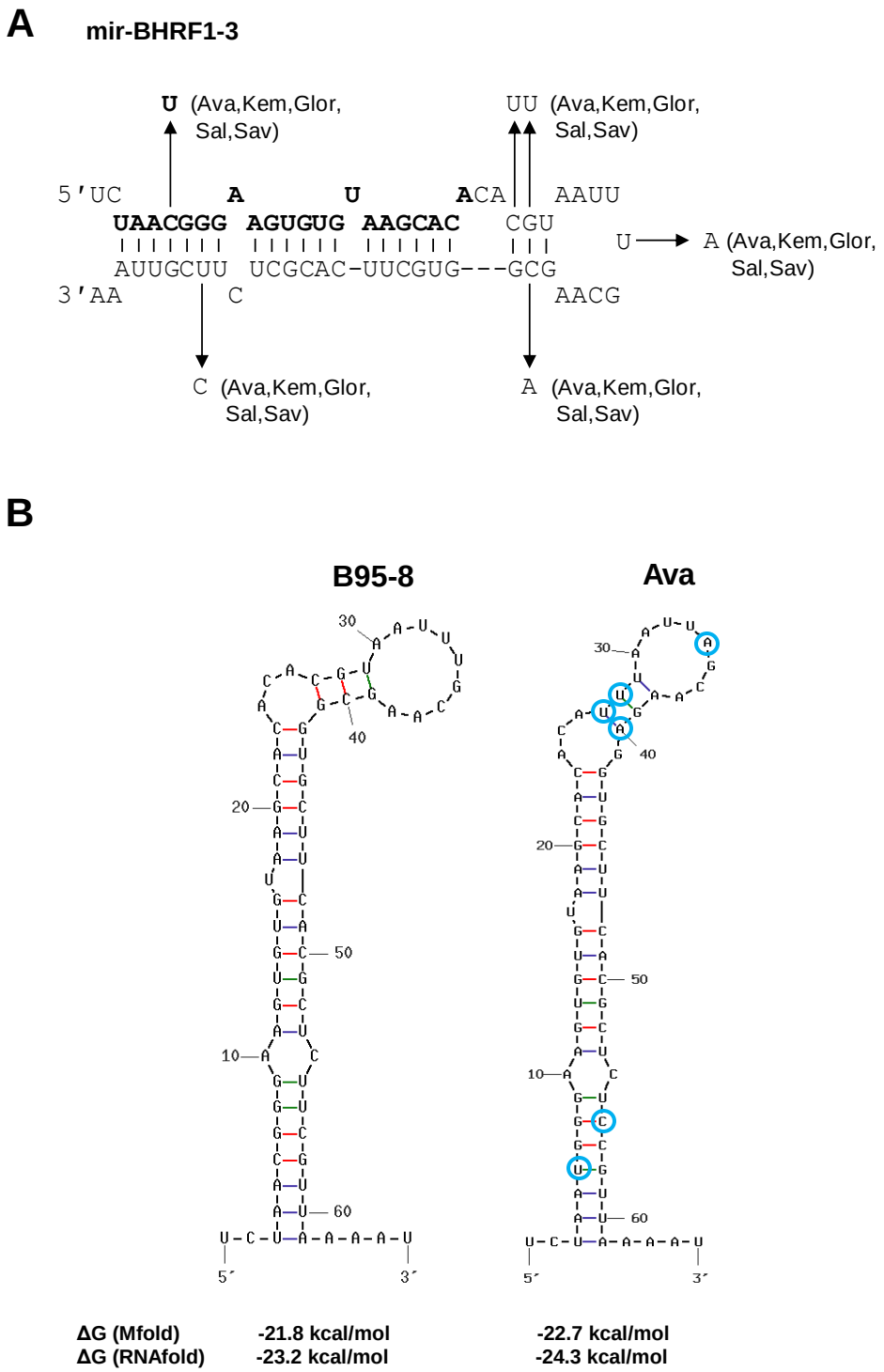

Fig. 3.12. Sequence variation in miR-BHRF1-3. **(A)** The prototype B95-8 sequence of the pre-miRNA is shown with the mature miRNA indicated in bold text. Sequence changes are marked by the arrows with the cell line indicated in brackets. **(B)** Structures of the folded B95-8 and Ava pre-miRNAs were predicted using Mfold. Minimum free energy ΔG was determined separately with Mfold and RNAfold.

all forms of latency. Since particular BART splice variants may favour the production of BART miRNAs (748), we quantified BART transcription in our test lines using two different PCR assays; the first specific for the conventional transcript containing exons 1, 2 and 3 (exon 2-3 assay) and the second specific for the exon 2-deleted variant (exon 1-3 assay). Subsequently we quantified a select panel of 9 BART miRNAs spanning both clusters 1 and 2 in the same lines.

3.5.1 Correlating BART miRNA expression and BART transcription

In contrast to BHRF1, BART transcripts were detected across all forms of latency, albeit at highly variable levels (Fig. 3.13A); BART transcripts containing exon 2-3 and exon 1-3 splice junctions appeared to be co-ordinately expressed. Screening the same samples for the presence of nine representative BART miRNAs, we found levels ranging from less than 10 to more than 400 copies per pg RNA (Figs. 3.13B-D). Overall it is clear that the B cell lines expressed lower levels of BART miRNAs than the epithelial cell line C666-1 (data included in Figs. 1.13B-D for comparison). Interestingly we observed up to a 50-fold variation between different BART miRNAs within a given cell line. BART miRNA levels also varied widely between cell lines but all showed the same hierarchy of BART miRNA expression, with miR-BART7 usually the most abundant and miR-BART13 the most scarce. Of note, EH LCL1 and EH LCL2 were generated from a recombinant prototype EBV strain which, like B95-8, lacks many of the BART miRNAs (Fig. 3.7B).

We next investigated how well BART transcription correlates with BART miRNA production. To this end we plotted the data sets of either the 1-3 or the 2-3 BART exon splice variant individually against miR-BART15 (cluster 1), miR-BART22 (cluster 2) or miR-BART2-5p (Fig. 3.14). Linear regression revealed that both BART exon splice variants

Fig. 3.13. Expression of BART transcripts and BART miRNAs in EBV-positive B cell lines. **(A)** BART transcripts were quantified by QPCR using assays specific for either the exon 1-3 or 2-3 splice variants in the same cell lines as shown in Fig. 3.5. Data were normalised to PGK expression and results are expressed relative to the EBV-positive epithelial tumour cell line C666-1. **(B)** and **(C)** show expression of cluster 1 and cluster 2 BART miRNAs, respectively while **(D)** shows miR-BART2-5p expression. Data were normalised to RNU48 expression and expressed as copy numbers per pg input RNA. Shown in separate panels are two replicate assay measurements obtained from a single preparation of RNA. Data points highlighted with † correspond to cell lines carrying a BART deletion. For comparison, copy numbers of BART miRNAs per pg C666-1 RNA are shown in parentheses in each histogram.

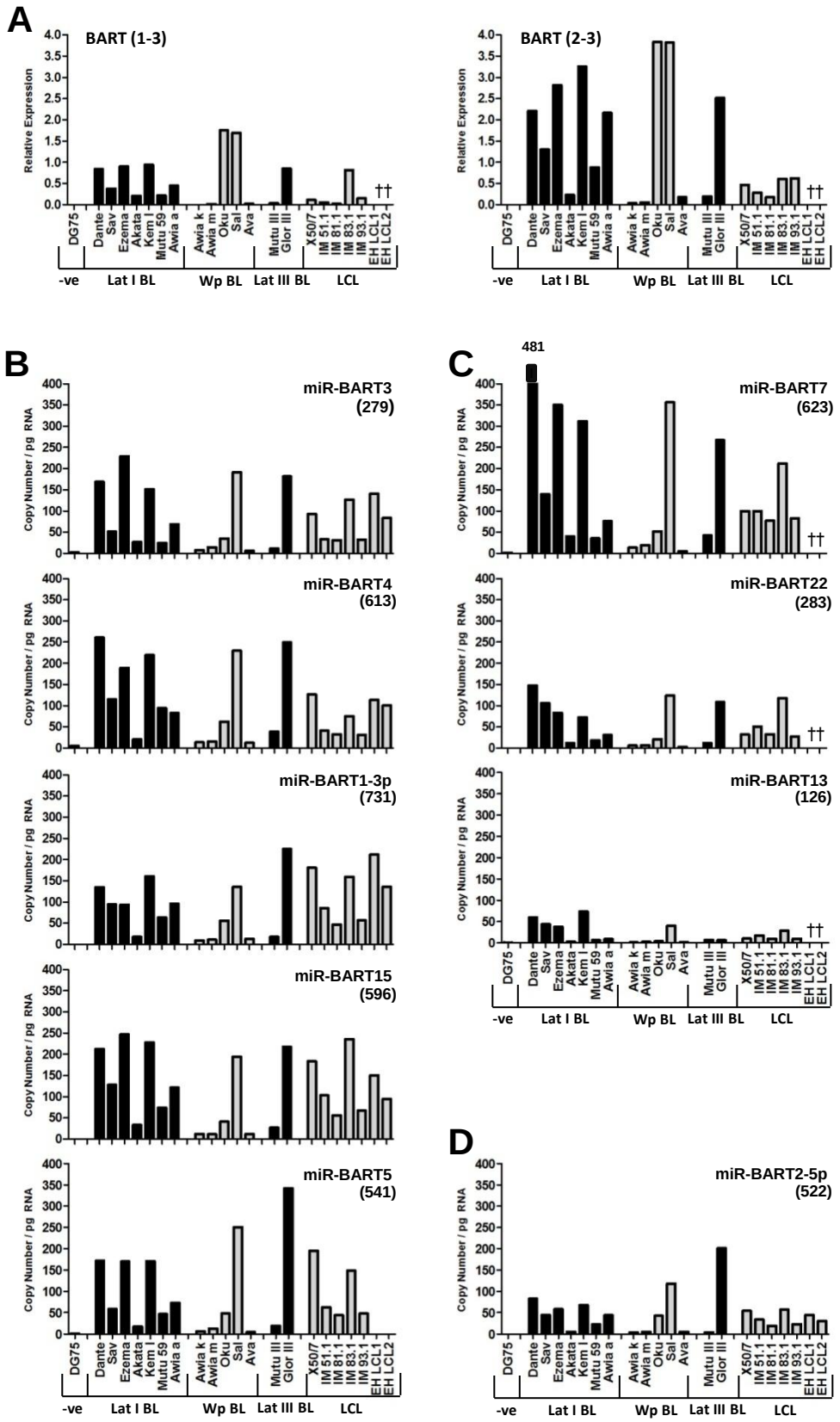
A
BART (1-3)
BART (2-3)
Relative Expression
B
miR-BART3 (279)
miR-BART4 (613)
miR-BART1-3p (731)
miR-BART15 (596)
miR-BART5 (541)
C
481
miR-BART7 (623)
miR-BART22 (283)
miR-BART13 (126)
D
miR-BART2-5p (522)
Copy Number / pg RNA
DG75
Dante
Sav
Ezema
Akata
Kem I
Mutu 59
Awia a
Awia k
Awia m
Oku
Sal
Ava
Mutu III
Glor III
X50/7
IM 51.1
IM 81.1
IM 83.1
IM 93.1
EH LCL1
EH LCL2
-ve
Lat I BL
Wp BL
Lat III BL
LCL
††

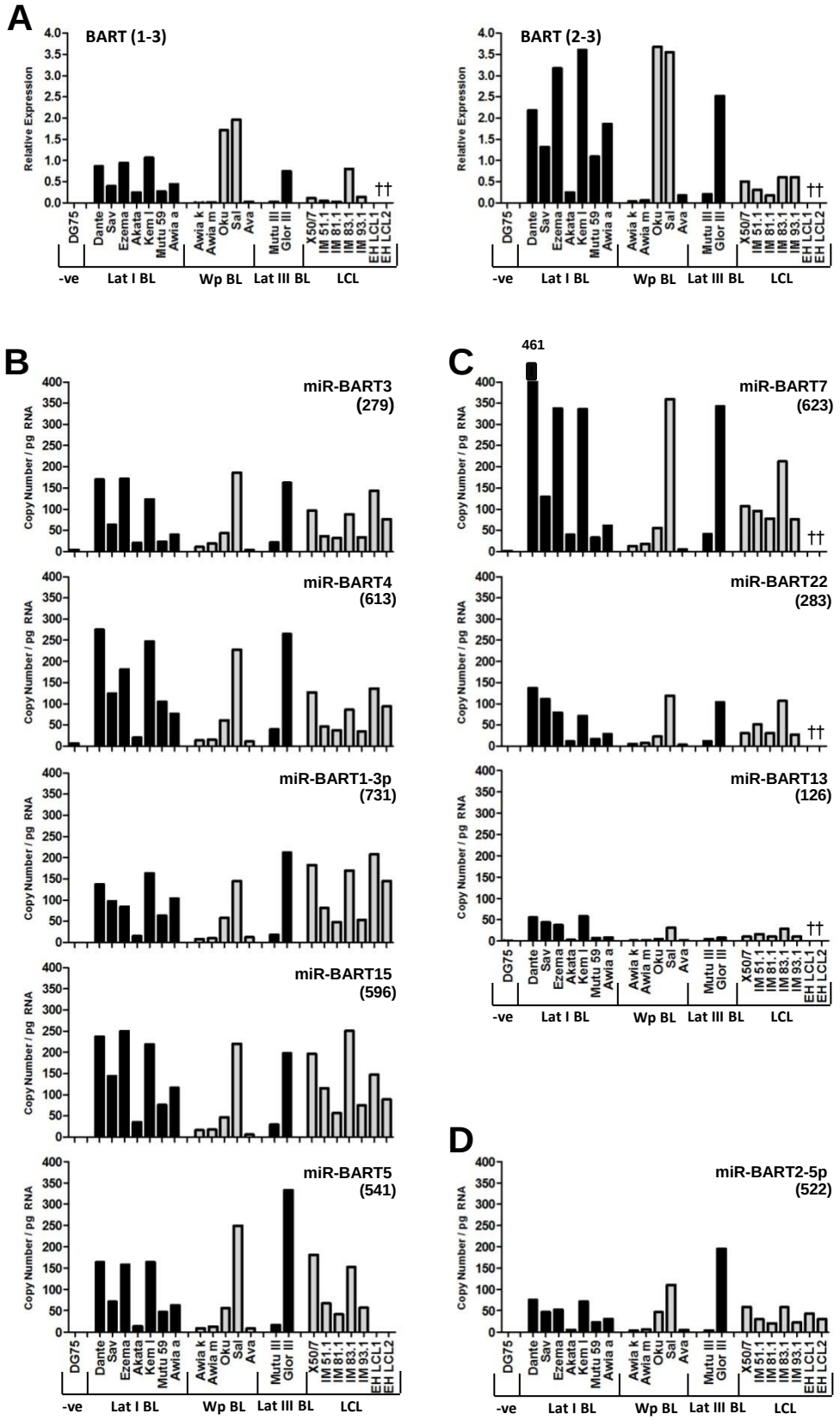
A
BART (1-3)
BART (2-3)
Relative Expression
B
miR-BART3 (279)
miR-BART4 (613)
miR-BART1-3p (731)
miR-BART15 (596)
miR-BART5 (541)
C
461
miR-BART7 (623)
miR-BART22 (283)
miR-BART13 (126)
D
miR-BART2-5p (522)
Copy Number / pg RNA
DG75
Dante
Sav
Ezema
Akata
Kem I
Mutu 59
Awia a
Awia k
Awia m
Oku
Sal
Ava
Mutu III
Glor III
X50/7
IM 51.1
IM 81.1
IM 83.1
IM 93.1
EH LCL1
EH LCL2
-ve
Lat I BL
Wp BL
Lat III BL
LCL

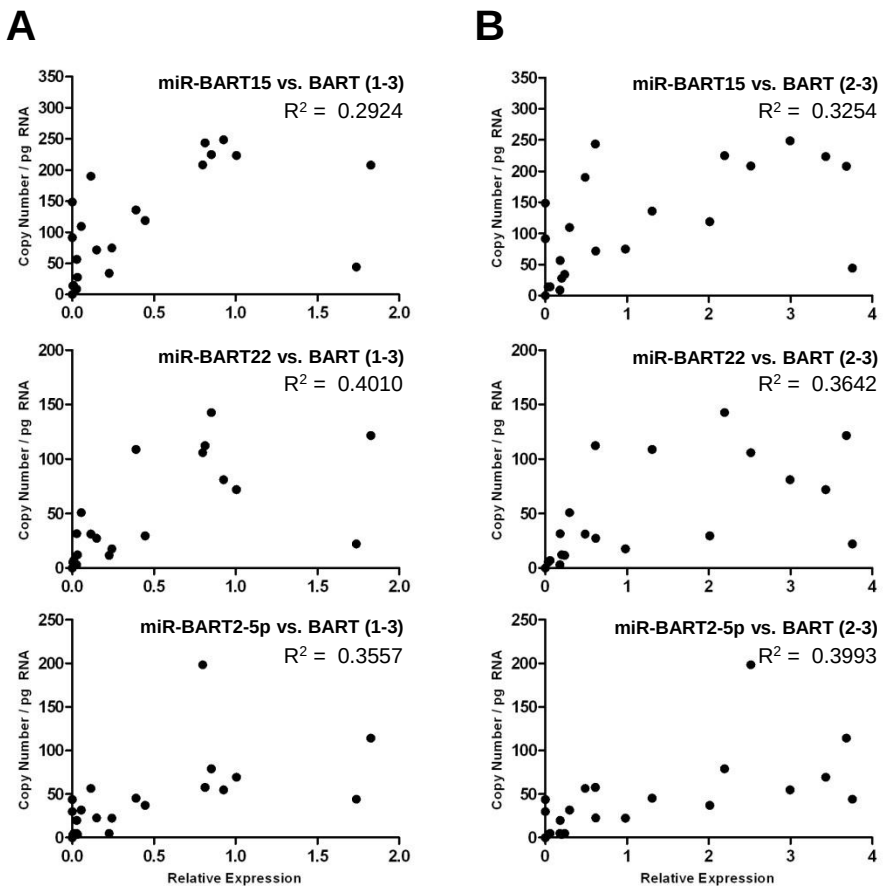

Fig. 3.14. Correlating levels of BART transcripts and BART miRNAs in EBV-positive B cell lines. Collective data from Fig. 3.13. were redrawn to plot either a cluster 1 (miR-BART15), a cluster 2 BART miRNA (miR-BART22) or the miR-BART2-5p miRNA individually against **(A)** BART (1-3) or **(B)** BART (2-3). Each point on the graph represents data from a single cell line. Linear regression analysis was performed to calculate R squared values.

correlated similarly with each of the three BART miRNAs examined, with R^2 values ranging between 0.3 and 0.4. These values indicate a closer relationship between BART transcription and BART miRNA production than is the case for latent BHRF1 and the BHRF1 miRNAs.

3.6 Quantifying Drosha and Dicer transcription in EBV positive B cell lines

Neither BHRF1 nor BART transcription could account for (a) the variation in EBV miRNA expression between different cell lines and (b) the wide variation in levels of individual miRNAs within a cell line. To address the former, we asked whether differences in the levels of Drosha and Dicer could account for some of the variation in BHRF1 or BART miRNA levels between our test lines. As discussed earlier (sections 1.2 and 1.5) Drosha and Dicer are key components of the miRNA biogenesis pathway whose levels impact on cellular miRNA accumulation. Therefore we performed QPCR for Drosha and Dicer transcripts in a select panel of B cell lines (Fig. 3.15A). Levels of Drosha and Dicer transcripts were within a 4 – 5 fold range in the cell lines tested. For comparison, we also calculated the mean copy number of BHRF1 and BART miRNAs for the same cell lines (Fig. 3.15B; using data from Fig. 3.8 and Fig. 3.13). It is clear that changes in miRNA levels are greater than changes in Drosha/Dicer, and show no correlation.

3.7 Stability of viral transcripts and miRNAs in EBV positive B cell lines

It has previously been reported that some miRNAs are intrinsically less stable than others, while conversely certain cell backgrounds have overall faster miRNA turnover rates (93, 95). Either scenario could account for some of the variation in the steady state levels of BHRF1 and BART miRNAs observed in our test lines. To investigate this theory in more detail, we

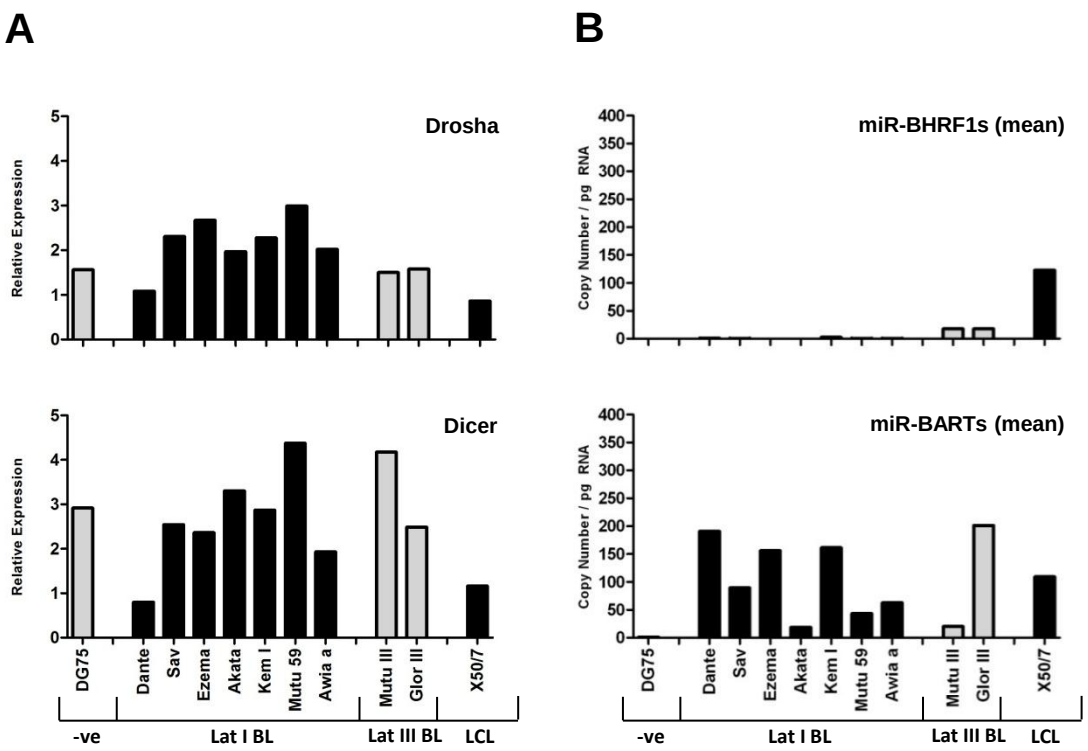

Fig. 3.15. Comparing levels of EBV miRNAs to Drosha and Dicer expression. **(A)** Drosha and Dicer transcripts were quantified by QPCR in a select panel of cell lines. Data were normalised to PGK expression and expressed relative to a reference LCL. Shown are the averages of two replicate assay measurements obtained from a single preparation of RNA **(B)** Data from Fig. 3.8. and Fig. 3.13. were used to generate mean BHRF1 and BART miRNA values for the same cell lines.

examined the half-life of selected miRNAs in three cell lines Sal-BL, X50/7 LCL and Ava-BL; these lines were chosen since they showed overall high, intermediate and low levels of BART miRNA expression (Fig. 3.13). Cells were cultured in the presence of the RNA synthesis inhibitor Actinomycin D and then harvested for analysis at various time points after treatment. Residual levels of BHRF1 and BART transcripts and derived miRNAs were then monitored by QPCR (Fig. 3.16, Fig. 3.17); as a control, we also assayed c-myc RNA since this transcript has been reported to have a very short half-life of around 12 minutes (782).

Fig. 3.16A and Fig. 3.17A show the individual data points from Sal-BL cells up to 24h post treatment, while Fig. 3.16B and Fig. 3.17B summarise the data from all three cell lines. In the case of Sal-BL, c-myc RNA levels decreased rapidly to less than 10% after 4h exposure to Actinomycin D while the latent BHRF1 transcripts also decreased but to a lesser extent (Fig. 3.16A). By contrast, the BHRF1 miRNAs decreased by less than 2-fold even at 24h post treatment. When we examined the BARTs, both the BART (1-3) transcript and three representative BART miRNAs were all relatively constant up to 24h (Fig. 3.17A). Similar data for the stability of the transcripts and miRNAs were obtained from X50/7 and Ava-BL (Fig. 3.16B, Fig. 3.17B). Although we have only tested a limited number of miRNAs, these data suggest that the EBV miRNAs are very stable and therefore changes in miRNA turnover cannot account for the observed differences in miRNA levels.

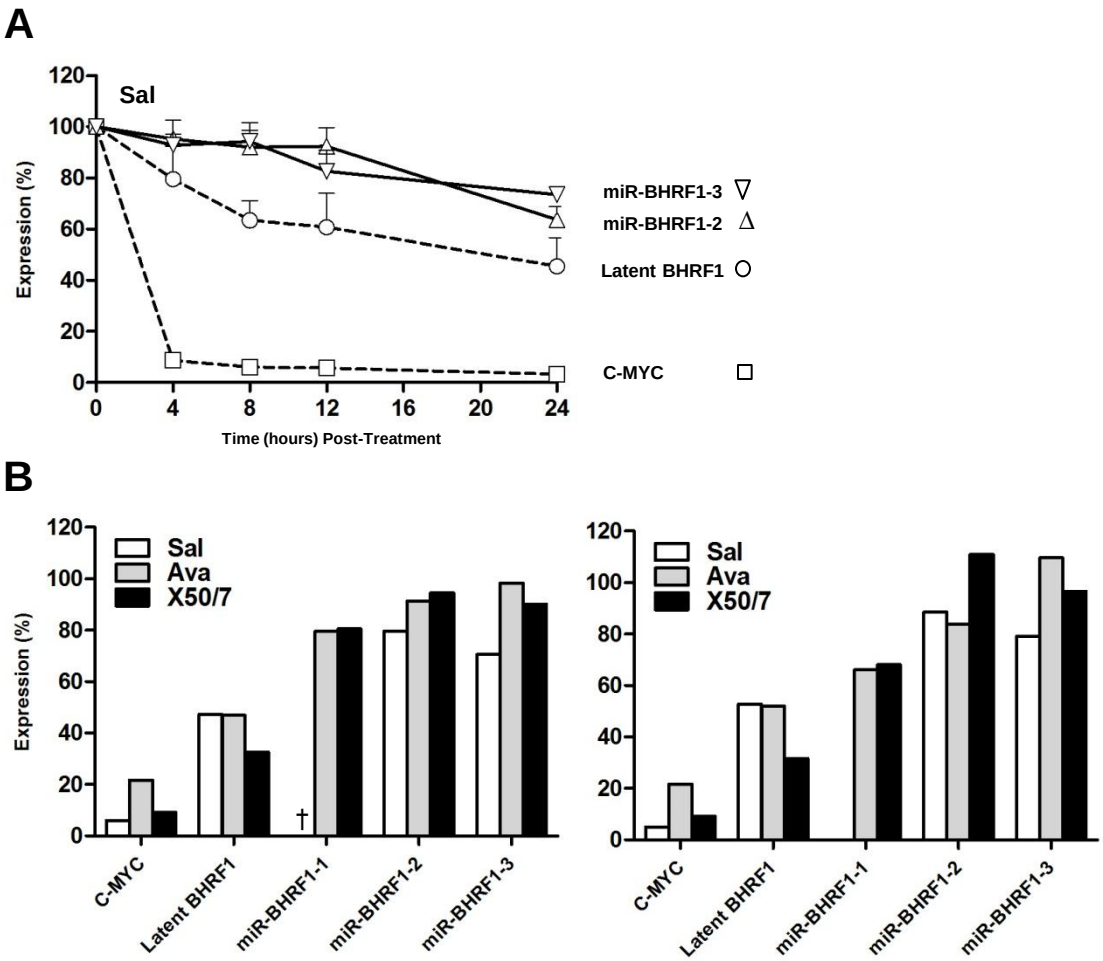

Fig. 3.16. Stability of EBV transcripts and miRNAs. **(A)** Sal-BL cells were treated with 5µg/ml actinomycin D, harvested at the indicated time points and then analysed for BHRF1 transcripts and miRNAs. Error bars indicate standard deviation of 3 replicate experiments **(B)** Summary of data from Sal-BL, Ava-BL and X50/7. The histograms indicate the expression of the indicated transcripts and miRNAs measured at 12 h after the addition of actinomycin D. Shown in separate panels are two replicate assay measurements obtained from a single preparation of RNA. Cellular c-myc RNA is unstable and served as a positive control for RNA decay. All data were normalised to RNA input.

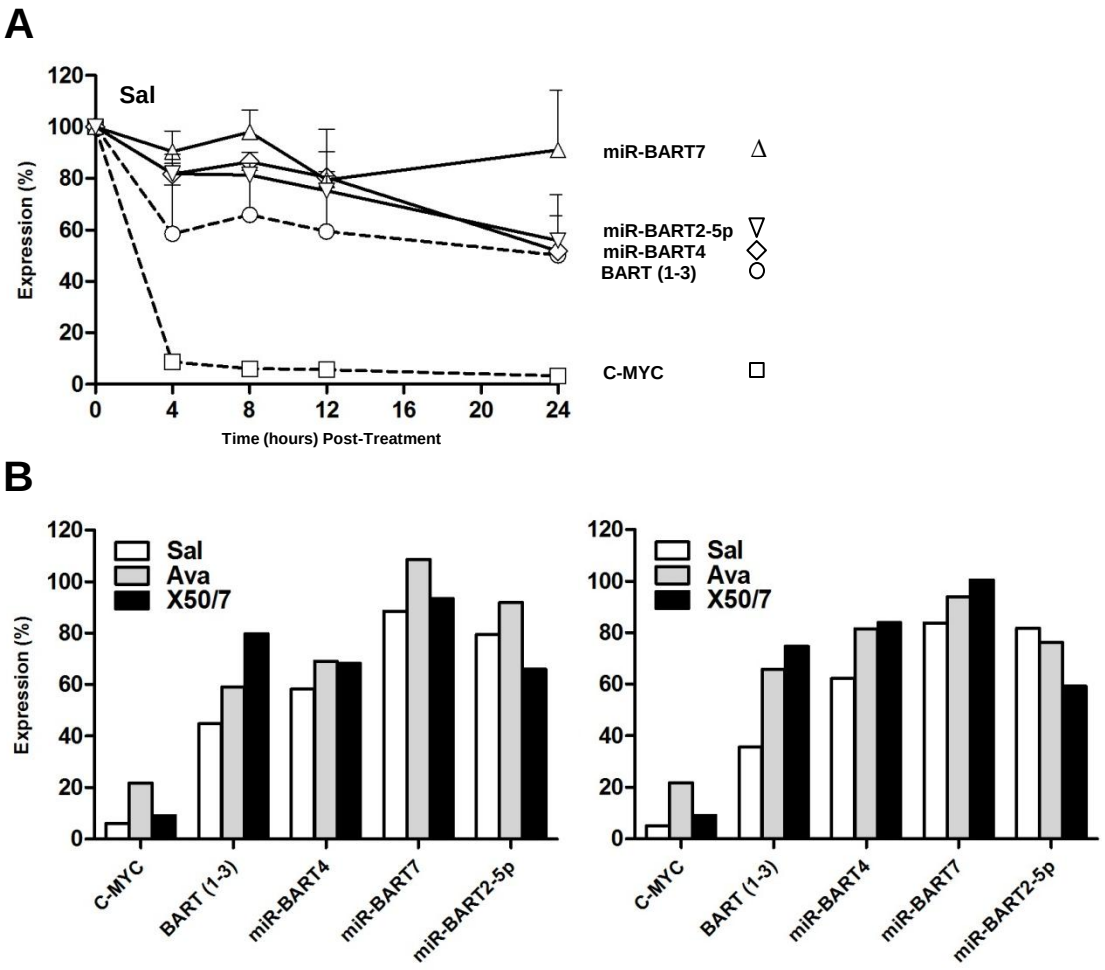

Fig. 3.17. Stability of EBV transcripts and miRNAs. **(A)** Sal-BL cells were treated with 5µg/ml actinomycin D, harvested at the indicated time points and then analysed for BART transcripts and miRNAs. Error bars indicate standard deviation of 3 replicate experiments. **(B)** Summary of data from Sal-BL, Ava-BL and X50/7. The histograms indicate the expression of the indicated transcripts and miRNAs measured at 12 h after the addition of actinomycin D. Shown in separate panels are two replicate assay measurements obtained from a single preparation of RNA. Cellular c-myc RNA is unstable and served as a positive control for RNA decay. All data were normalised to RNA input.

3.8 Discussion

3.8.1 Preliminary validation experiments

EBV miRNAs have attracted a lot of interest in recent years as they potentially contribute to the B cell growth transformation and the pathogenesis of EBV-associated tumours. However there was little information on the quantitative expression of these molecules in different types of infection. In the first part of our work we validated a panel of real time PCR assays to quantify expression of three BHRF1 miRNAs and nine representative BART miRNAs (including all five BART miRNAs present in the B95-8 prototype EBV genome). In a series of control experiments these assays were shown to be both specific and highly sensitive (Fig. 3.1 through Fig. 3.3).

In contrast to some earlier studies of EBV miRNAs, we carefully characterized latent viral promoter usage and protein expression in our 22 EBV-positive test cell lines (Fig. 3.5 and Fig. 3.6). The vast majority of our lines displayed the expected pattern of latent infection. One exception was Chep-BL which appeared to display an intermediate form of latency, characterized by the presence of Lat III transcripts but in the absence of detectable EBNA2 protein. The other exception was Awia-BL in which BHRF1 protein was nearly undetectable. We speculate that BHRF1 protein levels in these cells were too low for detection by western blot using the experimental conditions outlined in Table 2.2. Nonetheless these examples both highlight the importance of carefully validating cell lines before using them in research.

3.8.2 Viral miRNA expression in EBV positive B cell lines

Next we characterized the expression of 3 BHRF1 and 9 BART miRNAs in 21 EBV-positive lymphoid cell lines with well defined forms of latency. While this issue has been addressed in earlier studies, data have only been reported for a very limited number of lymphoid cell lines and these were not fully characterised in terms of virus gene expression (250, 738, 740, 744, 745, 748, 749).

Our work revealed that all three BHRF1 miRNAs are robustly expressed at comparable levels in Latency III cell lines which use Cp and/or Wp to drive EBNA transcription. While this finding is consistent with earlier Northern blot-based studies discussed in section 3.1 (738, 744), our data provide a number of novel findings. We demonstrate that the BHRF1 miRNAs are also abundantly expressed in a range of Wp BL lines (Fig. 3.8B). While the biological significance of this finding remains to be determined, it has previously been reported that Wp BL lines are much more resistant to cell death stimuli than standard Lat I BL lines (681). A number of recent reports (320, 511, 512) have focussed on the role of BHRF1, EBNA-LP and the EBNA3 proteins in providing a pro-survival signal in Wp BLs, but the current work now adds the BHRF1 miRNAs to the list of candidate genes which may mediate this phenotype. We also found that while some Lat I BL lines express extremely low levels of BHRF1 miRNAs, these signals are always accompanied by similar trace levels of Wp- and Cp-initiated transcripts, suggesting that a small population of cells have drifted to Latency III during passage *in vitro*. This finding further underlines the importance of carefully validating the patterns of virus promoter usage before drawing conclusions on miRNA expression.

Extending our studies to the BART region, our quantitative analysis confirms earlier reports that the BART miRNAs are readily detectable in all forms of virus latency, albeit at lower

levels than in EBV infected epithelial cell lines (250, 738, 743, 748). Our data also highlight the huge variation in overall BART miRNA levels between different cell lines. However, in sharp contrast to the coordinate expression of the BHRF1 miRNAs, different BART miRNAs were found to be expressed at dramatically different levels within a cell line, with miR-BART7, miR-BART4 and miR-BART15 frequently the most abundant and miR-BART2-5p and miR-BART13 consistently the least abundant (Fig. 3.13). While a similar hierarchy of miRNA expression has been noted in previous studies of B cells (743) and epithelial cells (739), it was unclear if this pattern reflected PCR artefacts arising from miRNA sequence polymorphisms or differences in miRNA processing and stability.

While this work was in progress, Pratt and co-workers (743) described a similar quantitative PCR study of EBV miRNA expression in EBV positive lymphoid cell lines. While their conclusions are broadly similar to those of the present work, our analysis included a larger collection of cell lines and examined a different panel of miRNAs. We also noted a number of discordant results between the two studies. Overall we found that the absolute level of BHRF1 and BART miRNAs were 5-20 fold higher than previously estimated (743).

Our data suggest that individual EBV miRNAs are expressed at a range of 100 – 4000 copies per cell, assuming that 1 cell contains 10 pg of RNA. For comparison, individual cellular miRNAs are expressed at a median of 633 copies per mouse liver cell and at a median of 178 copies per human hematopoietic progenitor cell (HSC) (783). Thus it is likely that EBV miRNAs are expressed at physiologically significant levels.

A number of recent studies have relied on deep sequencing techniques to profile miRNA expression in EBV positive lymphoid cell lines and tumours (763, 764, 784). The concept behind deep sequencing is reviewed in more detail elsewhere (785). Essentially millions of

small sequence reads are generated; individual miRNAs can then be quantified based on the number of times their sequence appears in the data set. Next generation sequencing techniques also appear capable of distinguishing between miRNA variants containing 3′ modifications; there is increasing evidence to suggest such reads are not just an artefact of sequencing (741, 763, 786). Sequencing is also suited for expression of individual miRNAs as a fraction of the total cellular miRNA pool. Thus Skalsky and co-workers found that up to 22% of all miRNA reads in a panel of B95-8 derived LCLs (Lat III) were virus associated (763). Imig and co-workers in turn found that around 1.7% of miRNA reads in EBV positive diffuse large B-cell lymphoma (DLBCL; Lat I) were virus associated (784).

There are a number of similarities between the present work and studies conducted by Skalsky, Imig and their respective co-workers (763, 784). They all agree with the notion that BHRF1 miRNAs are expressed during Latency III while BART miRNAs are found in all forms of latency. Furthermore they all found that the BART miRNAs were expressed at dramatically different levels within a given cell line or tumour. Finally, where examined there was a huge variation in overall EBV miRNA levels between different cell lines (763).

Nonetheless there were drastic differences concerning which EBV miRNAs were highest and lowest expressed within a given tumour background. We found that miR-BART7, miR-BART4 and miR-BART15 were frequently the most abundant and miR-BART2-5p and miR-BART13 consistently the least abundant of the BART miRNAs (Fig. 3.13). Imig and co-workers found that miR-BART10, miR-BART22 and miR-BART7 were frequently the most abundant and miR-BART15 and miR-BART20 consistently the least abundant of the BART miRNAs (784). Finally Skalsky and co-workers found that miR-BART1-5p (not tested in the present work) was frequently the most abundant of the BART miRNAs; relative levels of all the remaining BART miRNAs differed from one LCL to the next (763). They also noted that

the miR-BHRF1-1 was expressed at levels up to 16 fold greater than miR-BHRF1-2 and miR-BHRF1-3 in the majority of LCLs examined; the present work suggest that all three BHRF1 miRNAs are almost always expressed at similarly levels (Fig. 3.8). We speculate that these discrepancies are mainly due to differences in the cell line or tumour background studied, as opposed to differing methods of detection. Imig and co-workers demonstrated that quantitative data gathered by sequencing can in most cases be backed up by other techniques such as QPCR and northern blot (784).

On a final note QPCR and deep sequencing have all been used to characterize EBV miRNA expression in NPC tumours (739, 741, 786). Comparisons between these studies revealed that NPC does not have a characteristic EBV miRNA profile as the relative levels of each miRNA differs from one tumour to the next. For instance Chen *et al*. found miR-BART5-5p, miR-BART3-3p and miR-BART9-3p were the most abundant EBV miRNAs while Zhu *et al*. found miR-BART7-3p, miR-BART22 and miR-BART1-5p to be most abundant; this is despite both reports using a similar method of detection (sequencing) (741, 786). Cosmopoulos and co-workers in turn found miR-BART7, miR-BART17-5p and miR-BART16 to be the most abundant EBV miRNAs by means of QPCR (739). Overall the hierarchy of miRNA expression described in the present study agrees most closely with that described by Cosmopoulos *et al* (739).

3.8.3 Exploring the possible determinants of EBV miRNA accumulation

Our data highlight that alterations in BHRF1 transcription do not necessarily correlate with changes in steady state BHRF1 miRNA levels. This is best exemplified by the Wp-restricted BL lines which on average expressed ten-fold more latent BHRF1 transcripts than LCLs, but did not express higher levels of mature BHRF1 miRNAs (Fig. 3.8). We note that BHRF1 pre-

miRNAs may potentially be generated by processing of either a large BHRF1-containing intron present in all primary Cp/Wp-initiated EBNA transcripts (744) or from the 5' and 3' UTRs present within latent BHRF1 transcripts. Our data appear to suggest that this second pathway may be less important for determining the levels of BHRF1 miRNAs in latent infection. To some extent BART miRNA expression correlated with overall levels of BART transcription, although the correlation was better in the case of BL lines than LCLs (Fig. 3.13). Edwards *et al.* reported that BART miRNA production is favoured by the 1-3 BART exon splice form (748). Interestingly we found that 1-3 and 2-3 BART exon splice forms were similar in their correlation to selected BART miRNAs (Fig. 3.14). Nonetheless we appreciate this does not mean BART miRNAs are generated equally from both BART exon splice forms.

As discussed in section 1.3 there are a number of factors which affect miRNA accumulation aside from levels of precursor transcription (70). These factors include processing of the precursor miRNA as well as the inherent stability of a given mature miRNA. Similarly nucleotide polymorphisms in the pre-miRNA sequence have also been reported to disrupt processing of the mature miRNA (738, 743, 748, 787); examples include miR-BHRF1-3 in Raji BL or miR-BHRF1-1 in Jijoye BL.

Therefore we performed additional experiments in order to understand the discordant relationship between EBV precursor transcription and miRNA production. In the first we investigated Drosha and Dicer transcription due to their involvement in the miRNA biogenesis pathway. We found that RNA levels of both genes were relatively constant in the selection of cell lines tested (Fig. 3.15), implying that differences in Drosha and Dicer transcription can not explain differences in EBV miRNA expression. Nonetheless it remains possible that Drosha and Dicer protein levels accumulate differentially among our test lines.

Indeed a recent report has implicated miR-BART6 in the post-transcriptional regulation of Dicer (757).

Following this we investigated whether sequence polymorphisms in the pre-miRNA sequence were contributing to the variations in EBV miRNA measurements. A number of previous studies have already documented the high degree of sequence conservation of BART miRNAs in different EBV strains (738, 748). None of the nine BART miRNAs examined here have previously been reported to carry polymorphisms in the mature miRNA sequence, although some of the BART miRNAs examined here have been reported to carry polymorphisms in the pre-miRNA sequence; these changes were rare and predicted to have no effect on processing (748). Thus we argue that the differential accumulation of individual BART miRNAs is unlikely related to sequence variation.

A detailed investigation into BHRF1 miRNA sequence variation among different EBV positive cell lines revealed that the miR-BHRF1-1 (Fig. 3.10) and miR-BHRF1-2 (Fig. 3.11) sequences were well conserved in 12 virus genomes tested. In contrast, several cell lines contained six changes in the miR-BHRF1-3 pre-miRNA sequence. Remarkably these mutations appeared to maintain the base pairing within the pre-miRNA hairpin loop structure (Fig. 3.12) and did not significantly reduce miR-BHRF1-3 expression. Collectively these findings strongly support the view that BHRF1 miRNAs have been functionally conserved during EBV evolution.

We also note that when sequence variation occurs in the mature miRNA sequence, we cannot eliminate the possibility that the mutation affects PCR detection. This is compounded by the lack of data regarding the QPCR primer-probe sequences due to their commercial nature. Our data (Fig. 3.8) does however suggest that the single polymorphism seen in the mature miR-

BHRF1-3 sequence has little or no effect on PCR amplification; miR-BHRF1-3 was readily detectable in three cell lines (Sal BL, Ava BL and Glor III BL) carrying the nucleotide change, and at levels similar to other cell lines displaying a comparable pattern of latent gene expression.

Finally our data argue that variations in EBV miRNA expression are not due to differences in the stability of individual miRNAs within a cell line. BHRF1 transcripts and BHRF1 miRNAs have similar half lives in X50/7 LCL and two Wp BL lines, Sal-BL and Ava-BL (Fig. 3.16). Similarly all the BART miRNAs tested appeared to have half lives in excess of 12 h (Fig. 3.17).

Nonetheless, it is now known that many cellular miRNAs are also highly stable as compared to cellular transcripts (788). One study in particular found that most cellular miRNAs tested possess half lives in excess of 8h; miR-187, miR-224 and miR-378 in turn possessed half lives in excess of 48 h (93). Therefore we accept the possibility that differences in the stability of individual EBV miRNAs might only become apparent after 24 h.

Two recent studies by Kim *et al*. have provided a number of insights into BART miRNA transcription (789, 790). Firstly they found the BART miRNAs were, much like cellular miRNAs, transcribed by pol II and processed by Drosha and Dicer. Secondly they discovered an inverse correlation between BART miRNA expression and BART promoter methylation across a panel of lymphoid cell lines. Finally they demonstrated that the BART miRNAs were positively regulated by C/EBP β binding upstream of the BART promoters. While these findings may account for some of the variation in EBV miRNA levels between cell lines, they fail to explain why miRNAs derived from the same transcript accumulate to such different levels.

In summary we conclude that differences in steady state BHRF1 and BART miRNA levels are determined primarily by variations in the efficiency of miRNA maturation from their respective precursor transcripts. We will discuss this possibility further in section 6.

4. Quantitative study of EBV encoded miRNAs during EBV mediated B cell transformation and lytic replication

4.1 Introduction

In the first part of our study we investigated EBV miRNA expression in a panel of latently infected lymphoid cell lines. In the current section we will investigate viral miRNA expression during the early events of EBV mediated B cell transformation. Thereafter we will focus on viral miRNA expression following the induction of EBV replication.

4.2 Expression of viral miRNAs during the early events of EBV mediated B cell transformation

The kinetics of EBV gene expression following primary infection of human B cells are well established. Wp is activated immediately post infection (323, 326, 791), leading to the initial expression of EBNA2, EBNA-LP and also BHRF1 (320, 323, 324, 513). Wp activity then falls after 24 h as Cp activity becomes dominant, concomitant with the broadening of latent antigen expression to the full spectrum of EBNAs and LMPs. Nonetheless when we began our study there was no available information on the kinetics of EBV miRNA expression during the same events.

To address this issue we isolated primary B cells from peripheral blood using CD19 Dynabeads (Invitrogen) and subsequently exposed them to preparations of recombinant 2089 EBV at a multiplicity of infection (moi) of 100 using published methods (326). Infected cells were cultured in fresh medium and harvested at 0 h, 8 h, 12 h, 24 h, 48 h, 72 h and 120 h. By 120 h abundant lymphoblast formation was clearly visible by microscopic analysis implying

efficient transformation. Note that the recombinant 2089 EBV strain used in this work contains the same 12kb BamHI A deletion as the prototype B95-8 strain (Fig. 4.1B) (267); therefore in this experiment it was necessary to detect the BART transcripts using an alternative primer/probe combination which specifically amplified sequences across the exon 6-7 splice junction.

The data in Fig. 4.2A show the results of this BART6-7 assay, alongside standard assays to measure Wp-initiated transcripts, Cp-initiated transcripts and BHRF1 transcripts. As expected, Wp activity was already induced by 8 h post infection, peaked at 12 h and then fell as the level of Cp activity began to increase; latent BHRF1 expression was also robustly induced by 8 h (Fig. 4.2A). By contrast lytic BHRF1 was only transiently detectable in the first 24 h post-infection. The appearance of the BHRF1 miRNAs was significantly delayed relative to BHRF1 transcription, with weak signals first detected between 12-24 h which then gradually increased throughout the experiment (Fig. 4.2B). Kinetic analysis of BART RNAs also showed a similar lag in the appearance of mature BART miRNAs relative to BART transcription (Figs. 4.2A and 4.2B).

4.3 Expression of EBV miRNAs during lytic replication

As discussed in section 1.12, productive infection does not occur in *de novo* infected cultured B cells, even though BZLF1 is reportedly expressed within the first few hours post-infection (416). BHRF1 and BART transcripts are nonetheless both induced during lytic replication (275, 410, 747), although if and to what extent BHRF1 and BART miRNA levels also increase is less clear. We note that during lytic replication, BHRF1 and its associated miRNAs would be transcribed from an alternative promoter BHRF1p (747); as illustrated in

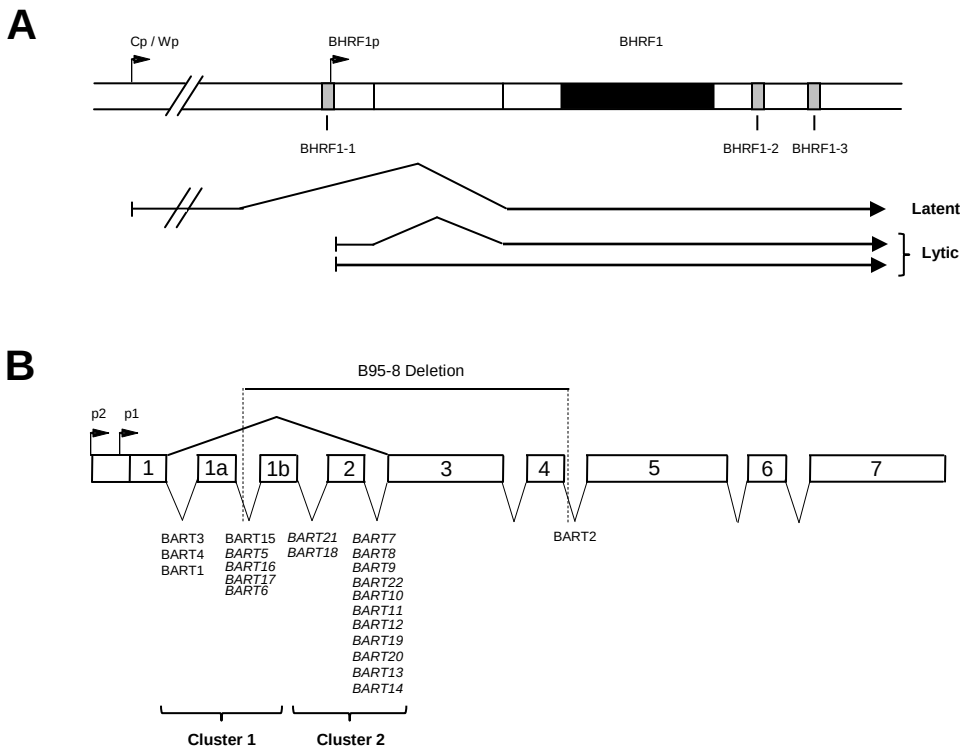

Fig. 4.1. Detailed structure of EBV transcripts and miRNAs. **(A)** BHRF1 transcripts and location of BHRF1-derived miRNAs. All three BHRF1 miRNAs may be generated during lateny either by processing of an intron present within the Cp/Wp initiated primary EBNA transcript or by processing of the 5′ and 3′ untranslated regions within latent BHRF1 transcripts with the W2-Y1-Y2-BHRF1 structure. In contrast lytic BHRF1 transcripts initiated from the alternative BHRF1p promoter only encode miR-BHRF1-2 and miR-BHRF1-3. **(B)** Detailed structure of the highly spliced BARTs and location of the BART-derived miRNAs (adapted from Edwards et al.) (748). The BART miRNAs form two clusters within the BART introns, with the exception of mirBART2 which lies further downstream. The prototype B95-8 EBV strain carries a 12kb deletion in this region which removes several cluster 1 miRNAs and all cluster 2 miRNAs (shown in italics).

Fig. 4.2. Expression of latent transcripts and EBV miRNAs in primary B cells infected with EBV in vitro. **(A)** Wp- and Cp-initiated transcripts, BHRF1 transcripts and BARTs were quantified by QPCR at the indicated time points post-infection. Since the recombinant EBV used in these experiments carries the same BamHI A deletion as the B95-8 strain, BARTs were detected using a primer/probe combination which amplified across the exon 6-7 splice junction. **(B)** Expression of selected BHRF1 and BART miRNAs measured by QPCR. Data were normalised to RNU48 expression and expressed as copy numbers per pg input RNA. Shown on each graph are representative time courses for two of three replicate experiments. Each data point corresponds to the average of two replicate assay measurements.

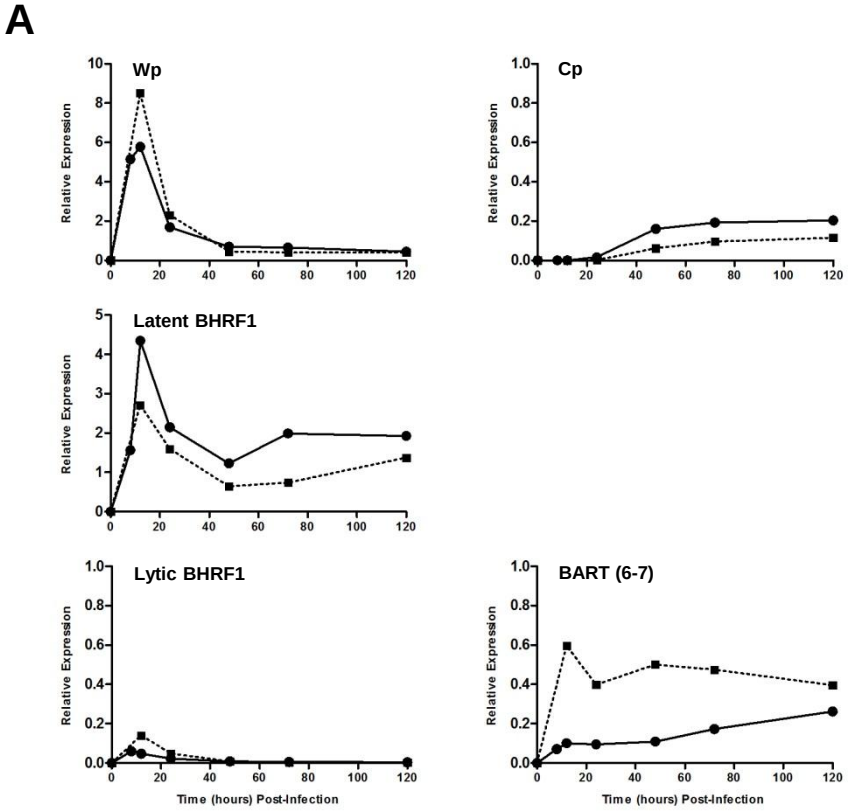
A
Wp
Cp
Latent BHRF1
Lytic BHRF1
BART (6-7)
Relative Expression
Time (hours) Post-Infection

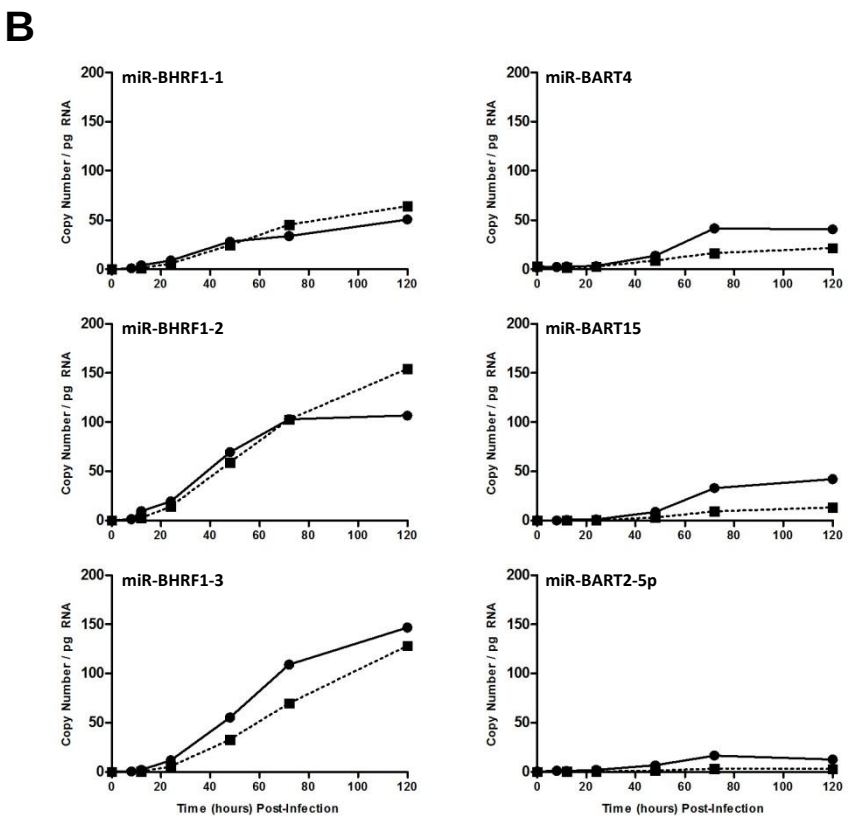
B
miR-BHRF1-1
miR-BART4
miR-BHRF1-2
miR-BART15
miR-BHRF1-3
miR-BART2-5p
Copy Number / pg RNA
Time (hours) Post-Infection

Fig. 4.1A, this lytic BHRF1 transcript overlaps the miR-BHRF1-1 sequence and therefore can only generate the two downstream BHRF1 miRNAs. Earlier studies have yielded contradictory findings on EBV miRNA expression during lytic infection (738, 743, 744). In order to resolve these issues we exploited the AKBM cell system in which EBV-positive Akata-BL cells are stably transfected with a GFP reporter gene under the control of the EBV lytic cycle BMRF1 promoter; following Ig crosslinking, a significant proportion of cells enter into lytic cycle and these cells can be identified by GFP expression (773). Note that unlike the B95-8 prototype strain, Akata-BL retains the entire BART region. Therefore in order to assess BART transcription we reverted back to the exon 1-3 assay; this assay measures the exon 2-deleted BART splice variant which, as discussed in section 3.1, favours the production of the BART miRNAs (748).

4.3.1 Short (24h) lytic induction of AKBM cells

In the first instance, we monitored the production of BHRF1 and BART transcripts and derived miRNAs in AKBM cells at various time points up to 24 h post induction. Entry into lytic cycle was confirmed by quantifying both the number of GFP and BZLF1 positive AKBM cells by flow cytometry (Fig. 4.3). BZLF1 positive lytic cells were detected by flow cytometry within 4 h and increased to around 22% of the culture at 24 h. GFP positive lytic cells appeared with similar albeit slightly delayed kinetics. In the experiments shown in Fig. 4.4, lytic BHRF1 transcripts appeared with similar kinetics to BZLF1 (Fig. 4.4A) and coincided with marked increases in miR-BHRF1-2 and 1-3 miRNAs, but not miR-BHRF1-1 (Fig. 4.4B); this is consistent with BHRF1 transcription being initiated from the lytic promoter BHRF1p, rather than the latent promoters Cp/Wp, at these early time points. In

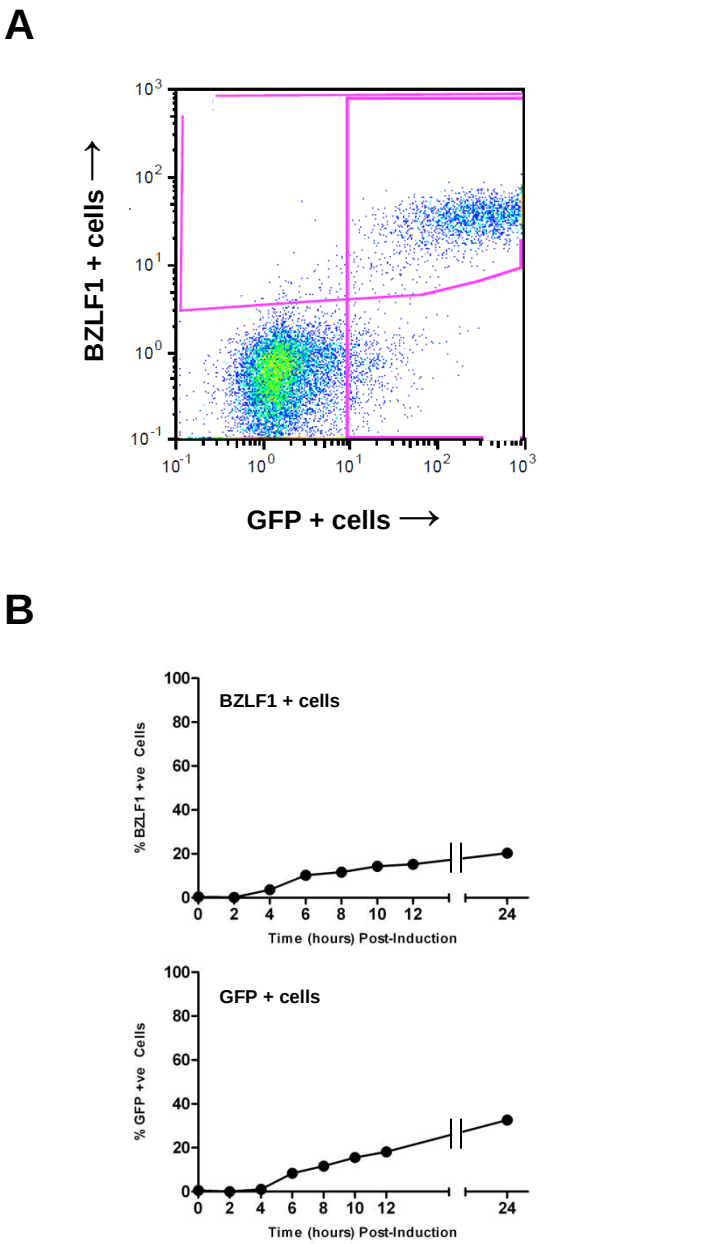

Fig. 4.3. Lytic induction of latent AKBM cultures over 24 hours. Lytic GFP-positive AKBM cells were enumerated at the indicated time points post-induction by flow cytometry. BZLF1 expression was assessed in the same samples by staining with BZ.1 anti BZLF1 antibody. **(A)** FACS plot illustrating the lytic GFP/BZLF1 double positive and latent GFP/BZLF1 double negative AKBM populations at 12 hours post-induction. **(B)** Percentage of lytic BZLF1 and GFP positive AKBM cells at each time point post-induction. Shown are representative data from one of two experiments.

Fig. 4.4. Expression of EBV transcripts and miRNAs in lytic AKBM cultures 24 h post-induction. **(A)** BHRF1 and BART transcripts quantified by QPCR at the indicated time points in the same culture shown in Fig. 4.3. Latent BHRF1 values are expressed relative to a reference LCL, while lytic BHRF1 values are expressed such a value of one is equivalent to 100% positive cells. **(B)** Expression of selected BHRF1 miRNAs and BART miRNAs determined by QPCR at the indicated time points. Data were normalised to RNU48 expression and expressed as copy numbers per pg input RNA. Shown on each graph are time courses for two replicate experiments. Each data point corresponds to the average of two replicate assay measurements.

A

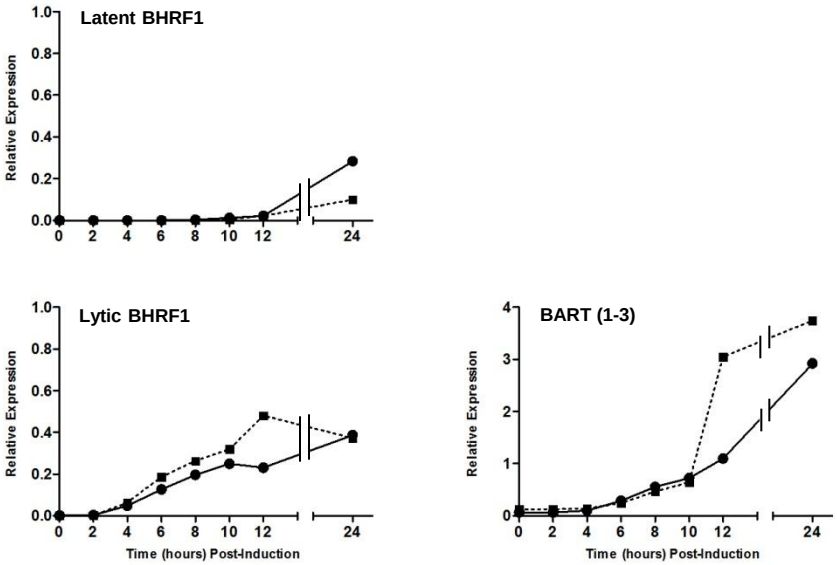
Latent BHRF1
Relative Expression
1.0
0.8
0.6
0.4
0.2
0.0
0 2 4 6 8 10 12 24
Lytic BHRF1
Relative Expression
Time (hours) Post-Induction
BART (1-3)
Relative Expression
4
3
2
1
0
Time (hours) Post-Induction

B

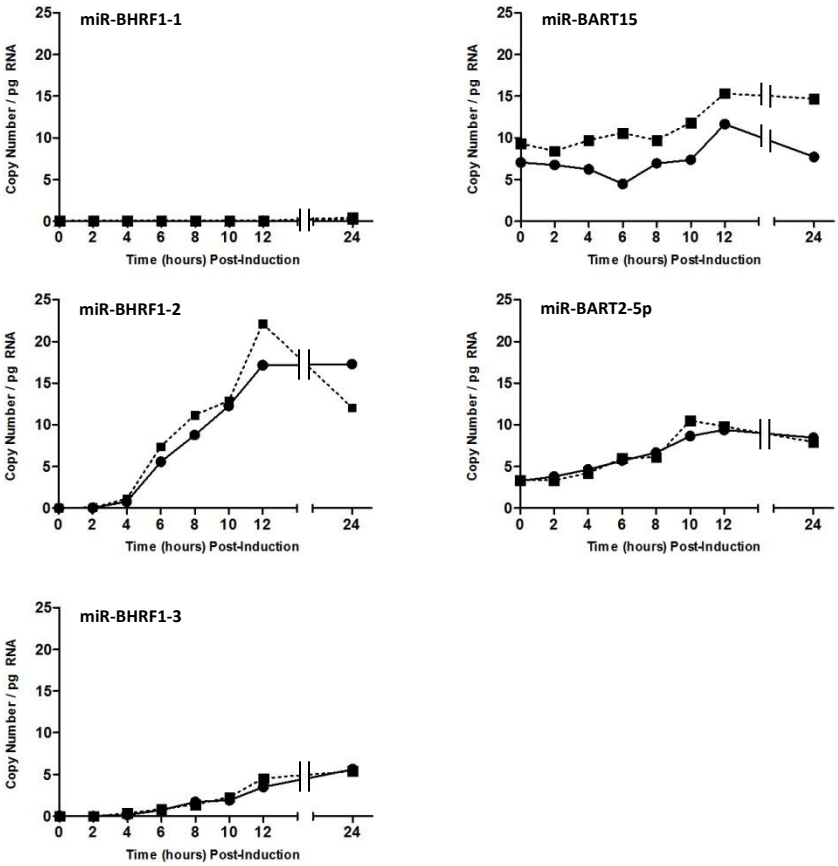
miR-BHRF1-1
Copy Number / pg RNA
25
20
15
10
5
0
0 2 4 6 8 10 12 24
Time (hours) Post-Induction
miR-BART15
miR-BHRF1-2
miR-BART2-5p
miR-BHRF1-3

contrast, levels of BART-derived miRNAs (here illustrated with data for miR-BART15 and miR-BART2-5p) barely increased during the same 24 h period despite the fact that BART transcript levels increased more than 45-fold (Figs. 4.4A and 4.4B).

4.3.2 Extended (120h) lytic induction of AKBM cells

To examine whether the relatively small increases in miR-BART miRNA expression might be due to a delay in processing the BART transcripts, we repeated the experiment but now analysed gene expression in the induced AKBM cells for up to 120 h post induction. Given the similar kinetics of GFP and BZLF1 induction in these experiments, we quantified the number of lytic AKBM cells by GFP alone (Fig. 4.5). The number of GFP positive AKBM cells detected at 24h was comparable to previous experiments (Fig. 4.3). Furthermore lytic BHRF1 and BART transcripts showed similar levels of induction at 24 h (Fig. 4.6A) to the previous experiments (Fig. 4.4) and thereafter remained relatively constant. However we now observed that latent BHRF1 transcripts became detectable at later time points, coincident with induction of the Lat III promoters Wp and Cp (Fig. 4.6A and data not shown) and broadening of miRNA expression to all three miR-BHRF1 miRNAs (Fig. 4.6B). Consistent with our earlier findings, we again noted a rapid and dramatic increase in BART transcription accompanied by only modest 5-8 fold increase in levels of miR-BART4, miR-BART15 and miR-BART2-5p.

4.3.3 Analysis of sorted lytic AKBM cells

The above findings suggested that BHRF1 miRNA production during virus replication is biphasic, with early lytic BHRF1 transcripts selectively generating miBHRF1-2 and miR-

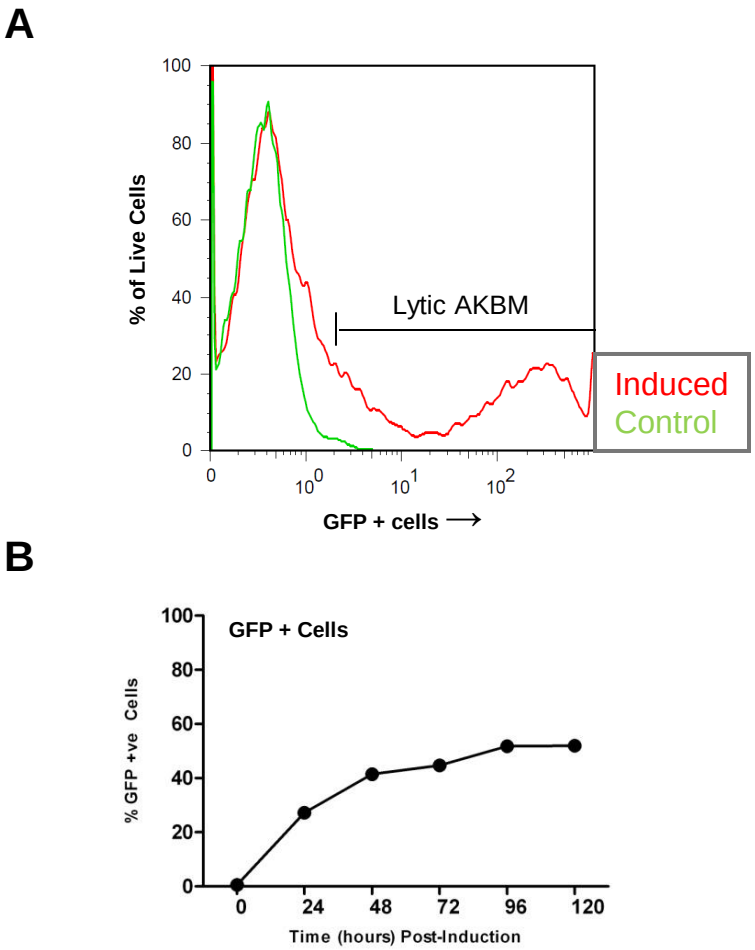

Fig. 4.5. Lytic induction of latent AKBM cultures over 120 hours. Lytic GFP-positive AKBM cells were enumerated at the indicated time points post-induction by flow cytometry. **(A)** FACS histogram illustrating lytic and latent populations in induced AKBM cells at 24h post-induction. Non-induced AKBM cells were used as negative controls. **(B)** Percentage of lytic GFP positive AKBM cells in the induced population at each time point post-induction.

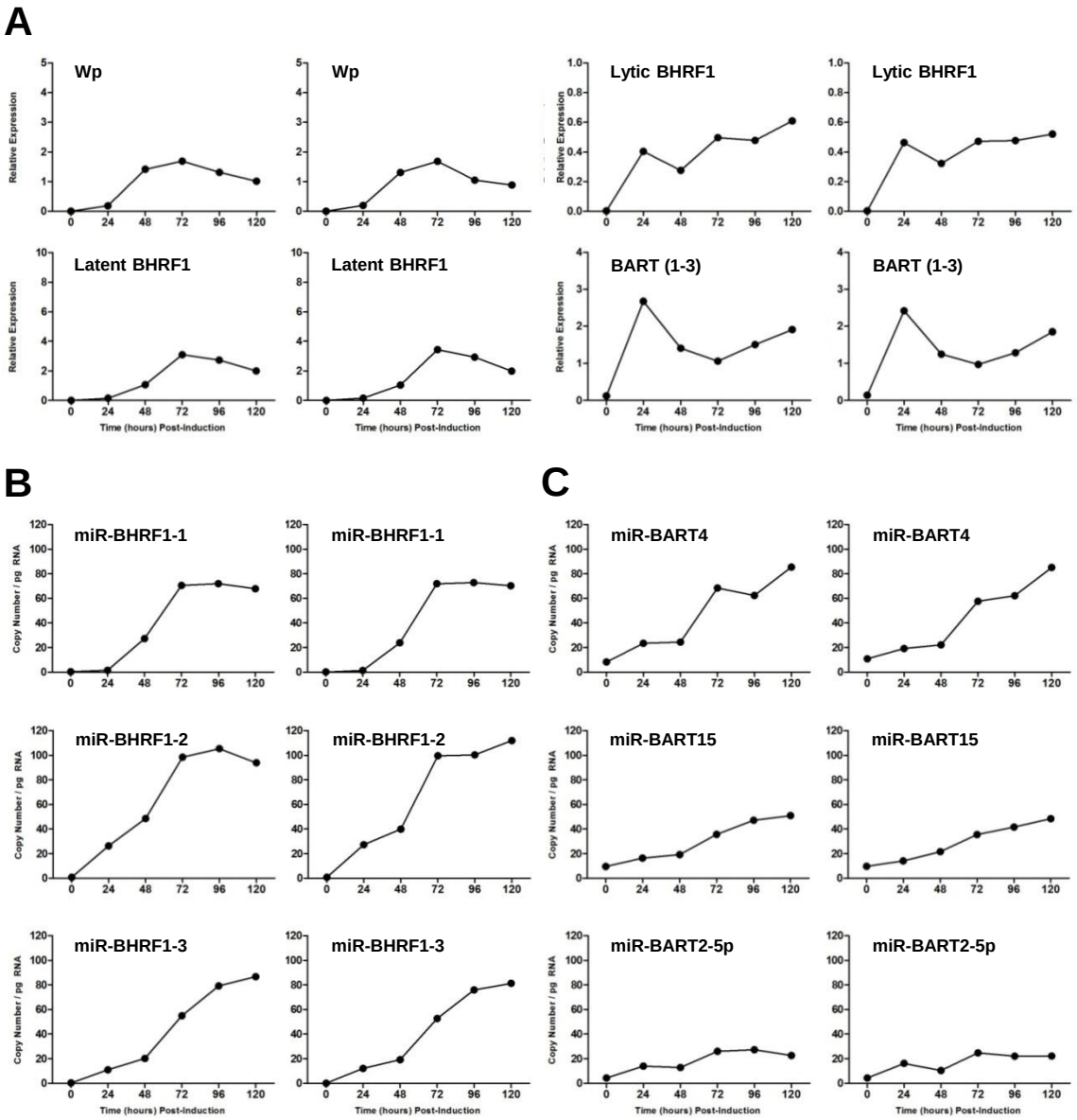

Fig. 4.6. Extended time course showing expression of EBV transcripts and miRNAs in lytic AKBM cultures. **(A)** Wp, latent BHRF1 and lytic BHRF1 transcripts and BARTs (exon 1-3 splice form) were quantified by QPCR in the same induced cells shown in Fig. 4.5. **(B)** and **(C)** show expression of selected BHRF1 and BART miRNAs, respectively, determined by QPCR. Shown in separate panels are two replicate assay measurements obtained from a single experiment.

BHRF1-3, while delayed latent BHRF1 transcripts are processed to give all three miR-BHRF1 miRNAs. This is consistent with the appearance of Lat III transcripts during the later stages of virus replication (Fig. 4.6), in agreement with an earlier study (744). To further examine the role of Lat III transcripts in miRNA production we next confirmed that the latent transcripts were present in the lytic AKBM population. Briefly, AKBM cells were induced into lytic cycle as before and then sorted into GFP-positive (lytic) and GFP-negative (latent) populations at 48 h post induction. We found that both latent and lytic BHRF1 transcripts, and all three miR-BHRF1 miRNAs, were greatly enriched in the GFP-positive fraction relative to the GFP-negative population (Fig. 4.7).

4.3.4 Using acyclovir to inhibit lytic replication in AKBM cells

We speculated that the Lat III transcripts seen in lytic AKBM cultures were being transcribed from the very high copy numbers of newly replicated EBV genomes, since such genomes are unmethylated and could therefore act as templates for Wp- and Cp-initiated transcription. To test this hypothesis, we induced AKBM cells in the presence of acyclovir (ACV) to block viral DNA replication. In the absence of ACV, we confirmed that the average EBV genome load increased from around 50 genomes per cell to as much as 16,000 genomes per cell in induced control AKBM cells. The addition of ACV completely blocked this genome amplification (Fig. 4.8A) and also ablated induction of Latency III Wp, Cp and BHRF1 transcripts as well as miR-BHRF1-1 (Figs. 4.8B and 4.8C); these data support the view that these transcripts are dependent on viral DNA synthesis. In contrast, ACV treatment only modestly reduced levels of lytic BHRF1 and BART transcripts (~2-fold and less than 5-fold, respectively) (Fig. 4.8B) and made little difference to expression of the two remaining miR-

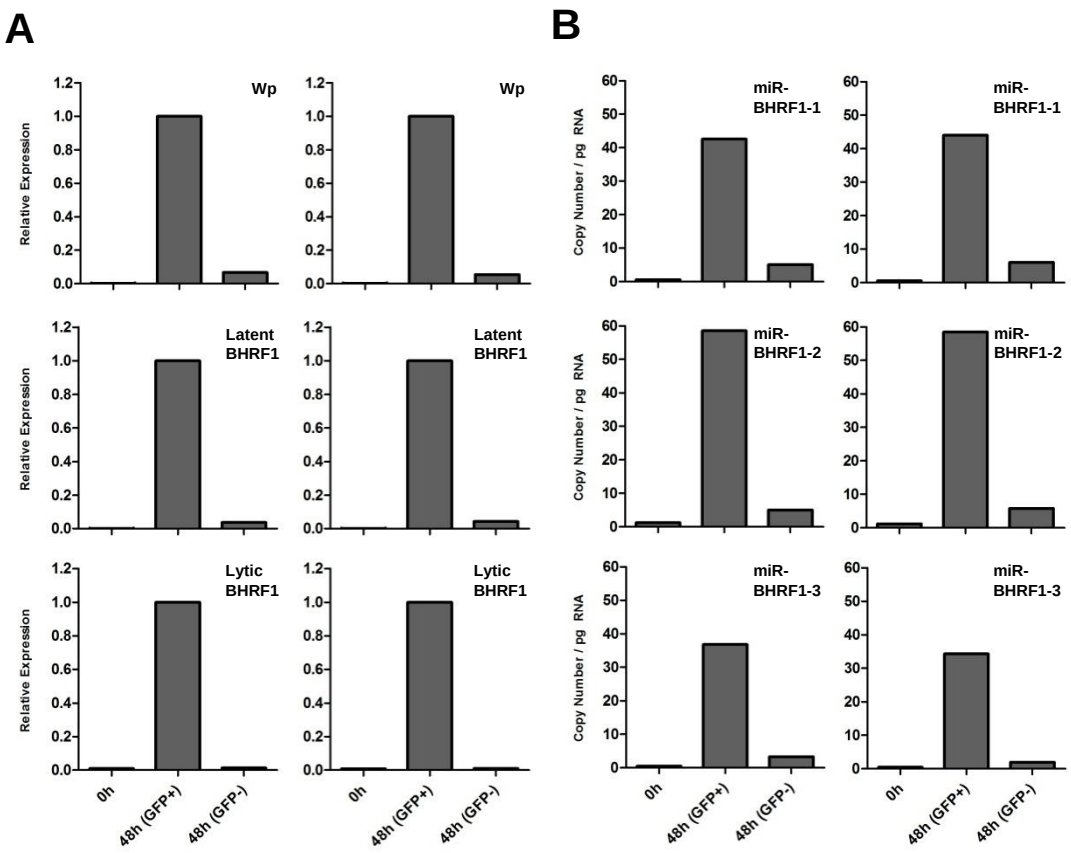

Fig. 4.7. GFP sorting of induced AKBM cells. AKBM cells were induced and sorted at 48 hours for GFP expression. **(A)** Wp and BHRF1 (latent and lytic) transcripts were quantified by QPCR. Data are expressed relative to the 48h GFP + ve population (set at one). **(B)** Expression of BHRF1 miRNAs in the same populations as determined by QPCR. Data were normalised to RNU48 expression and expressed as absolute copy numbers per pg total RNA. Shown in separate panels are two replicate assay measurements obtained from one of two replicate experiments.

Fig. 4.8. Effect of ACV on expression of EBV transcripts and miRNAs in induced AKBM cultures. **(A)** EBV genome load quantified by QPCR 48 h post induction. Data were normalised to cellular beta-2-microblobulin copies and expressed as EBV genomes per cell. **(B)** Wp, Cp, latent and lytic BHRF1 transcripts and BARTs (exon 1-3 splice) quantified by QPCR 48 h post induction. Data are expressed relative to values seen in the uninhibited culture. **(C)** and **(D)** show expression of selected BHRF1 and BART miRNAs, respectively, determined by QPCR. Data were normalised to RNU48 expression and expressed as copy numbers per pg input RNA. Shown on each graph are two replicate experiments. Each data point corresponds to the average of two replicate assay measurements.

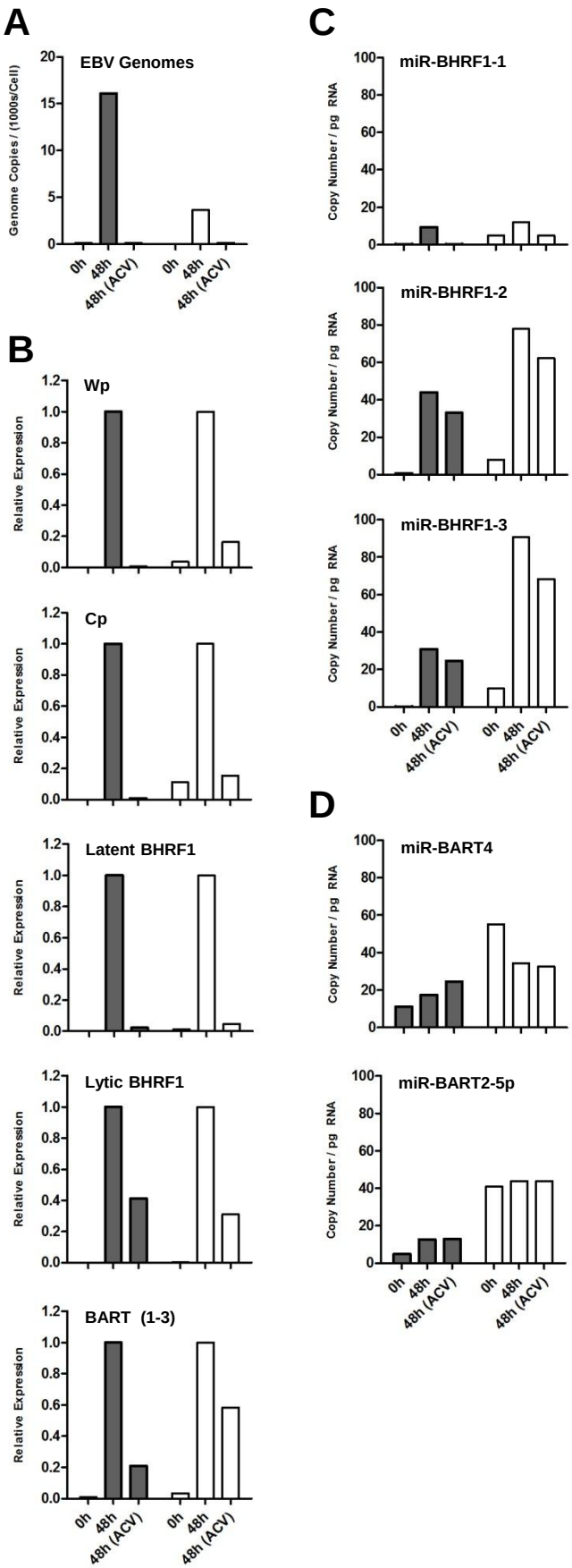
A
EBV Genomes
Genome Copies / (1000s/Cell)
0h
48h
48h (ACV)
B
Wp
Cp
Latent BHRF1
Lytic BHRF1
BART (1-3)
Relative Expression
C
miR-BHRF1-1
miR-BHRF1-2
miR-BHRF1-3
Copy Number / pg RNA
D
miR-BART4
miR-BART2-5p

BHRF1 miRNAs or the BART miRNAs tested (miR-BART4 and miR-BART2-5p) (Figs. 4.8C and 4.8D).

4.3.5 Stability of BART miRNAs in latent vs. lytic AKBM cells

In a final experiment, we asked whether the failure to significantly increase BART miRNA expression during virus replication was due to changes in BART transcript or BART miRNA stability. Briefly, AKBM cells were induced as before and then 12 h post induction, the cells were either cultured in normal medium or transferred to medium containing Actinomycin D to block further RNA transcription. We found that the BART transcripts and the three BART miRNAs (miR-BART4, miR-BART7 and miR-BART2-5p) examined had similar long half lives in lytically induced and latent AKBM cultures (Fig. 4.9). These half lives were also comparable to latently infected cell lines examined previously (Fig. 3.17), arguing that the weak induction of the BART miRNAs was not due to increased miRNA turnover during lytic cycle.

4.4 Discussion

4.4.1 Viral miRNA expression during EBV mediated transformation of B cells

In the first set of experiments we looked at miRNA expression during the early events of B cell transformation. Interestingly we found that EBV miRNA production was delayed with respect to the induction of BHRF1 and BART transcripts (Fig. 4.2). In the case of the BHRF1 miRNAs, one possible explanation for the delay in miRNA production could be that the pre-

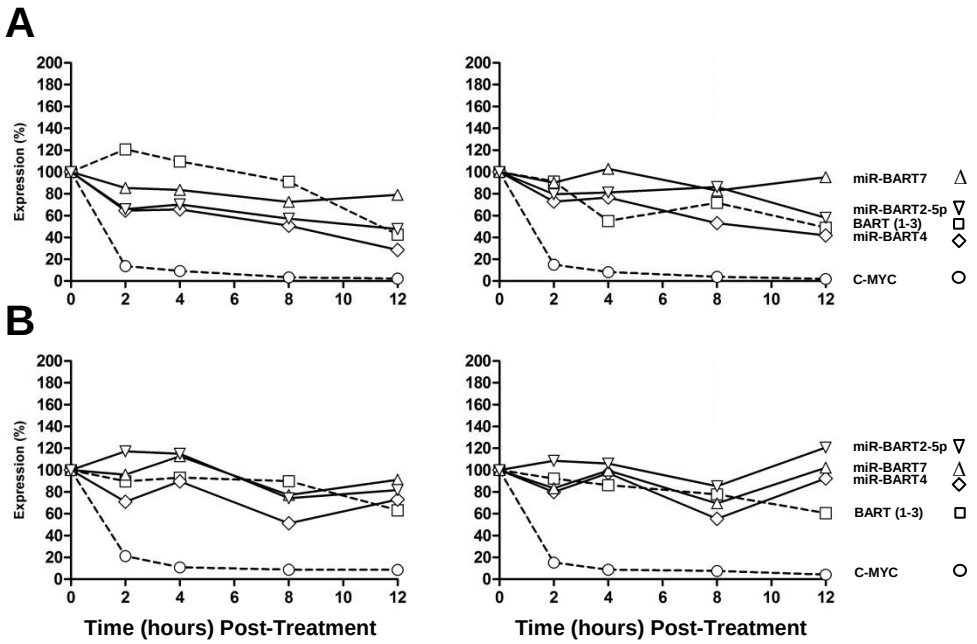

Fig. 4.9. Stability of BART transcripts and miRNAs in latent and induced AKBM cultures. AKBM cells were split into two populations and **(A)** cultured normally for 12h or **(B)** induced for the same duration. Both populations were then treated with 5µg/ml actinomycin D, harvested at the indicated time points and analysed for BART transcripts and miRNAs. Cellular c-myc RNA is unstable and served as a positive control for RNA decay. Shown in separate panels are two replicate assay measurements obtained from a single experiment. All data were normalised to RNA input.

miRNAs are only efficiently processed once the Wp-to-Cp switch has occurred between 24-48h post infection (323, 326, 791). Interestingly BART transcripts can also be expressed from two alternative promoters, P1, which is expressed early post-infection, and P2, which is only activated after 48 h (729). It remains to be tested whether BART miRNAs are preferentially generated from P2-initiated BART transcripts. An alternative possibility is that precursor miRNAs are actually transcribed much earlier than 48h but their processing is delayed. On that note Nourse *et al.* observed that EBV miRNAs are maintained as precursors (pre-miRNAs) throughout the initial stages of B cell infection (unpublished data).

The presence of the EBV miRNAs throughout early EBV infection means they could potentially contribute to B cell transformation. The lack of significant levels of EBV miRNAs at early time points, when EBNA2 and EBNA-LP are already abundantly expressed (323, 324), argues that they are not essential for the initiation of B cell growth transformation. On this point a recent study demonstrated that EBV mutants lacking the BHRF1 miRNAs (Δ123) display a reduced transforming capacity (750). However they only detected discernable differences between wild type and Δ123 EBV after 5 days post infection at which point the BHRF1 miRNAs are clearly expressed (Fig. 4.2). Another study demonstrated that the BHRF1 miRNAs protect B cells against apoptosis and promote cell cycle progression during the early stages of B cell infection (751). Again these effects were observed after 5 days post infection.

The contributions of the BART miRNAs throughout the early stages of B cell infection remain unclear. The efficient transformation mediated by the prototype B95-8 virus clearly demonstrates that many of the BART miRNAs are dispensable for transformation *in vitro*. Conversely reconstitution of the deleted BART miRNAs in the B95-8 strain does not result in noticeably increased proliferation or survival of *de novo* infected B cells (751). Nonetheless

these observations do not exclude the possibility that BART miRNAs still present in the B95-8 virus contribute to transformation. On that note miR-BART1 and miR-BART3 have been found to target Bim while miR-BART2 targets the viral polymerase BALF5 (754, 759). We appreciate that these studies were mostly conducted using epithelial as opposed to lymphoid cell lines. Nonetheless it is still tempting to speculate that the BART miRNAs might provide survival signals to *de novo* infected B cells whilst suppressing viral reactivation once latency has been established.

4.4.2 Viral miRNA expression following EBV lytic replication

A number of previous studies have reported contradictory findings on EBV miRNA expression during virus replication (738, 743, 744). Northern blot studies by Cai and co-workers showed that with the exception of miR-BHRF1-1, all BHRF1 and BART miRNAs tested were increased following lytic induction. By contrast similar studies by Xing and Kieff showed that all BHRF1 miRNAs were increased following lytic induction while levels of the BART miRNAs remained unchanged (744). Similar results were obtained by Pratt and co-workers using a different detection method (QPCR) (743). Overall our data seems to agree most with the latter two studies.

We clearly demonstrate that all three BHRF1 miRNAs are strongly induced in lytic cycle, approaching levels seen in Latency III LCLs. Our detailed kinetic studies show that both lytic and latent BHRF1 transcripts potentially contribute to this increase in BHRF1 miRNAs (Fig. 4.6), thus the initial increases in miR-BHRF1-2 and miR-BHRF1-3 correlated with the induction of early lytic BHRF1 transcripts, while the expression of BHRF1-1 was delayed until after the induction of Cp/Wp-initiated transcripts (410) and dependent on new viral DNA

replication (Fig. 4.8). The up regulation of the BHRF1 miRNAs during viral replication suggest they could participate in immune evasion or in protecting virus producing cells from apoptosis; this would agree with the observations that miR-BHRF1-1 and miR-BHRF1-3 target p53 and CXCL11, respectively. Alternatively the BHRF1 miRNAs may function to regulate EBV lytic cycle genes.

In contrast, virus replication was associated with relatively modest (5-8 fold) increases in BART miRNA levels (Figs. 4.4 and 4.6), in agreement with two earlier studies (743, 744). However this latter finding is difficult to reconcile with the much bigger increases in overall BART transcription during lytic cycle. As the BART miRNAs are very stable in both latent and lytic cycle, we conclude that the BART transcripts which accumulate during replication are inefficiently processed into mature miRNAs. These observations raise the question as to the role of the BARTs in the context of virus replication. On this point, several open reading frames (RPMS1, A73) have previously been identified within the BART transcripts and a number of studies have proposed that these may give rise to functional proteins (727, 731). While there is no evidence to date to support the view that these protein products are naturally expressed in latently infected cells (721, 732, 735, 736), our data would suggest that such protein products might be detectable in productive infection where there are dramatically elevated levels of BART transcripts. Alternatively, the BARTs might have other roles, such as encoding a recently identified small nucleolar RNA, v-snoRNA1 (742).

5. Investigating the function of the BHRF1 miRNAs in the context of BL

5.1 Introduction

In the previous chapters we correlated viral miRNA expression with levels of BHRF1 and BART transcripts in a variety of cell lines with different forms of EBV infection. Our study demonstrated for the first time that the three BHRF1 miRNAs are abundantly expressed in Wp-restricted BL (Wp BL) but not Latency I BL (Lat I BL) cell lines.

Earlier studies have demonstrated that the broader viral antigen expression found in Wp BL lines grants these cells more resistance to induced cell death than their Lat I counterparts (681). Previous reports have investigated the contributions of gene products expressed in Wp BL but not Lat I BL (BHRF1, EBNA-LP and EBNA3) towards the increased pro-survival signal (320, 511, 512). The observation that the BHRF1 miRNAs support B cell growth and survival (750, 751) prompted us to ask whether the BHRF1 miRNAs also contribute to the pro-survival phenotype of Wp- restricted Burkitt lymphoma (681).

Thus we wanted to establish which genes, either cellular or viral, are targeted by the BHRF1 miRNAs and test if such targets may contribute to the underlying mechanism of apoptosis resistance in Wp BL. In order to achieve this we undertook two complementary approaches. Firstly we attempted to knock down the BHRF1 miRNAs in Wp BL lines using antisense oligonucleotide inhibitors. Secondly we attempted to express the BHRF1 miRNAs in either an EBV negative or Lat I BL line. In the first part of this chapter, we will focus on the design and validation of the methodologies used to investigate BHRF1 miRNA function. In the second part of this chapter we will investigate the effects of the BHRF1 miRNAs on the

transcriptome of a BL cell line as well as their contribution towards cell growth and cell survival.

5.2 Establishing a reporter system to assess functional changes in BHRF1 miRNA expression

Before developing methodologies for knockdown or expression of the BHRF1 miRNAs, we needed to have a system to detect functional changes in BHRF1 miRNA levels. For this we exploited the pMIR-REPORT^{TM} miRNA expression reporter vector system by Ambion®.

5.2.1 Cloning of the BHRF1 miRNA reporter constructs

The firefly luciferase construct (pMIR-REPORT^{TM} Luciferase) contains a multiple cloning site (MCS) in the luciferase gene 3′ UTR for cloning of known or artificial miRNA targets. This allows the miRNA of interest to negatively regulate firefly luciferase activity. We therefore cloned DNA oligonucleotide sequences representing individual BHRF1 miRNA binding sites (Fig. 5.1B) between the HindIII and SacI cloning sites of pMIR-REPORT^{TM} Luciferase (Fig. 5.1A). The resulting miR-BHRF1-1, 1-2 and 1-3 reporter constructs each had a single perfectly complementary miR-BHRF1-1, 1-2 and 1-3 binding site, respectively, in the luciferase gene 3′ UTR.

5.2.2 Validation of the BHRF1 miRNA reporter constructs

To test that the luciferase activities of the BHRF1 miRNA reporter constructs were specifically reduced in the presence BHRF1 miRNAs, we transfected each construct into the

A

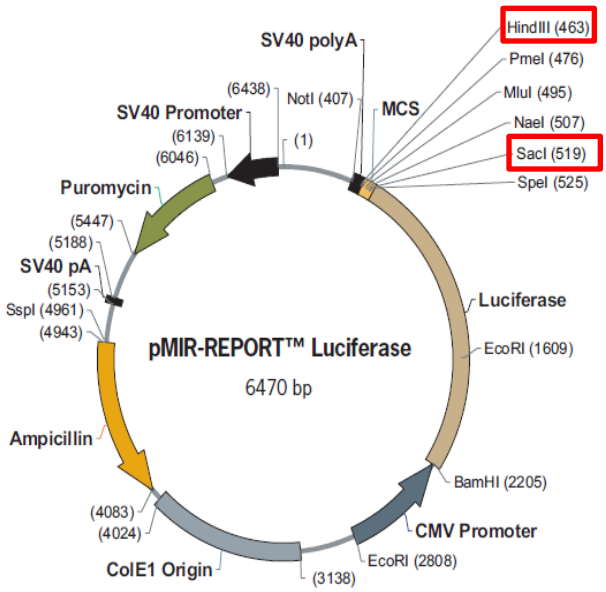

B

	(Hind III)	(Sac I)
miR-BHRF1-1 Binding Site	5'-AGCTTTAACCTGATCAGCCCCGGAGTTGAGCT-3'	
	3'- AATTGGACTAGTCGGGGCCTCAAC-5'	
miR-BHRF1-2 Binding Site	5'-AGCTTTATCTTTTGCGGCAGAAATTGAGAGCT-3'	
	3'-AATAGAAAACGCCGTCTTTAACTC-5'	
miR-BHRF1-3 Binding Site	5'-AGCTTTAACGGGAAGTGTGTAAGCACAGAGCT-3'	
	3'-AATTGCCCTTCACACATTCGTGTC-5'	

Fig. 5.1. Schematic describing the generation of the BHRF1 miRNA luciferase reporter constructs. **(A)** The miRNA firefly reporter vector pMIR-REPORT™ Luciferase, commercially available from Ambion®, served as a starting point for the generation of the BHRF1 miRNA reporter constructs. Sequences corresponding to miRNA target sites are introduced into the multiple cloning site of the luciferase 3′ UTR such that luciferase expression will be inhibited if the target miRNA is expressed in the transfected host cell. **(B)** DNA oligonucleotide sequences corresponding to individual BHRF1 miRNA binding sites were inserted between the HindIII and SacI cloning sites of pMIR-REPORT™ Luciferase to yield the miRBHRF1-1, 1-2 and 1-3 reporter constructs.

EBV negative BL line DG75 and the EBV positive Wp-restricted BL line Oku-BL (Fig. 5.2). The results show that in the presence of the BHRF1 miRNAs (Oku BL), all three miRNA reporter constructs were significantly down-regulated ($P < 0.05$); luciferase activities of the BHRF1-1 and BHRF1-3 miRNA reporters were reduced between 3-4 fold relative to the unmodified pMIR-REPORT^{TM} construct while that of the BHRF1-2 miRNA reporter was reduced nearly 10 fold. In the absence of the BHRF1 miRNAs (DG75 BL) however, all three BHRF1 miRNA reporters showed similar activities to the unmodified pMIR-REPORT^{TM} construct with differences rarely exceeding 15%. Thus expression of all three miRNA reporters was specifically inhibited in the presence of BHRF1 miRNAs.

5.3 Investigating antisense technology as a means to knockdown the BHRF1 miRNAs

Having established a system to monitor the suppressive effects of the BHRF1 miRNAs, next we wanted to determine whether we could functionally knock down the BHRF1 miRNAs using anti-miRNA oligonucleotides (AMOs).

5.3.1 An introduction to anti-miRNA oligonucleotides (AMOs)

The current knowledge of AMOs has been reviewed by Lennox and Behlke (792). While antisense technology itself has been around for over 30 years, more recently it has been successfully adapted to the study of small non-coding RNAs such as miRNAs. In order to functionally inhibit a miRNA, an AMO needs to contain a sequence that is the reverse complement of the target miRNA seed. Possible mechanisms by which AMOs inhibit miRNA

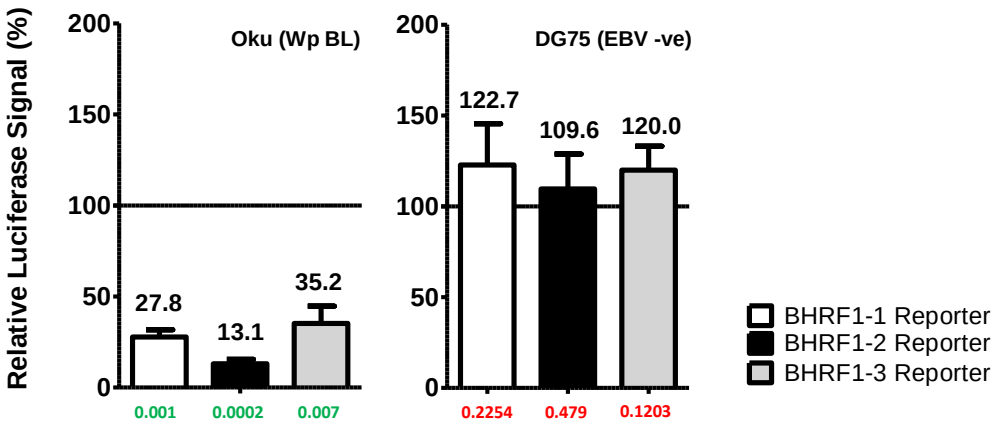

Fig. 5.2. The BHRF1 miRNAs are capable of specifically down regulating an artificial reporter construct. EBV positive Oku (Wp BL) cells were transfected with either the empty control pMIR-REPORT^{TM} firefly reporter construct or derivatives containing a single binding site for miR-BHRF1-1, 1-2 or 1-3. The same cells were co-transfected with the pRL SV40 *Renilla* reporter construct, commercially available from Promega. Firefly luciferase activity was measured in cell lysates prepared 24h post-transfection and normalized to *Renilla* luciferase activity measured in the same samples. Normalized luciferase data was expressed relative to the empty control pMIR-REPORT^{TM} firefly reporter (set at 100%). These values are listed above each column. DG75 (EBV negative) cells were used as a control. Error bars indicate standard deviation of three separate experiments. Normalized luciferase activity for each BHRF1 miRNA reporter was compared to that of the control reporter in each cell line, using a paired t test with a P value cut off set to 0.05. P values are listed below each column using green and red text to denote statistical significance and insignificance respectively.

function are to cause its degradation or sequester it in an inactive duplex; precisely which occurs may be dependent on the chemical nature of the AMO in question (793). It is also possible to design an AMO that interferes with miRNA processing (794).

The potency of an antisense miRNA inhibitor depends amongst other things on its ability to resist nuclease degradation, to specifically and strongly interact with its target, and to be efficiently taken up by the cell (792). Straightforward DNA based AMOs are rapidly degraded when exposed to serum nucleases (795). Their stability and overall efficacy may be boosted by any number of previously tried and tested chemical modifications used in mRNA knockdown studies (792, 796). For instance several earlier studies have achieved miRNA knockdown using 2′-O-alkyl RNA such as 2′-O-methyl RNA (2′OMe) and 2′-O-methoxy-ethyl RNA (MOE) (797-800). The presence of a 2′-O-alkyl group in place of a 2′-OH group on the ribose ring of this class of AMO confers greater nuclease resistance and target affinity as compared to DNA. Similarly other groups have incorporated phosphorothioate (PS) linkages into their miRNA inhibitors, which interfere with the ability of nucleases to degrade the phosphate bond between nucleotides (801, 802).

Nowadays there are a large number of effective chemical modifications and combinations thereof available (792). In the following sections we will investigate two relatively novel types of AMOs, which incorporate Locked nucleic acids (LNA^{TM}) and Morpholino oligos respectively.

5.3.2 Locked nucleic acid (LNA^{TM}) miRNA inhibitors

Locked nucleic acid (LNA^{TM}) differs from DNA in that it is conformationally restricted via a methylene bridge on the ribose ring linking the 2′ O atom and 4′ C atom (803-805). This

results in remarkable nuclease resistance and high target binding affinity. LNA™ inhibitors have been successfully applied to the study of cellular and viral (EBV and KSHV) miRNAs (764, 792, 806). They presumably function by retaining the mature miRNA in an inactive duplex without inducing target degradation (793).

The specific inhibitors used in our knockdown experiments are the miRCURY LNA™ miRNA Power Inhibitors (Exiqon) (http://www.exiqon.com/mirna-inhibitors). They differ from conventional LNA™ miRNA inhibitors in that they incorporate PS linkages in the phosphate backbone, resulting in increased stability. They are designed to achieve optimum potency at low doses (1-100nM) in order to avoid cellular toxicity.

Using our BHRF1 miRNA reporter constructs, we investigated whether and to what extent we could achieve BHRF1 miRNA knockdown in Oku BL cells using LNA™ miRNA inhibitors. Briefly we transfected Oku BL cells with inhibitors designed against either the miR-BHRF1-3 or miR-BHRF1-1 miRNA in combination with the relevant BHRF1 miRNA reporter construct and assessed knockdown at 24h post-transfection (Fig. 5.3). In the representative experiment shown in Fig. 5.3A, the 500nM concentration of the miR-BHRF1-3 inhibitor de-repressed luciferase activity of the miR-BHRF1-3 reporter by 2.3 fold, compared to a much smaller 1.3 fold change for the control reporter. This indicates a partial functional knockdown of miR-BHRF1-3. Barely any knockdown was observed when using a 100nM concentration of the miR-BHRF1-3 inhibitor.

Repeating the experiment using the miR-BHRF1-1 inhibitor, our results show that the control firefly reporter displayed a greater fold increase in luciferase activity than did the miR-BHRF1-1 reporter at both the 100nM and 500nM inhibitor concentration (Fig. 5.3B).

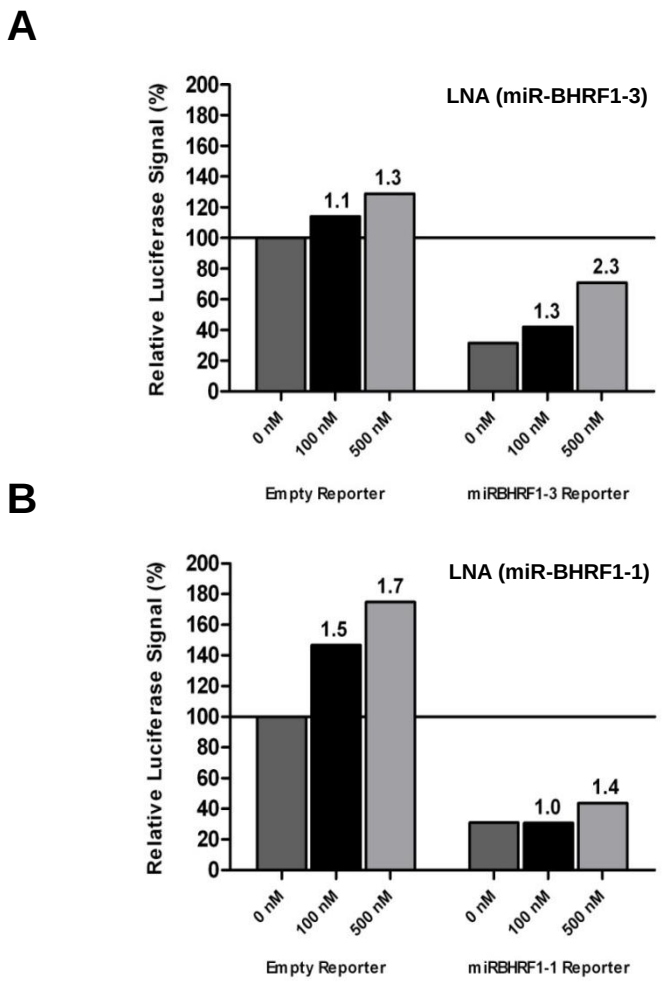

Fig. 5.3. Knockdown of the BHRF1 miRNAs using locked nucleic acid (LNA^{TM}) miRNA inhibitors. EBV positive Oku (Wp BL) cells were co-transfected with increasing doses of a LNA against **(A)** miR-BHRF1-3 or **(B)** miR-BHRF1-1 and either the empty control pMIR-REPORT^{TM} firefly reporter construct or a derivative containing a single binding site for miR-BHRF1-1 or miR-BHRF1-3. Cells were co-transfected with a β-Gal control vector, commercially available from Ambion®. Firefly luciferase activity was measured in cell lysates prepared 24h post-transfection and normalized to β-Gal activity measured in the same samples. Normalized luciferase data was expressed relative to the uninhibited empty control pMIR-REPORT^{TM} firefly reporter (set at 100%). Data for the miR-BHRF1-3 inhibitor correspond to one of two replicate experiments, while the miR-BHRF1-1 inhibitor data are from a single experiment. The numbers above the columns indicate fold increases in relative luciferase signal attributed to the LNA inhibitor.

Consequently it is not possible to distinguish between genuine miR-BHRF1-1 knockdown and off target effects.

5.3.3 Morpholino miRNA inhibitors

In parallel work, we also tested the effects of Morpholino inhibitors against the BHRF1 miRNAs. Morpholino nucleotides differ from DNA in that their backbone contains morpholine rings in place of deoxyribose rings and incorporate uncharged phosphorodiamidate (PN) linkages in place of phosphodiester (PO) linkages (796). Morpholino AMOs have been used in a number of miRNA knockdown experiments; a complete list of publications can be viewed on the Gene Tools, LLC website (http://www.gene-tools.com/node/31#miRNAcitations). Our Morpholino BHRF1 miRNA inhibitors were synthesized by Gene Tools, LLC and designed to not only be highly stable and target specific, but simultaneously interfere with both mature miRNA function and miRNA processing. Note that it was not possible to design a Morpholino inhibitor against miR-BHRF1-1 (see Discussion)

Oku BL cells were transfected with inhibitors designed to functionally inhibit either miR-BHRF1-2 or miR-BHRF1-3 in combination with the relevant BHRF1 miRNA reporter construct; knockdown was assessed at 24h post-transfection (Fig. 5.4). In the representative experiment shown in Fig. 5.4A, the 10μM and 20μM concentrations of the miR-BHRF1-3 inhibitor de-repressed luciferase activity of the miR-BHRF1-3 firefly reporter by 1.8 and 1.9 fold, respectively, without de-repressing the control reporter. This indicates a partial functional knockdown of miR-BHRF1-3.

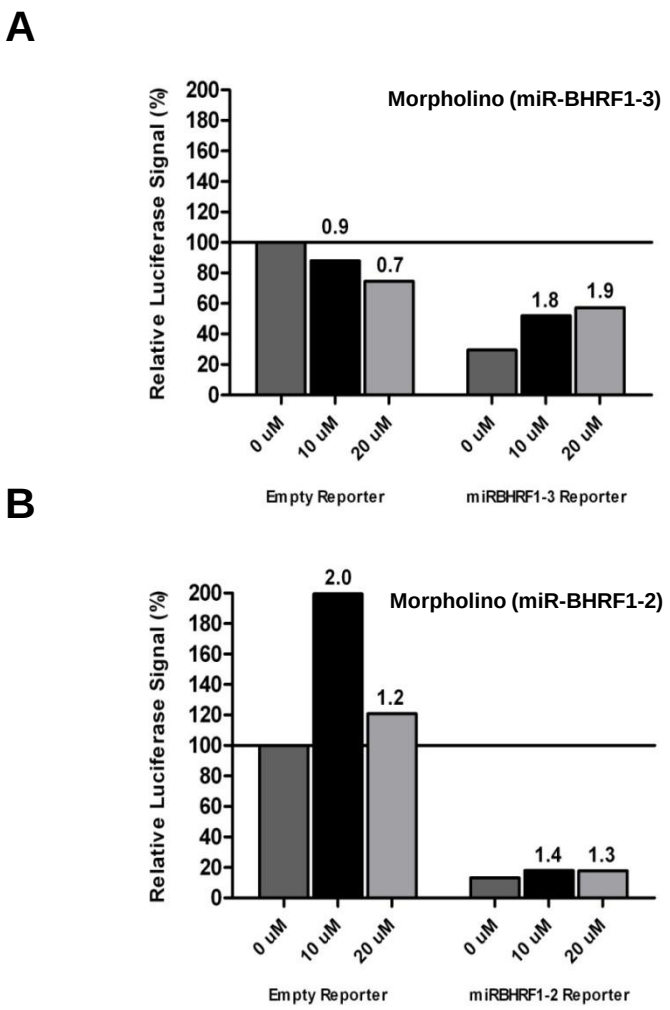

Fig. 5.4. Knockdown of the BHRF1 miRNAs using Morpholino miRNA inhibitors. EBV positive Oku (Wp BL) cells were co-transfected with increasing doses of a Morpholino against **(A)** miR-BHRF1-3 or **(B)** miR-BHRF1-2 and either the empty control pMIR-REPORT™ firefly reporter construct or a derivative containing a single binding site for miR-BHRF1-2 or miR-BHRF1-3. Cells were co-transfected with a β-Gal control vector. Firefly luciferase activity was measured in cell lysates prepared 24h post-transfection and normalized to β-Gal activity measured in the same samples. Normalized luciferase data was expressed relative to the uninhibited empty control pMIR-REPORT™ firefly reporter (set at 100%). Data for the miR-BHRF1-3 inhibitor correspond to one of two replicate experiments, while the miR-BHRF1-2 data are from a single experiment. The numbers above the columns indicate fold increases in relative luciferase signal attributed to the Morpholino inhibitor.

Neither dose of the miR-BHRF1-2 inhibitor caused a noticeable de-repression of the miR-BHRF1-2 firefly reporter when compared to the control reporter (Fig. 5.4B). We noted that the 10μM dose of the miR-BHRF1-2 inhibitor caused a 2 fold change in normalized luciferase activity of the control reporter. However closer inspection of the data revealed that this was caused by a technical issue with β-gal detection in this sample, rather than reflecting a real change in normalized luciferase activity (see Discussion). In conclusion we were only able to achieve knockdown of one BHRF1 miRNA when using LNA^{TM} or Morpholino AMOs. Consequently we chose to abandon the use of antisense oligonucleotides as a means to study the BHRF1 miRNAs.

5.4 Establishing a lentivirus system for the stable, inducible expression of the BHRF1 miRNAs

Previous studies have demonstrated the expression of functional miRNAs using a lentivirus delivery system (807, 808). The appeal of a lentivirus lies in its ability to stably integrate into the host genome to allow continuous expression of the miRNA cassette. Earlier we observed that all three BHRF1 miRNAs were expressed during Lat III infection whilst during lytic cycle miR-BHRF1-2 and miR-BHRF1-3 were expressed in the absence of miR-BHRF1-1 (809). Therefore we designed two separate BHRF1 miRNA constructs to mimic these two scenarios.

Our cloning strategy was designed to include a number of useful features necessary in the final constructs. First miRNA expression should be under the control of a pol II promoter, since RNA pol II transcribes the viral miRNAs in the context of the virus genome (789). Second our miRNA expression cassettes should be inducible so that we can completely

control their expression. Thirdly our final constructs should constitutively express GFP to facilitate sorting of lentivirus transduced cells.

Our cloning strategy used two lentivirus vectors termed FTGW and FH1t(INSR)UTG which were kindly supplied by Marco Herold (Fig 5.5) (810). FTGW was used as the intermediate cloning vector in our strategy (Fig 5.5A). It expresses eGFP under the control of the pol II CMV immediate-early promoter TREX-p; TREX-p contains two tetracycline operator (TetO) sites and is therefore repressed by binding of the tetracycline repressor (TetR). Note that in this vector, TREX-p is constitutively active because FTGW lacks a TetR gene. FH1t(INSR)UTG served as the final lentivirus vector in our strategy (Fig 5.5B). It expresses eGFP and TetR under the control of the constitutively active ubiquitin promoter (hUbc-p). Note that in the parental FH1t(INSR)UTG vector, there is an expression cassette encoding a shRNA (IR5) against the insulin receptor (INSR) expressed from the H1tetO promoter (811, 812); this cassette is replaced in the final construct with the TREX-p-miRNA cassette, as described below.

5.4.1 Generation of the intermediate lentiviral BHRF1 miRNA expression constructs

The first step of our cloning strategy is illustrated in Fig. 5.6. Briefly we used PCR to amplify a fragment spanning a 553 bp region of the Oku-BL BHRF1 3′ UTR encompassing miR-BHRF1-2 and miR-BHRF1-3; primers were designed to include an internal PacI site as well as terminal *Eco*RI and *Bam*HI sites. This fragment was then inserted immediately downstream of TREX-p using *Eco*RI and *Bam*HI sites, replacing eGFP in the process (Fig. 5.6A). The resulting vector was dubbed FTGW (BHRF1-2/1-3). In parallel we generated a second

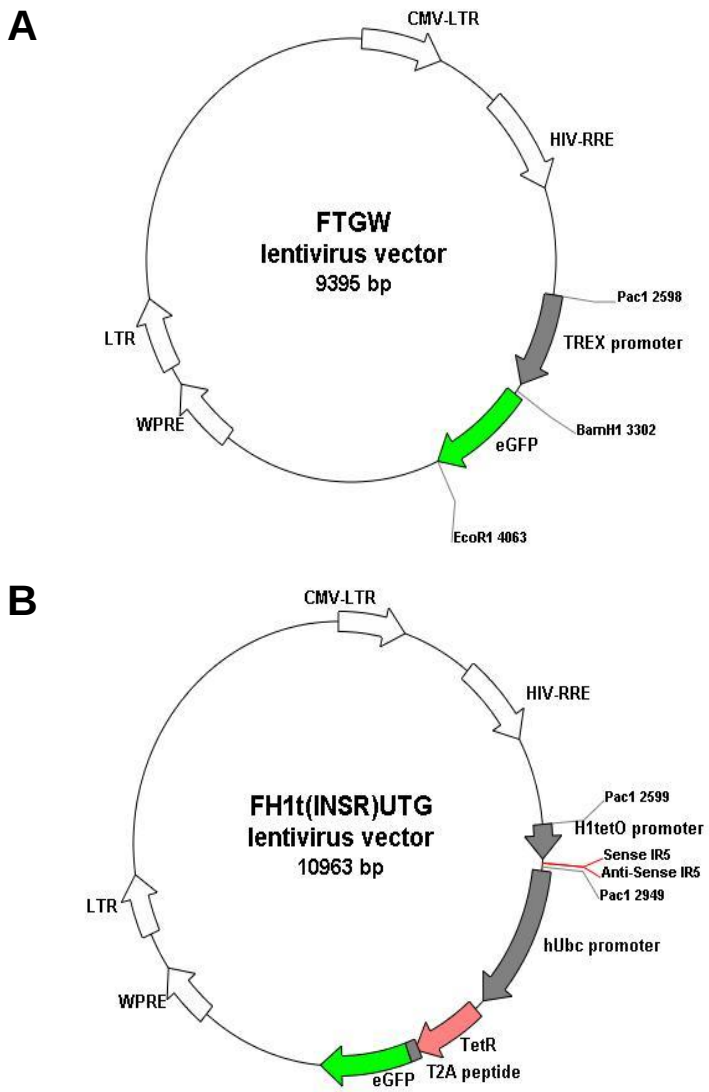

Fig. 5.5. Schematic describing the starting vectors used to generate lentiviral constructs for the tetracycline inducible expression of the BHRF1 miRNAs. **(A)** FTGW expresses eGFP under the control of the pol II tetracycline inducible promoter TREX-p. **(B)** FH1t(INSR)UTG expresses a small hairpin RNA (shRNA) against the insulin receptor (INSR) under the control of the pol III tetracycline inducible promoter H1tetO-p. It also expresses the tetracycline repressor protein (TetR) and eGFP under the control of the constitutively active ubiquitin promoter (hUbc-p). Both vectors transcribe the viral RNA genome from a pol II CMV promoter. Rev-dependent nuclear export of the nascent genome is mediated by the HIV Rev response element (HIV-RRE). The long terminal repeats (LTR) mediate integration of lentiviral DNA. The wood chuck hepatitis virus post-transcriptional regulatory element (WPRE) increases transgene expression. Both vectors were designed and kindly supplied by Marco Herold (810).

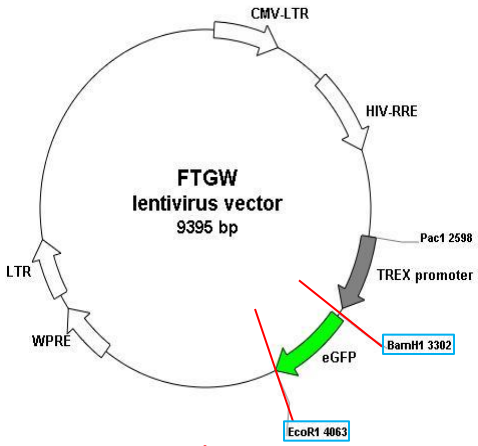
CMV-LTR
HIV-RRE
FTGW
lentivirus vector
9395 bp
Pac1 2598
TREX promoter
LTR
WPRE
eGFP
BamH1 3302
EcoR1 4063

A

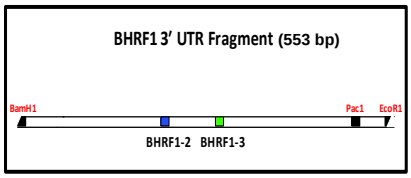
BHRF1 3′ UTR Fragment (553 bp)
BamH1
Pac1
EcoR1
BHRF1-2
BHRF1-3

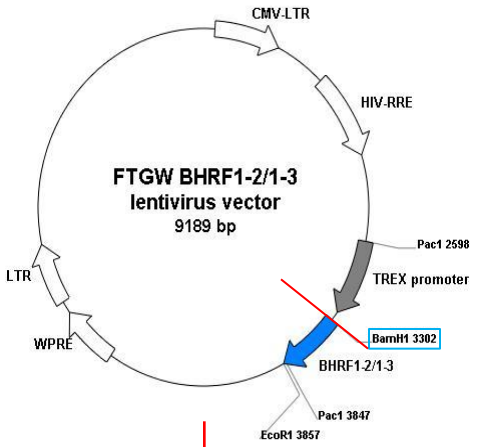
CMV-LTR
HIV-RRE
FTGW BHRF1-2/1-3
lentivirus vector
9189 bp
Pac1 2598
TREX promoter
LTR
WPRE
BamH1 3302
BHRF1-2/1-3
Pac1 3847
EcoR1 3857

B

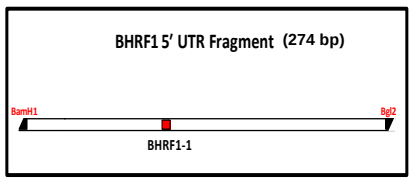
BHRF1 5′ UTR Fragment (274 bp)
BamH1
Bgl2
BHRF1-1

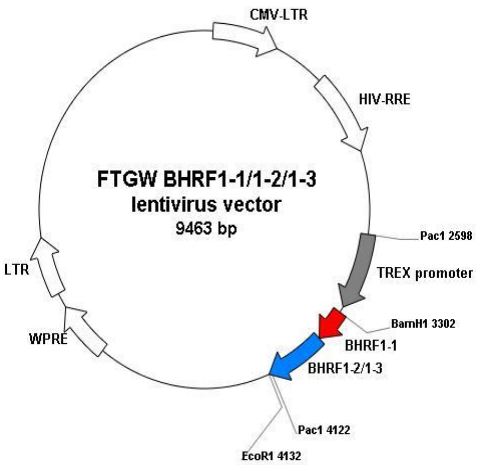
CMV-LTR
HIV-RRE
FTGW BHRF1-1/1-2/1-3
lentivirus vector
9463 bp
Pac1 2598
TREX promoter
LTR
WPRE
BamH1 3302
BHRF1-1
BHRF1-2/1-3
Pac1 4122
EcoR1 4132

Fig. 5.6. Schematic describing the first step in the generation of the lentiviral BHRF1 miRNA expression constructs. **(A)** PCR was used to amplify a fragment of the BHRF1 3′ UTR containing miR-BHRF1-2 and miR-BHRF1-3; primers were designed to include EcoRI, BamHI and PacI sites. The fragment was then inserted downstream of the FTGW TREX promoter using EcoRI and BamHI sites to generate the FTGW(BHRF1-2/1-3) vector. **(B)** Similarly a fragment of the BHRF1 5′ UTR containing miR-BHRF1-1 was inserted into the BamHI site downstream of the FTGW(BHRF1-2/1-3) TREX promoter to generate the FTWG(BHRF1-1/1-2/1-3) vector. Note that BglII and BamHI sticky ends are compatible with one another.

intermediate vector containing all 3 BHRF1 miRNAs, by using PCR to amplify a fragment spanning a 274 bp region of the Oku BL BHRF1 5′ UTR encompassing miR-BHRF1-1; primers were designed to include terminal *Bgl*II and *Bam*HI sites. This fragment was then inserted into the *Bam*HI site between TREX-p and BHRF1-2/1-3 (Fig 5.6B) to form FTWG (BHRF1-1/1-2/1-3).

5.4.2 Confirming expression of the BHRF1 miRNAs from intermediate lentiviral vectors FTGW (BHRF1-2/1-3) and FTGW (BHRF1-1/1-2/1-3)

In preliminary experiments, we wanted to test whether the intermediate FTGW-derived lentiviral vectors could generate detectable levels of the BHRF1 miRNAs. Therefore we transfected EBV negative DG75 BL cells with either FTGW BHRF1-2/1-3 or FTGW BHRF1-1/1-2/1-3, and assessed cells for BHRF1 miRNA expression 72h later (Fig. 5.7). Our results clearly show that both FTGW vectors express miR-BHRF1-2 and miR-BHRF1-3 at much higher levels than seen in control DG75 cells. FTGW BHRF1-1/1-2/1-3 additionally expresses miR-BHRF1-1 as expected. Given this positive result we then proceeded with the final step of the lentiviruses cloning.

5.4.3 Generation of the final lentiviral BHRF1 miRNA expression constructs

The final step in our cloning strategy is illustrated in Fig. 5.8 and is identical for both the FTGW (BHRF1-2/1-3) and FTGW (BHRF1-1/1-2/1-3). The complete TREX-p – BHRF1 miRNA expression cassette was excised via two *Pac*I sites and cloned into FH1t(INSR)UTG

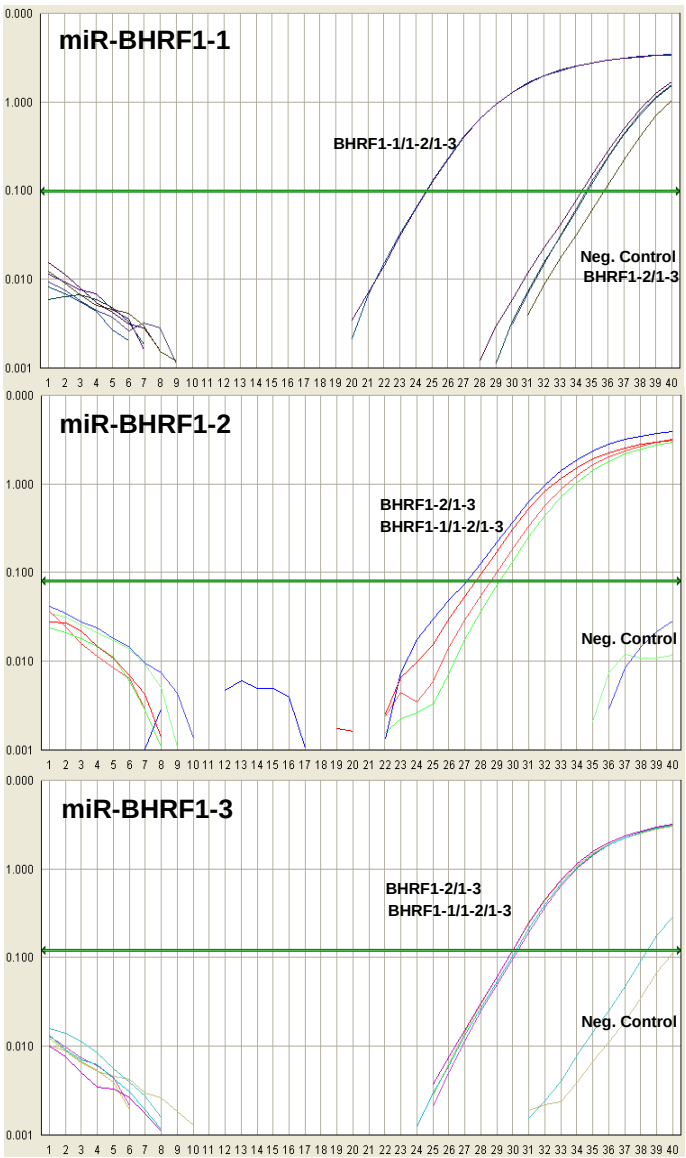

Fig. 5.7. Expression of the BHRF1 miRNAs from the intermediate FTGW lentiviral vectors. EBV negative DG75 BL cells were transfected with lentiviral BHRF1 miRNA expression vectors (FTGW BHRF1-2/1-3 or FTGW BHRF1-1/1-2/1-3) and assessed for BHRF1 miRNA expression. Shown are PCR amplification plots for each BHRF1 miRNA, with untransfected DG75 BL cells used as a negative control. Note that BHRF1-2/1-3 does not express miR-BHRF1-1.

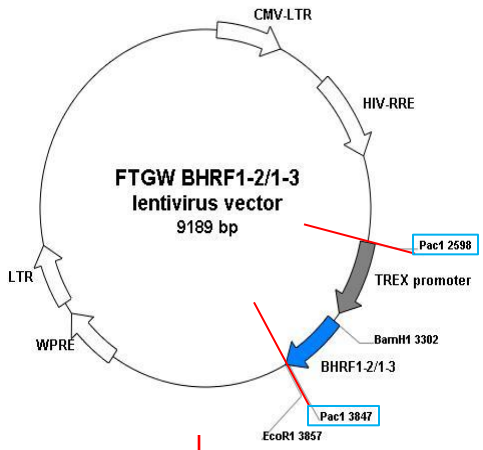
CMV-LTR
HIV-RRE
FTGW BHRF1-2/1-3
lentivirus vector
9189 bp
Pac1 2598
TREX promoter
LTR
WPRE
BamH1 3302
BHRF1-2/1-3
Pac1 3847
EcoR1 3857

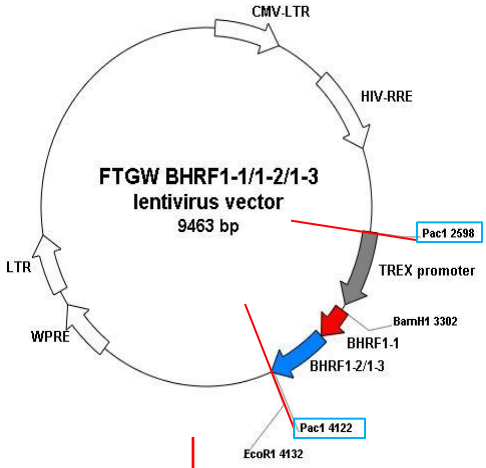
CMV-LTR
HIV-RRE
FTGW BHRF1-1/1-2/1-3
lentivirus vector
9463 bp
Pac1 2598
TREX promoter
LTR
WPRE
BamH1 3302
BHRF1-1
BHRF1-2/1-3
Pac1 4122
EcoR1 4132

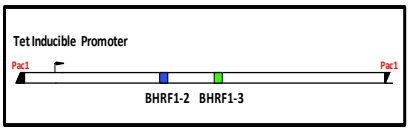
Tet Inducible Promoter
Pac1
Pac1
BHRF1-2 BHRF1-3

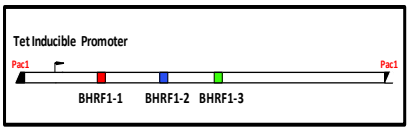
Tet Inducible Promoter
Pac1
Pac1
BHRF1-1 BHRF1-2 BHRF1-3

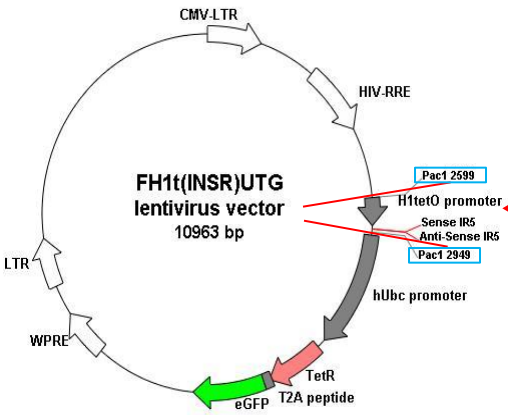
CMV-LTR
HIV-RRE
FH1t(INSR)UTG
lentivirus vector
10963 bp
Pac1 2599
H1tetO promoter
Sense IR5
Anti-Sense IR5
Pac1 2949
LTR
hUbc promoter
WPRE
TetR
eGFP
T2A peptide

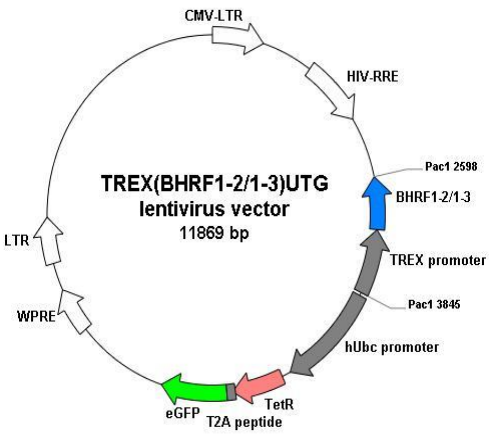
CMV-LTR
HIV-RRE
TREX(BHRF1-2/1-3)UTG
lentivirus vector
11869 bp
Pac1 2598
BHRF1-2/1-3
LTR
TREX promoter
Pac1 3845
WPRE
hUbc promoter
eGFP
TetR
T2A peptide

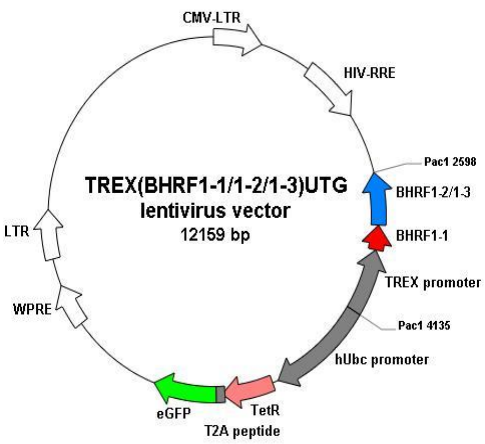
CMV-LTR
HIV-RRE
TREX(BHRF1-1/1-2/1-3)UTG
lentivirus vector
12159 bp
Pac1 2598
BHRF1-2/1-3
LTR
BHRF1-1
TREX promoter
Pac1 4135
WPRE
hUbc promoter
eGFP
TetR
T2A peptide

Fig. 5.8. Schematic describing the final step in the generation of lentiviral constructs for the tetracycline inducible expression of the BHRF1 miRNAs. The TREX-p – BHRF1 miRNA expression cassette was excised from from both the FTGW(BHRF1-2/1-3) and FTGW(BHRF1-1/1-2/1-3) intermediate vectors by PacI digest. Each cassette was then cloned individually into FH1t(INSR)UTG using PacI sites to generate the TREX(BHRF1-2/1-3)UTG and TREX(BHRF1-1/1-2/1-3)UTG vectors respectively. Note that each expression cassette was inserted into FH1t(INSR)UTG in the reverse orientation relative to the direction in which the viral genome is transcribed. The final constructs express either miR-BHRF1-2 and miR-BHRF1-3 or all three BHRF1 miRNAs from a pol II tetracycline inducible promoter; additionally the constitutively express TetR and eGFP from promoter hUbc.

thus replacing the H1tetO promoter and IR5 shRNA; note the fragment was inserted in the reverse orientation relative to the direction in which the viral genome is transcribed (see discussion). The final BHRF1 miRNA expression vectors were dubbed TREX(BHRF1-2/1-3)UTG and TREX(BHRF1-1/1-2/1-3)UTG respectively. Both vectors expressed the relevant combinations of BHRF1 miRNAs from a tetracycline inducible pol II promoter and constitutively expressed eGFP and TetR.

To generate an appropriate control vector we excised the H1tetO-p – shRNA expression cassette from FH1t(INSR)UTG to create an empty vector dubbed CON(empty)UTG. We sequenced across two overlapping regions of the TREX-p – BHRF1 miRNA expression cassette in TREX(BHRF1-2/1-3)UTG and TREX(BHRF1-1/1-2/1-3)UTG and checked the size of each vector backbone using a range of suitable digests (data not shown). Neither construct displayed any unexpected sequence changes and/or digest patterns.

5.4.4 Sorting of TREX(BHRF1-2/1-3)UTG and TREX(BHRF1-1/1-2/1-3) transduced BL lines

After generating suitable lentivirus stocks, two EBV negative BL lines (BL41 and BL30) and two Lat I BL lines (Akata and Mutu59) were then individually transduced with TREX(BHRF1-2/1-3)UTG, TREX(BHRF1-1/1-2/1-3)UTG) and CON(empty)UTG. Roughly two weeks post-transduction each lentivirus transduced BL line was assessed for GFP expression by FACS; representative measurements for the BL41 and Akata BL lines are shown in Fig. 5.9. Transduction efficiencies varied widely both with different constructs and different BL lines. Generally the BL41 and Akata BL cells were easier to transduce (always >40% GFP positive) than were BL30 and Mutu59 BL cells (always <40% GFP positive) (Fig.

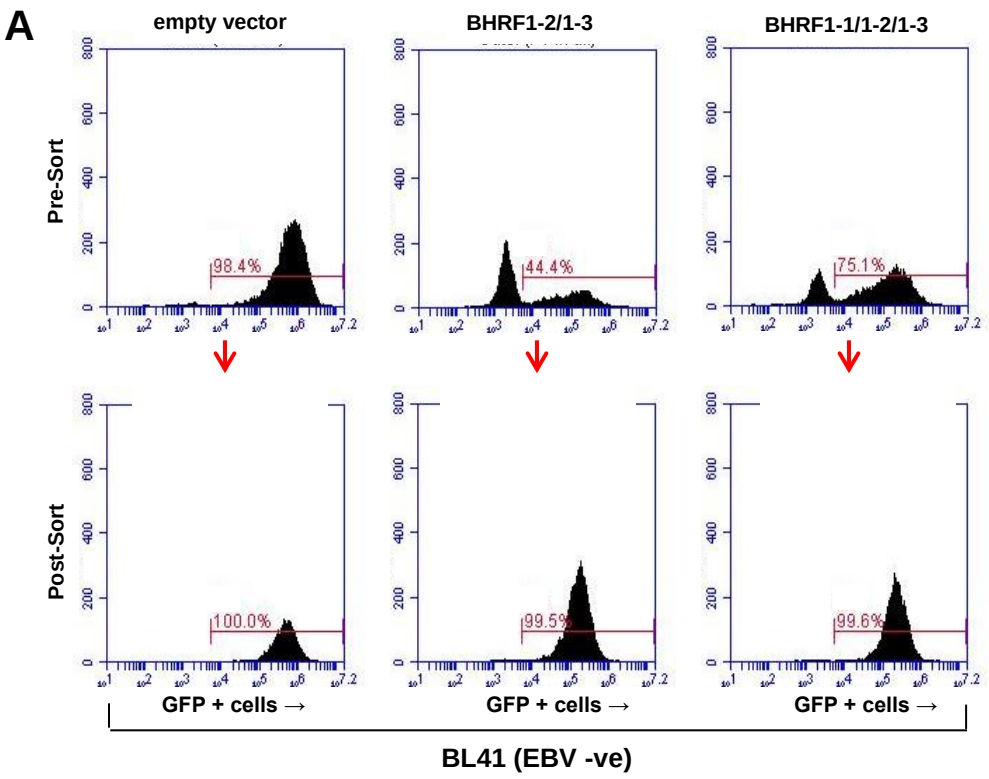
A
empty vector
BHRF1-2/1-3
BHRF1-1/1-2/1-3
Pre-Sort
Post-Sort
98.4%
44.4%
75.1%
100.0%
99.5%
99.6%
GFP + cells →
GFP + cells →
GFP + cells →
BL41 (EBV -ve)

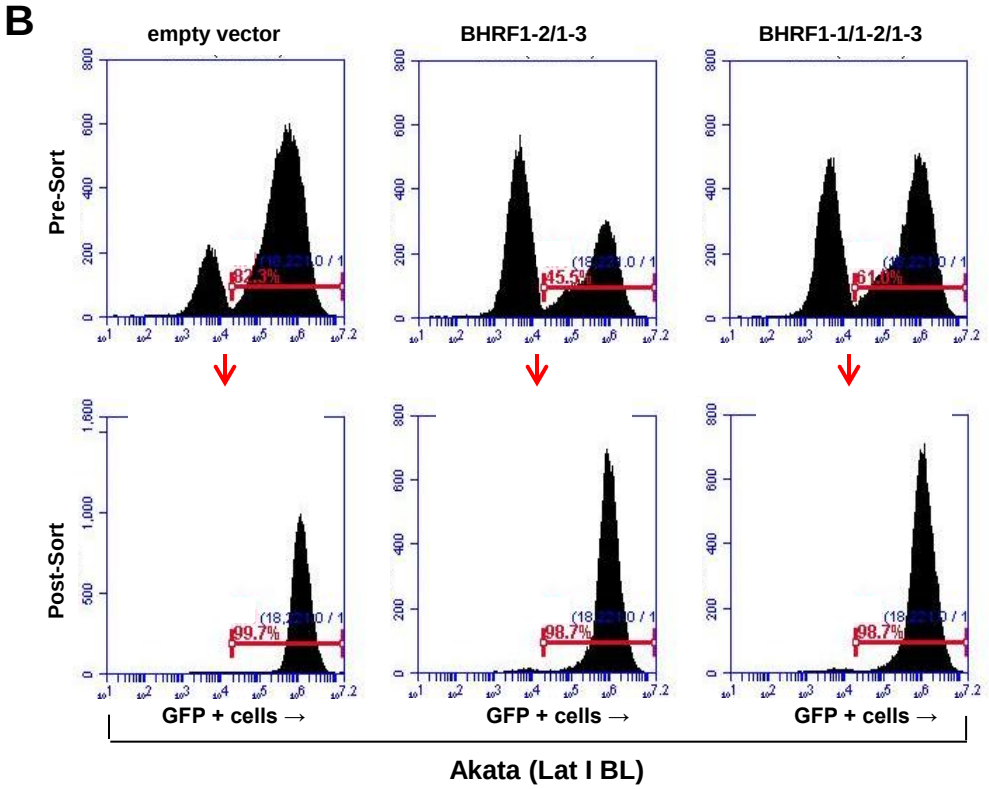
B
empty vector
BHRF1-2/1-3
BHRF1-1/1-2/1-3
Pre-Sort
Post-Sort
99.7%
98.7%
98.7%
GFP + cells →
GFP + cells →
GFP + cells →
Akata (Lat I BL)

Fig. 5.9. Sorting of lentivirus transduced BL lines. EBV negative BL41 and BL30 BL cells and EBV positive Lat I Akata and Mutu59 BL cells were transduced with a lentiviral BHRF1 miRNA expression vector (empty vector, BHRF1-2/1-3 or BHRF1-1/1-2/1-3). Shown are representative FACS measurements for the BL41 BL **(A)** and Akata BL **(B)** lines. The first set of measurements were taken a day before sorting, approximately two weeks post-transduction (pre-sort). The second set of measurements were taken four weeks after sorting (post-sort).

5.9 and data not shown); similarly the CON(empty)UTG) virus transduced cells much more efficiently than did either the TREX(BHRF1-2/1-3)UTG or TREX(BHRF1-1/1-2/1-3)UTG virus.

GFP positive cells were subsequently sorted from each lentivirus transduced BL line; where possible we sorted each BL line in triplicate, i.e. BL41(empty vector), BL41(BHRF1-2/1-3) and BL41(BHRF1-1/1-2/1-3), to similar mean GFP intensities. Sorted BL lines were returned to culture and assessed for GFP expression on a bimonthly basis to ensure that they were still 100% GFP positive; the data in Fig. 5.9 are representative measurements taken one month post-sort.

5.4.5 Quantifying BHRF1 miRNA expression from TREX lentiviral vectors

Having established lentivirus transduced BL lines, we next investigated if they could express the BHRF1 miRNAs. To this end cells were treated with a tetracycline derivative (doxycycline) for 72h, and BHRF1 miRNA expression was subsequently measured by QPCR (Fig. 5.10). Our data show that all four BL lines transduced with TREX(BHRF1-2/1-3)UTG expressed miR-BHRF1-2 and miR-BHRF1-3 in the absence of miR-BHRF1-1. In turn all BL lines transduced with TREX(BHRF1-1/1-2/1-3)UTG expressed all three BHRF1 miRNAs. We noted that while both vectors produced comparable levels of miR-BHRF1-2 in the same BL line, miR-BHRF1-3 expression from TREX(BHRF1-1/1-2/1-3)UTG was markedly reduced. Overall the copy numbers of miR-BHRF1-1 and BHRF1-2 ranged between 50-100 copies per pg RNA and 25-100 copies per pg RNA respectively; this is the same range seen in Wp BL (Fig. 3.8B). Overall the copy numbers of miR-BHRF1-3 were reduced as compared those detected in Wp BL, but still generally similar to copy numbers seen in Lat III BL. As

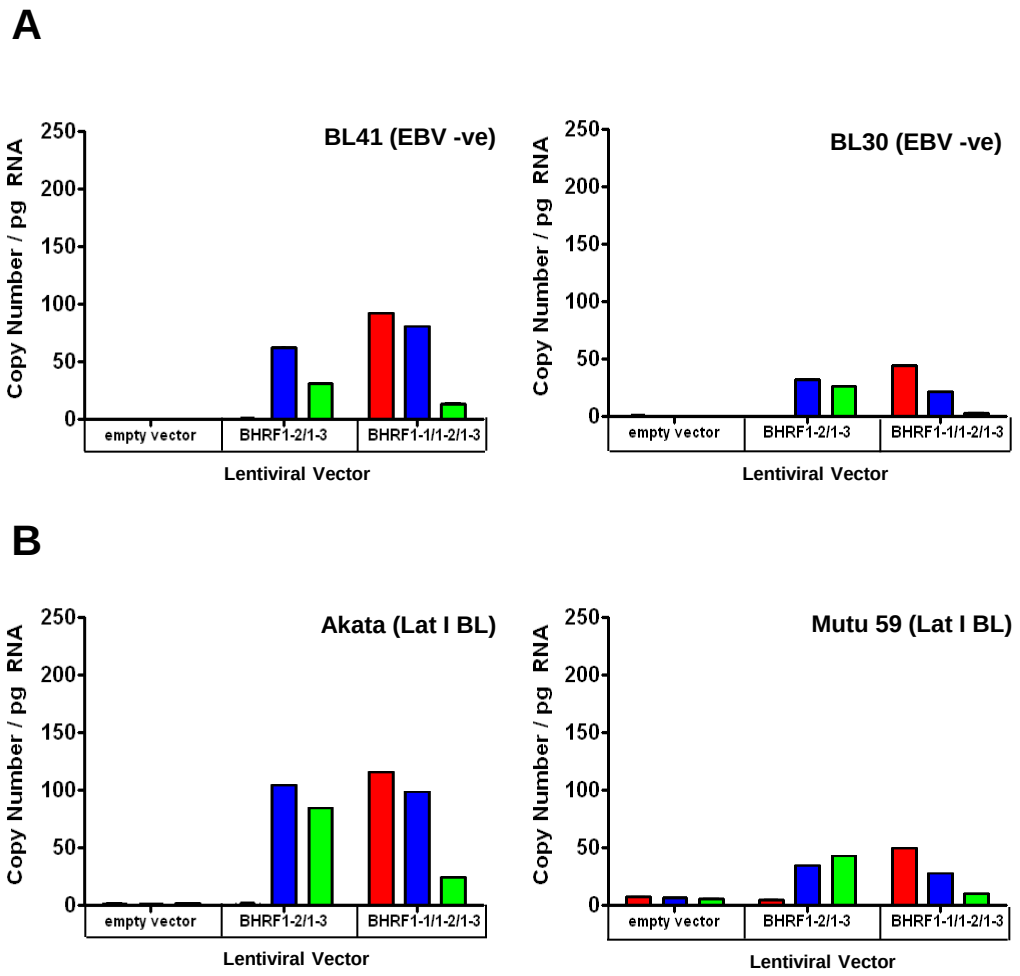

Fig. 5.10. Expression of the BHRF1 miRNAs from the final lentiviral vectors. **(A)** EBV negative BL41 and BL30 BL cells and **(B)** EBV positive Lat I Akata and Mutu 59 BL cells transduced with a lentiviral BHRF1 miRNA expression vector (empty vector, BHRF1-2/1-3 or BHRF1-1/1-2/1-3) were assessed for BHRF1 miRNA expression. Different BHRF1 miRNAs are colour coded using red (miR-BHRF1-1), blue (miR-BHRF1-2) and green (miR-BHRF1-3). Data were quantified by QPCR and expressed as absolute copy numbers per pg total RNA. Each data point corresponds to the average of two replicate assay measurements. Note that BHRF1-2/1-3 does not express miR-BHRF1-1.

expected the BHRF1 miRNAs were only detectable at low background levels in CON(empty)UTG transduced BL lines. The only exception was Mutu 59 BL for which trace levels of all BHRF1 miRNAs could be detected; this is likely due to some cells having drifted toward Lat III (781). Consequently Mutu 59 BL was removed from future studies.

5.4.6 BHRF1 miRNAs expressed from lentivectors are capable of specifically down regulating an artificial target

Next we asked whether the lentiviral expressed BHRF1 miRNAs could functionally knock down a reporter target. BL41 and Akata BL cells stably transduced with TREX(BHRF1-2/1-3)UTG, TREX(BHRF1-1/1-2/1-3)UTG or CON(empty)UTG were treated with doxycycline for 72h as before and transfected individually with each BHRF1 miRNA reporter construct (Fig. 5.11).

As expected the BHRF1-2 and BHRF1-3 reporters, but not the BHRF1-1 reporter, were significantly down regulated in TREX(BHRF1-2/1-3)UTG transduced BL41 and Akata BL cells ($P < 0.05$). In turn the BHRF1-1 and BHRF1-2 reporters, but not the BHRF1-3 reporter, were significantly down regulated in cells transduced with TREX(BHRF1-1/1-2/1-3)UTG. This is consistent with the pattern of miRNA expression shown in Fig. 5.10 and confirms that miR-BHRF1-3 is expressed at lower levels from TREX(BHRF1-1/1-2/1-3)UTG than from TREX(BHRF1-2/1-3)UTG. Luciferase knockdown, when it occurred, was similar for all three BHRF1 miRNA reporters and ranged from 40% to 50% in the BL41 BL background and from 50% to 60% in the Akata BL background. This is also consistent with our QPCR data showing that overall levels of the BHRF1 miRNAs are higher in Akata cells (Fig 5.10).

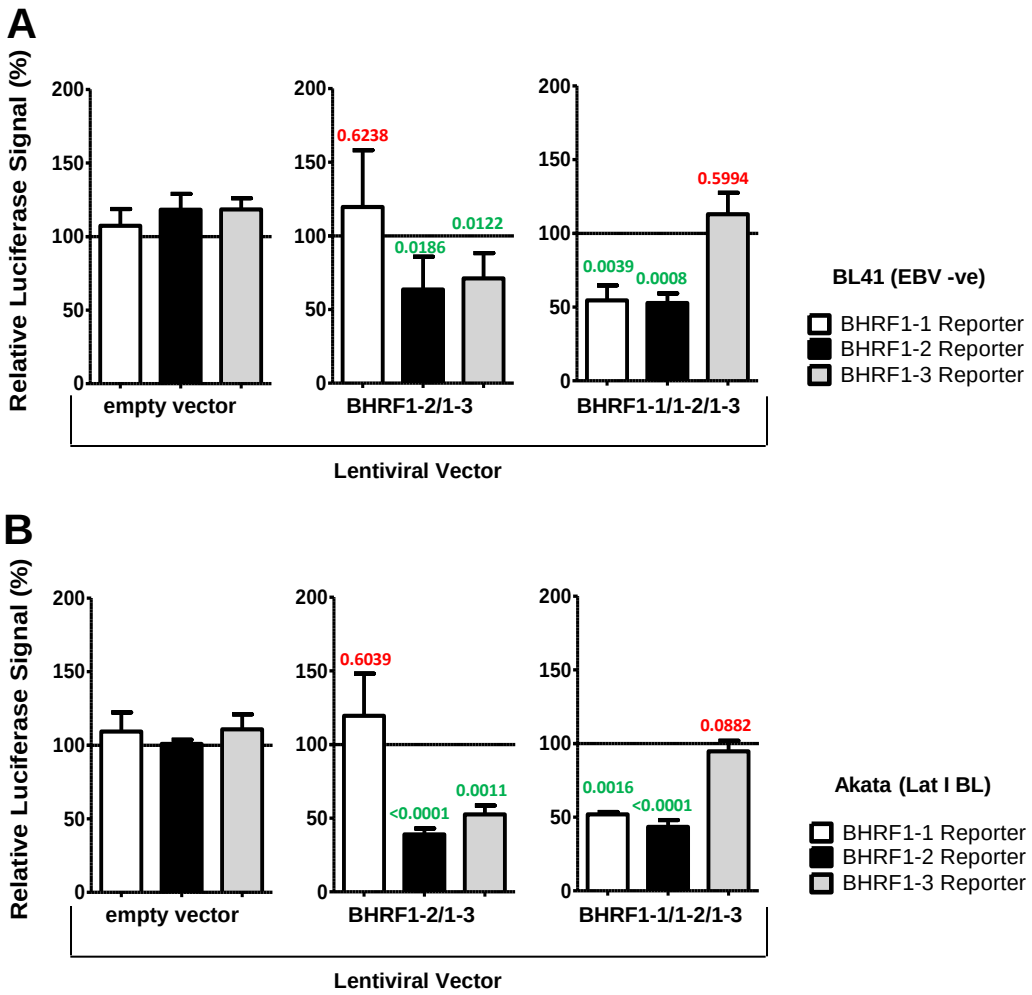

Fig. 5.11. The BHRF1 miRNAs expressed from lentivectors are capable of specifically down regulating an artificial target. Lentiviral vector (empty vector, BHRF1-2/1-3 or BHRF1-1/1-2/1-3) transduced EBV negative BL41 **(A)** cells or EBV positive Akata **(B)** cells were transfected with either the control pMIR-REPORT™ firefly reporter construct or derivatives containing a single binding site for miR-BHRF1-1, 1-2 or 1-3. The same cells were co-transfected with the pRL SV40 *Renilla* reporter construct. Firefly luciferase activity was measured in cell lysates prepared 24h post-transfection and normalized to *Renilla* luciferase activity measured in the same samples. Normalized luciferase data was expressed relative to the empty control pMIR-REPORT™ firefly reporter (set at 100%). Error bars indicate standard deviation of three separate experiments. Normalized luciferase activity in BHRF1-2/1-3 and BHRF1-1/1-2/1-3 transduced cells was compared to that of empty vector transduced cells for each BHRF1 miRNA reporter, using an unpaired t test with a P value cut off set to 0.05. P values are listed above each column using green and red text to denote statistical significance and insignificance respectively

5.4.7 Assessing the inducibility of BHRF1 miRNA expression from TREX lentiviral vectors

In a final validation experiment we tested the inducibility of our TREX lentiviral vectors. BL41 and Akata BL cells stably transduced with TREX(BHRF1-2/1-3)UTG, TREX(BHRF1-1/1-2/1-3)UTG or CON(empty)UTG were cultured either in the presence or absence of doxycycline for 72h. Subsequently cells were assessed both for BHRF1 miRNAs expression and BHRF1 miRNA reporter construct knockdown as before.

Shown in Fig. 5.12 are representative data for the TREX(BHRF1-1/1-2/1-3)UTG transduced BL41 and Akata BL lines. Both lentivirus transduced BL lines were characterized by similar levels of leaky BHRF1 miRNAs expression in the absence of doxycycline (Fig. 5.12A). Upon doxycycline treatment, levels of miR-BHRF1-1, miR-BHRF1-2 and miR-BHRF1-3 in the lentivirus transduced BL41 BL line increased by 4.1, 3.5 and 1.9 fold, respectively. By comparison miR-BHRF1-1, miR-BHRF1-2 and miR-BHRF1-3 in Akata BL increased by 9.3, 7.5 and 3.4, respectively.

Doxycycline induced BHRF1 miRNAs repressed the BHRF1-1 and 1-2 reporters, but not the BHRF1-3 reporter construct, in both BL lines tested (Fig. 5.12B). This is consistent with the reporter knockdown data shown in Fig. 5.11. Interestingly, leaky BHRF1 miRNA expression in doxycycline untreated BL41 cells caused a similar degree of BHRF1 miRNA reporter knockdown as induced BHRF1 miRNA expression in doxycycline treated BL41 cells. By contrast, leaky BHRF1 miRNA expression in doxycycline untreated Akata cells had no effect on BHRF1 miRNA reporter activity.

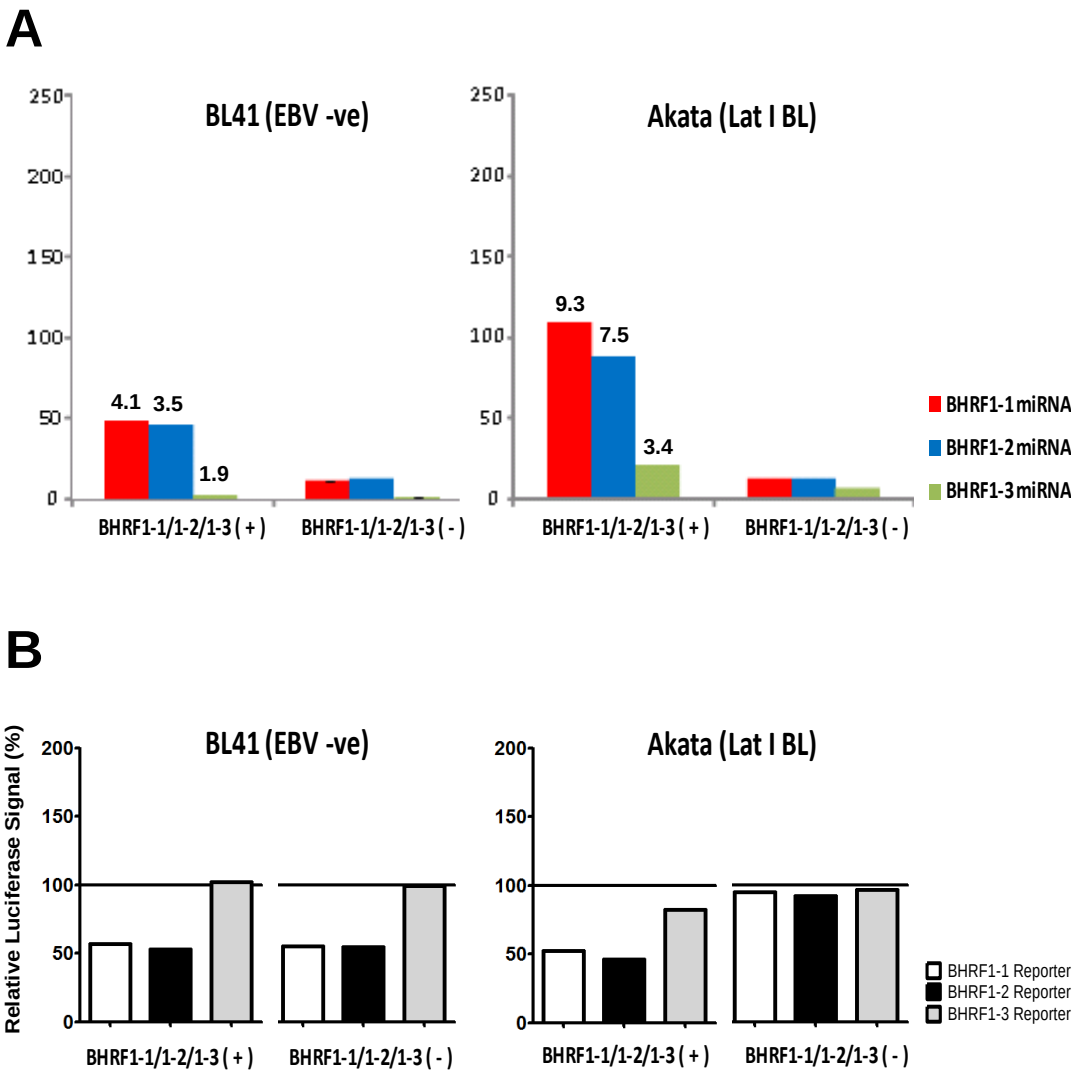

Fig. 5.12. Inducibility of the BHRF1 miRNAs from the final lentiviral vectors. **(A)** EBV negative BL41 BL cells and EBV positive Lat I Akata BL cells transduced with TREX(BHRF1-1/1-2/1-3)UTG lentiviral expression vector were cultured in parallel either in the presence (+) or absence (-) of doxycycline and assessed for BHRF1 miRNA expression. Different BHRF1 miRNAs are colour coded using red (miR-BHRF1-1), blue (miR-BHRF1-2) and green (miR-BHRF1-3). The numbers above the columns indicate fold increases in miRNA levels attributed to doxycycline treatment. Shown are the averages of two replicate assay measurements obtained from a single preparation of RNA. **(B)** The same cells were transfected with either the control pMIR-REPORT™ firefly reporter construct or derivatives containing a single binding site for miR-BHRF1-1, 1-2 or 1-3. Luciferase data were expressed relative to the empty control pMIR-REPORT™ firefly reporter (set at 100%). Each data point corresponds to the average of two replicate assay measurements obtained from the same preparation of cell lysate.

5.5 Investigating the effects of the BHRF1 miRNAs on cellular transcripts

In chapter 1.4 we discussed the variety of transcriptional and post-transcriptional mechanisms by which miRNAs silence their targets. One possibility is that they interfere with translation initiation or elongation, thereby decreasing the levels of target protein but not target mRNA. Conversely they can decrease levels of target mRNA either by deadenylation and degradation or, in rare cases, by endonucleolytic cleavage. It has been estimated that up to 85% of cellular miRNA induced protein changes result from decreases in mRNA levels (151). Interestingly a number of validated EBV miRNA targets are also repressed at the transcript level; these include cellular CXCL11 (miR-BHRF1-3), Dicer (miR-BART6-5p), PUMA (miR-BART5) as well as viral BALF5 (miR-BART2) and LMP1 (miR-BART9) (753, 756, 757, 759, 762). Furthermore we note that any EBV miRNA associated changes to the cellular proteome may well exert secondary downstream effects on cellular transcription.

5.5.1 Array analysis of Akata BL cells stably expressing BHRF1 miRNAs

In the next series of experiments, we used gene expression profiling to ask whether the BHRF1 miRNAs were capable of altering the levels of cellular transcripts in BL cells. To this end we screened total RNA preparations using the whole transcript (WT) GeneChip® Human Gene 1.0 ST Array system (Affymetrix). Unlike standard 3′ arrays, the HG 1.0 ST array contains probes which are spread evenly throughout the length of the gene; consequently they can detect differentially spliced transcripts, truncated transcripts and transcripts with alternative polyadenylation sites. Importantly microarrays have reliably been used to detect target genes for both KSHV (MAF) and EBV (PUMA) miRNAs (754, 806), providing further rationale for our approach.

In preparation for the array analysis, Akata BL cells stably transduced with the TREX(BHRF1-2/1-3)UTG, TREX(BHRF1-1/1-2/1-3)UTG or CON(empty)UTG constructs were treated with doxycycline for 72 h. Subsequently each cell line was split into three separate cultures; one was used to generate RNA for the array while the others were used to assess miRNA expression by QPCR (Fig. 5.10) and the effects of the BHRF1 miRNAs on a reporter target (Fig. 5.11). This routine was performed a total of three times in order to gain three experimental RNA replicates for our array. Using the 2100 Bioanalyzer (Agilent Technologies), the overall quality of the RNA was deemed to be excellent. Samples were then submitted to the Affymetrix Microarray Facility within the School of Cancer Sciences (University of Birmingham) for analysis.

The raw array data were initially processed using the AltAnalyze software package (http://www.altanalyze.org/) (780). Differentially expressed genes were then identified using Limma analysis (813). A p-value cut off of 0.01 and a fold change cut off to 1.5 were applied; note that smaller fold changes would be difficult to reliably validate by other RNA detection methods. These data have been summarized as a Venn diagram in Fig. 5.13. Using these criteria, 77 genes were differentially regulated between Akata BL cells expressing miR-BHRF1-2 and miR-BHRF1-3 vs. the empty control. The same number of genes was differentially regulated between Akata BL cells expressing all BHRF1 miRNAs vs. the empty vector. Finally 88 genes were differentially regulated between Akata BL cells expressing all BHRF1 miRNAs vs. miR-BHRF1-2 and miR-BHRF1-3 alone. Note that at this point we are not distinguishing between up or down regulated genes. Names, fold changes and P values of differentially regulated genes found across the three biological comparisons have been listed in Table 5.1.

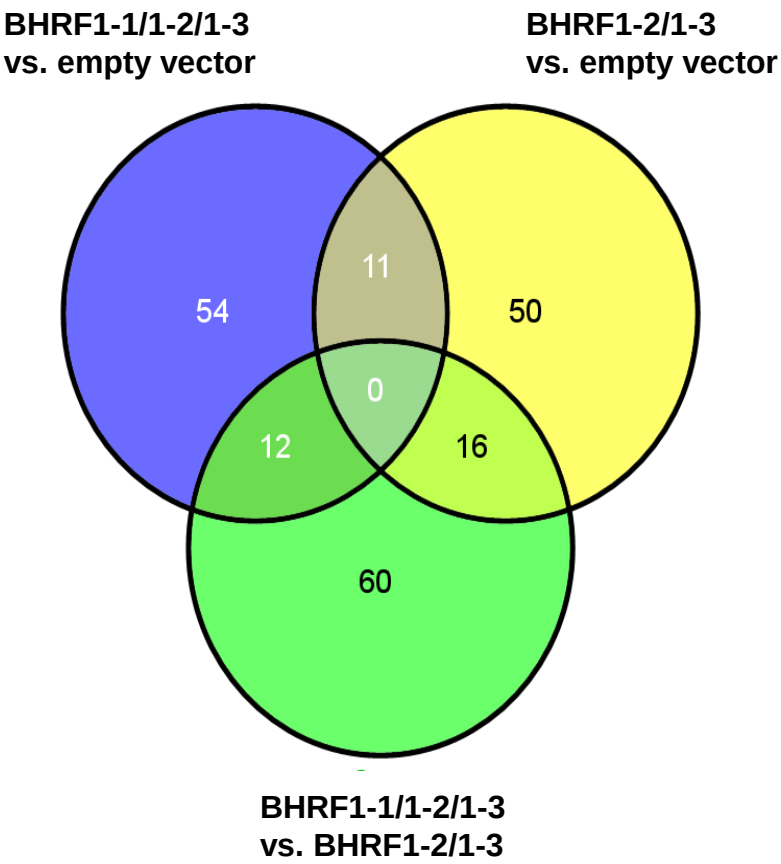

Fig. 5.13. Investigating the effects of the BHRF1 miRNAs on cellular transcription. Lentiviral vector (empty vector, BHRF1-2/1-3 or BHRF1-1/1-2/1-3) transduced EBV positive Akata BL cells were subjected to total cellular transcript analysis using the GeneChip® Human Gene 1.0 ST Array system (Affymetrix). Data were initially processed using the AltAnalyse software. Differentially expressed genes were identified using limma. The p-value cut off was set to 0.01 and the fold change cut off to 1.5. The total number of genes differentially expressed between the three TREX lentivirus transduced Akata BL lines are summarized in the Venn Diagram.

BHRF1-1/1-2/1-3 vs. empty vector			BHRF1-2/1-3 vs. empty vector			BHRF1-1/1-2/1-3 vs. BHRF1-2/1-3		
Gene Symbol	Fold Change	P.Value	Gene Symbol	Fold Change	P.Value	Gene Symbol	Fold Change	P.Value
ADAM18	-5.00	0.00280	ANO5	-4.47	0.00300	ADAM18	-3.71	0.00550
OCA2	-2.99	0.00363	KIAA1598	-4.20	0.00005	SYCP2	-3.25	0.00174
MTMR11	-2.91	0.00930	MERTK	-3.19	0.00138	FCRL2	-2.29	0.00387
FERMT1	-2.60	0.00030	PTPRO	-2.79	0.00114	ANKAR	-2.19	0.00802
EPS8L1	-2.40	0.00420	LIPI	-2.24	0.00188	OVCH2	-2.16	0.00897
MAGEB1	-1.98	0.00171	C6orf154	-2.11	0.00053	TSPAN9	-2.11	0.00968
TFEC	-1.89	0.00019	C14orf48	-2.09	0.00943	SLC9B1	-2.06	0.00780
MAN1B1	-1.89	0.00111	ASZ1	-2.05	0.00015	MAN1B1	-2.05	0.00034
ALS2CR12	-1.86	0.00588	KIFC3	-2.05	0.00032	RNY4P5	-2.01	0.00551
ASZ1	-1.83	0.00089	POU6F2	-2.02	0.00004	RP11-192H23.4	-1.95	0.00058
TMTC2	-1.83	0.00344	SIGLEC12	-1.98	0.00065	LRIG3	-1.85	0.00056
LIPI	-1.80	0.00065	ADCY10	-1.96	0.00380	snoU13	-1.80	0.00722
SNX31	-1.79	0.00004	GLUL	-1.94	0.00019	C20orf118	-1.79	0.00503
ZIM2	-1.78	0.00708	FGF13	-1.89	0.00137	AC133485.1	-1.79	0.00665
ZNF563	-1.78	0.00957	TANC1	-1.84	0.00106	TP53TG3B	-1.79	0.00665
C6orf97	-1.77	0.00653	NPR3	-1.82	0.00217	RP11-397P14.3	-1.79	0.00234
MIPEP	-1.71	0.00480	FAM71F1	-1.80	0.00718	DAZL	-1.76	0.00225
ZNF487P	-1.70	0.00956	PCSK1N	-1.77	0.00005	MAGEB1	-1.76	0.00089
COL4A6	-1.69	0.00051	GJA5	-1.75	0.00798	RS1	-1.74	0.00256
GABRB3	-1.68	0.00384	EMILIN3	-1.74	0.00932	IL5RA	-1.73	0.00061
FEZ1	-1.67	0.00712	FHL1	-1.73	0.00749	Y_RNA	-1.73	0.00034
C20orf118	-1.67	0.00937	GAS2L1	-1.73	0.00202	NCOA7	-1.70	0.00075
GBP3	-1.62	0.00172	CYP3A7	-1.72	0.00167	AL353774.1	-1.69	0.00183
UACA	-1.62	0.00651	SLC5A4	-1.69	0.00035	Y_RNA	-1.69	0.00827
RP11-196D18.6	-1.60	0.00079	GLULP4	-1.69	0.00232	SYT15	-1.67	0.00627
STOX2	-1.59	0.00410	NPL	-1.67	0.00133	IMPA2	-1.66	0.00192
FBN1	-1.59	0.00560	GABRB3	-1.67	0.00259	FAM20A	-1.66	0.00792
NEUROD1	-1.59	0.00730	RP11-196D18.6	-1.67	0.00046	STOX2	-1.65	0.00334
ZNF734	-1.58	0.00080	ZNF734	-1.64	0.00041	AC097374.2	-1.64	0.00591
SMAP1	-1.56	0.00170	IL1R1	-1.64	0.00061	IFLTD1	-1.64	0.00168
MYH8	-1.55	0.00295	EPB41L5	-1.64	0.00351	HAUS6	-1.63	0.00891
NCOA7	-1.55	0.00044	RNY4P16	-1.61	0.00847	FBXL21	-1.63	0.00804
WFDC6	-1.55	0.00281	FAM153B	-1.60	0.00901	ATP9A	-1.61	0.00112
MFAP2	-1.54	0.00208	ALDH1B1	-1.59	0.00239	TAT	-1.59	0.00916
NRCAM	-1.54	0.00043	DMRTC1B	-1.58	0.00102	MC1R	-1.58	0.00549
C1orf168	-1.53	0.00314	PCDHA8	-1.57	0.00174	AKR1CL1	-1.58	0.00462
MYT1	-1.53	0.00549	OSBPL6	-1.56	0.00450	ALPK2	-1.57	0.00672
TDRD5	-1.52	0.00251	DMRTC1	-1.56	0.00084	UACA	-1.55	0.00907
KIAA1377	-1.51	0.00063	C15orf29	-1.54	0.00294	TFEC	-1.54	0.00129
TBC1D16	-1.51	0.00046	PLD1	-1.53	0.00509	DYNC2LI1	-1.54	0.00682
Y_RNA	-1.50	0.00257	VLDLR	-1.52	0.00650	CCDC111	-1.53	0.00559
MX2	1.50	0.00072	IFIT5	-1.52	0.00305	C17orf42	-1.52	0.00539
C10orf116	1.50	0.00091	KCNIP1	-1.52	0.00729	Y_RNA	-1.52	0.00945
RILP	1.51	0.00312	PRRG2	-1.52	0.00199	NPAS3	-1.51	0.00715
CYP2C9	1.51	0.00853	RUNX1T1	-1.52	0.00238	ABHD5	-1.51	0.00153
LHX6	1.51	0.00574	ATP1B4	-1.52	0.00316	TDRD7	-1.51	0.00163
						AL512325.1	-1.50	0.00682
						TMEM156	-1.50	0.00867

BHRF1-1/1-2/1-3 vs. empty vector			BHRF1-2/1-3 vs. empty vector			BHRF1-1/1-2/1-3 vs. BHRF1-2/1-3		
Gene Symbol	Fold Change	P.Value	Gene Symbol	Fold Change	P.Value	Gene Symbol	Fold Change	P.Value
PIP5KL1	1.52	0.00482	C10orf116	1.52	0.00943	VASH1	1.51	0.00901
SYN3	1.54	0.00330	APBB3	1.53	0.00084	DUSP6	1.52	0.00516
OTOGL	1.55	0.00019	PRR19	1.54	0.00701	ATP1B4	1.52	0.00572
LHX2	1.55	0.00382	CHRD	1.54	0.00837	C6orf154	1.52	0.00324
MRO	1.57	0.00597	SESN3	1.56	0.00091	GUCY2F	1.52	0.00141
GUCY2F	1.57	0.00110	CAPS2	1.57	0.00179	ANKRD43	1.53	0.00040
KLRF1	1.58	0.00548	ALLC	1.57	0.00251	IL3	1.53	0.00476
LCN1P1	1.59	0.00226	RP11-397P14.3	1.58	0.00021	TMEM150B	1.54	0.00304
MRPL55	1.59	0.00458	MLF1	1.59	0.00122	MAP7D2	1.54	0.00901
SH3BP2	1.59	0.00526	MX2	1.61	0.00132	AIF1	1.54	0.00463
SLC2A9	1.62	0.00354	DAZL	1.61	0.00472	U6	1.54	0.00977
FRZB	1.65	0.00735	IFLTD1	1.61	0.00823	FGF13	1.55	0.00686
CAPS2	1.65	0.00609	SLC22A14	1.63	0.00269	PIEZO1	1.55	0.00404
RP5-1004I9.1	1.71	0.00841	MGAT4C	1.65	0.00734	SERPINF2	1.58	0.00766
CAPN11	1.72	0.00193	GLI2	1.65	0.00392	CKMT2	1.58	0.00133
PNPLA3	1.72	0.00532	ANO4	1.65	0.00220	FAM83G	1.61	0.00543
TYRO3	1.80	0.00802	IFT80	1.68	0.00435	PLIN1	1.62	0.00775
ITGA5	1.81	0.00248	ANKRD20A9P	1.69	0.00080	TAS1R1	1.63	0.00798
CRYBG3	1.87	0.00157	HSD3B2	1.70	0.00355	ZNF385A	1.63	0.00533
TTC38	1.93	0.00571	CNTLN	1.72	0.00308	RASAL3	1.64	0.00119
ZNF619	1.93	0.00778	FCRL2	1.73	0.00217	SNX15	1.65	0.00211
OR10J1	1.98	0.00672	GULP1	1.77	0.00026	EMILIN3	1.66	0.00751
AC117472.2	2.03	0.00472	RS1	1.79	0.00154	UNC5C	1.67	0.00688
IQSEC2	2.21	0.00075	RP11-192H23.4	1.80	0.00228	GLT8D2	1.68	0.00136
HSPA4L	2.23	0.00503	ITGA5	1.81	0.00698	NCKAP5L	1.68	0.00647
CCDC157	2.61	0.00015	SPATA13	1.83	0.00675	ADCY10	1.71	0.00550
CLCA2	2.66	0.00051	TTLL13	1.91	0.00019	GPC3	1.71	0.00374
ANKRD30BL	2.98	0.00363	NHSL1	1.95	0.00353	TP53BP2	1.81	0.00740
DUOX1	3.31	0.00051	TTC38	1.96	0.00561	ASB9	1.83	0.00186
EFCAB5	3.36	0.00148	TYRO3	2.03	0.00378	MUC5B	1.92	0.00484
DSCR8	6.89	0.00308	SYCP2	2.11	0.00557	GRM5	2.05	0.00080
						CELF2	2.07	0.00195
						MMP14	2.19	0.00114
						KIFC3	2.25	0.00335
						DDO	2.26	0.00010
						KIAA1598	2.33	0.00242
						TIAM2	2.41	0.00015
						CCDC157	2.45	0.00011
						SLC36A3	2.47	0.00033
						MERTK	2.66	0.00358
						PTPRO	3.77	0.00077
						DSCR8	10.42	0.00082

Table 5.1. Investigating the effects of the BHRF1 miRNAs on cellular transcription. Lentiviral vector (empty vector, BHRF1-2/1-3 or BHRF1-1/1-2/1-3) transduced EBV positive Akata BL cells were subjected to total cellular transcript analysis using the GeneChip® Human Gene 1.0 ST Array system (Affymetrix). Data were initially processed using the AltAnalyse software. Differentially expressed genes were identified using limma. The p-value cut off was set to 0.01 and the fold change cut off to 1.5.

5.5.2 QPCR validation of genes found differentially regulated on the array

Next we investigated if these gene changes could be validated by another method of RNA detection. Therefore we randomly selected 15 differentially expressed genes for further validation by QPCR. In preliminary experiments we tested each QPCR assay using a small panel of lymphoid and epithelial cell lines in order to find suitable positive reference lines (data not shown). These lines included the EBV positive Akata BL and EH LCL2 B cell lines described in section 3.3, the EBV positive epithelial line C666.1 and the EBV negative NK line NKL. Five genes were found to be undetectable in Akata BL (ADAM18, DSCR8, ASZ1, HSPA4L and GRM5) and thus excluded from further analysis.

Expression of the remaining genes (MIPEP, TDRD7, CRYBG3, FCRL2, IQSEC2, CELF2, MAN1B1, MMP14, OCA2 and ITGA5) was assessed by QPCR in the same RNA samples used in the microarray analysis. Relative expression levels of each gene are shown in Fig. 5. 14, alongside the paired array data. According to the array analysis, transcript levels of all ten genes varied by 1.5-3 fold between Akata cultures transduced with different lentiviral vectors (Fig. 5.14A). For instance TDRD7 was up-regulated by 1.51 fold in BHRF1-2/1-3 transduced Akata cells relative to the BHRF1-1/1-2/1-3 vector. OCA2 in turn was down-regulated by 2.99 fold in BHRF1-1/1-2/1-3 transduced Akata cells relative to the empty vector. Remarkably none of these changes could be reproduced when detection was carried out using QPCR (Fig. 5.14B); levels of all genes, including TDRD7 and OCA2, were near identical between for all three lentiviral vector transduced Akata cultures.

In order to better understand the lack of correlation between the array and QPCR data sets, we re-analyzed our raw array data with R/Bioconductor using the XPS software package (http://www.bioconductor.org). From this new normalized dataset we then examined

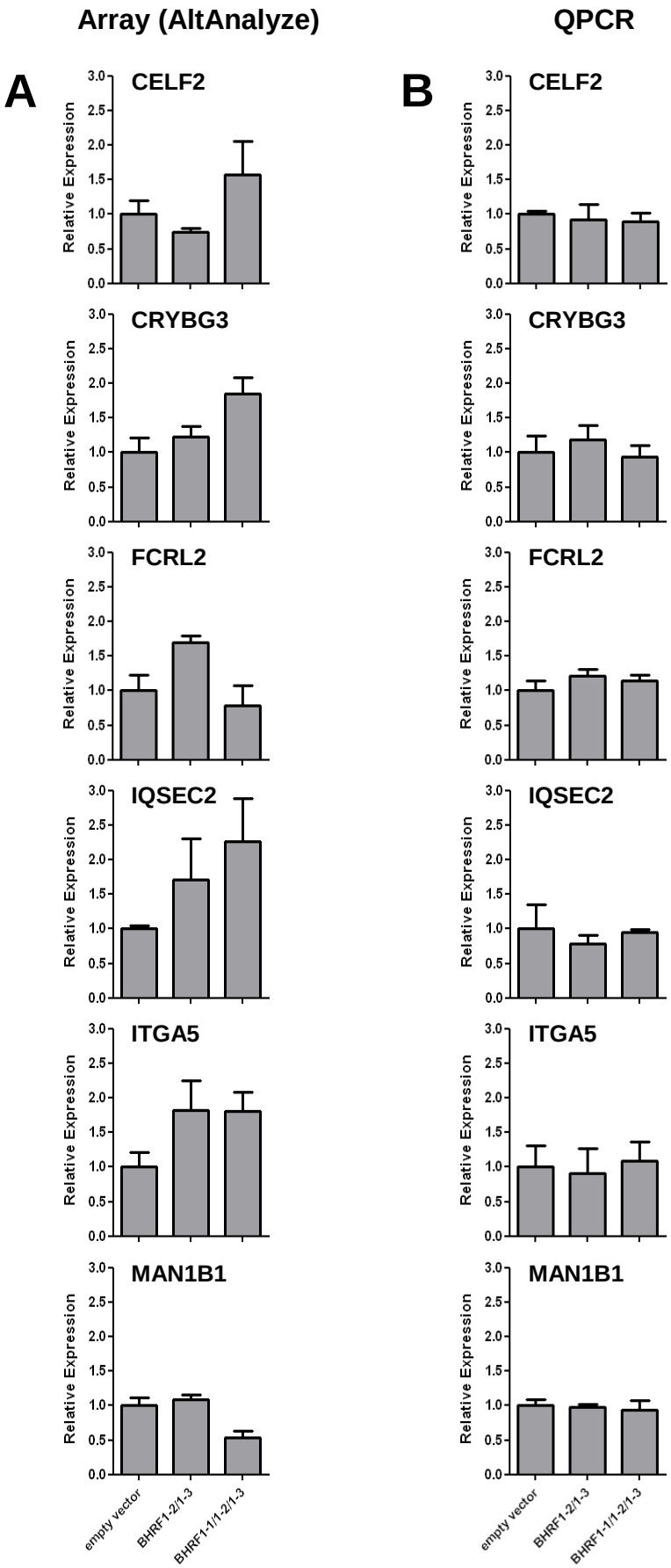
Array (AltAnalyze)
QPCR
A
B
CELF2
CRYBG3
FCRL2
IQSEC2
ITGA5
MAN1B1
Relative Expression
3.0
2.5
2.0
1.5
1.0
0.5
0.0
empty vector
BHRF1-2/1-3
BHRF1-1/1-2/1-3

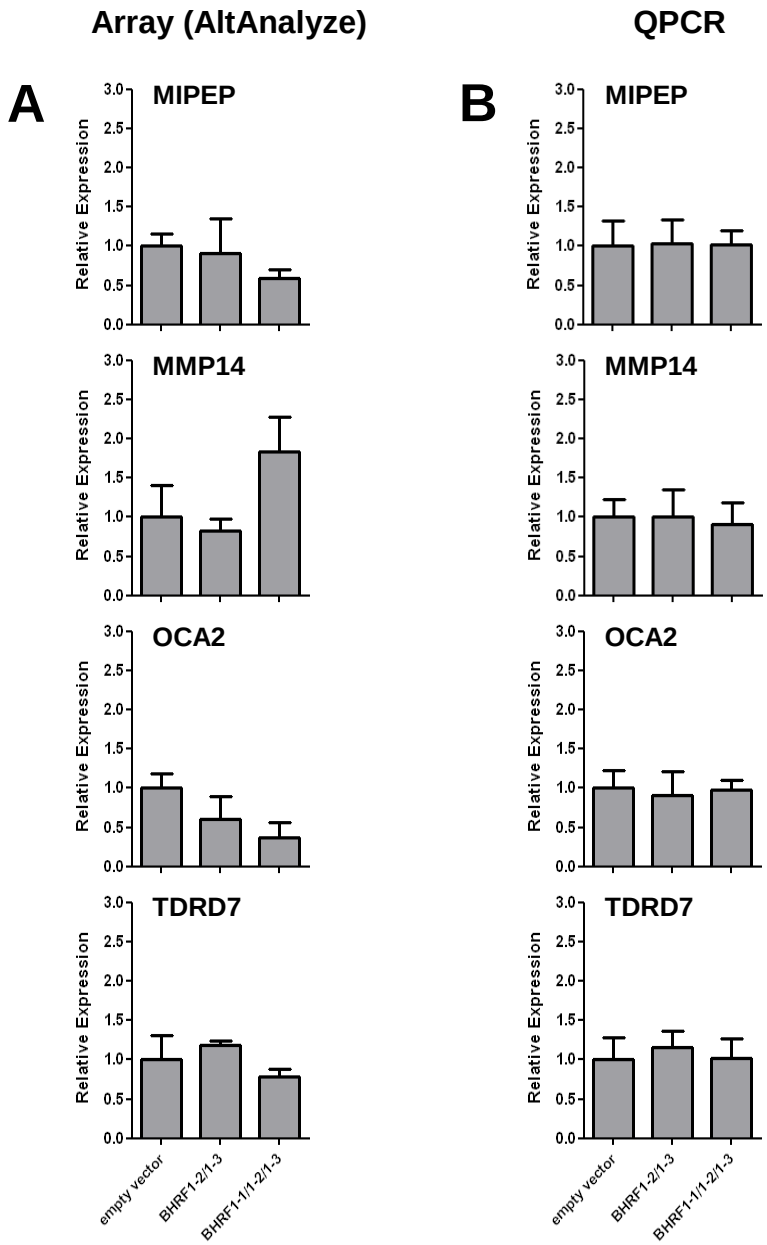

Fig. 5.14. Investigating the effects of the BHRF1 miRNAs on cellular transcription. **(A)** Lentiviral vector (empty vector, BHRF1-2/1-3 or BHRF1-1/1-2/1-3) transduced EBV positive Akata cells were subjected to total cellular transcription analysis using the GeneChip® Human Gene 1.0 ST Array system (Affymetrix). Data were processed using the AltAnalyse software. **(B)** Transcriptional changes seen in array were validated by QPCR for a random selection of genes. Data are expressed relative to the empty vector control (set at one). Error bars indicate standard deviation of three separate experiments.

expression levels of nine genes shown earlier in Fig. 5.14. These new XPS-generated values are shown in Fig. 5.15, also alongside the paired QPCR data. In contrast to the AltAnalyze data, the XPS data indicates that all nine genes (MIPEP, TDRD7, FCRL2, IQSEC2, CELF2 MAN1B1, MMP14, OCA2 and ITGA5) are expressed to similar levels in all three lentiviral vector transduced Akata cultures (Fig. 5.15A). These data clearly agree more with QPCR data (Fig. 5.15B) than the AltAnalyze data (Fig. 5.14A). Overall these findings suggest that all 15 genes originally identified as differentially expressed from the AltAnalyze data set were false positives. Unfortunately due to lack of time, it was not possible to perform a Limma analysis to identify potential differentially regulated genes from the new XPS data set.

5.5.3 Analysis of CXCL11 expression

In a final attempt to validate our array data, we asked whether our array data was consistent with previous studies which had identified BHRF1 miRNA targets. At the time of this study only two groups had investigated the effects of the BHRF1 miRNAs at both protein and mRNA levels. Li *et al.* found that miR-BHRF1-1 reduced levels of p53 protein but not p53 mRNA (752), while Xia *et al.* reported that miR-BHRF1-3 reduced both levels of CXCL11 protein and mRNA (753). Out of our two BHRF1 miRNA expression vectors, the BHRF1-2/1-3 construct generated higher levels of miR-BHRF1-3 sufficient to knock down a target reporter (Fig. 5.16A). Consequently we interrogated our array data for CXCL11 transcript levels in empty vector vs. BHRF1-2/1-3 transduced Akata BL cells but our data did not reveal any reduction in CXCL11 mRNA levels in the presence of miR-BHRF1-3 (Fig. 5.16B). However we can not draw any concrete conclusions on the overall validity of our array data until we have fully analyzed the data using the alternative XPS analysis.

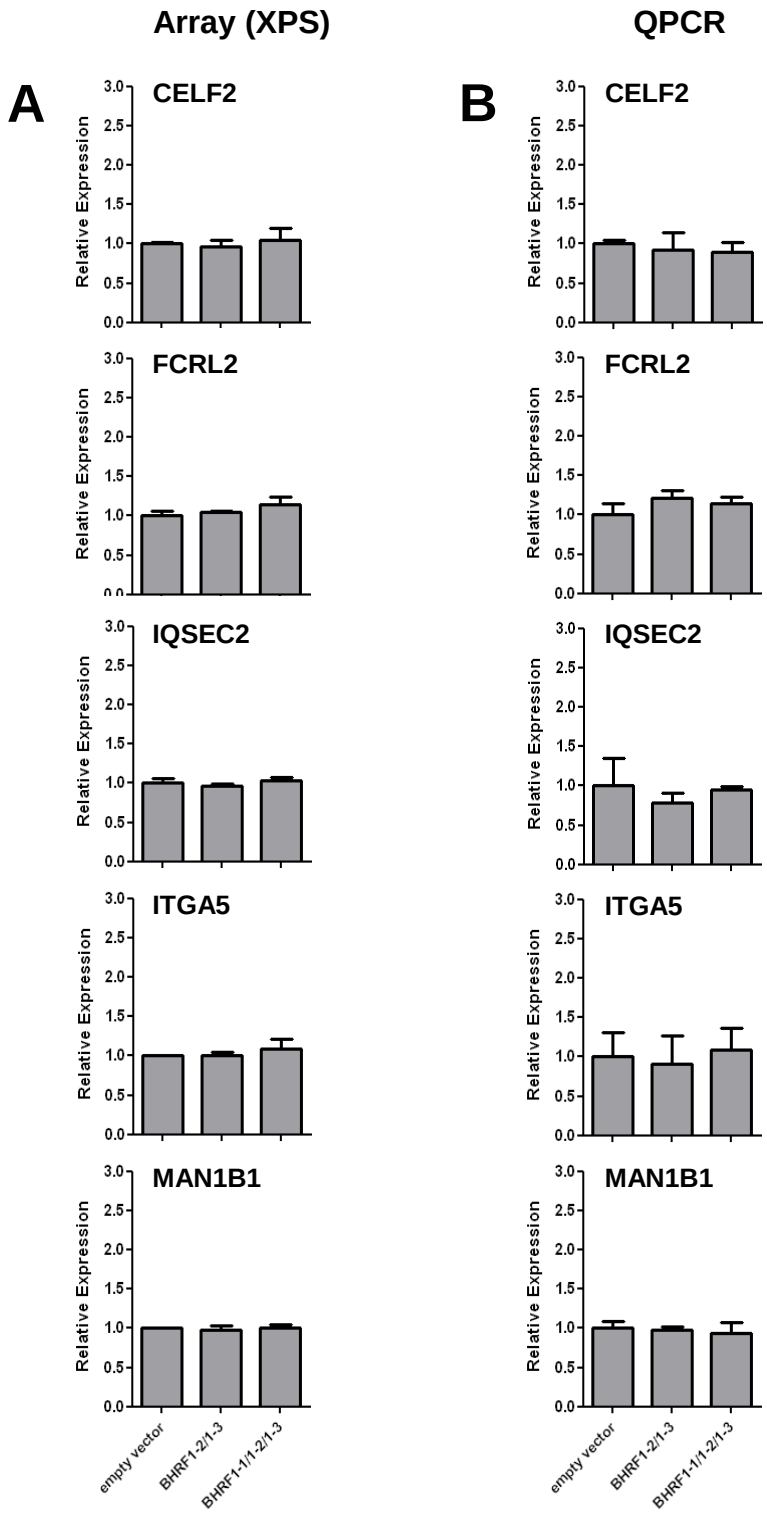
Array (XPS)
QPCR
A
B
CELF2
FCRL2
IQSEC2
ITGA5
MAN1B1
Relative Expression
3.0
2.5
2.0
1.5
1.0
0.5
0.0
empty vector
BHRF1-2/1-3
BHRF1-1/1-2/1-3

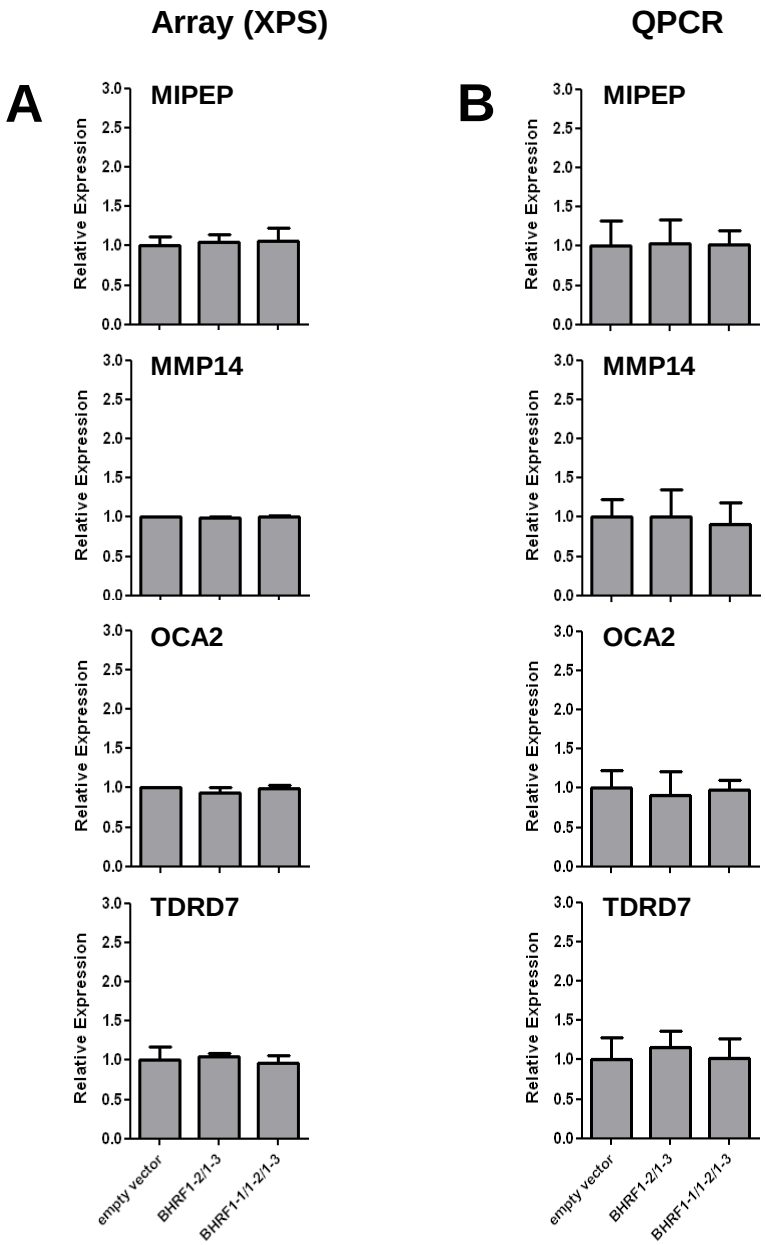

Fig. 5.15. Investigating the effects of the BHRF1 miRNAs on cellular transcription. **(A)** Lentiviral vector (empty vector, BHRF1-2/1-3 or BHRF1-1/1-2/1-3) transduced EBV positive Akata cells were subjected to total cellular transcription analysis using the GeneChip® Human Gene 1.0 ST Array system (Affymetrix). Data were processed using the XPS software **(B)** Transcriptional changes seen in array were validated by QPCR for a random selection of genes. Data are expressed relative to the empty vector control (set at one). Error bars indicate standard deviation of three separate experiments.

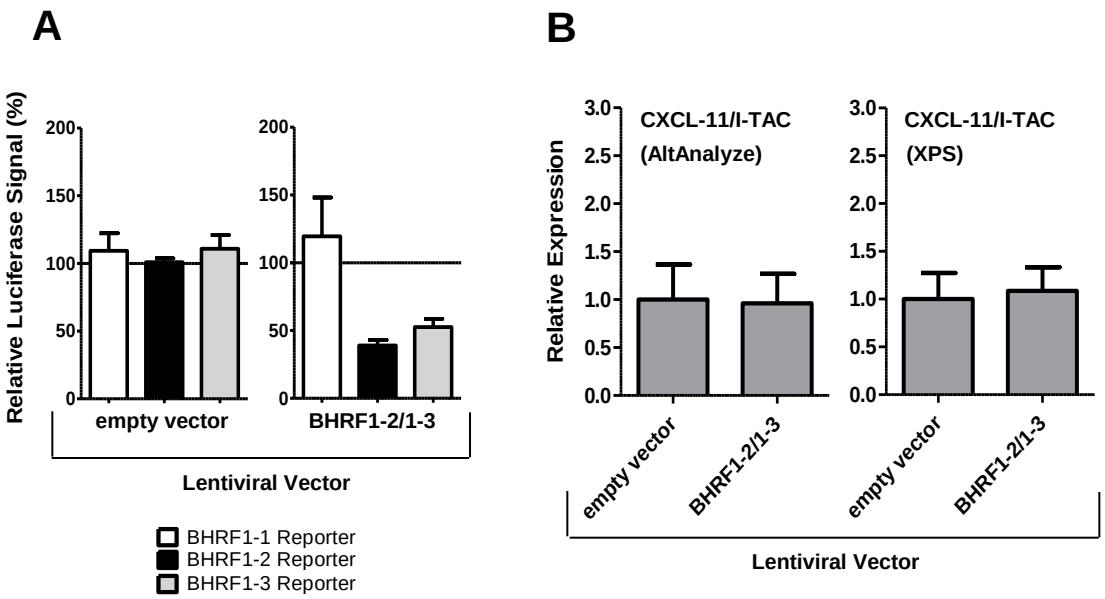

Fig. 5.16. Validation of a published BHRF1 miRNA target. **(A)** Data presented in Fig. 5.11 revealed that the BHRF1-2 and BHRF1-3 firefly reporter constructs are specifically repressed in EBV positive Akata cells transduced with the BHRF1-2/1-3 but not the empty lentiviral expression vector. **(B)** Affymetrix array data for the same cells, processed either using the AltAnalyse or XPS software, reveals no corresponding change in the levels of CXCL11 mRNA.

5.6 Investigating the effects of the BHRF1 miRNAs on cell growth

In chapter 1.5 we described how cellular miRNAs regulate proliferation. Most cellular miRNAs exert anti-proliferative effects through the targeting of cyclins and CDK family members (199). A number of KSHV and EBV miRNAs exert pro-proliferative effects by targeting inhibitors of proliferation. Thus KSHV miRNAs target CDK inhibitors such as WEE1 (miR-K12-1 and miR-K12-12), p21 (miR-K12-1), p27 (miR-K12-11) and PP2A (miR-K12-1) (814-817). EBV miRNAs can also target inhibitors of proliferation such as p53 (miR-BHRF1-1) (752). Furthermore the EBV BART miRNAs are predicted to target numerous cell cycle proteins while the BHRF1 miRNAs are known to assist in cell cycle progression during early EBV infection (750, 751, 764).

Therefore we asked whether the BHRF1 miRNAs might confer a proliferative advantage to BL cells. To this end EBV negative BL41 cells and EBV positive Lat I Akata BL cells, both stably transduced with lentivirus (empty vector, BHRF1-2/1-3 or BHRF1-1/1-2/1-3), were treated with doxycycline for 72 h as before. Cells were seeded at 10^5 cells/ml, and viable GFP-positive cells were subsequently enumerated at 24 h, 48 h and 72 h using flow cytometry. The representative experiments illustrated in Fig. 5.17 show that the growth rates of BL41 cells in the presence or absence of the BHRF1 miRNAs are remarkably similar; similar results can be observed for Akata BL cells. Thus the BHRF1 miRNAs do not appear to alter the growth rates of the BL tumour lines, at least under *in vitro* conditions.

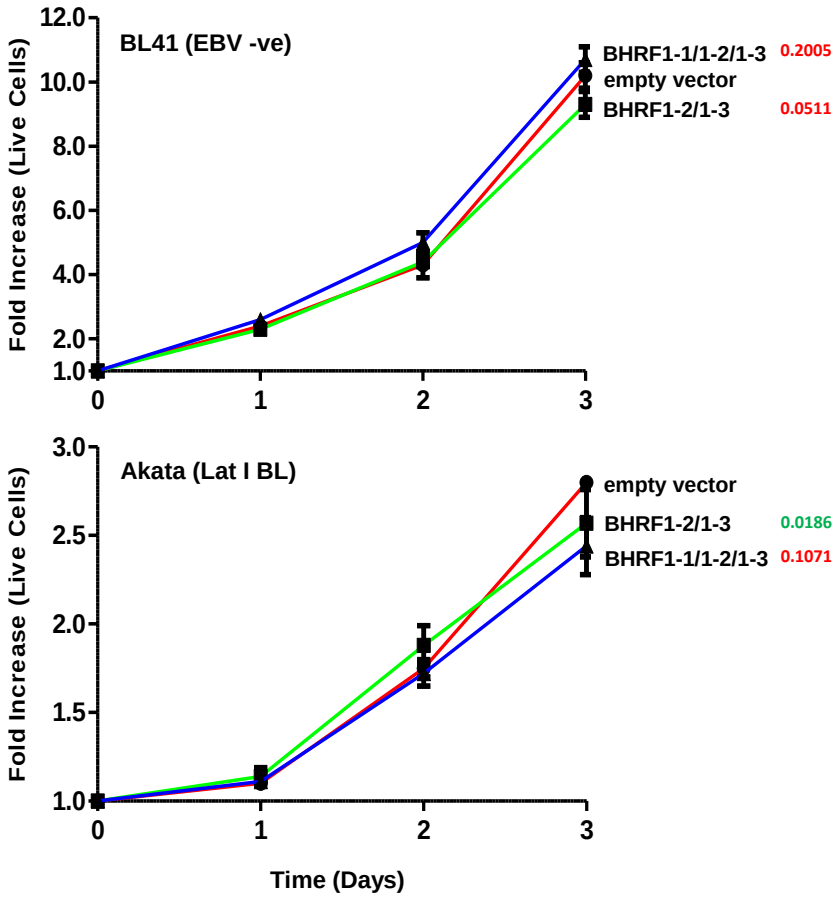

Fig. 5.17. Investigating the effects of the BHRF1 miRNAs on cell growth. Lentiviral vector (empty vector, BHRF1-2/1-3 or BHRF1-1/1-2/1-3) transduced EBV negative BL41 BL cells and EBV positive Lat I Akata BL cells were seeded at low density (10^5 cells/ml). Live GFP-positive cells were enumerated daily over a 3 day period using flow cytometry. One of two representative experiments are shown for each BL line tested. Error bars indicate standard deviation of three replicate measurements. Fold changes in live cell counts for BHRF1 miRNA expressing cultures were compared to those of empty vector transduced cells on day 3 using an unpaired t test with a P value cut off set to 0.05. P values are listed to the right of each graph using green and red text to denote statistical significance and insignificance respectively.

5.7 Investigating the effects of the BHRF1 miRNAs on apoptosis

In chapter 1.5 we also described how many cellular miRNAs regulate apoptosis (programmed cell death). Apoptosis can occur through the intrinsic pathway, which is regulated by Bcl-2 family members, and the extrinsic pathway, which is regulated by cell-cell signalling (188). In the intrinsic pathway, pro- and anti-apoptotic members of the Bcl-2 family interact to carefully control mitochondrial cytochrome c release which consequently triggers cell death. EBV BART miRNAs are already known to enhance cell survival by repressing pro-apoptotic Bcl-2 family members such PUMA (miR-BART5) and Bim (miR-BART 1, 3, 9, 11 and 12) (754, 756). Likewise the BHRF1 miRNAs are reported to confer cell survival during early EBV infection, though their precise targets remain unclear (751).

5.7.1 Expression of Bcl-2 family proteins in BL41 BL cells stably expressing BHRF1 miRNAs

To address the possibility that the BHRF1 miRNAs also target Bcl-2 family members, we initially screened our array data for changes in transcript levels of Bcl-2 family genes using the AltAnalyze array data set. There were no changes which were both greater than 1.5 fold and statistically significant ($p<0.01$) (data not shown). Consequently any potential regulation of Bcl-2 family members by the BHRF1 miRNAs would most likely be post-transcriptional. To investigate this further, EBV negative BL41 cells stably transduced with lentivirus (empty vector, BHRF1-2/1-3 or BHRF1-1/1-2/1-3) were cultured for 72 h either in the presence or absence of doxycycline. Subsequently cells were assessed by western blot for the expression of pro-apoptotic (Bak, Bax, PUMA, Bim, Noxa and Bid) and anti-apoptotic (Bcl-2, Bcl-XL and Mcl-1) Bcl-2 family members (Fig. 5.18); note that Bcl-6 is not a Bcl-2 family member

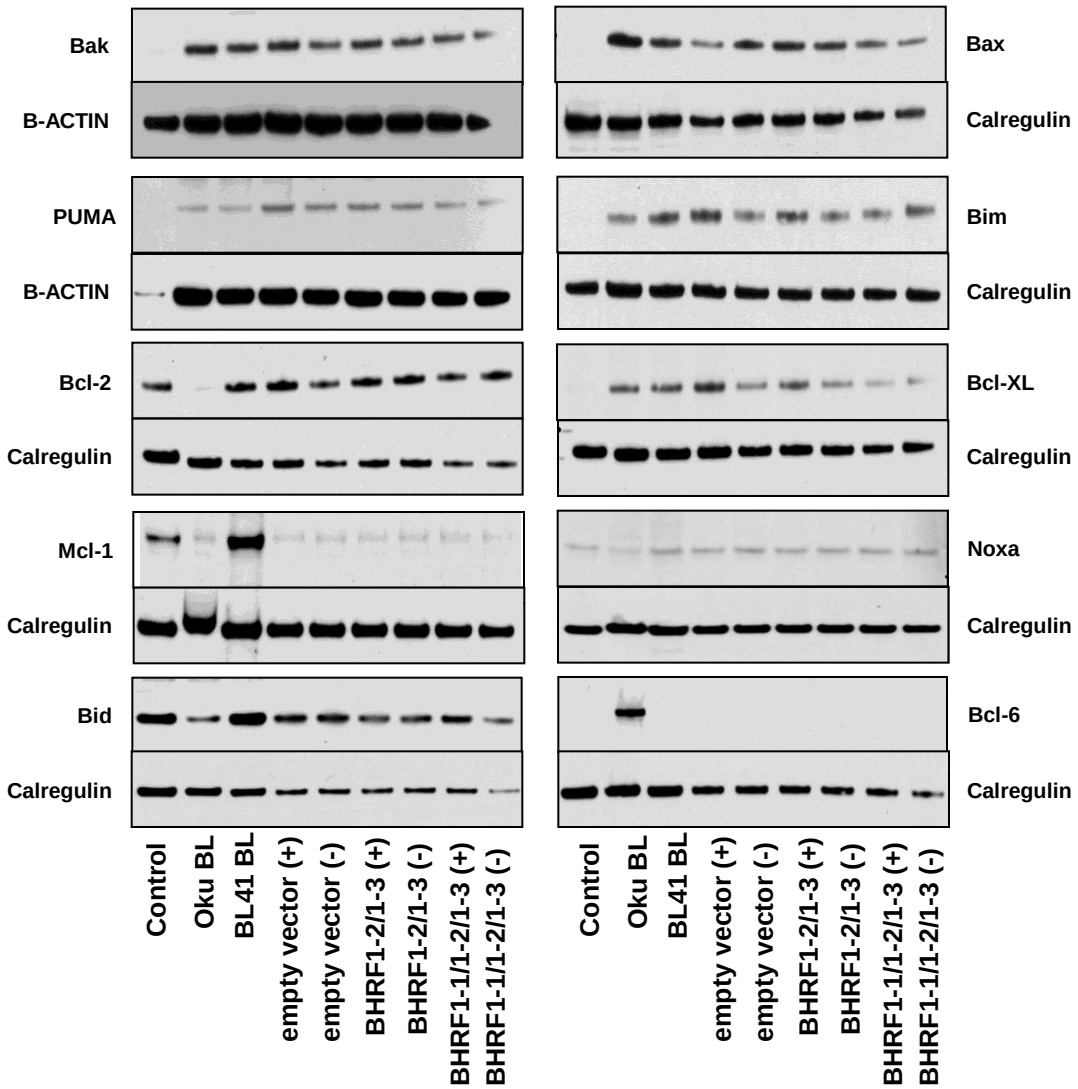

Fig. 5.18. Expression of Bcl-2 family member proteins in a lentivirus transduced BL line. Pro-apoptotic (Bak, Bax, PUMA, Bim, Noxa and Bid) and anti-apoptotic (Bcl-2, Bcl-XL and Mcl-1) members of the Bcl-2 family were detected by western blot in EBV negative BL41 BL cells transduced with a lentiviral BHRF1 miRNA expression vector (empty vector, BHRF1-2/1-3 or BHRF1-1/1-2/1-3). Where indicated, BL41 BL cells were cultured in parallel either in the presence (+) or absence (-) of doxycycline. Parental BL41 BL and Oku BL lines were included as BHRF1 miRNA negative and positive controls respectively. DG75 (Bak and Bax), 293 ft (PUMA), BL2 (Bim) and Kem I (Bcl-XL and Bcl-6) were included as negative controls. EH LCL2 (Bcl-2) was included as a positive control. No suitable controls were known/available for Mcl-2, Noxa and Bid. Detection of either B-Actin or Calregulin was performed as a loading control.

but was added to the list because it is a predicted target of the miR-BHRF1-2 seed (AUCUUUU) according to Targetscan (102, 107).

In general, levels of all Bcl-2 family members tested were similar in BL41 cells transduced with the BHRF1-2/1-3, BHRF1-1/1-2/1-3 or empty lentiviral expression construct; this was true for both the doxycycline treated and untreated samples. In some cases, minor differences between protein band intensities were observed but these were almost always mirrored by similar changes in the loading control e.g. Bid and calregulin levels in untreated BHRF1-1/1-2/1-3 transduced cells. One exception was Bcl-XL which appeared to be reduced in BL41 cells transduced with the BHRF1-1/1-2/1-3 construct; however this result was not reproducible in every experiment (data not shown). We were unable to confirm if miR-BHRF1-2 regulates Bcl-6 as it was undetectable in the BL41 cell line.

5.7.2 Survival of BL cells stably expressing the BHRF1 miRNAs cultured in the presence of ionomycin

In a final experiment we asked if the BHRF1 miRNAs conferred any resistance to cell death in the BL cell line model. Therefore we treated lentiviral vector (empty vector, BHRF1-2/1-3, BHRF1-1/1-2/1-3 or BHRF1 protein) transduced EBV negative BL41 and BL30 cells and EBV positive Lat I Akata BL cells for 48 h with doxycycline. Thereafter cells were cultured in the presence or absence of ionomycin for an additional 48 h; note that ionomycin induces apoptosis via the intrinsic apoptosis pathway by increasing intracellular Ca^{2+} levels (818-820). Total cell death was then assessed by flow cytometry, using syto17 and PI to stain for live and dead cells, respectively (Fig. 5.19).

Fig. 5.19. Investigating the effects of the BHRF1 miRNAs on cell survival. Lentiviral vector (empty vector, BHRF1-2/1-3, BHRF1-1/1-2/1-3 or BHRF1 protein) transduced EBV negative BL41 and BL30 BL cells and EBV positive Lat I Akata BL cells were treated for 48h with the apoptosis-inducing drug ionomycin. **(A)** Total cell death was enumerated using flow cytometry. Live cells were stained using syto17; this is a membrane permeable dye which brightly stains live, but not apoptotic and dead cells. Dead cells were stained using PI; this is a membrane impermeable dye and thus only stains cells with degenerate membranes. **(B)** Two replicate experiments are shown for each BL line tested. Error bars indicate standard deviation of three replicate measurements. Total cell death in BHRF1 miRNA and protein expressing cultures was compared to that in empty vector transduced cells using an unpaired t test with a P value cut off set to 0.05. P values are listed above each column using green and red text to denote statistical significance and insignificance respectively.

A

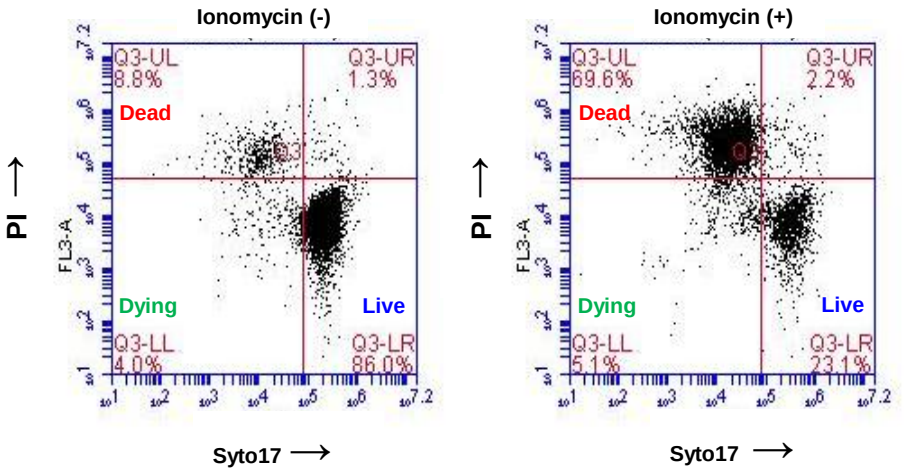
Ionomycin (-)
Ionomycin (+)
PI
FL3-A
Syto17
Q3-UL
8.8%
Q3-UR
1.3%
Dead
Dying
Live
Q3-LL
4.0%
Q3-LR
86.0%
Q3-UL
69.6%
Q3-UR
2.2%
Dead
Dying
Live
Q3-LL
5.1%
Q3-LR
23.1%

B

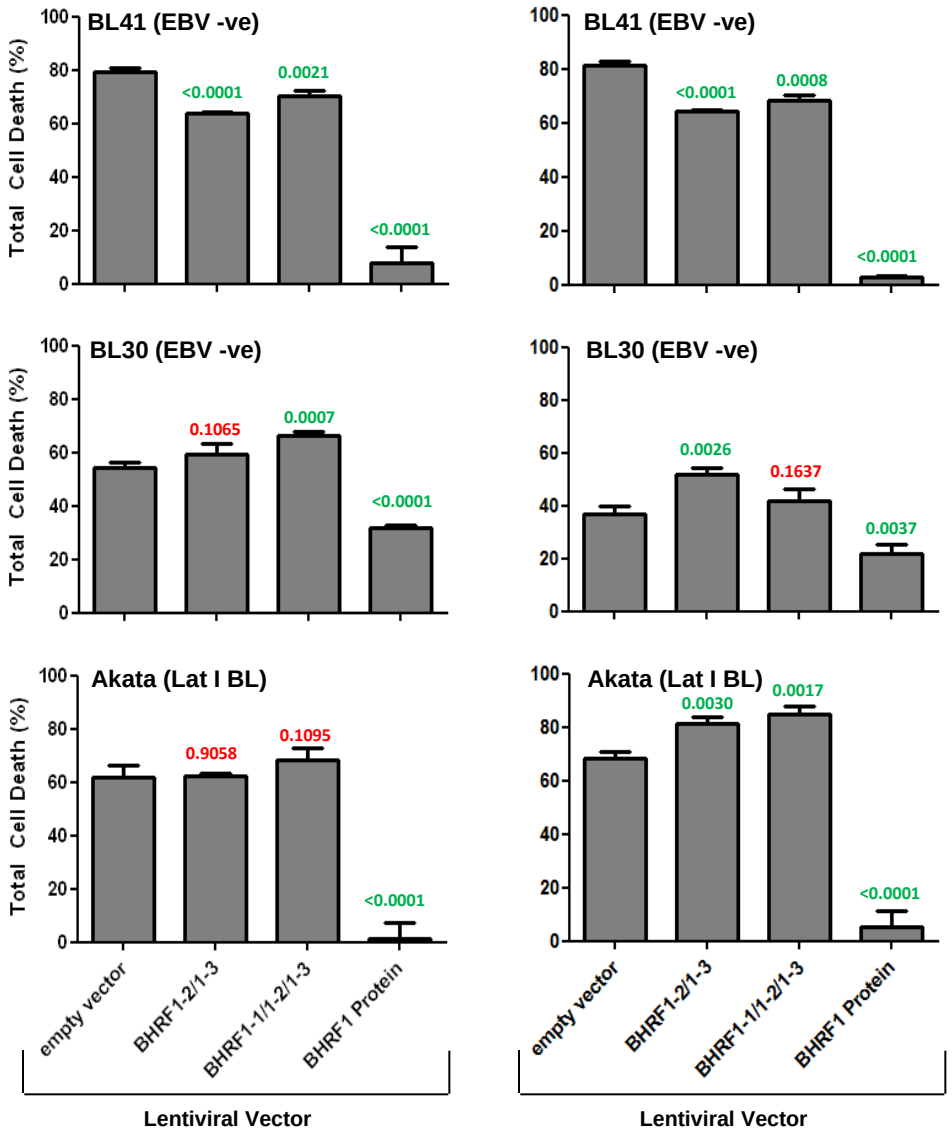
BL41 (EBV -ve)
BL30 (EBV -ve)
Akata (Lat I BL)
Total Cell Death (%)
<0.0001
0.0021
<0.0001
0.0008
0.1065
0.0007
<0.0001
0.0026
0.1637
0.0037
0.9058
0.1095
<0.0001
0.0030
0.0017
<0.0001
empty vector
BHRF1-2/1-3
BHRF1-1/1-2/1-3
BHRF1 Protein
Lentiviral Vector

Broadly speaking BL41 cells transduced with the BHRF1 miRNAs expression constructs (BHRF1-2/1-3 or BHRF1-1/1-2/1-3) appeared slightly more resistant to cell death than cells transduced with the empty vector. By contrast BL30 cells transduced with the BHRF1 miRNAs expression constructs appeared slightly more sensitive to cell death than cells transduced with the empty vector. Finally the sensitivities to cell death were broadly similar for all three TREX lentivirus transduced Akata BL lines.

As a control we included BL41, BL30 and Akata BL cells stably transduced with a BHRF1 protein expression construct (kindly provided by Leah Fitzsimmons). BHRF1 is the main viral Bcl-2 homolog and is considered an important contributor to the survival advantage of Wp-BL over Lat I BL (320, 681). All three BL lines tested were significantly ($P < 0.05$) and reproducibly protected from cell death in the presence of the BHRF1 protein. The level of protection ranged from ~2 fold (BL30) to nearly absolute protection (BL41 BL and Akata BL). By comparison the effects of the BHRF1 miRNAs on cell death were remarkably small in all BL lines tested and lacked reproducibility.

5.8 Discussion

5.8.1 Detecting functional changes in BHRF1 miRNA expression

A wide range of methodologies have been used to investigate the function of EBV miRNAs. These include genetic deletion, down regulation by AMOs, down regulation by sponge constructs or artificial expression of the miRNA of interest (750-752, 755, 764). We investigated a number of these methodologies as possible means by which to study the function of the BHRF1 miRNAs in the context of Wp BL.

As a first step we designed luciferase reporter constructs with individual BHRF1 miRNA binding sites to detect functional changes in miRNA levels (Fig. 5.1). These constructs were successful in that inhibition was only observed in a cell line expressing relevant BHRF1 miRNAs (Fig. 5.2). Interestingly, we observed a greater repression of the BHRF1-2 miRNA construct as compared to the other reporters. This is unlikely due to an excess of the BHRF1-2 miRNA, as copy numbers of all three BHRF1 miRNAs in Oku BL are within a 2-fold range (Fig. 3.8B) (743). This result could represent a higher affinity of the BHRF1-2 miRNA for its binding site in the luciferase mRNA 3′ UTR.

Our reporter system used perfectly complementary binding sites for each of the BHRF1 miRNAs. Use of physiological binding sites for miR-BHRF1-1 or miR-BHRF1-2 was not possible as there were no validated targets for these miRNAs at the time we developed our reporter system. Although miR-BHRF1-3 was shown to target CXCL11, it was presumed to do so via a 100% complementary sequence (250, 753). Consequently the miR-BHRF1-3 binding site in our reporter system could be seen as physiological. The use of perfectly complementary binding sites is advantageous when designing a sensitive reporter system as perfect miRNA-target associations result in stronger repression than do imperfect miRNA-target matches (821).

5.8.2 Using anti-miRNA oligonucleotides to study BHRF1 miRNA function

The successfully application of LNA^{TM} inhibitors to the study of cellular miRNAs has been extensively documented (792). More recently LNA^{TM} inhibitors have also been to study the function of viral miRNAs; miRNA knockdown studies have implicated KSHV miRNAs (miR-K12-6 and miR-K12-11) in targeting the cellular transcription factor MAF (806) and an

EBV miRNA (miR-BART10-3p) in targeting BHRF1 (764). The use of Morpholino inhibitors to study cellular miRNAs has also has been extensively documented (http://www.gene-tools.com/node/31#miRNAcitations). Success stories include demonstrating that miR-24a regulates apoptosis during retinal development (822) while miR-125b regulates p53 expression in humans and zebrafish (823). Thus we had ample evidence to suggest that LNA^{TM} and Morpholinos inhibitors could be used to successfully knockdown the BHRF1 miRNAs.

Thus having designed our BHRF1 miRNA reporter constructs, we investigated whether we could achieve BHRF1 miRNA knockdown in Oku BL using inhibitors, and which inhibitor (LNA^{TM} and Morpholinos) would give us the best results (Fig. 5.3 and 5.4). We concluded that miR-BHRF1-3 knockdown was achievable using both inhibitors. While higher doses of Morpholinos were required to achieve an effect, as compared to LNA^{TM}, the overall price per quantity was much cheaper, making the former a more cost effective approach. Following our success with both of the miR-BHRF1-3 inhibitors we then proceeded to test an LNA^{TM} inhibitor against miR-BHRF1-1 and a Morpholino inhibitor against miR-BHRF1-2. The LNA^{TM} inhibitor against miR-BHRF1-1 increased reporter activity in a non-specific manner i.e. both the BHRF1-1 and the control reporters were affected. We speculate our inhibitor could be in part acting as carrier DNA by improving plasmid uptake; the effects of carrier DNA on transfection have been documented elsewhere (824). Thus we could not distinguish genuine miR-BHRF1-1 knockdown from off target effects. Because of this result we chose not to order an LNA^{TM} inhibitor against miR-BHRF1-2.

Results with the Morpholino inhibitor against miR-BHRF1-2 were difficult to interpret due to technical issues with our β-gal assay. Briefly the duplicate β-gal readings taken for each sample often deviated from each other by more than two fold. Consequently when we

normalized our firefly luciferase data to β-gal we occasionally obtained nonsensical results, such as the apparent 2-fold increase in control reporter activity at the 10μM inhibitor concentration. We eventually resolved this issue by using the pRL SV40 *Renilla* reporter construct for data normalization. Nonetheless it was clear that the miR-BHRF1-2 inhibitor could not achieve satisfactory miR-BHRF1-2 knockdown; doubling the inhibitor dose made no difference to our results. Note that Gene Tool, LLC were unable to design a Morpholino inhibitor against miR-BHRF1-1; a tetra-G sequence in the inhibitor would render it water insoluble (http://www.gene-tools.com/node/18). Consequently it would not have been possible to knockdown all three BHRF1 miRNAs using LNA^{TM} inhibitors, Morpholino inhibitors, or combinations thereof.

Oku BL expresses broadly similar levels of all three BHRF1 miRNAs (Fig. 3.8B). Therefore if we assume that neither the LNA^{TM} inhibitor against miR-BHRF1-1 nor the Morpholino inhibitor against miR-BHRF1-2 was defective, then the only way to explain our lack of success with both is that they are less efficient in mediating target knockdown than either miR-BHRF1-3 inhibitor. Therefore it follows that the amount of miR-BHRF1-1 and miR-BHRF1-2 inhibitor taken up by the cell was likely insufficient to mediate target knockdown. On that note Wp BL lines are very difficult to transfect; this could explain our overall lack of success with anti-miRNA oligonucleotides (AMOs).

Issues with transfection efficiencies may well have complicated future attempts to deliver a pool of inhibitors capable of simultaneously knocking down multiple BHRF1 miRNAs. Likewise it impacts on the cost of our experiments as higher doses of inhibitor per transfection are required to achieve knockdown. Adding to the issue of cost are the scrambled miRNA inhibitors required to control for non-specific effects for each type of inhibitor used in our experiments; the process of introducing foreign DNA to the cell may itself affect cell

cycle progression and apoptosis (825), two cellular process previously associated with the BHRF1 miRNAs (750, 751).

A recent study by Obad *et al*. documented the use of small LNA^{TM} inhibitors against the miRNA seed (826). These inhibitors were found to target closely related miRNAs without causing off-target effects; specifically, binding of small LNA^{TM} inhibitors to sites in the ORF and UTR regions of mRNA did not influence protein output. Small LNA^{TM} inhibitors, by virtue of their size, may also have allowed for more efficient cellular delivery than those inhibitors used in the present study. Unfortunately we were unaware of the existence of these inhibitors at the time we conducted our AMO experiments. Thus the overall unsatisfactory results and high cost of this line of work led us to seek alternative methodologies to study BHRF1 miRNA function.

5.8.3 Using lentivirus expression vectors to study BHRF1 miRNA function

One alternative approach to study the function of the BHRF1 miRNAs is to use lentiviral constructs to express the BHRF1 miRNAs in a panel of EBV negative and Lat I lines (Fig 5.5 – Fig 5.8). As reviewed by Liu and Berkhout, the use of lentiviruses to express miRNAs has a number of advantages as well as potential drawbacks (827). The main advantage is that lentivirus vectors stably integrate into the host genome thereby allowing continuous expression of the miRNA expression cassette. A major disadvantage is the theoretical ability of the miRNA expression cassette to interfere with virus production in producer cells. If the cassette is inserted in the sense orientation, then the viral RNA genome will contain Drosha cleavage sites; if the cassette is inserted in the antisense orientation then the viral RNA genome will contain miRNA target sites.

Our BHRF1 miRNA expression cassettes were inserted in the reverse orientation thus avoiding the presence of Drosha cleavage sites in the viral RNA genome (Fig 5.8). The accumulation of the tetracycline repressor protein (TetR) in producer cells should in theory minimize BHRF1 miRNA expression and potential targeting of the viral RNA genome. A possible issue with inserting the BHRF1 miRNA expression cassette in the reverse orientation is that the viral RNA genome would contain the BHRF1 poly-A signal. This could lead to reduced viral titre by inducing early transcriptional termination of the viral RNA genome (828). On the other hand removal of the BHRF1 poly-A signal might have destabilized the miRNA precursor transcript (828). However we speculated that a reduction in virus titre could be compensated for by sorting cells with high GFP expression.

We generated two BHRF1 miRNA expression constructs; one to express the combination of miR-BHRF1-2 and miR-BHRF1-3, and the other to express all three BHRF1 miRNAs, thus mimicking BHRF1 miRNA expression in lytic cycle and Lat III, respectively. Overall we found that the same construct produced similar BHRF1 miRNA copy numbers across all four BL backgrounds (BL41, BL30, Akata BL, Mutu 59 BL); the small variations in BHRF1 miRNA expression between BL lines likely reflects differences in transduction efficiency (Fig 5.10). Importantly the observed levels of BHRF1 miRNA expression were physiologically comparable to Wp BL and Lat III BL (809). Specifically the copy numbers measured for miR-BHRF1-1 and BHRF1-2 were comparable to those seen in Wp BL while those of miR-BHRF1-3 were comparable to Lat III BL.

At this point we noted a few technical issues with our BHRF1 miRNA expression system. In all BL lines tested we found a degree of leaky BHRF1 miRNA expression in the absence of doxycycline (Fig. 5.12 and data not shown). We assessed the effects of leaky BHRF1 miRNA expression on relevant target reporters in the BL41 and Akata BL lines. Interestingly

knockdown was only seen in BL41 cells, despite both lines expressing similar background levels of the BHRF1 miRNAs. It is tempting to speculate that BHRF1 miRNAs might function more effectively in some backgrounds over others, perhaps because they are able to associate with miRISC more easily. On that note, Riley *et al*. observed that a small group of just 12 BART miRNAs appeared to compete for 22% of all Ago sites in the Jijoye BL line. The BHRF1 miRNAs would have to compete with the BART miRNAs for Ago sites in Akata BL, but not BL41, possibly explaining the discrepancies in BHRF1 miRNA function between these lines. More importantly, the leaky BHRF1 miRNA expression posed a problem in that we could not necessarily rely on using doxycycline untreated cells as a negative control in our experiments. For this reason we generated the empty control vector CON(empty)UTG.

We also found that miR-BHRF1-3 copy numbers were notably reduced in the construct expressing all three BHRF1 miRNAs as compared to the construct expressing just miR-BHRF1-2 and miR-BHRF1-3. Due to the artificial nature of our construct, we can only speculate as to why joining parts of the BHRF1 5′ UTR (miR-BHRF1-1) and 3′ UTR (miR-BHRF1-2 and miR-BHRF1-3) would result in diminished miR-BHRF1-3 expression. Changes in the miR-BHRF1-2 sequence can impair processing of the miR-BHRF1-3, which means that sequences outside the pre-miRNA can also affect miRNA processing (829). Nonetheless we find it strange that the presence of the miR-BHRF1-1 sequence would impair miR-BHRF1-3 processing but not that of the adjacent miR-BHRF1-2. The ability of the pri-miRNA tertiary structure to trigger the differential accumulation of individual miRNAs within the same cluster has been documented (830). Thus it is possible that the presence of the miR-BHRF1-1 sequence triggers a conformational change in the pri-miRNA structure that makes miR-BHRF1-3 less accessible to miRNA processing machinery.

With these caveats in mind, we proceeded to assess the functional impact of all three BHRF1 miRNAs on our firefly reporter system (Fig 5.11). The results were highly satisfactory. Firstly there was a very good correlation between BHRF1 miRNA expression and luciferase knockdown. Secondly knockdown was satisfactory, usually ranging between 40% and 60%. Thirdly the same degree of knockdown was highly reproducible across three separate experiments. Consequently we chose to use our BHRF1 miRNA expression system to investigate the function of the BHRF1 miRNAs in the context of Wp BL.

5.8.4 Investigating potential phenotypes conferred by the BHRF1 miRNAs

The majority of cellular miRNAs are believed to fine-tune gene expression rather than completely shut off expression of their target (106). Nonetheless some miRNAs are able to mediate dramatic phenotypic changes e.g. transgenic expression of miR-155 causes B cell malignancies in mice (218). Thus there is a rationale for investigating potential miRNA associated phenotypes as opposed to merely elucidating their 3′ UTR binding sites. So far only two phenotypic studies have been conducted on the EBV miRNAs, both of which demonstrated a contributing role for the BHRF1 miRNAs in B cell growth transformation (750, 751).

Seto *et al.* were first to note that, when compared to the wild type 2089 strain, a BHRF1 miRNA deleted variant (Δ123 EBV) was 4-5 fold reduced in its ability to mediate B cell outgrowth over the first 5-12 days post infection; note that later time points were not investigated (751). Consistent with the impaired transforming phenotype, fewer B cells infected with Δ123 EBV survived over the same time frame and only half as many were found to be undergoing DNA synthesis (S phase), compared to cells infected with the wild

type virus. Feederle performed a similar study at later time points using a Δ123 EBV variant of the B95-8 strain (750). Compared to the wild type B95-8 strain, they observed that outgrowth of Δ123 EBV infected B cells was reduced by ~2.5 fold at 29 days cells post-infection under conditions of bulk infection . This effect was found to be amplified at 8 weeks post-infection under stringent culture conditions i.e. low cell density. In agreement with Seto *et al.*, fewer Δ123 EBV infected B cells were noted to have entered into S phase. Interestingly Feederle *et al.* noted higher relative levels of both Cp and Wp transcription in Δ123 EBV infected B cells between 11 and 73 days post-infection which was generally mirrored by higher levels of latent protein production.

Thus we chose to investigate whether the BHRF1 miRNAs could confer a survival or growth advantage in the context of malignant BL cells (Figs. 5.17 through 5.19). However we found little evidence to suggest that the growth rates of either BL line tested were altered in the presence of the BHRF1 miRNAs. Similarly the BHRF1 miRNAs did not appear to alter the Bcl-2 family profile or protect from ionomycin induced cell death.

The lack of a detectable phenotype under *in vitro* conditions could be due to a number of technical differences between the past and present studies. For instance our BHRF1-1/1-2/1-3 lentiviral construct generated high levels of miR-BHRF1-1 and miR-BHRF1-2, but lower amounts of miR-BHRF1-3 (Fig. 5.10); it is possible that abundant levels of all three BHRF1 miRNAs are necessary to cooperate to alter the growth and survival characteristics of BL cells. Interestingly Seto *et al* observed 8000-12000 copies of BHRF1 miRNAs in the majority of established LCL lines tested (751), levels which are much higher than previously reported in LCL lines (743, 809). By comparison our BL lines stably only expressed between 500-1000 copies of miR-BHRF1-1 and miR-BHRF1-2 per cell and 250-1000 copies of miR-BHRF1-3 per cell; perhaps these levels were insufficient to cause an overt phenotypic change.

Another difference between the past and present studies is that Seto et al. and Feederle et al. did not exclude the possibility that alterations in the levels of the BHRF1 protein are contributing to the observed phenotype. BHRF1 protein is known to contribute towards growth transformation by protecting *de novo* infected B cells from apoptosis (513). While both groups noted similar levels of BHRF1 transcript in the wild type and Δ123 EBV strains, scrambling parts of the BHRF1 5′ and 3′ UTR regions may have affected the efficiency of BHRF1 translation.

Another possible reason we did not see a change in the growth or survival phenotype of BL lines stably expressing the BHRF1 miRNAs is because the roles of the BHRF1 miRNAs in resting B cells and established tumour lines are fundamentally different. In the context of primary infection, the BHRF1 miRNAs likely contribute towards early LCL formation. Such contributions may become redundant as the developing LCL acquires a number of additional changes during the immortalization process; as discussed in section 1.10 these changes include telomerase activation, (355-358), chromosomal aberrations (361), p53 mutations (362), enhanced tumour-like growth properties (362) and an altered resistance to cytotoxic drugs (363). On this point, Seto *et al*. observed no apparent contribution of the BHRF1 miRNAs towards survival in established LCL lines whilst the cell cycle distribution was only marginally altered in these cells (751). Similarly Feederle *et al.* found that the relatively high levels Cp and Wp activity observed in Δ123 EBV infected B cells began to tail off between 36 days and 73 days post-infection (750). These findings support the idea that the phenotypic contributions of the BHRF1 miRNAs gradually become dispensable as immortalization progresses.

Similarly one could argue that the BHRF1 miRNAs confer growth and survival advantages during the formation of BL but not once the tumours have been established. The near 100%

association of EBV with endemic BL and the monoclonal origin of the tumour imply an essential role for the virus in tumour formation (254, 473, 474, 492). Nonetheless, at least in some BL lines, EBV is dispensable for tumour growth *in vitro* as demonstrated by the formation of spontaneous EBV loss clones (500). Thus in the context of BL, the c-myc translocation and p53 mutations could gradually diminish the requirement for EBV growth promoting and survival properties (477, 480, 481, 502, 503). For instance, the ability of EBNA1 to destabilize p53 via HAUSP may be important during early BL tumour formation, but not in established BL carrying p53 aberrations. Similarly the BHRF1 miRNAs may simply not confer overt growth or survival advantages in established BL tumours.

5.8.5 Microarray analysis of BL lines stably expressing the BHRF1 miRNAs

In order to pin point possible genes and pathways regulated by the BHRF1 miRNAs, we performed a whole transcript array analysis and then used the AltAnalyze software (780) for data pre-processing, such as elimination of background noise, filtering of probe sets, data summarization and normalization. This revealed a total of 203 differentially regulated genes between all three biological comparisons (empty vector vs. BHRF1-2/1-3, empty vector vs. BHRF1-1/1-2/1-3 and BHRF1-2/1-3 vs. BHRF1-1/1-2/1-3). Subsequently 15 differentially regulated genes were selected at random for validation by QPCR but unfortunately not one of these gene changes could be confirmed. These findings imply a false positivity rate of at least 7.4%, although this number is likely to be much larger considering we randomly selected gene changes for validation. Notably many of the identified genes were expressed at very low levels in the test lines, consistent with the finding that five genes (ADAM18, DSCR8, ASZ1, HSPA4L and GRM5) were not even detectable by QPCR.

It is important to note that the probe sets screened by AltAnalyze and primer/probe combinations used in the QPCR assays were targetted against constitutive exons i.e. those present in all splice variants of a given mRNA species. Thus the discordant results cannot be accounted for by the detection of different splice variants by the two methods. It remains possible that the high rate of false positives predicted in the array analysis simply reflects the fact that the BHRF1 miRNAs regulate their targets at a post-transcriptional level. However this is difficult to reconcile with the general observation that ~84% of miRNA induced protein changes are associated with reductions in mRNA levels (151). Furthermore any significant changes to the cellular proteome would be expected to have some degree of downstream transcriptional effect.

Towards the end of our study, we chose to reanalyze the raw array data using the XPS software. Using this approach, the array results for the same set of 15 validation genes agreed more closely with the QPCR data. This highlights a number of important issues about the interpretation of microarray analysis. First using different software algorithms to calculate changes in gene expression can yield a very different gene list (831). There is still no “best” way to analyze microarray data and consequently the development of analysis algorithms is a very busy area of research (832). Unfortunately due to time constraints we were unable to generate a list of differentially regulated genes based on the XPS data. It would be interesting to determine the degree of overlap between the AltAnalyze and XPS data sets, as such a comparison might help us chose more reliable targets for validation by QPCR.

6. Conclusions and future work

In the first part of this thesis, we described an in depth investigation into the expression of EBV miRNAs in a variety of cell lines with different forms of EBV infection. Our study provided a number of novel findings. First, we demonstrated that all three BHRF1 miRNAs are abundantly expressed in Wp-restricted BL (Wp BL), but not in Latency I BL (Lat I BL) cell lines in which the Cp and Wp promoters are silent; this is the first example of BHRF1 miRNA expression in the context of a BL tumour background. Second, in contrast to some earlier studies, we show that the BART miRNAs are abundantly expressed in cells of B lymphoid origin. While these findings help resolve controversies in the literature regarding the expression of the BART miRNAs in different cell lineages (738, 748), they also highlighted the widely different levels of individual BART miRNAs within a cell line. Finally we demonstrated that changes in BHRF1 and BART transcription are not necessarily reflected in altered miRNA levels, suggesting that miRNA maturation is a key step in regulating steady-state levels of EBV miRNAs.

Studies on EBV miRNA expression have provided us with a number of vital clues as to their possible roles in different stages of the viral life cycle and tumour pathogenesis. For instance, the presence of the BHRF1 miRNAs in B cells early after EBV infection provided a rationale for investigating their potential contribution to B cell transformation (750, 751), while the finding that the BHRF1 miRNAs are present in a subset of BL tumours raises the possibility that they can also contribute to BL pathogenesis. However, in light of recent studies, it may be informative to determine not just the total levels of EBV miRNAs but also the amount of miRNAs specifically associated with Ago proteins. On this note, Riley *et al*. recently used high throughput sequencing (HITS-CLIP) to quantify only those miRNAs bound to Ago

proteins in the Jijoye BL cell line (764). This study not only revealed that 25% of all Ago-bound miRNAs were EBV-derived but that the 12 highest expressed BART miRNAs (which included miR-BART10, miR-BART13, miR-BART4, miR-BART7 and miR-BART22) comprised 90% of all EBV miRNA sequence reads. By contrast the BHRF1 miRNAs were barely detected in this study, a result which is in stark contrast to previous northern blot analyses of Jijoye cells (738, 741, 748, 764). These findings raise two interesting possibilities. Firstly, EBV miRNAs might be preferentially loaded into miRISC complexes compared to cellular miRNAs. Secondly, the frequency with which individual EBV miRNAs bind Ago, and thus can exert their biological effects, may not necessarily correlate with absolute miRNA copy numbers.

One striking finding of our study was the observation that individual BART miRNAs are present at widely different levels within a given cell line. Factors involved in regulating the maturation of cellular miRNAs were discussed earlier in section 1.3. For instance, SMAD, KSRP, p53 and ADAR are all capable of regulating pri-miRNA processing by the micro-processor complex in the nucleus, while TUT4 has been shown to regulate pre-miRNA processing by Dicer in the cytoplasm. There is also evidence that pre-miRNA export from the nucleus is regulated by an, as yet, unidentified mechanism. At present the contribution of these factors to the differential accumulation of EBV miRNAs remains mostly unexplored. It has recently been suggested that four EBV pri-miRNAs sequences (miR-BHRF1-1, miR-BART8, miR-BART16 and miR-BART6) are subject to editing by ADAR deaminases, which converts adenosine to inosine (757); this would lead to impaired Drosha processing and eventual degradation by the ribonuclease Tudor-SN, which specifically recognizes inosine containing dsRNA (76). Interestingly, A – I editing of the mature miRNA seed sequence may also direct a given miRNA to target an entirely different set of genes (833). Further studies are

therefore clearly required to understand how EBV miRNA levels are regulated by the complex miRNA maturation pathway.

In the second part of our work we sought to explore the functions of the BHRF1 miRNAs in the context of a BL cell line model. Our phenotypic studies revealed that the growth rates and survival properties of BL cells were unaffected by BHRF1 miRNAs. However attempts to identify potential BHRF1 miRNA targets using a whole transcriptome approach are at this point inconclusive, possibly due to technical issues involving the data processing (section 5.8.5). Further analysis of the raw array data may yet provide us with meaningful insight into BHRF1 miRNA function.

At present we speculate that the BHRF1 miRNAs contribute to the pro-survival phenotype Wp BL but may be functionally redundant in the context of EBV negative and Lat I BL lines. Vereide and Sugden recently assessed the contributions of EBV to a number of virus-associated malignancies by using dominant negative EBNA1 inhibitors to force genome loss (834, 835). Overall they observed a strong correlation between the number of different latent gene products expressed in a given tumour cell and its dependence on the growth and survival properties of EBV. Thus PTLD tumour lines (Lat III) and Oku BL cells (Wp BL) which had lost the EBV genome were more susceptible to spontaneous cell death than EBV loss derivatives of Lat I BL cells. Similarly PTLD cells and Oku-BL cells were more dependent on the presence of the EBV genome for proliferation when compared to Lat I BL cells. It has been hypothesized that the reduced dependence of Lat I BL cells on EBV is due to a greater accumulation of cellular mutations (834). In agreement with this prediction, Wp BL lines appear to carry wild type p53 whilst Lat I BL cells are usually characterized by p53 mutations (503, 511). Interestingly a recent study by Schmitz *et al.* observed that 38% of sporadic BL tumours and 2% of endemic BL tumours produced a highly stable mutant of cyclin-D3 (836).

Similarly 70% of sporadic BL and 40% of endemic BL tumours contained mutations in transcription factor 3 (TCF3) or its inhibitor, ID3. Collectively these mutations would favour cell cycle progression, cell survival and an increased expression of genes important in germinal centre development. Since the present study largely focused on an EBV positive Lat I BL line (Akata) and two EBV negative sporadic BL lines (BL30 and BL41) (276, 344), it is possible that the function of the BHRF1 miRNAs in these cells may be redundant due to additional cellular genetic changes.

It is also likely that BHRF1 miRNA function may depend on the presence of other Lat III associated EBV gene products e.g. EBNA-LP, EBNA3 and BHRF1 which are expressed in Lat III infection and in Wp BLs, but not in Lat I BLs or EBV negative lines. This also raises the possibility that the BHRF1 miRNAs may regulate EBV gene products themselves, a view supported by the observation that Lat III gene expression is apparently deregulated in LCLs infected with a recombinant EBV lacking all three BHRF1 miRNAs (750). However Skalsky and co-workers concluded that there are no predicted BHRF1 miRNA binding sites in the latent EBV transcripts (763). Alternatively the BHRF1 miRNAs could function to counteract the effects of EBV latent gene products on cellular gene expression. For instance the BHRF1 miRNAs could regulate any of the hundreds of cellular genes predicted to be targeted by one or more of the EBNA3 proteins (612). Another possibility is that the BHRF1 miRNAs mediate some or all of their effects by cooperating with cellular miRNAs; in this context Lat III associated gene products may first be required to alter the cellular miRNA profile (745).

Originally we had aimed to answer these specific questions in the context of Wp BL by setting up a methodology for the efficient knockdown of the BHRF1 miRNAs (section 5.3); however such attempts using anti miRNA inhibitors had only limited success. As an alternative strategy, preliminary work was initiated to construct a miRNA “sponge” ie. a

transcribed RNA species with multiple binding sites complementary to the miRNA of interest (837). Such miRNA sponges can be highly effective in mediating miRNA knockdown and have been successfully applied to the study of EBV and KSHV miRNAs (755, 815). Unlike anti-miRNA oligonucleotides, lentivirus mediated sponge expression would allow transduced cells to be sorted using a GFP marker, thus eliminating the problem of the inherently low transfection efficiency associated with Wp BL lines.

To this end, we had already begun construction of a sponge carrying nine binding sites against miR-BHRF1-2, with a view to knocking down expression of miR-BHRF1-2 in Wp BL cell lines. This work could be continued, in the first instance, by validating knockdown of miR-BHRF1-2 using our newly developed luciferase reporters. If this proved successful, we would then try to incorporate binding sites for different combinations of all three BHRF1 miRNAs into the sponge. Ultimately we would envision performing Ago precipitation (e.g. HITS-CLIP) on sponge-transduced cells followed by deep sequencing or microarray analysis. To counter the argument that such approaches may not detect post transcriptional changes, we could also exploit techniques such as SILAC to perform a quantitative analysis of protein levels in cells expressing different combinations of sponge sequences. In this way, we would hope to study the function of the BHRF1 miRNAs in the more physiologically relevant setting of endemic Wp BL lines, rather than in EBV negative sporadic BL or Lat I BL cells used in the current work.

We note that, even today, very little is known about the specific roles of the BHRF1 miRNAs in virus mediated oncogenesis, with the possible exception of B cell transformation (750, 751), and, despite extensive studies, very few EBV miRNA targets have been fully validated (754, 755, 759, 760, 763, 764). Indeed we still have a poor understanding of what makes a good or bad miRNA target. In some cases, EBV miRNAs can regulate transcripts lacking a

predicted binding site (miR-BART3 and BACH1), while in others they fail to regulate a target with a predicted binding site (miR-BART2 and CLIC4) (763). It is therefore important to understand the different methods which are used to identify potential miRNA targets.

Much of what we know about miRNA-mRNA interactions has come from target prediction software. Indeed almost every published study on EBV miRNAs has attempted to use a computational approach to predict target genes for a given miRNA of interest. Some commonly used target prediction software and algorithms were discussed briefly in section 1.4. We therefore decided to investigate target predictions for miR-BHRF1-1, miR-BHRF1-2, miR-BHRF1-2* and miR-BHRF1-3 from three commonly used software packages (TargetScan v5.2, RepTar and Diana-microT v3.0) (1, 114, 838, 839). Surprisingly there was very little overlap in the target predictions generated from the three data sets (Fig. 6.1); only 25 target genes were common all three programs, and only nine of those were predicted to be targeted by the exact same BHRF1 miRNA. As a postive control, we confirmed that the Diana-microT algorithm could predict Dicer as a target of miR-BART6-5p (757). These findings clearly highlight the shortcomings of relying solely on computational approaches to identify miRNA targets, and identify a need for comprehensive, robust biochemical analysis (114).

One such biochemical approach involves deep sequencing of miRNA-containing Ago complexes. However despite the huge amounts of data generated by this method, there still appears to be little overlap between EBV miRNA targetomes predicted by different studies. Recent reports by Skalsky *et al.* and Dolken *et al.* both obtained data sets for potential BHRF1 miRNA target genes (758, 763), either in the context of an LCL, or in the case of Dolken *et al.* using the Jijoye BL line. An overlap of the putative BHRF1 miRNA targets revealed in these two studies, together with the 203 differentially regulated genes from our array, is

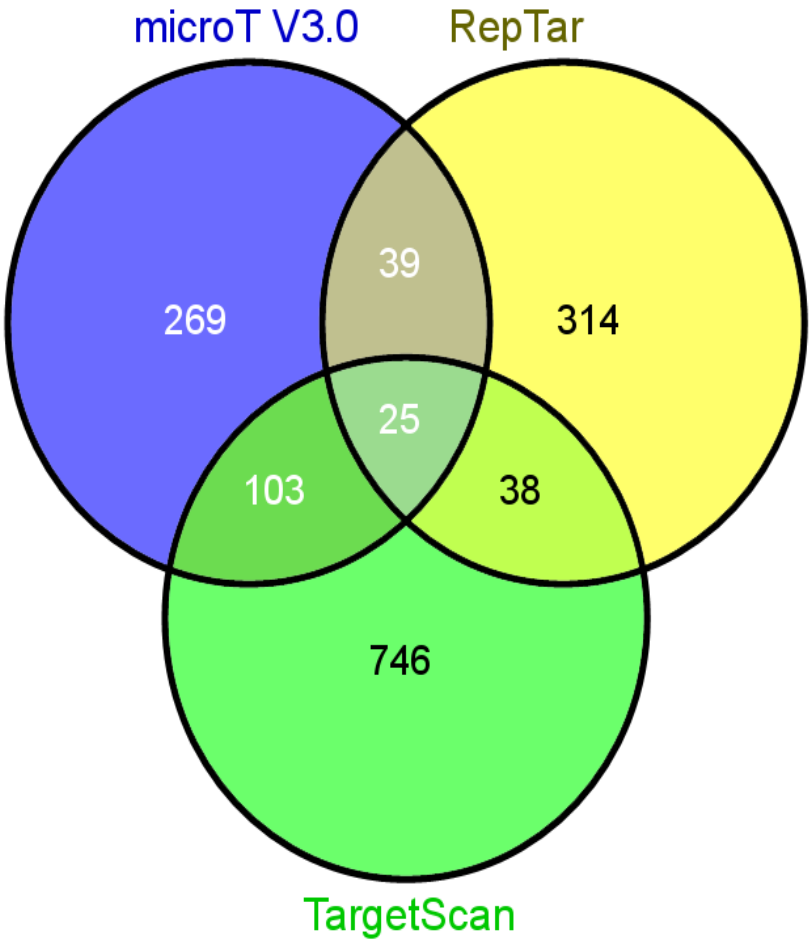

Fig 6.1. A comparison of three different miRNA prediction software programs. Predicted targets of miR-BHRF1-1, miR-BHRF1-2 and miR-BHRF1-3 were determined with TargetScan version 5.2 (1), RepTar (838) and Diana-microT version 3.0 (839) using standard parameters. The total number of genes predicted to be targeted by one or more of the BHRF1 miRNAs has been summarized for each program in the Venn Diagram

illustrated in Fig. 6.2. Note that Dolken *et al.* did not assign specific miRNAs to the majority of their predicted 44 EBV miRNA targeted transcripts. Therefore we included only those genes in our comparison which were predicted to be targeted by one or more BHRF1 miRNA in at least one of the target prediction packages. Using these criteria, we found zero overlap between the predicted genes in any of the three studies (Fig. 6.2).

Very recently, a third study by Riley *et al.* identified more than 1500 EBV miRNA targets using HITS-CLIP of Ago bound RNA species (764). Collectively these three studies used similar methods to investigate either the LCL (Skalsky and Dolken) or the Jijoye BL (Dolken and Riley) miRNA targetome. We therefore compared all three published studies, but restricted our analysis to a single miRNA, miR-BART4 (Fig. 6.3). In this case, there was a small degree of overlap based on pairwise comparisons but no individual gene was identified by all three studies. Whether these discrepancies arise from different methodologies or the use of different cell types warrants further investigation.

Putting aside this lack of agreement between published studies, EBV miRNAs are predicted to target genes involved in cell cycle, apoptosis, transcription and Wnt signalling. These comprehensive profiling studies have clearly demonstrated their merits by identifying new targets and validating some of those discovered in earlier studies e.g. PUMA, MICB and IPO7 (755, 756, 758, 763, 764). Interestingly a number of studies have confirmed the same targets in different cellular contexts, but find them to be regulated by a different set of EBV miRNAs. For instance four groups have confirmed that LMP1 is an EBV miRNA target (760, 762-764); Lo *et al.* showed miR-BART1-5p, 16-5p and 17-5p regulate LMP1, Skalsky *et al.* confirmed the interaction with miR-BART1-5p, Riley *et al* suggested that miR-BART5-5p and miR-BART19-5p were involved whilst Ramakrishnan *et al*. validated miR-BART9.

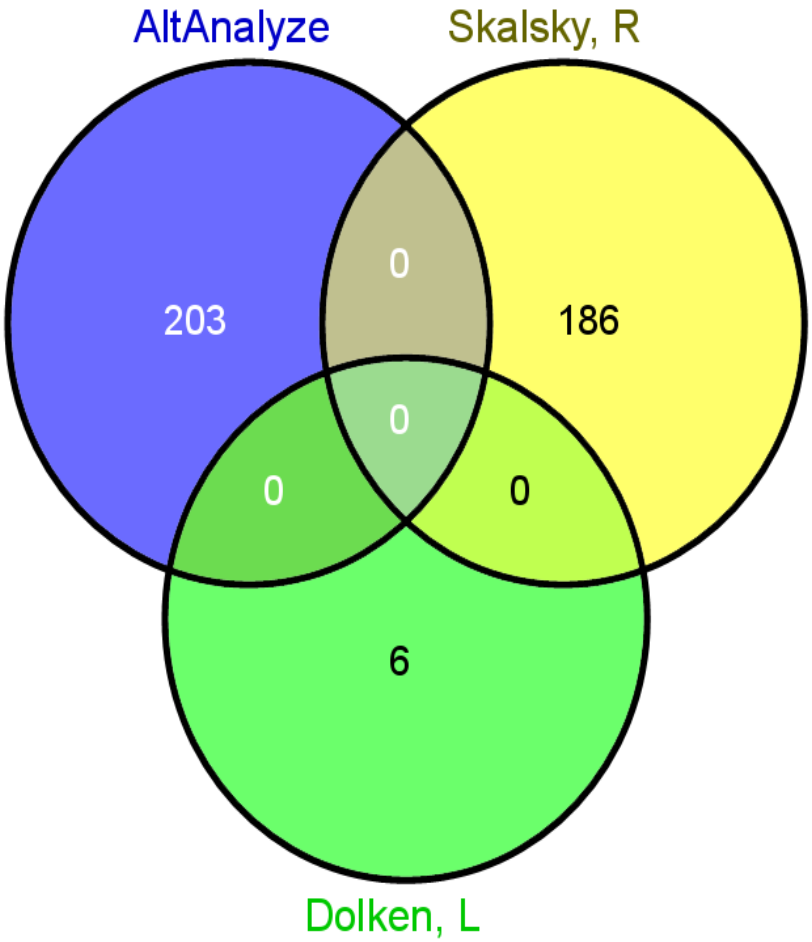

Fig 6.2. A comparison of candidate BHRF1 miRNA targets from three studies. The total number of genes differentially expressed between the three TREX lentivirus transduced Akata BL lines (AltAnalyze) was compared to the total number of genes predicted to be targeted by one or more BHRF1 miRNAs in the studies conducted by Dolken *et al.* (758) and Skalsky *et al*. (763). Data have been summarized in the Venn Diagram.

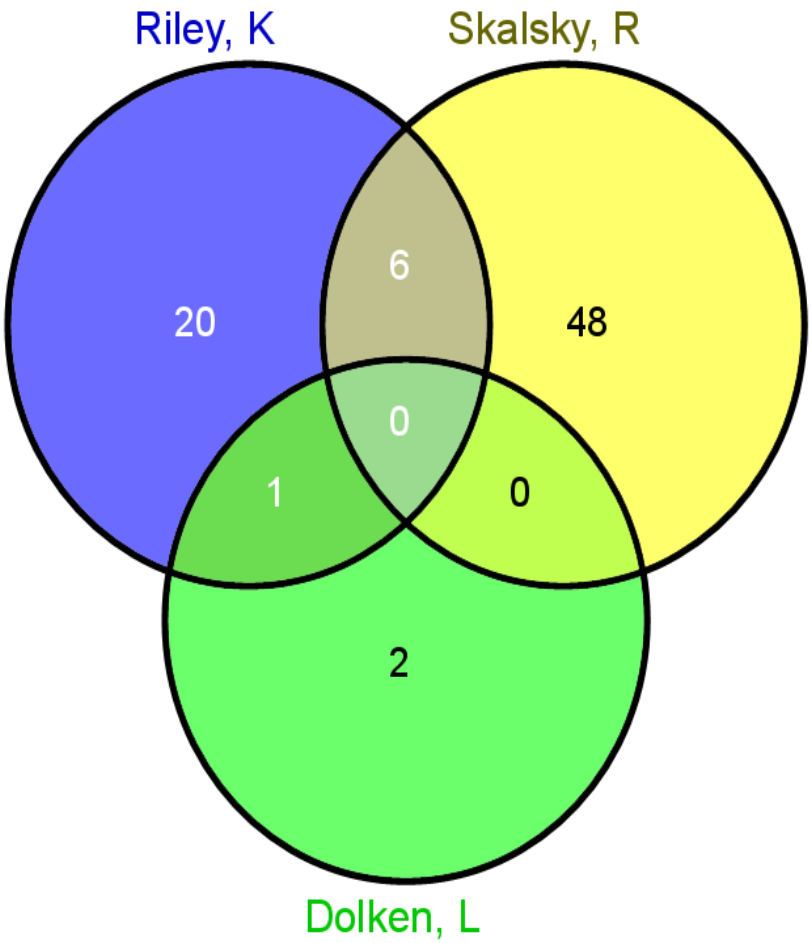

Fig 6.3. A comparison of miR-BART4 targets predicted by three similar studies. The total number of genes predicted to be targeted miRBART4 in the studies conducted by Dolken *et al.* (758), Riley *et al.* (764) and Skalsky *et al.* (763) have been summarized for each study in the Venn Diagram.

In summary, our knowledge of EBV miRNAs and their roles in EBV infection and lymphomagenesis is steadily increasing, but several fundamental questions still remain unanswered. In terms of EBV miRNA expression, we need to better understand the cellular mechanisms which control the biogenesis and maturation of EBV miRNAs from the BHRF1 and BART transcripts. Further studies are also required to investigate if EBV miRNAs can selectively gain access into miRISC silencing complexes. On the question of EBV miRNA function, the current literature is both confusing and contradictory. Therefore future studies will need to combine complementary genetic and biochemical approaches in order to fully characterise the relationship between the EBV miRNA targetome and cell phenotype. Finally our increased understanding of the role of EBV miRNAs in lymphomagenesis may lead to the identification of novel therapeutic targets for the treatment of EBV associated lymphomas.

References

1. Lewis BP, Burge CB, Bartel DP. Conserved seed pairing, often flanked by adenosines, indicates that thousands of human genes are microRNA targets. Cell. 2005 Jan 14;120(1):15-20.
2. Lee RC, Feinbaum RL, Ambros V. The C. elegans heterochronic gene lin-4 encodes small RNAs with antisense complementarity to lin-14. Cell. 1993 Dec 3;75(5):843-54.
3. Reinhart BJ, Slack FJ, Basson M, Pasquinelli AE, Bettinger JC, Rougvie AE, et al. The 21-nucleotide let-7 RNA regulates developmental timing in Caenorhabditis elegans. Nature. 2000 Feb 24;403(6772):901-6.
4. Lagos-Quintana M, Rauhut R, Lendeckel W, Tuschl T. Identification of novel genes coding for small expressed RNAs. Science. 2001 Oct 26;294(5543):853-8.
5. Lau NC, Lim LP, Weinstein EG, Bartel DP. An abundant class of tiny RNAs with probable regulatory roles in Caenorhabditis elegans. Science. 2001 Oct 26;294(5543):858-62.
6. Lee RC, Ambros V. An extensive class of small RNAs in Caenorhabditis elegans. Science. 2001 Oct 26;294(5543):862-4.
7. Wightman B, Burglin TR, Gatto J, Arasu P, Ruvkun G. Negative regulatory sequences in the lin-14 3'-untranslated region are necessary to generate a temporal switch during Caenorhabditis elegans development. Genes Dev. 1991 Oct;5(10):1813-24.
8. Wightman B, Ha I, Ruvkun G. Posttranscriptional regulation of the heterochronic gene lin-14 by lin-4 mediates temporal pattern formation in C. elegans. Cell. 1993 Dec 3;75(5):855-62.
9. Slack FJ, Basson M, Liu Z, Ambros V, Horvitz HR, Ruvkun G. The lin-41 RBCC gene acts in the C. elegans heterochronic pathway between the let-7 regulatory RNA and the LIN-29 transcription factor. Mol Cell. 2000 Apr;5(4):659-69.
10. Pasquinelli AE, Reinhart BJ, Slack F, Martindale MQ, Kuroda MI, Maller B, et al. Conservation of the sequence and temporal expression of let-7 heterochronic regulatory RNA. Nature. 2000 Nov 2;408(6808):86-9.
11. Lagos-Quintana M, Rauhut R, Meyer J, Borkhardt A, Tuschl T. New microRNAs from mouse and human. RNA. 2003 Feb;9(2):175-9.
12. Houbaviy HB, Murray MF, Sharp PA. Embryonic stem cell-specific MicroRNAs. Dev Cell. 2003 Aug;5(2):351-8.
13. Dostie J, Mourelatos Z, Yang M, Sharma A, Dreyfuss G. Numerous microRNPs in neuronal cells containing novel microRNAs. RNA. 2003 Feb;9(2):180-6.
14. Aravin AA, Lagos-Quintana M, Yalcin A, Zavolan M, Marks D, Snyder B, et al. The small RNA profile during Drosophila melanogaster development. Dev Cell. 2003 Aug;5(2):337-50.
15. Ambros V, Lee RC, Lavanway A, Williams PT, Jewell D. MicroRNAs and other tiny endogenous RNAs in C. elegans. Curr Biol. 2003 May 13;13(10):807-18.
16. Mourelatos Z, Dostie J, Paushkin S, Sharma A, Charroux B, Abel L, et al. miRNPs: a novel class of ribonucleoproteins containing numerous microRNAs. Genes Dev. 2002 Mar 15;16(6):720-8.
17. Lagos-Quintana M, Rauhut R, Yalcin A, Meyer J, Lendeckel W, Tuschl T. Identification of tissue-specific microRNAs from mouse. Curr Biol. 2002 Apr 30;12(9):735-9.
18. Kim J, Krichevsky A, Grad Y, Hayes GD, Kosik KS, Church GM, et al. Identification of many microRNAs that copurify with polyribosomes in mammalian neurons. Proc Natl Acad Sci U S A. 2004 Jan 6;101(1):360-5.
19. Michael MZ, SM OC, van Holst Pellekaan NG, Young GP, James RJ. Reduced accumulation of specific microRNAs in colorectal neoplasia. Mol Cancer Res. 2003 Oct;1(12):882-91.
20. Lim LP, Lau NC, Weinstein EG, Abdelhakim A, Yekta S, Rhoades MW, et al. The microRNAs of Caenorhabditis elegans. Genes Dev. 2003 Apr 15;17(8):991-1008.

21. Lim LP, Glasner ME, Yekta S, Burge CB, Bartel DP. Vertebrate microRNA genes. Science. 2003 Mar 7;299(5612):1540.
22. Griffiths-Jones S, Saini HK, van Dongen S, Enright AJ. miRBase: tools for microRNA genomics. Nucleic Acids Res. 2008 Jan;36(Database issue):D154-8.
23. Kozomara A, Griffiths-Jones S. miRBase: integrating microRNA annotation and deep-sequencing data. Nucleic Acids Res. 2011 Jan;39(Database issue):D152-7.
24. Bushati N, Cohen SM. microRNA functions. Annu Rev Cell Dev Biol. 2007;23:175-205.
25. Kim VN, Han J, Siomi MC. Biogenesis of small RNAs in animals. Nat Rev Mol Cell Biol. 2009 Feb;10(2):126-39.
26. Rodriguez A, Griffiths-Jones S, Ashurst JL, Bradley A. Identification of mammalian microRNA host genes and transcription units. Genome Res. 2004 Oct;14(10A):1902-10.
27. Saini HK, Enright AJ, Griffiths-Jones S. Annotation of mammalian primary microRNAs. BMC Genomics. 2008;9:564.
28. Lee Y, Kim M, Han J, Yeom KH, Lee S, Baek SH, et al. MicroRNA genes are transcribed by RNA polymerase II. EMBO J. 2004 Oct 13;23(20):4051-60.
29. Cai X, Hagedorn CH, Cullen BR. Human microRNAs are processed from capped, polyadenylated transcripts that can also function as mRNAs. RNA. 2004 Dec;10(12):1957-66.
30. Gregory RI, Yan KP, Amuthan G, Chendrimada T, Doratotaj B, Cooch N, et al. The Microprocessor complex mediates the genesis of microRNAs. Nature. 2004 Nov 11;432(7014):235-40.
31. Han J, Lee Y, Yeom KH, Nam JW, Heo I, Rhee JK, et al. Molecular basis for the recognition of primary microRNAs by the Drosha-DGCR8 complex. Cell. 2006 Jun 2;125(5):887-901.
32. Lee Y, Ahn C, Han J, Choi H, Kim J, Yim J, et al. The nuclear RNase III Drosha initiates microRNA processing. Nature. 2003 Sep 25;425(6956):415-9.
33. Okamura K, Hagen JW, Duan H, Tyler DM, Lai EC. The mirtron pathway generates microRNA-class regulatory RNAs in Drosophila. Cell. 2007 Jul 13;130(1):89-100.
34. Ruby JG, Jan CH, Bartel DP. Intronic microRNA precursors that bypass Drosha processing. Nature. 2007 Jul 5;448(7149):83-6.
35. Berezikov E, Chung WJ, Willis J, Cuppen E, Lai EC. Mammalian mirtron genes. Mol Cell. 2007 Oct 26;28(2):328-36.
36. Lund E, Guttinger S, Calado A, Dahlberg JE, Kutay U. Nuclear export of microRNA precursors. Science. 2004 Jan 2;303(5654):95-8.
37. Yi R, Doehle BP, Qin Y, Macara IG, Cullen BR. Overexpression of exportin 5 enhances RNA interference mediated by short hairpin RNAs and microRNAs. RNA. 2005 Feb;11(2):220-6.
38. Gwizdek C, Ossareh-Nazari B, Brownawell AM, Doglio A, Bertrand E, Macara IG, et al. Exportin-5 mediates nuclear export of minihelix-containing RNAs. J Biol Chem. 2003 Feb 21;278(8):5505-8.
39. Zeng Y, Cullen BR. Structural requirements for pre-microRNA binding and nuclear export by Exportin 5. Nucleic Acids Res. 2004;32(16):4776-85.
40. Brownawell AM, Macara IG. Exportin-5, a novel karyopherin, mediates nuclear export of double-stranded RNA binding proteins. J Cell Biol. 2002 Jan 7;156(1):53-64.
41. Kehlenbach RH, Dickmanns A, Kehlenbach A, Guan T, Gerace L. A role for RanBP1 in the release of CRM1 from the nuclear pore complex in a terminal step of nuclear export. J Cell Biol. 1999 May 17;145(4):645-57.
42. Hutvagner G, McLachlan J, Pasquinelli AE, Balint E, Tuschl T, Zamore PD. A cellular function for the RNA-interference enzyme Dicer in the maturation of the let-7 small temporal RNA. Science. 2001 Aug 3;293(5531):834-8.
43. Ketting RF, Fischer SE, Bernstein E, Sijen T, Hannon GJ, Plasterk RH. Dicer functions in RNA interference and in synthesis of small RNA involved in developmental timing in C. elegans. Genes Dev. 2001 Oct 15;15(20):2654-9.

44. Zhang H, Kolb FA, Brondani V, Billy E, Filipowicz W. Human Dicer preferentially cleaves dsRNAs at their termini without a requirement for ATP. EMBO J. 2002 Nov 1;21(21):5875-85.
45. Zhang H, Kolb FA, Jaskiewicz L, Westhof E, Filipowicz W. Single processing center models for human Dicer and bacterial RNase III. Cell. 2004 Jul 9;118(1):57-68.
46. Ma JB, Ye K, Patel DJ. Structural basis for overhang-specific small interfering RNA recognition by the PAZ domain. Nature. 2004 May 20;429(6989):318-22.
47. Song JJ, Liu J, Tolia NH, Schneiderman J, Smith SK, Martienssen RA, et al. The crystal structure of the Argonaute2 PAZ domain reveals an RNA binding motif in RNAi effector complexes. Nat Struct Biol. 2003 Dec;10(12):1026-32.
48. MacRae IJ, Ma E, Zhou M, Robinson CV, Doudna JA. In vitro reconstitution of the human RISC-loading complex. Proc Natl Acad Sci U S A. 2008 Jan 15;105(2):512-7.
49. Chendrimada TP, Gregory RI, Kumaraswamy E, Norman J, Cooch N, Nishikura K, et al. TRBP recruits the Dicer complex to Ago2 for microRNA processing and gene silencing. Nature. 2005 Aug 4;436(7051):740-4.
50. Gregory RI, Chendrimada TP, Cooch N, Shiekhattar R. Human RISC couples microRNA biogenesis and posttranscriptional gene silencing. Cell. 2005 Nov 18;123(4):631-40.
51. Maniataki E, Mourelatos Z. A human, ATP-independent, RISC assembly machine fueled by pre-miRNA. Genes Dev. 2005 Dec 15;19(24):2979-90.
52. Schwarz DS, Hutvagner G, Du T, Xu Z, Aronin N, Zamore PD. Asymmetry in the assembly of the RNAi enzyme complex. Cell. 2003 Oct 17;115(2):199-208.
53. Khvorova A, Reynolds A, Jayasena SD. Functional siRNAs and miRNAs exhibit strand bias. Cell. 2003 Oct 17;115(2):209-16.
54. Noland CL, Ma E, Doudna JA. siRNA repositioning for guide strand selection by human Dicer complexes. Mol Cell. 2011 Jul 8;43(1):110-21.
55. Diederichs S, Haber DA. Dual role for argonautes in microRNA processing and posttranscriptional regulation of microRNA expression. Cell. 2007 Dec 14;131(6):1097-108.
56. Shin C. Cleavage of the star strand facilitates assembly of some microRNAs into Ago2-containing silencing complexes in mammals. Mol Cells. 2008 Sep 30;26(3):308-13.
57. Wang B, Li S, Qi HH, Chowdhury D, Shi Y, Novina CD. Distinct passenger strand and mRNA cleavage activities of human Argonaute proteins. Nat Struct Mol Biol. 2009 Dec;16(12):1259-66.
58. Meister G, Landthaler M, Patkaniowska A, Dorsett Y, Teng G, Tuschl T. Human Argonaute2 mediates RNA cleavage targeted by miRNAs and siRNAs. Mol Cell. 2004 Jul 23;15(2):185-97.
59. Liu J, Carmell MA, Rivas FV, Marsden CG, Thomson JM, Song JJ, et al. Argonaute2 is the catalytic engine of mammalian RNAi. Science. 2004 Sep 3;305(5689):1437-41.
60. Ozsolak F, Poling LL, Wang Z, Liu H, Liu XS, Roeder RG, et al. Chromatin structure analyses identify miRNA promoters. Genes Dev. 2008 Nov 15;22(22):3172-83.
61. Saini HK, Griffiths-Jones S, Enright AJ. Genomic analysis of human microRNA transcripts. Proc Natl Acad Sci U S A. 2007 Nov 6;104(45):17719-24.
62. Tam W. Identification and characterization of human BIC, a gene on chromosome 21 that encodes a noncoding RNA. Gene. 2001 Aug 22;274(1-2):157-67.
63. Tarasov V, Jung P, Verdoodt B, Lodygin D, Epanchintsev A, Menssen A, et al. Differential regulation of microRNAs by p53 revealed by massively parallel sequencing: miR-34a is a p53 target that induces apoptosis and G1-arrest. Cell Cycle. 2007 Jul 1;6(13):1586-93.
64. Raver-Shapira N, Marciano E, Meiri E, Spector Y, Rosenfeld N, Moskovits N, et al. Transcriptional activation of miR-34a contributes to p53-mediated apoptosis. Mol Cell. 2007 Jun 8;26(5):731-43.
65. He L, He X, Lim LP, de Stanchina E, Xuan Z, Liang Y, et al. A microRNA component of the p53 tumour suppressor network. Nature. 2007 Jun 28;447(7148):1130-4.
66. He L, Thomson JM, Hemann MT, Hernando-Monge E, Mu D, Goodson S, et al. A microRNA polycistron as a potential human oncogene. Nature. 2005 Jun 9;435(7043):828-33.

67. O'Donnell KA, Wentzel EA, Zeller KI, Dang CV, Mendell JT. c-Myc-regulated microRNAs modulate E2F1 expression. Nature. 2005 Jun 9;435(7043):839-43.
68. Thomson JM, Newman M, Parker JS, Morin-Kensicki EM, Wright T, Hammond SM. Extensive post-transcriptional regulation of microRNAs and its implications for cancer. Genes Dev. 2006 Aug 15;20(16):2202-7.
69. Obernosterer G, Leuschner PJ, Alenius M, Martinez J. Post-transcriptional regulation of microRNA expression. RNA. 2006 Jul;12(7):1161-7.
70. Treiber T, Treiber N, Meister G. Regulation of microRNA biogenesis and function. Thromb Haemost. 2012 Apr;107(4):605-10.
71. Davis BN, Hilyard AC, Nguyen PH, Lagna G, Hata A. Smad proteins bind a conserved RNA sequence to promote microRNA maturation by Drosha. Mol Cell. 2010 Aug 13;39(3):373-84.
72. Davis BN, Hilyard AC, Lagna G, Hata A. SMAD proteins control DROSHA-mediated microRNA maturation. Nature. 2008 Jul 3;454(7200):56-61.
73. Suzuki HI, Yamagata K, Sugimoto K, Iwamoto T, Kato S, Miyazono K. Modulation of microRNA processing by p53. Nature. 2009 Jul 23;460(7254):529-33.
74. Trabucchi M, Briata P, Garcia-Mayoral M, Haase AD, Filipowicz W, Ramos A, et al. The RNA-binding protein KSRP promotes the biogenesis of a subset of microRNAs. Nature. 2009 Jun 18;459(7249):1010-4.
75. Zhang X, Wan G, Berger FG, He X, Lu X. The ATM kinase induces microRNA biogenesis in the DNA damage response. Mol Cell. 2011 Feb 18;41(4):371-83.
76. Yang W, Chendrimada TP, Wang Q, Higuchi M, Seeburg PH, Shiekhattar R, et al. Modulation of microRNA processing and expression through RNA editing by ADAR deaminases. Nat Struct Mol Biol. 2006 Jan;13(1):13-21.
77. Lee EJ, Baek M, Gusev Y, Brackett DJ, Nuovo GJ, Schmittgen TD. Systematic evaluation of microRNA processing patterns in tissues, cell lines, and tumors. RNA. 2008 Jan;14(1):35-42.
78. Melo SA, Moutinho C, Ropero S, Calin GA, Rossi S, Spizzo R, et al. A genetic defect in exportin-5 traps precursor microRNAs in the nucleus of cancer cells. Cancer Cell. 2010 Oct 19;18(4):303-15.
79. Newman MA, Thomson JM, Hammond SM. Lin-28 interaction with the Let-7 precursor loop mediates regulated microRNA processing. RNA. 2008 Aug;14(8):1539-49.
80. Rybak A, Fuchs H, Smirnova L, Brandt C, Pohl EE, Nitsch R, et al. A feedback loop comprising lin-28 and let-7 controls pre-let-7 maturation during neural stem-cell commitment. Nat Cell Biol. 2008 Aug;10(8):987-93.
81. Hagan JP, Piskounova E, Gregory RI. Lin28 recruits the TUTase Zcchc11 to inhibit let-7 maturation in mouse embryonic stem cells. Nat Struct Mol Biol. 2009 Oct;16(10):1021-5.
82. Heo I, Joo C, Cho J, Ha M, Han J, Kim VN. Lin28 mediates the terminal uridylation of let-7 precursor MicroRNA. Mol Cell. 2008 Oct 24;32(2):276-84.
83. Heo I, Joo C, Kim YK, Ha M, Yoon MJ, Cho J, et al. TUT4 in concert with Lin28 suppresses microRNA biogenesis through pre-microRNA uridylation. Cell. 2009 Aug 21;138(4):696-708.
84. Yeom KH, Heo I, Lee J, Hohng S, Kim VN, Joo C. Single-molecule approach to immunoprecipitated protein complexes: insights into miRNA uridylation. EMBO Rep. 2011 Jul;12(7):690-6.
85. Richards M, Tan SP, Tan JH, Chan WK, Bongso A. The transcriptome profile of human embryonic stem cells as defined by SAGE. Stem Cells. 2004;22(1):51-64.
86. Viswanathan SR, Daley GQ, Gregory RI. Selective blockade of microRNA processing by Lin28. Science. 2008 Apr 4;320(5872):97-100.
87. Grosshans H, Johnson T, Reinert KL, Gerstein M, Slack FJ. The temporal patterning microRNA let-7 regulates several transcription factors at the larval to adult transition in C. elegans. Dev Cell. 2005 Mar;8(3):321-30.

88. Guo Y, Chen Y, Ito H, Watanabe A, Ge X, Kodama T, et al. Identification and characterization of lin-28 homolog B (LIN28B) in human hepatocellular carcinoma. Gene. 2006 Dec 15;384:51-61.
89. Johnson SM, Grosshans H, Shingara J, Byrom M, Jarvis R, Cheng A, et al. RAS is regulated by the let-7 microRNA family. Cell. 2005 Mar 11;120(5):635-47.
90. Lee YS, Dutta A. The tumor suppressor microRNA let-7 represses the HMGA2 oncogene. Genes Dev. 2007 May 1;21(9):1025-30.
91. Mayr C, Hemann MT, Bartel DP. Disrupting the pairing between let-7 and Hmga2 enhances oncogenic transformation. Science. 2007 Mar 16;315(5818):1576-9.
92. Sampson VB, Rong NH, Han J, Yang Q, Aris V, Soteropoulos P, et al. MicroRNA let-7a down-regulates MYC and reverts MYC-induced growth in Burkitt lymphoma cells. Cancer Res. 2007 Oct 15;67(20):9762-70.
93. Bail S, Swerdel M, Liu H, Jiao X, Goff LA, Hart RP, et al. Differential regulation of microRNA stability. RNA. 2010 May;16(5):1032-9.
94. Yu Z, Hecht NB. The DNA/RNA-binding protein, translin, binds microRNA122a and increases its in vivo stability. J Androl. 2008 Sep-Oct;29(5):572-9.
95. Krol J, Busskamp V, Markiewicz I, Stadler MB, Ribi S, Richter J, et al. Characterizing light-regulated retinal microRNAs reveals rapid turnover as a common property of neuronal microRNAs. Cell. 2010 May 14;141(4):618-31.
96. Rybak A, Fuchs H, Hadian K, Smirnova L, Wulczyn EA, Michel G, et al. The let-7 target gene mouse lin-41 is a stem cell specific E3 ubiquitin ligase for the miRNA pathway protein Ago2. Nat Cell Biol. 2009 Dec;11(12):1411-20.
97. Ender C, Meister G. Argonaute proteins at a glance. J Cell Sci. 2010 Jun 1;123(Pt 11):1819-23.
98. Grimson A, Farh KK, Johnston WK, Garrett-Engele P, Lim LP, Bartel DP. MicroRNA targeting specificity in mammals: determinants beyond seed pairing. Mol Cell. 2007 Jul 6;27(1):91-105.
99. Lytle JR, Yario TA, Steitz JA. Target mRNAs are repressed as efficiently by microRNA-binding sites in the 5' UTR as in the 3' UTR. Proc Natl Acad Sci U S A. 2007 Jun 5;104(23):9667-72.
100. Forman JJ, Coller HA. The code within the code: microRNAs target coding regions. Cell Cycle. 2010 Apr 15;9(8):1533-41.
101. Jones-Rhoades MW, Bartel DP, Bartel B. MicroRNAS and their regulatory roles in plants. Annu Rev Plant Biol. 2006;57:19-53.
102. Lewis BP, Shih IH, Jones-Rhoades MW, Bartel DP, Burge CB. Prediction of mammalian microRNA targets. Cell. 2003 Dec 26;115(7):787-98.
103. Rhoades MW, Reinhart BJ, Lim LP, Burge CB, Bartel B, Bartel DP. Prediction of plant microRNA targets. Cell. 2002 Aug 23;110(4):513-20.
104. Brennecke J, Stark A, Russell RB, Cohen SM. Principles of microRNA-target recognition. PLoS Biol. 2005 Mar;3(3):e85.
105. Doench JG, Sharp PA. Specificity of microRNA target selection in translational repression. Genes Dev. 2004 Mar 1;18(5):504-11.
106. Bartel DP. MicroRNAs: target recognition and regulatory functions. Cell. 2009 Jan 23;136(2):215-33.
107. Friedman RC, Farh KK, Burge CB, Bartel DP. Most mammalian mRNAs are conserved targets of microRNAs. Genome Res. 2009 Jan;19(1):92-105.
108. Krek A, Grun D, Poy MN, Wolf R, Rosenberg L, Epstein EJ, et al. Combinatorial microRNA target predictions. Nat Genet. 2005 May;37(5):495-500.
109. John B, Enright AJ, Aravin A, Tuschl T, Sander C, Marks DS. Human MicroRNA targets. PLoS Biol. 2004 Nov;2(11):e363.
110. Betel D, Wilson M, Gabow A, Marks DS, Sander C. The microRNA.org resource: targets and expression. Nucleic Acids Res. 2008 Jan;36(Database issue):D149-53.

111. Kertesz M, Iovino N, Unnerstall U, Gaul U, Segal E. The role of site accessibility in microRNA target recognition. Nat Genet. 2007 Oct;39(10):1278-84.
112. Gaidatzis D, van Nimwegen E, Hausser J, Zavolan M. Inference of miRNA targets using evolutionary conservation and pathway analysis. BMC Bioinformatics. 2007;8:69.
113. Kiriakidou M, Nelson PT, Kouranov A, Fitziev P, Bouyioukos C, Mourelatos Z, et al. A combined computational-experimental approach predicts human microRNA targets. Genes Dev. 2004 May 15;18(10):1165-78.
114. Sethupathy P, Megraw M, Hatzigeorgiou AG. A guide through present computational approaches for the identification of mammalian microRNA targets. Nat Methods. 2006 Nov;3(11):881-6.
115. Lam LT, Lu X, Zhang H, Lesniewski R, Rosenberg S, Semizarov D. A microRNA screen to identify modulators of sensitivity to BCL2 inhibitor ABT-263 (navitoclax). Mol Cancer Ther. 2010 Nov;9(11):2943-50.
116. Sethupathy P, Corda B, Hatzigeorgiou AG. TarBase: A comprehensive database of experimentally supported animal microRNA targets. RNA. 2006 Feb;12(2):192-7.
117. Schmitter D, Filkowski J, Sewer A, Pillai RS, Oakeley EJ, Zavolan M, et al. Effects of Dicer and Argonaute down-regulation on mRNA levels in human HEK293 cells. Nucleic Acids Res. 2006;34(17):4801-15.
118. Behm-Ansmant I, Rehwinkel J, Doerks T, Stark A, Bork P, Izaurralde E. mRNA degradation by miRNAs and GW182 requires both CCR4:NOT deadenylase and DCP1:DCP2 decapping complexes. Genes Dev. 2006 Jul 15;20(14):1885-98.
119. Pillai RS, Artus CG, Filipowicz W. Tethering of human Ago proteins to mRNA mimics the miRNA-mediated repression of protein synthesis. RNA. 2004 Oct;10(10):1518-25.
120. Bohmert K, Camus I, Bellini C, Bouchez D, Caboche M, Benning C. AGO1 defines a novel locus of Arabidopsis controlling leaf development. EMBO J. 1998 Jan 2;17(1):170-80.
121. Peters L, Meister G. Argonaute proteins: mediators of RNA silencing. Mol Cell. 2007 Jun 8;26(5):611-23.
122. Tolia NH, Joshua-Tor L. Slicer and the argonautes. Nat Chem Biol. 2007 Jan;3(1):36-43.
123. Cerutti L, Mian N, Bateman A. Domains in gene silencing and cell differentiation proteins: the novel PAZ domain and redefinition of the Piwi domain. Trends Biochem Sci. 2000 Oct;25(10):481-2.
124. Jinek M, Doudna JA. A three-dimensional view of the molecular machinery of RNA interference. Nature. 2009 Jan 22;457(7228):405-12.
125. Yuan YR, Pei Y, Ma JB, Kuryavyi V, Zhadina M, Meister G, et al. Crystal structure of A. aeolicus argonaute, a site-specific DNA-guided endoribonuclease, provides insights into RISC-mediated mRNA cleavage. Mol Cell. 2005 Aug 5;19(3):405-19.
126. Boland A, Tritschler F, Heimstadt S, Izaurralde E, Weichenrieder O. Crystal structure and ligand binding of the MID domain of a eukaryotic Argonaute protein. EMBO Rep. 2010 Jul;11(7):522-7.
127. Djuranovic S, Zinchenko MK, Hur JK, Nahvi A, Brunelle JL, Rogers EJ, et al. Allosteric regulation of Argonaute proteins by miRNAs. Nat Struct Mol Biol. 2010 Feb;17(2):144-50.
128. Song JJ, Smith SK, Hannon GJ, Joshua-Tor L. Crystal structure of Argonaute and its implications for RISC slicer activity. Science. 2004 Sep 3;305(5689):1434-7.
129. Eulalio A, Huntzinger E, Izaurralde E. GW182 interaction with Argonaute is essential for miRNA-mediated translational repression and mRNA decay. Nat Struct Mol Biol. 2008 Apr;15(4):346-53.
130. Fabian MR, Mathonnet G, Sundermeier T, Mathys H, Zipprich JT, Svitkin YV, et al. Mammalian miRNA RISC recruits CAF1 and PABP to affect PABP-dependent deadenylation. Mol Cell. 2009 Sep 24;35(6):868-80.

131. Takimoto K, Wakiyama M, Yokoyama S. Mammalian GW182 contains multiple Argonaute-binding sites and functions in microRNA-mediated translational repression. RNA. 2009 Jun;15(6):1078-89.
132. Till S, Lejeune E, Thermann R, Bortfeld M, Hothorn M, Enderle D, et al. A conserved motif in Argonaute-interacting proteins mediates functional interactions through the Argonaute PIWI domain. Nat Struct Mol Biol. 2007 Oct;14(10):897-903.
133. Yao B, Li S, Lian SL, Fritzler MJ, Chan EK. Mapping of Ago2-GW182 functional interactions. Methods Mol Biol. 2011;725:45-62.
134. Pasquinelli AE. MicroRNAs and their targets: recognition, regulation and an emerging reciprocal relationship. Nat Rev Genet. 2012 Apr;13(4):271-82.
135. Yekta S, Shih IH, Bartel DP. MicroRNA-directed cleavage of HOXB8 mRNA. Science. 2004 Apr 23;304(5670):594-6.
136. Elbashir SM, Martinez J, Patkaniowska A, Lendeckel W, Tuschl T. Functional anatomy of siRNAs for mediating efficient RNAi in Drosophila melanogaster embryo lysate. EMBO J. 2001 Dec 3;20(23):6877-88.
137. Jackson AL, Bartz SR, Schelter J, Kobayashi SV, Burchard J, Mao M, et al. Expression profiling reveals off-target gene regulation by RNAi. Nat Biotechnol. 2003 Jun;21(6):635-7.
138. Bagga S, Bracht J, Hunter S, Massirer K, Holtz J, Eachus R, et al. Regulation by let-7 and lin-4 miRNAs results in target mRNA degradation. Cell. 2005 Aug 26;122(4):553-63.
139. Giraldez AJ, Mishima Y, Rihel J, Grocock RJ, Van Dongen S, Inoue K, et al. Zebrafish MiR-430 promotes deadenylation and clearance of maternal mRNAs. Science. 2006 Apr 7;312(5770):75-9.
140. Wu L, Belasco JG. Micro-RNA regulation of the mammalian lin-28 gene during neuronal differentiation of embryonal carcinoma cells. Mol Cell Biol. 2005 Nov;25(21):9198-208.
141. Braun JE, Huntzinger E, Fauser M, Izaurralde E. GW182 proteins directly recruit cytoplasmic deadenylase complexes to miRNA targets. Mol Cell. 2011 Oct 7;44(1):120-33.
142. Chekulaeva M, Mathys H, Zipprich JT, Attig J, Colic M, Parker R, et al. miRNA repression involves GW182-mediated recruitment of CCR4-NOT through conserved W-containing motifs. Nat Struct Mol Biol. 2011 Nov;18(11):1218-26.
143. Fabian MR, Cieplak MK, Frank F, Morita M, Green J, Srikumar T, et al. miRNA-mediated deadenylation is orchestrated by GW182 through two conserved motifs that interact with CCR4-NOT. Nat Struct Mol Biol. 2011 Nov;18(11):1211-7.
144. Kuzuoglu-Ozturk D, Huntzinger E, Schmidt S, Izaurralde E. The Caenorhabditis elegans GW182 protein AIN-1 interacts with PAB-1 and subunits of the PAN2-PAN3 and CCR4-NOT deadenylase complexes. Nucleic Acids Res. 2012 Jul 1;40(12):5651-65.
145. Rehwinkel J, Behm-Ansmant I, Gatfield D, Izaurralde E. A crucial role for GW182 and the DCP1:DCP2 decapping complex in miRNA-mediated gene silencing. RNA. 2005 Nov;11(11):1640-7.
146. Kulkarni M, Ozgur S, Stoecklin G. On track with P-bodies. Biochem Soc Trans. 2010 Feb;38(Pt 1):242-51.
147. Liu J, Rivas FV, Wohlschlegel J, Yates JR, 3rd, Parker R, Hannon GJ. A role for the P-body component GW182 in microRNA function. Nat Cell Biol. 2005 Dec;7(12):1261-6.
148. Liu J, Valencia-Sanchez MA, Hannon GJ, Parker R. MicroRNA-dependent localization of targeted mRNAs to mammalian P-bodies. Nat Cell Biol. 2005 Jul;7(7):719-23.
149. Sen GL, Blau HM. Argonaute 2/RISC resides in sites of mammalian mRNA decay known as cytoplasmic bodies. Nat Cell Biol. 2005 Jun;7(6):633-6.
150. Eystathioy T, Jakymiw A, Chan EK, Seraphin B, Cougot N, Fritzler MJ. The GW182 protein colocalizes with mRNA degradation associated proteins hDcp1 and hLSm4 in cytoplasmic GW bodies. RNA. 2003 Oct;9(10):1171-3.
151. Guo H, Ingolia NT, Weissman JS, Bartel DP. Mammalian microRNAs predominantly act to decrease target mRNA levels. Nature. 2010 Aug 12;466(7308):835-40.

152. Humphreys DT, Westman BJ, Martin DI, Preiss T. MicroRNAs control translation initiation by inhibiting eukaryotic initiation factor 4E/cap and poly(A) tail function. Proc Natl Acad Sci U S A. 2005 Nov 22;102(47):16961-6.
153. Pillai RS, Bhattacharyya SN, Artus CG, Zoller T, Cougot N, Basyuk E, et al. Inhibition of translational initiation by Let-7 MicroRNA in human cells. Science. 2005 Sep 2;309(5740):1573-6.
154. Kiriakidou M, Tan GS, Lamprinaki S, De Planell-Saguer M, Nelson PT, Mourelatos Z. An mRNA m7G cap binding-like motif within human Ago2 represses translation. Cell. 2007 Jun 15;129(6):1141-51.
155. Frank F, Fabian MR, Stepinski J, Jemielity J, Darzynkiewicz E, Sonenberg N, et al. Structural analysis of 5'-mRNA-cap interactions with the human AGO2 MID domain. EMBO Rep. 2011 May;12(5):415-20.
156. Kinch LN, Grishin NV. The human Ago2 MC region does not contain an eIF4E-like mRNA cap binding motif. Biol Direct. 2009;4:2.
157. Chendrimada TP, Finn KJ, Ji X, Baillat D, Gregory RI, Liebhaber SA, et al. MicroRNA silencing through RISC recruitment of eIF6. Nature. 2007 Jun 14;447(7146):823-8.
158. Ceci M, Gaviraghi C, Gorrini C, Sala LA, Offenhauser N, Marchisio PC, et al. Release of eIF6 (p27BBP) from the 60S subunit allows 80S ribosome assembly. Nature. 2003 Dec 4;426(6966):579-84.
159. Cooke A, Prigge A, Wickens M. Translational repression by deadenylases. J Biol Chem. 2010 Sep 10;285(37):28506-13.
160. Olsen PH, Ambros V. The lin-4 regulatory RNA controls developmental timing in Caenorhabditis elegans by blocking LIN-14 protein synthesis after the initiation of translation. Dev Biol. 1999 Dec 15;216(2):671-80.
161. Seggerson K, Tang L, Moss EG. Two genetic circuits repress the Caenorhabditis elegans heterochronic gene lin-28 after translation initiation. Dev Biol. 2002 Mar 15;243(2):215-25.
162. Petersen CP, Bordeleau ME, Pelletier J, Sharp PA. Short RNAs repress translation after initiation in mammalian cells. Mol Cell. 2006 Feb 17;21(4):533-42.
163. Nottrott S, Simard MJ, Richter JD. Human let-7a miRNA blocks protein production on actively translating polyribosomes. Nat Struct Mol Biol. 2006 Dec;13(12):1108-14.
164. Vasudevan S, Steitz JA. AU-rich-element-mediated upregulation of translation by FXR1 and Argonaute 2. Cell. 2007 Mar 23;128(6):1105-18.
165. Eiring AM, Harb JG, Neviani P, Garton C, Oaks JJ, Spizzo R, et al. miR-328 functions as an RNA decoy to modulate hnRNP E2 regulation of mRNA translation in leukemic blasts. Cell. 2010 Mar 5;140(5):652-65.
166. Forstemann K, Tomari Y, Du T, Vagin VV, Denli AM, Bratu DP, et al. Normal microRNA maturation and germ-line stem cell maintenance requires Loquacious, a double-stranded RNA-binding domain protein. PLoS Biol. 2005 Jul;3(7):e236.
167. Knight SW, Bass BL. A role for the RNase III enzyme DCR-1 in RNA interference and germ line development in Caenorhabditis elegans. Science. 2001 Sep 21;293(5538):2269-71.
168. Wienholds E, Koudijs MJ, van Eeden FJ, Cuppen E, Plasterk RH. The microRNA-producing enzyme Dicer1 is essential for zebrafish development. Nat Genet. 2003 Nov;35(3):217-8.
169. Bernstein E, Kim SY, Carmell MA, Murchison EP, Alcorn H, Li MZ, et al. Dicer is essential for mouse development. Nat Genet. 2003 Nov;35(3):215-7.
170. Abrahante JE, Daul AL, Li M, Volk ML, Tennessen JM, Miller EA, et al. The Caenorhabditis elegans hunchback-like gene lin-57/hbl-1 controls developmental time and is regulated by microRNAs. Dev Cell. 2003 May;4(5):625-37.
171. Lin SY, Johnson SM, Abraham M, Vella MC, Pasquinelli A, Gamberi C, et al. The C elegans hunchback homolog, hbl-1, controls temporal patterning and is a probable microRNA target. Dev Cell. 2003 May;4(5):639-50.

172. Moss EG, Lee RC, Ambros V. The cold shock domain protein LIN-28 controls developmental timing in C. elegans and is regulated by the lin-4 RNA. Cell. 1997 Mar 7;88(5):637-46.
173. Bettinger JC, Lee K, Rougvie AE. Stage-specific accumulation of the terminal differentiation factor LIN-29 during Caenorhabditis elegans development. Development. 1996 Aug;122(8):2517-27.
174. Rougvie AE, Ambros V. The heterochronic gene lin-29 encodes a zinc finger protein that controls a terminal differentiation event in Caenorhabditis elegans. Development. 1995 Aug;121(8):2491-500.
175. Maller Schulman BR, Liang X, Stahlhut C, DelConte C, Stefani G, Slack FJ. The let-7 microRNA target gene, Mlin41/Trim71 is required for mouse embryonic survival and neural tube closure. Cell Cycle. 2008 Dec 15;7(24):3935-42.
176. Wulczyn FG, Smirnova L, Rybak A, Brandt C, Kwidzinski E, Ninnemann O, et al. Post-transcriptional regulation of the let-7 microRNA during neural cell specification. FASEB J. 2007 Feb;21(2):415-26.
177. Kloosterman WP, Wienholds E, Ketting RF, Plasterk RH. Substrate requirements for let-7 function in the developing zebrafish embryo. Nucleic Acids Res. 2004;32(21):6284-91.
178. Sokol NS, Xu P, Jan YN, Ambros V. Drosophila let-7 microRNA is required for remodeling of the neuromusculature during metamorphosis. Genes Dev. 2008 Jun 15;22(12):1591-6.
179. Caygill EE, Johnston LA. Temporal regulation of metamorphic processes in Drosophila by the let-7 and miR-125 heterochronic microRNAs. Curr Biol. 2008 Jul 8;18(13):943-50.
180. Lin YC, Hsieh LC, Kuo MW, Yu J, Kuo HH, Lo WL, et al. Human TRIM71 and its nematode homologue are targets of let-7 microRNA and its zebrafish orthologue is essential for development. Mol Biol Evol. 2007 Nov;24(11):2525-34.
181. Xu N, Papagiannakopoulos T, Pan G, Thomson JA, Kosik KS. MicroRNA-145 regulates OCT4, SOX2, and KLF4 and represses pluripotency in human embryonic stem cells. Cell. 2009 May 15;137(4):647-58.
182. Melton C, Judson RL, Blelloch R. Opposing microRNA families regulate self-renewal in mouse embryonic stem cells. Nature. 2010 Feb 4;463(7281):621-6.
183. Ivey KN, Muth A, Arnold J, King FW, Yeh RF, Fish JE, et al. MicroRNA regulation of cell lineages in mouse and human embryonic stem cells. Cell Stem Cell. 2008 Mar 6;2(3):219-29.
184. Zhao Y, Samal E, Srivastava D. Serum response factor regulates a muscle-specific microRNA that targets Hand2 during cardiogenesis. Nature. 2005 Jul 14;436(7048):214-20.
185. Delaloy C, Liu L, Lee JA, Su H, Shen F, Yang GY, et al. MicroRNA-9 coordinates proliferation and migration of human embryonic stem cell-derived neural progenitors. Cell Stem Cell. 2010 Apr 2;6(4):323-35.
186. Tarantino C, Paolella G, Cozzuto L, Minopoli G, Pastore L, Parisi S, et al. miRNA 34a, 100, and 137 modulate differentiation of mouse embryonic stem cells. FASEB J. 2010 Sep;24(9):3255-63.
187. Vecchione A, Croce CM. Apoptomirs: small molecules have gained the license to kill. Endocr Relat Cancer. 2010 Mar;17(1):F37-50.
188. Ola MS, Nawaz M, Ahsan H. Role of Bcl-2 family proteins and caspases in the regulation of apoptosis. Mol Cell Biochem. 2011 May;351(1-2):41-58.
189. Cimmino A, Calin GA, Fabbri M, Iorio MV, Ferracin M, Shimizu M, et al. miR-15 and miR-16 induce apoptosis by targeting BCL2. Proc Natl Acad Sci U S A. 2005 Sep 27;102(39):13944-9.
190. Cole KA, Attiyeh EF, Mosse YP, Laquaglia MJ, Diskin SJ, Brodeur GM, et al. A functional screen identifies miR-34a as a candidate neuroblastoma tumor suppressor gene. Mol Cancer Res. 2008 May;6(5):735-42.
191. Yamakuchi M, Ferlito M, Lowenstein CJ. miR-34a repression of SIRT1 regulates apoptosis. Proc Natl Acad Sci U S A. 2008 Sep 9;105(36):13421-6.
192. Zhang CZ, Zhang JX, Zhang AL, Shi ZD, Han L, Jia ZF, et al. MiR-221 and miR-222 target PUMA to induce cell survival in glioblastoma. Mol Cancer. 2010;9:229.

193. Ventura A, Young AG, Winslow MM, Lintault L, Meissner A, Erkeland SJ, et al. Targeted deletion reveals essential and overlapping functions of the miR-17 through 92 family of miRNA clusters. Cell. 2008 Mar 7;132(5):875-86.
194. Kirchhoff SR, Gupta S, Knowlton AA. Cytosolic heat shock protein 60, apoptosis, and myocardial injury. Circulation. 2002 Jun 18;105(24):2899-904.
195. Latchman DS. Heat shock proteins and cardiac protection. Cardiovasc Res. 2001 Sep;51(4):637-46.
196. Xu C, Lu Y, Pan Z, Chu W, Luo X, Lin H, et al. The muscle-specific microRNAs miR-1 and miR-133 produce opposing effects on apoptosis by targeting HSP60, HSP70 and caspase-9 in cardiomyocytes. J Cell Sci. 2007 Sep 1;120(Pt 17):3045-52.
197. Sayed D, He M, Hong C, Gao S, Rane S, Yang Z, et al. MicroRNA-21 is a downstream effector of AKT that mediates its antiapoptotic effects via suppression of Fas ligand. J Biol Chem. 2010 Jun 25;285(26):20281-90.
198. Ovcharenko D, Kelnar K, Johnson C, Leng N, Brown D. Genome-scale microRNA and small interfering RNA screens identify small RNA modulators of TRAIL-induced apoptosis pathway. Cancer Res. 2007 Nov 15;67(22):10782-8.
199. Bueno MJ, Malumbres M. MicroRNAs and the cell cycle. Biochim Biophys Acta. 2011 May;1812(5):592-601.
200. Takeshita F, Patrawala L, Osaki M, Takahashi RU, Yamamoto Y, Kosaka N, et al. Systemic delivery of synthetic microRNA-16 inhibits the growth of metastatic prostate tumors via downregulation of multiple cell-cycle genes. Mol Ther. 2010 Jan;18(1):181-7.
201. Liu Q, Fu H, Sun F, Zhang H, Tie Y, Zhu J, et al. miR-16 family induces cell cycle arrest by regulating multiple cell cycle genes. Nucleic Acids Res. 2008 Sep;36(16):5391-404.
202. Linsley PS, Schelter J, Burchard J, Kibukawa M, Martin MM, Bartz SR, et al. Transcripts targeted by the microRNA-16 family cooperatively regulate cell cycle progression. Mol Cell Biol. 2007 Mar;27(6):2240-52.
203. Wang F, Fu XD, Zhou Y, Zhang Y. Down-regulation of the cyclin E1 oncogene expression by microRNA-16-1 induces cell cycle arrest in human cancer cells. BMB Rep. 2009 Nov 30;42(11):725-30.
204. Lal A, Kim HH, Abdelmohsen K, Kuwano Y, Pullmann R, Jr., Srikantan S, et al. p16(INK4a) translation suppressed by miR-24. PLoS One. 2008;3(3):e1864.
205. Malhas A, Saunders NJ, Vaux DJ. The nuclear envelope can control gene expression and cell cycle progression via miRNA regulation. Cell Cycle. 2010 Feb 1;9(3):531-9.
206. Huang L, Luo J, Cai Q, Pan Q, Zeng H, Guo Z, et al. MicroRNA-125b suppresses the development of bladder cancer by targeting E2F3. Int J Cancer. 2011 Apr 15;128(8):1758-69.
207. Schultz J, Lorenz P, Gross G, Ibrahim S, Kunz M. MicroRNA let-7b targets important cell cycle molecules in malignant melanoma cells and interferes with anchorage-independent growth. Cell Res. 2008 May;18(5):549-57.
208. Lal A, Navarro F, Maher CA, Maliszewski LE, Yan N, O'Day E, et al. miR-24 Inhibits cell proliferation by targeting E2F2, MYC, and other cell-cycle genes via binding to "seedless" 3'UTR microRNA recognition elements. Mol Cell. 2009 Sep 11;35(5):610-25.
209. Qi J, Yu JY, Shcherbata HR, Mathieu J, Wang AJ, Seal S, et al. microRNAs regulate human embryonic stem cell division. Cell Cycle. 2009 Nov 15;8(22):3729-41.
210. Butz H, Liko I, Czirjak S, Igaz P, Khan MM, Zivkovic V, et al. Down-regulation of Wee1 kinase by a specific subset of microRNA in human sporadic pituitary adenomas. J Clin Endocrinol Metab. 2010 Oct;95(10):E181-91.
211. Shi W, Alajez NM, Bastianutto C, Hui ABY, Mocanu JD, Ito E, et al. Significance of Plk1 regulation by miR-100 in human nasopharyngeal cancer. International Journal of Cancer. 2010 May 1;126(9):2036-48.

212. Lu J, Getz G, Miska EA, Alvarez-Saavedra E, Lamb J, Peck D, et al. MicroRNA expression profiles classify human cancers. Nature. 2005 Jun 9;435(7043):834-8.
213. Volinia S, Calin GA, Liu CG, Ambs S, Cimmino A, Petrocca F, et al. A microRNA expression signature of human solid tumors defines cancer gene targets. Proc Natl Acad Sci U S A. 2006 Feb 14;103(7):2257-61.
214. Wang Y, Lee CG. MicroRNA and cancer--focus on apoptosis. J Cell Mol Med. 2009 Jan;13(1):12-23.
215. Lages E, Guttin A, El Atifi M, Ramus C, Ipas H, Dupre I, et al. MicroRNA and target protein patterns reveal physiopathological features of glioma subtypes. PLoS One. 2011;6(5):e20600.
216. Eis PS, Tam W, Sun L, Chadburn A, Li Z, Gomez MF, et al. Accumulation of miR-155 and BIC RNA in human B cell lymphomas. Proc Natl Acad Sci U S A. 2005 Mar 8;102(10):3627-32.
217. Kluiver J, Poppema S, de Jong D, Blokzijl T, Harms G, Jacobs S, et al. BIC and miR-155 are highly expressed in Hodgkin, primary mediastinal and diffuse large B cell lymphomas. J Pathol. 2005 Oct;207(2):243-9.
218. Costinean S, Zanesi N, Pekarsky Y, Tili E, Volinia S, Heerema N, et al. Pre-B cell proliferation and lymphoblastic leukemia/high-grade lymphoma in E(mu)-miR155 transgenic mice. Proc Natl Acad Sci U S A. 2006 May 2;103(18):7024-9.
219. Chen Y, Knosel T, Kristiansen G, Pietas A, Garber ME, Matsuhashi S, et al. Loss of PDCD4 expression in human lung cancer correlates with tumour progression and prognosis. J Pathol. 2003 Aug;200(5):640-6.
220. Mudduluru G, Medved F, Grobholz R, Jost C, Gruber A, Leupold JH, et al. Loss of programmed cell death 4 expression marks adenoma-carcinoma transition, correlates inversely with phosphorylated protein kinase B, and is an independent prognostic factor in resected colorectal cancer. Cancer. 2007 Oct 15;110(8):1697-707.
221. Zhu S, Si ML, Wu H, Mo YY. MicroRNA-21 targets the tumor suppressor gene tropomyosin 1 (TPM1). J Biol Chem. 2007 May 11;282(19):14328-36.
222. Asangani IA, Rasheed SA, Nikolova DA, Leupold JH, Colburn NH, Post S, et al. MicroRNA-21 (miR-21) post-transcriptionally downregulates tumor suppressor Pdcd4 and stimulates invasion, intravasation and metastasis in colorectal cancer. Oncogene. 2008 Apr 3;27(15):2128-36.
223. Calin GA, Sevignani C, Dumitru CD, Hyslop T, Noch E, Yendamuri S, et al. Human microRNA genes are frequently located at fragile sites and genomic regions involved in cancers. Proc Natl Acad Sci U S A. 2004 Mar 2;101(9):2999-3004.
224. Sarhadi VK, Wikman H, Salmenkivi K, Kuosma E, Sioris T, Salo J, et al. Increased expression of high mobility group A proteins in lung cancer. J Pathol. 2006 Jun;209(2):206-12.
225. Iorio MV, Ferracin M, Liu CG, Veronese A, Spizzo R, Sabbioni S, et al. MicroRNA gene expression deregulation in human breast cancer. Cancer Res. 2005 Aug 15;65(16):7065-70.
226. Akao Y, Nakagawa Y, Naoe T. let-7 microRNA functions as a potential growth suppressor in human colon cancer cells. Biol Pharm Bull. 2006 May;29(5):903-6.
227. Yanaihara N, Caplen N, Bowman E, Seike M, Kumamoto K, Yi M, et al. Unique microRNA molecular profiles in lung cancer diagnosis and prognosis. Cancer Cell. 2006 Mar;9(3):189-98.
228. Guessous F, Zhang Y, Kofman A, Catania A, Li Y, Schiff D, et al. microRNA-34a is tumor suppressive in brain tumors and glioma stem cells. Cell Cycle. 2010 Mar 15;9(6):1031-6.
229. Jiang Q, Wang Y, Hao Y, Juan L, Teng M, Zhang X, et al. miR2Disease: a manually curated database for microRNA deregulation in human disease. Nucleic Acids Res. 2009 Jan;37(Database issue):D98-104.
230. Beroukhim R, Mermel CH, Porter D, Wei G, Raychaudhuri S, Donovan J, et al. The landscape of somatic copy-number alteration across human cancers. Nature. 2010 Feb 18;463(7283):899-905.
231. Brosh R, Rotter V. When mutants gain new powers: news from the mutant p53 field. Nat Rev Cancer. 2009 Oct;9(10):701-13.

232. Lodygin D, Tarasov V, Epanchintsev A, Berking C, Knyazeva T, Korner H, et al. Inactivation of miR-34a by aberrant CpG methylation in multiple types of cancer. Cell Cycle. 2008 Aug 15;7(16):2591-600.
233. Lujambio A, Ropero S, Ballestar E, Fraga MF, Cerrato C, Setien F, et al. Genetic unmasking of an epigenetically silenced microRNA in human cancer cells. Cancer Res. 2007 Feb 15;67(4):1424-9.
234. Zhang L, Coukos G. MicroRNAs: a new insight into cancer genome. Cell Cycle. 2006 Oct;5(19):2216-9.
235. Saito-Ohara F, Imoto I, Inoue J, Hosoi H, Nakagawara A, Sugimoto T, et al. PPM1D is a potential target for 17q gain in neuroblastoma. Cancer Res. 2003 Apr 15;63(8):1876-83.
236. Calin GA, Dumitru CD, Shimizu M, Bichi R, Zupo S, Noch E, et al. Frequent deletions and down-regulation of micro- RNA genes miR15 and miR16 at 13q14 in chronic lymphocytic leukemia. Proc Natl Acad Sci U S A. 2002 Nov 26;99(24):15524-9.
237. Merritt WM, Lin YG, Han LY, Kamat AA, Spannuth WA, Schmandt R, et al. Dicer, Drosha, and outcomes in patients with ovarian cancer. N Engl J Med. 2008 Dec 18;359(25):2641-50.
238. Sand M, Gambichler T, Skrygan M, Sand D, Scola N, Altmeyer P, et al. Expression levels of the microRNA processing enzymes Drosha and dicer in epithelial skin cancer. Cancer Invest. 2010 Jul;28(6):649-53.
239. Sugito N, Ishiguro H, Kuwabara Y, Kimura M, Mitsui A, Kurehara H, et al. RNASEN regulates cell proliferation and affects survival in esophageal cancer patients. Clin Cancer Res. 2006 Dec 15;12(24):7322-8.
240. Chiosea S, Jelezcova E, Chandran U, Acquafondata M, McHale T, Sobol RW, et al. Up-regulation of dicer, a component of the MicroRNA machinery, in prostate adenocarcinoma. Am J Pathol. 2006 Nov;169(5):1812-20.
241. Chiosea S, Jelezcova E, Chandran U, Luo J, Mantha G, Sobol RW, et al. Overexpression of Dicer in precursor lesions of lung adenocarcinoma. Cancer Res. 2007 Mar 1;67(5):2345-50.
242. Karube Y, Tanaka H, Osada H, Tomida S, Tatematsu Y, Yanagisawa K, et al. Reduced expression of Dicer associated with poor prognosis in lung cancer patients. Cancer Sci. 2005 Feb;96(2):111-5.
243. Boominathan L. The tumor suppressors p53, p63, and p73 are regulators of microRNA processing complex. PLoS One. 2010;5(5):e10615.
244. Jazdzewski K, Murray EL, Franssila K, Jarzab B, Schoenberg DR, de la Chapelle A. Common SNP in pre-miR-146a decreases mature miR expression and predisposes to papillary thyroid carcinoma. Proc Natl Acad Sci U S A. 2008 May 20;105(20):7269-74.
245. Permuth-Wey J, Thompson RC, Burton Nabors L, Olson JJ, Browning JE, Madden MH, et al. A functional polymorphism in the pre-miR-146a gene is associated with risk and prognosis in adult glioma. J Neurooncol. 2011 Dec;105(3):639-46.
246. Xu B, Feng NH, Li PC, Tao J, Wu D, Zhang ZD, et al. A functional polymorphism in Pre-miR-146a gene is associated with prostate cancer risk and mature miR-146a expression in vivo. Prostate. 2010 Apr 1;70(5):467-72.
247. Meyer B, Loeschke S, Schultze A, Weigel T, Sandkamp M, Goldmann T, et al. HMGA2 overexpression in non-small cell lung cancer. Mol Carcinog. 2007 Jul;46(7):503-11.
248. Di Cello F, Hillion J, Hristov A, Wood LJ, Mukherjee M, Schuldenfrei A, et al. HMGA2 participates in transformation in human lung cancer. Mol Cancer Res. 2008 May;6(5):743-50.
249. Rickinson A, Kieff E. Epstein-Barr Virus. In: DM K, PM H, editors. Fields Virology. Philadelphia: Lippincott Williams and Wilkins; 2006. p. 2655-700.
250. Pfeffer S, Zavolan M, Grasser FA, Chien M, Russo JJ, Ju J, et al. Identification of virus-encoded microRNAs. Science. 2004 Apr 30;304(5671):734-6.
251. Burkitt D. A sarcoma involving the jaws in African children. Br J Surg. 1958 Nov;46(197):218-23.

252. Burkitt DP. The discovery of Burkitt's lymphoma. Cancer. 1983 May 15;51(10):1777-86.
253. Burkitt D. A children's cancer dependent on climatic factors. Nature. 1962 Apr 21;194:232-4.
254. Epstein MA, Achong BG, Barr YM. Virus Particles in Cultured Lymphoblasts from Burkitt's Lymphoma. Lancet. 1964 Mar 28;1(7335):702-3.
255. Epstein MA, Henle G, Achong BG, Barr YM. Morphological and Biological Studies on a Virus in Cultured Lymphoblasts from Burkitt's Lymphoma. J Exp Med. 1965 May 1;121:761-70.
256. Henle G, Henle W. Immunofluorescence in cells derived from Burkitt's lymphoma. J Bacteriol. 1966 Mar;91(3):1248-56.
257. Burkitt DP. Etiology of Burkitt's lymphoma--an alternative hypothesis to a vectored virus. J Natl Cancer Inst. 1969 Jan;42(1):19-28.
258. Whittle HC, Brown J, Marsh K, Greenwood BM, Seidelin P, Tighe H, et al. T-cell control of Epstein-Barr virus-infected B cells is lost during P. falciparum malaria. Nature. 1984 Nov 29-Dec 5;312(5993):449-50.
259. Henle G, Henle W, Diehl V. Relation of Burkitt's tumor-associated herpes-ytpe virus to infectious mononucleosis. Proc Natl Acad Sci U S A. 1968 Jan;59(1):94-101.
260. Niederman JC, McCollum RW, Henle G, Henle W. Infectious mononucleosis. Clinical manifestations in relation to EB virus antibodies. JAMA. 1968 Jan 15;203(3):205-9.
261. Henle W, Diehl V, Kohn G, Zur Hausen H, Henle G. Herpes-type virus and chromosome marker in normal leukocytes after growth with irradiated Burkitt cells. Science. 1967 Sep 1;157(3792):1064-5.
262. Miller G. The oncogenicity of Epstein-Barr virus. J Infect Dis. 1974 Aug;130(2):187-205.
263. Davison AJ, Eberle R, Ehlers B, Hayward GS, McGeoch DJ, Minson AC, et al. The order Herpesvirales. Arch Virol. 2009;154(1):171-7.
264. Kieff E, Dambaugh T, Heller M, King W, Cheung A, van Santen V, et al. The biology and chemistry of Epstein-Barr virus. J Infect Dis. 1982 Oct;146(4):506-17.
265. Pope JH, Achong BG, Epstein MA. Cultivation and fine structure of virus-bearing lymphoblasts from a second New Guinea Burkitt lymphoma: establishment of sublines with unusual cultural properties. Int J Cancer. 1968 Mar 15;3(2):171-82.
266. Dambaugh T, Raab-Traub N, Heller M, Beisel C, Hummel M, Cheung A, et al. Variations among isolates of Epstein-Barr virus. Ann N Y Acad Sci. 1980;354:309-25.
267. Baer R, Bankier AT, Biggin MD, Deininger PL, Farrell PJ, Gibson TJ, et al. DNA sequence and expression of the B95-8 Epstein-Barr virus genome. Nature. 1984 Jul 19-25;310(5974):207-11.
268. Dambaugh T, Beisel C, Hummel M, King W, Fennewald S, Cheung A, et al. Epstein-Barr virus (B95-8) DNA VII: molecular cloning and detailed mapping. Proc Natl Acad Sci U S A. 1980 May;77(5):2999-3003.
269. Arrand JR, Rymo L, Walsh JE, Bjorck E, Lindahl T, Griffin BE. Molecular cloning of the complete Epstein-Barr virus genome as a set of overlapping restriction endonuclease fragments. Nucleic Acids Res. 1981 Jul 10;9(13):2999-3014.
270. Kalla M, Hammerschmidt W. Human B cells on their route to latent infection--early but transient expression of lytic genes of Epstein-Barr virus. Eur J Cell Biol. 2012 Jan;91(1):65-9.
271. Dolan A, Addison C, Gatherer D, Davison AJ, McGeoch DJ. The genome of Epstein-Barr virus type 2 strain AG876. Virology. 2006 Jun 20;350(1):164-70.
272. Kwok H, Tong AH, Lin CH, Lok S, Farrell PJ, Kwong DL, et al. Genomic sequencing and comparative analysis of Epstein-Barr virus genome isolated from primary nasopharyngeal carcinoma biopsy. PLoS One. 2012;7(5):e36939.
273. Liu P, Fang X, Feng Z, Guo YM, Peng RJ, Liu T, et al. Direct sequencing and characterization of a clinical isolate of Epstein-Barr virus from nasopharyngeal carcinoma tissue by using next-generation sequencing technology. J Virol. 2011 Nov;85(21):11291-9.

274. Zeng MS, Li DJ, Liu QL, Song LB, Li MZ, Zhang RH, et al. Genomic sequence analysis of Epstein-Barr virus strain GD1 from a nasopharyngeal carcinoma patient. J Virol. 2005 Dec;79(24):15323-30.
275. Hummel M, Kieff E. Epstein-Barr virus RNA. VIII. Viral RNA in permissively infected B95-8 cells. J Virol. 1982 Jul;43(1):262-72.
276. van Santen V, Cheung A, Kieff E. Epstein-Barr virus RNA VII: size and direction of transcription of virus-specified cytoplasmic RNAs in a transformed cell line. Proc Natl Acad Sci U S A. 1981 Mar;78(3):1930-4.
277. Powell AL, King W, Kieff E. Epstein-Barr virus-specific RNA. III. Mapping of DNA encoding viral RNA in restringent infection. J Virol. 1979 Jan;29(1):261-74.
278. King W, Thomas-Powell AL, Raab-Traub N, Hawke M, Kieff E. Epstein-Barr virus RNA. V. Viral RNA in a restringently infected, growth-transformed cell line. J Virol. 1980 Nov;36(2):506-18.
279. King W, Van Santen V, Kieff E. Epstein-Barr virus RNA. VI. Viral RNA in restringently and abortively infected Raji cells. J Virol. 1981 May;38(2):649-60.
280. Given D, Kieff E. DNA of Epstein-Barr virus. VI. Mapping of the internal tandem reiteration. J Virol. 1979 Aug;31(2):315-24.
281. Hayward SD, Nogee L, Hayward GS. Organization of repeated regions within the Epstein-Barr virus DNA molecule. J Virol. 1980 Jan;33(1):507-21.
282. Heller M, van Santen V, Kieff E. Simple repeat sequence in Epstein-Barr virus DNA is transcribed in latent and productive infections. J Virol. 1982 Oct;44(1):311-20.
283. Dambaugh TR, Kieff E. Identification and nucleotide sequences of two similar tandem direct repeats in Epstein-Barr virus DNA. J Virol. 1982 Dec;44(3):823-33.
284. Kintner CR, Sugden B. The structure of the termini of the DNA of Epstein-Barr virus. Cell. 1979 Jul;17(3):661-71.
285. Given D, Yee D, Griem K, Kieff E. DNA of Epstein-Barr virus. V. Direct repeats of the ends of Epstein-Barr virus DNA. J Virol. 1979 Jun;30(3):852-62.
286. Adldinger HK, Delius H, Freese UK, Clarke J, Bornkamm GW. A putative transforming gene of Jijoye virus differs from that of Epstein-Barr virus prototypes. Virology. 1985 Mar;141(2):221-34.
287. Sample J, Young L, Martin B, Chatman T, Kieff E, Rickinson A. Epstein-Barr virus types 1 and 2 differ in their EBNA-3A, EBNA-3B, and EBNA-3C genes. J Virol. 1990 Sep;64(9):4084-92.
288. Dambaugh T, Hennessy K, Chamnankit L, Kieff E. U2 region of Epstein-Barr virus DNA may encode Epstein-Barr nuclear antigen 2. Proc Natl Acad Sci U S A. 1984 Dec;81(23):7632-6.
289. Falk K, Gratama JW, Rowe M, Zou JZ, Khanim F, Young LS, et al. The role of repetitive DNA sequences in the size variation of Epstein-Barr virus (EBV) nuclear antigens, and the identification of different EBV isolates using RFLP and PCR analysis. J Gen Virol. 1995 Apr;76 (Pt 4):779-90.
290. Rowe M, Young LS, Cadwallader K, Petti L, Kieff E, Rickinson AB. Distinction between Epstein-Barr virus type A (EBNA 2A) and type B (EBNA 2B) isolates extends to the EBNA 3 family of nuclear proteins. J Virol. 1989 Mar;63(3):1031-9.
291. Habeshaw G, Yao QY, Bell AI, Morton D, Rickinson AB. Epstein-barr virus nuclear antigen 1 sequences in endemic and sporadic Burkitt's lymphoma reflect virus strains prevalent in different geographic areas. J Virol. 1999 Feb;73(2):965-75.
292. Khanna R, Slade RW, Poulsen L, Moss DJ, Burrows SR, Nicholls J, et al. Evolutionary dynamics of genetic variation in Epstein-Barr virus isolates of diverse geographical origins: evidence for immune pressure-independent genetic drift. J Virol. 1997 Nov;71(11):8340-6.
293. Sandvej K, Gratama JW, Munch M, Zhou XG, Bolhuis RL, Andresen BS, et al. Sequence analysis of the Epstein-Barr virus (EBV) latent membrane protein-1 gene and promoter region: identification of four variants among wild-type EBV isolates. Blood. 1997 Jul 1;90(1):323-30.
294. Busson P, Edwards RH, Tursz T, Raab-Traub N. Sequence polymorphism in the Epstein-Barr virus latent membrane protein (LMP)-2 gene. J Gen Virol. 1995 Jan;76 (Pt 1):139-45.

295. Fingeroth JD, Weis JJ, Tedder TF, Strominger JL, Biro PA, Fearon DT. Epstein-Barr virus receptor of human B lymphocytes is the C3d receptor CR2. Proc Natl Acad Sci U S A. 1984 Jul;81(14):4510-4.

296. Nemerow GR, Wolfert R, McNaughton ME, Cooper NR. Identification and characterization of the Epstein-Barr virus receptor on human B lymphocytes and its relationship to the C3d complement receptor (CR2). J Virol. 1985 Aug;55(2):347-51.

297. Jondal M, Klein G, Oldstone MB, Bokish V, Yefenof E. Surface markers on human B and T lymphocytes. VIII. Association between complement and Epstein-Barr virus receptors on human lymphoid cells. Scand J Immunol. 1976;5(4):401-10.

298. Nemerow GR, Mullen JJ, 3rd, Dickson PW, Cooper NR. Soluble recombinant CR2 (CD21) inhibits Epstein-Barr virus infection. J Virol. 1990 Mar;64(3):1348-52.

299. Tanner J, Weis J, Fearon D, Whang Y, Kieff E. Epstein-Barr virus gp350/220 binding to the B lymphocyte C3d receptor mediates adsorption, capping, and endocytosis. Cell. 1987 Jul 17;50(2):203-13.

300. Nemerow GR, Mold C, Schwend VK, Tollefson V, Cooper NR. Identification of gp350 as the viral glycoprotein mediating attachment of Epstein-Barr virus (EBV) to the EBV/C3d receptor of B cells: sequence homology of gp350 and C3 complement fragment C3d. J Virol. 1987 May;61(5):1416-20.

301. Nemerow GR, Houghten RA, Moore MD, Cooper NR. Identification of an epitope in the major envelope protein of Epstein-Barr virus that mediates viral binding to the B lymphocyte EBV receptor (CR2). Cell. 1989 Feb 10;56(3):369-77.

302. Li Q, Spriggs MK, Kovats S, Turk SM, Comeau MR, Nepom B, et al. Epstein-Barr virus uses HLA class II as a cofactor for infection of B lymphocytes. J Virol. 1997 Jun;71(6):4657-62.

303. Molesworth SJ, Lake CM, Borza CM, Turk SM, Hutt-Fletcher LM. Epstein-Barr virus gH is essential for penetration of B cells but also plays a role in attachment of virus to epithelial cells. J Virol. 2000 Jul;74(14):6324-32.

304. Wang X, Hutt-Fletcher LM. Epstein-Barr virus lacking glycoprotein gp42 can bind to B cells but is not able to infect. J Virol. 1998 Jan;72(1):158-63.

305. Anagnostopoulos I, Hummel M, Kreschel C, Stein H. Morphology, immunophenotype, and distribution of latently and/or productively Epstein-Barr virus-infected cells in acute infectious mononucleosis: implications for the interindividual infection route of Epstein-Barr virus. Blood. 1995 Feb 1;85(3):744-50.

306. Henle G, Henle W. Epstein-Barr virus-specific IgA serum antibodies as an outstanding feature of nasopharyngeal carcinoma. Int J Cancer. 1976 Jan 15;17(1):1-7.

307. Tao Q, Ho FC, Loke SL, Srivastava G. Epstein-Barr virus is localized in the tumour cells of nasal lymphomas of NK, T or B cell type. Int J Cancer. 1995 Jan 27;60(3):315-20.

308. Harabuchi Y, Yamanaka N, Kataura A, Imai S, Kinoshita T, Mizuno F, et al. Epstein-Barr virus in nasal T-cell lymphomas in patients with lethal midline granuloma. Lancet. 1990 Jan 20;335(8682):128-30.

309. Shannon-Lowe CD, Neuhierl B, Baldwin G, Rickinson AB, Delecluse HJ. Resting B cells as a transfer vehicle for Epstein-Barr virus infection of epithelial cells. Proc Natl Acad Sci U S A. 2006 May 2;103(18):7065-70.

310. Imai S, Nishikawa J, Takada K. Cell-to-cell contact as an efficient mode of Epstein-Barr virus infection of diverse human epithelial cells. J Virol. 1998 May;72(5):4371-8.

311. Herrmann K, Frangou P, Middeldorp J, Niedobitek G. Epstein-Barr virus replication in tongue epithelial cells. J Gen Virol. 2002 Dec;83(Pt 12):2995-8.

312. Frangou P, Buettner M, Niedobitek G. Epstein-Barr virus (EBV) infection in epithelial cells in vivo: rare detection of EBV replication in tongue mucosa but not in salivary glands. J Infect Dis. 2005 Jan 15;191(2):238-42.

313. Fischer E, Delibrias C, Kazatchkine MD. Expression of CR2 (the C3dg/EBV receptor, CD21) on normal human peripheral blood T lymphocytes. J Immunol. 1991 Feb 1;146(3):865-9.
314. Sauvageau G, Stocco R, Kasparian S, Menezes J. Epstein-Barr virus receptor expression on human CD8+ (cytotoxic/suppressor) T lymphocytes. J Gen Virol. 1990 Feb;71 (Pt 2):379-86.
315. Rowe M, Lear AL, Croom-Carter D, Davies AH, Rickinson AB. Three pathways of Epstein-Barr virus gene activation from EBNA1-positive latency in B lymphocytes. J Virol. 1992 Jan;66(1):122-31.
316. Sample J, Hummel M, Braun D, Birkenbach M, Kieff E. Nucleotide sequences of mRNAs encoding Epstein-Barr virus nuclear proteins: a probable transcriptional initiation site. Proc Natl Acad Sci U S A. 1986 Jul;83(14):5096-100.
317. Speck SH, Pfitzner A, Strominger JL. An Epstein-Barr virus transcript from a latently infected, growth-transformed B-cell line encodes a highly repetitive polypeptide. Proc Natl Acad Sci U S A. 1986 Dec;83(24):9298-302.
318. Bodescot M, Perricaudet M. Epstein-Barr virus mRNAs produced by alternative splicing. Nucleic Acids Res. 1986 Sep 11;14(17):7103-14.
319. Woisetschlaeger M, Yandava CN, Furmanski LA, Strominger JL, Speck SH. Promoter switching in Epstein-Barr virus during the initial stages of infection of B lymphocytes. Proc Natl Acad Sci U S A. 1990 Mar;87(5):1725-9.
320. Kelly GL, Long HM, Stylianou J, Thomas WA, Leese A, Bell AI, et al. An Epstein-Barr virus anti-apoptotic protein constitutively expressed in transformed cells and implicated in burkitt lymphomagenesis: the Wp/BHRF1 link. PLoS Pathog. 2009 Mar;5(3):e1000341.
321. Hurley EA, Thorley-Lawson DA. B cell activation and the establishment of Epstein-Barr virus latency. J Exp Med. 1988 Dec 1;168(6):2059-75.
322. Sugden B, Phelps M, Domoradzki J. Epstein-Barr virus DNA is amplified in transformed lymphocytes. J Virol. 1979 Sep;31(3):590-5.
323. Alfieri C, Birkenbach M, Kieff E. Early events in Epstein-Barr virus infection of human B lymphocytes. Virology. 1991 Apr;181(2):595-608.
324. Allday MJ, Crawford DH, Griffin BE. Epstein-Barr virus latent gene expression during the initiation of B cell immortalization. J Gen Virol. 1989 Jul;70 (Pt 7):1755-64.
325. Shannon-Lowe C, Adland E, Bell AI, Delecluse HJ, Rickinson AB, Rowe M. Features distinguishing Epstein-Barr virus infections of epithelial cells and B cells: viral genome expression, genome maintenance, and genome amplification. J Virol. 2009 Aug;83(15):7749-60.
326. Shannon-Lowe C, Baldwin G, Feederle R, Bell A, Rickinson A, Delecluse HJ. Epstein-Barr virus-induced B-cell transformation: quantitating events from virus binding to cell outgrowth. J Gen Virol. 2005 Nov;86(Pt 11):3009-19.
327. Woisetschlaeger M, Strominger JL, Speck SH. Mutually exclusive use of viral promoters in Epstein-Barr virus latently infected lymphocytes. Proc Natl Acad Sci U S A. 1989 Sep;86(17):6498-502.
328. Tierney RJ, Kao KY, Nagra JK, Rickinson AB. Epstein-Barr virus BamHI W repeat number limits EBNA2/EBNA-LP coexpression in newly infected B cells and the efficiency of B-cell transformation: a rationale for the multiple W repeats in wild-type virus strains. J Virol. 2011 Dec;85(23):12362-75.
329. Puglielli MT, Woisetschlaeger M, Speck SH. oriP is essential for EBNA gene promoter activity in Epstein-Barr virus-immortalized lymphoblastoid cell lines. J Virol. 1996 Sep;70(9):5758-68.
330. Schlager S, Speck SH, Woisetschlager M. Transcription of the Epstein-Barr virus nuclear antigen 1 (EBNA1) gene occurs before induction of the BCR2 (Cp) EBNA gene promoter during the initial stages of infection in B cells. J Virol. 1996 Jun;70(6):3561-70.

331. Woisetschlaeger M, Jin XW, Yandava CN, Furmanski LA, Strominger JL, Speck SH. Role for the Epstein-Barr virus nuclear antigen 2 in viral promoter switching during initial stages of infection. Proc Natl Acad Sci U S A. 1991 May 1;88(9):3942-6.
332. Puglielli MT, Desai N, Speck SH. Regulation of EBNA gene transcription in lymphoblastoid cell lines: characterization of sequences downstream of BCR2 (Cp). J Virol. 1997 Jan;71(1):120-8.
333. Pope JH, Horne MK, Scott W. Transformation of foetal human keukocytes in vitro by filtrates of a human leukaemic cell line containing herpes-like virus. Int J Cancer. 1968 Nov 15;3(6):857-66.
334. Lindhout E, Lakeman A, Mevissen ML, de Groot C. Functionally active Epstein-Barr virus-transformed follicular dendritic cell-like cell lines. J Exp Med. 1994 Apr 1;179(4):1173-84.
335. Palmero I, Holder A, Sinclair AJ, Dickson C, Peters G. Cyclins D1 and D2 are differentially expressed in human B-lymphoid cell lines. Oncogene. 1993 Apr;8(4):1049-54.
336. Hollyoake M, Stuhler A, Farrell P, Gordon J, Sinclair A. The normal cell cycle activation program is exploited during the infection of quiescent B lymphocytes by Epstein-Barr virus. Cancer Res. 1995 Nov 1;55(21):4784-7.
337. Cannell EJ, Farrell PJ, Sinclair AJ. Epstein-Barr virus exploits the normal cell pathway to regulate Rb activity during the immortalisation of primary B-cells. Oncogene. 1996 Oct 3;13(7):1413-21.
338. Thorley-Lawson DA. Epstein-Barr virus: exploiting the immune system. Nat Rev Immunol. 2001 Oct;1(1):75-82.
339. Baumann MA, Paul CC. Interleukin-5 is an autocrine growth factor for Epstein-Barr virus-transformed B lymphocytes. Blood. 1992 Apr 1;79(7):1763-7.
340. Tosato G, Tanner J, Jones KD, Revel M, Pike SE. Identification of interleukin-6 as an autocrine growth factor for Epstein-Barr virus-immortalized B cells. J Virol. 1990 Jun;64(6):3033-41.
341. Burdin N, Peronne C, Banchereau J, Rousset F. Epstein-Barr virus transformation induces B lymphocytes to produce human interleukin 10. J Exp Med. 1993 Feb 1;177(2):295-304.
342. Nakagomi H, Dolcetti R, Bejarano MT, Pisa P, Kiessling R, Masucci MG. The Epstein-Barr virus latent membrane protein-1 (LMP1) induces interleukin-10 production in Burkitt lymphoma lines. Int J Cancer. 1994 Apr 15;57(2):240-4.
343. Wang F, Gregory CD, Rowe M, Rickinson AB, Wang D, Birkenbach M, et al. Epstein-Barr virus nuclear antigen 2 specifically induces expression of the B-cell activation antigen CD23. Proc Natl Acad Sci U S A. 1987 May;84(10):3452-6.
344. Calender A, Billaud M, Aubry JP, Banchereau J, Vuillaume M, Lenoir GM. Epstein-Barr virus (EBV) induces expression of B-cell activation markers on in vitro infection of EBV-negative B-lymphoma cells. Proc Natl Acad Sci U S A. 1987 Nov;84(22):8060-4.
345. Wade M, Allday MJ. Epstein-Barr virus suppresses a G(2)/M checkpoint activated by genotoxins. Mol Cell Biol. 2000 Feb;20(4):1344-60.
346. Birkenbach M, Josefsen K, Yalamanchili R, Lenoir G, Kieff E. Epstein-Barr virus-induced genes: first lymphocyte-specific G protein-coupled peptide receptors. J Virol. 1993 Apr;67(4):2209-20.
347. Burgstahler R, Kempkes B, Steube K, Lipp M. Expression of the chemokine receptor BLR2/EBI1 is specifically transactivated by Epstein-Barr virus nuclear antigen 2. Biochem Biophys Res Commun. 1995 Oct 13;215(2):737-43.
348. Gibbons DL, Rowe M, Cope AP, Feldmann M, Brennan FM. Lymphotoxin acts as an autocrine growth factor for Epstein-Barr virus-transformed B cells and differentiated Burkitt lymphoma cell lines. Eur J Immunol. 1994 Aug;24(8):1879-85.
349. Mosialos G, Hanissian SH, Jawahar S, Vara L, Kieff E, Chatila TA. A Ca2+/calmodulin-dependent protein kinase, CaM kinase-Gr, expressed after transformation of primary human B lymphocytes by Epstein-Barr virus (EBV) is induced by the EBV oncogene LMP1. J Virol. 1994 Mar;68(3):1697-705.

350. Kaye KM, Izumi KM, Kieff E. Epstein-Barr virus latent membrane protein 1 is essential for B-lymphocyte growth transformation. Proc Natl Acad Sci U S A. 1993 Oct 1;90(19):9150-4.
351. Tomkinson B, Robertson E, Kieff E. Epstein-Barr virus nuclear proteins EBNA-3A and EBNA-3C are essential for B-lymphocyte growth transformation. J Virol. 1993 Apr;67(4):2014-25.
352. Mannick JB, Cohen JI, Birkenbach M, Marchini A, Kieff E. The Epstein-Barr virus nuclear protein encoded by the leader of the EBNA RNAs is important in B-lymphocyte transformation. J Virol. 1991 Dec;65(12):6826-37.
353. Hertle ML, Popp C, Petermann S, Maier S, Kremmer E, Lang R, et al. Differential gene expression patterns of EBV infected EBNA-3A positive and negative human B lymphocytes. PLoS Pathog. 2009 Jul;5(7):e1000506.
354. Humme S, Reisbach G, Feederle R, Delecluse HJ, Bousset K, Hammerschmidt W, et al. The EBV nuclear antigen 1 (EBNA1) enhances B cell immortalization several thousandfold. Proc Natl Acad Sci U S A. 2003 Sep 16;100(19):10989-94.
355. Counter CM, Avilion AA, LeFeuvre CE, Stewart NG, Greider CW, Harley CB, et al. Telomere shortening associated with chromosome instability is arrested in immortal cells which express telomerase activity. EMBO J. 1992 May;11(5):1921-9.
356. Counter CM, Botelho FM, Wang P, Harley CB, Bacchetti S. Stabilization of short telomeres and telomerase activity accompany immortalization of Epstein-Barr virus-transformed human B lymphocytes. J Virol. 1994 May;68(5):3410-4.
357. Sugimoto M, Furuichi Y, Ide T, Goto M. Incorrect us of "immortalization" for B-lymphoblastoid cell lines transformed by Epstein-Barr virus. J Virol. 1999 Nov;73(11):9690-1.
358. Sugimoto M, Ide T, Goto M, Furuichi Y. Reconsideration of senescence, immortalization and telomere maintenance of Epstein-Barr virus-transformed human B-lymphoblastoid cell lines. Mech Ageing Dev. 1999 Feb 1;107(1):51-60.
359. Tahara H, Tokutake Y, Maeda S, Kataoka H, Watanabe T, Satoh M, et al. Abnormal telomere dynamics of B-lymphoblastoid cell strains from Werner's syndrome patients transformed by Epstein-Barr virus. Oncogene. 1997 Oct 16;15(16):1911-20.
360. Kataoka H, Tahara H, Watanabe T, Sugawara M, Ide T, Goto M, et al. Immortalization of immunologically committed Epstein-Barr virus-transformed human B-lymphoblastoid cell lines accompanied by a strong telomerase activity. Differentiation. 1997 Dec;62(4):203-11.
361. Okubo M, Tsurukubo Y, Higaki T, Kawabe T, Goto M, Murase T, et al. Clonal chromosomal aberrations accompanied by strong telomerase activity in immortalization of human B-lymphoblastoid cell lines transformed by Epstein-Barr virus. Cancer Genet Cytogenet. 2001 Aug;129(1):30-4.
362. Takahashi T, Kawabe T, Okazaki Y, Itoh C, Noda K, Tajima M, et al. In vitro establishment of tumorigenic human B-lymphoblastoid cell lines transformed by Epstein-Barr virus. DNA Cell Biol. 2003 Nov;22(11):727-35.
363. Okada M, Goto M, Furuichi Y, Sugimoto M. Differential effects of cytotoxic drugs on mortal and immortalized B-lymphoblastoid cell lines from normal and Werner's syndrome patients. Biol Pharm Bull. 1998 Mar;21(3):235-9.
364. Joncas J, Boucher J, Granger-Julien M, Filion C. Epstein-Barr virus infection in the neonatal period and in childhood. Can Med Assoc J. 1974 Jan 5;110(1):33-7.
365. Hoagland RJ. The transmission of infectious mononucleosis. Am J Med Sci. 1955 Mar;229(3):262-72.
366. Karajannis MA, Hummel M, Anagnostopoulos I, Stein H. Strict lymphotropism of Epstein-Barr virus during acute infectious mononucleosis in nonimmunocompromised individuals. Blood. 1997 Apr 15;89(8):2856-62.
367. Tao Q, Srivastava G, Chan AC, Chung LP, Loke SL, Ho FC. Evidence for lytic infection by Epstein-Barr virus in mucosal lymphocytes instead of nasopharyngeal epithelial cells in normal individuals. J Med Virol. 1995 Jan;45(1):71-7.

368. Shannon-Lowe C, Rowe M. Epstein-Barr virus infection of polarized epithelial cells via the basolateral surface by memory B cell-mediated transfer infection. PLoS Pathog. 2011 May;7(5):e1001338.
369. Hadinoto V, Shapiro M, Sun CC, Thorley-Lawson DA. The dynamics of EBV shedding implicate a central role for epithelial cells in amplifying viral output. PLoS Pathog. 2009 Jul;5(7):e1000496.
370. Pegtel DM, Middeldorp J, Thorley-Lawson DA. Epstein-Barr virus infection in ex vivo tonsil epithelial cell cultures of asymptomatic carriers. J Virol. 2004 Nov;78(22):12613-24.
371. Tugizov SM, Berline JW, Palefsky JM. Epstein-Barr virus infection of polarized tongue and nasopharyngeal epithelial cells. Nat Med. 2003 Mar;9(3):307-14.
372. Callan MF, Annels N, Steven N, Tan L, Wilson J, McMichael AJ, et al. T cell selection during the evolution of CD8+ T cell memory in vivo. Eur J Immunol. 1998 Dec;28(12):4382-90.
373. Sheldon PJ, Hemsted EH, Papamichail M, Holborow EJ. Thymic origin of atypical lymphoid cells in infectious mononucleosis. Lancet. 1973 May 26;1(7813):1153-5.
374. Miller G, Niederman JC, Andrews LL. Prolonged oropharyngeal excretion of Epstein-Barr virus after infectious mononucleosis. N Engl J Med. 1973 Feb 1;288(5):229-32.
375. Nilsson K, Klein G, Henle W, Henle G. The establishment of lymphoblastoid lines from adult and fetal human lymphoid tissue and its dependence on EBV. Int J Cancer. 1971 Nov 15;8(3):443-50.
376. Babcock GJ, Decker LL, Volk M, Thorley-Lawson DA. EBV persistence in memory B cells in vivo. Immunity. 1998 Sep;9(3):395-404.
377. Thorley-Lawson DA, Gross A. Persistence of the Epstein-Barr virus and the origins of associated lymphomas. N Engl J Med. 2004 Mar 25;350(13):1328-37.
378. Young LS, Rickinson AB. Epstein-Barr virus: 40 years on. Nat Rev Cancer. 2004 Oct;4(10):757-68.
379. Kurth J, Spieker T, Wustrow J, Strickler GJ, Hansmann LM, Rajewsky K, et al. EBV-infected B cells in infectious mononucleosis: viral strategies for spreading in the B cell compartment and establishing latency. Immunity. 2000 Oct;13(4):485-95.
380. Babcock GJ, Hochberg D, Thorley-Lawson AD. The expression pattern of Epstein-Barr virus latent genes in vivo is dependent upon the differentiation stage of the infected B cell. Immunity. 2000 Oct;13(4):497-506.
381. Gires O, Zimber-Strobl U, Gonnella R, Ueffing M, Marschall G, Zeidler R, et al. Latent membrane protein 1 of Epstein-Barr virus mimics a constitutively active receptor molecule. EMBO J. 1997 Oct 15;16(20):6131-40.
382. Mosialos G, Birkenbach M, Yalamanchili R, VanArsdale T, Ware C, Kieff E. The Epstein-Barr virus transforming protein LMP1 engages signaling proteins for the tumor necrosis factor receptor family. Cell. 1995 Feb 10;80(3):389-99.
383. Caldwell RG, Wilson JB, Anderson SJ, Longnecker R. Epstein-Barr virus LMP2A drives B cell development and survival in the absence of normal B cell receptor signals. Immunity. 1998 Sep;9(3):405-11.
384. Longnecker R, Druker B, Roberts TM, Kieff E. An Epstein-Barr virus protein associated with cell growth transformation interacts with a tyrosine kinase. J Virol. 1991 Jul;65(7):3681-92.
385. Yates J, Warren N, Reisman D, Sugden B. A cis-acting element from the Epstein-Barr viral genome that permits stable replication of recombinant plasmids in latently infected cells. Proc Natl Acad Sci U S A. 1984 Jun;81(12):3806-10.
386. Kurth J, Hansmann ML, Rajewsky K, Kuppers R. Epstein-Barr virus-infected B cells expanding in germinal centers of infectious mononucleosis patients do not participate in the germinal center reaction. Proc Natl Acad Sci U S A. 2003 Apr 15;100(8):4730-5.

387. Chaganti S, Ma CS, Bell AI, Croom-Carter D, Hislop AD, Tangye SG, et al. Epstein-Barr virus persistence in the absence of conventional memory B cells: IgM+IgD+CD27+ B cells harbor the virus in X-linked lymphoproliferative disease patients. Blood. 2008 Aug 1;112(3):672-9.
388. Chaganti S, Heath EM, Bergler W, Kuo M, Buettner M, Niedobitek G, et al. Epstein-Barr virus colonization of tonsillar and peripheral blood B-cell subsets in primary infection and persistence. Blood. 2009 Jun 18;113(25):6372-81.
389. Scheeren FA, Nagasawa M, Weijer K, Cupedo T, Kirberg J, Legrand N, et al. T cell-independent development and induction of somatic hypermutation in human IgM+ IgD+ CD27+ B cells. J Exp Med. 2008 Sep 1;205(9):2033-42.
390. Tangye SG, Good KL. Human IgM+CD27+ B cells: memory B cells or "memory" B cells? J Immunol. 2007 Jul 1;179(1):13-9.
391. Weller S, Reynaud CA, Weill JC. Splenic marginal zone B cells in humans: where do they mutate their Ig receptor? Eur J Immunol. 2005 Oct;35(10):2789-92.
392. Niedobitek G, Kremmer E, Herbst H, Whitehead L, Dawson CW, Niedobitek E, et al. Immunohistochemical detection of the Epstein-Barr virus-encoded latent membrane protein 2A in Hodgkin's disease and infectious mononucleosis. Blood. 1997 Aug 15;90(4):1664-72.
393. Laichalk LL, Thorley-Lawson DA. Terminal differentiation into plasma cells initiates the replicative cycle of Epstein-Barr virus in vivo. J Virol. 2005 Jan;79(2):1296-307.
394. Niedobitek G, Agathanggelou A, Herbst H, Whitehead L, Wright DH, Young LS. Epstein-Barr virus (EBV) infection in infectious mononucleosis: virus latency, replication and phenotype of EBV-infected cells. J Pathol. 1997 Jun;182(2):151-9.
395. Brandtzaeg P, Baekkevold ES, Farstad IN, Jahnsen FL, Johansen FE, Nilsen EM, et al. Regional specialization in the mucosal immune system: what happens in the microcompartments? Immunol Today. 1999 Mar;20(3):141-51.
396. Brandtzaeg P, Farstad IN, Haraldsen G. Regional specialization in the mucosal immune system: primed cells do not always home along the same track. Immunol Today. 1999 Jun;20(6):267-77.
397. Golden HD, Chang RS, Prescott W, Simpson E, Cooper TY. Leukocyte-transforming agent: prolonged excretion by patients with mononucleosis and excretion by normal individuals. J Infect Dis. 1973 Apr;127(4):471-3.
398. Countryman J, Miller G. Activation of expression of latent Epstein-Barr herpesvirus after gene transfer with a small cloned subfragment of heterogeneous viral DNA. Proc Natl Acad Sci U S A. 1985 Jun;82(12):4085-9.
399. Takada K, Shimizu N, Sakuma S, Ono Y. trans activation of the latent Epstein-Barr virus (EBV) genome after transfection of the EBV DNA fragment. J Virol. 1986 Mar;57(3):1016-22.
400. Adamson AL, Darr D, Holley-Guthrie E, Johnson RA, Mauser A, Swenson J, et al. Epstein-Barr virus immediate-early proteins BZLF1 and BRLF1 activate the ATF2 transcription factor by increasing the levels of phosphorylated p38 and c-Jun N-terminal kinases. J Virol. 2000 Feb;74(3):1224-33.
401. Flemington EK, Goldfeld AE, Speck SH. Efficient transcription of the Epstein-Barr virus immediate-early BZLF1 and BRLF1 genes requires protein synthesis. J Virol. 1991 Dec;65(12):7073-7.
402. Liu P, Speck SH. Synergistic autoactivation of the Epstein-Barr virus immediate-early BRLF1 promoter by Rta and Zta. Virology. 2003 Jun 5;310(2):199-206.
403. Ragoczy T, Miller G. Autostimulation of the Epstein-Barr virus BRLF1 promoter is mediated through consensus Sp1 and Sp3 binding sites. J Virol. 2001 Jun;75(11):5240-51.
404. Sinclair AJ, Brimmell M, Shanahan F, Farrell PJ. Pathways of activation of the Epstein-Barr virus productive cycle. J Virol. 1991 May;65(5):2237-44.
405. Farrell PJ, Rowe DT, Rooney CM, Kouzarides T. Epstein-Barr virus BZLF1 trans-activator specifically binds to a consensus AP-1 site and is related to c-fos. EMBO J. 1989 Jan;8(1):127-32.

406. Chang YN, Dong DL, Hayward GS, Hayward SD. The Epstein-Barr virus Zta transactivator: a member of the bZIP family with unique DNA-binding specificity and a dimerization domain that lacks the characteristic heptad leucine zipper motif. J Virol. 1990 Jul;64(7):3358-69.
407. Packham G, Economou A, Rooney CM, Rowe DT, Farrell PJ. Structure and function of the Epstein-Barr virus BZLF1 protein. J Virol. 1990 May;64(5):2110-6.
408. Cho MS, Tran VM. A concatenated form of Epstein-Barr viral DNA in lymphoblastoid cell lines induced by transfection with BZLF1. Virology. 1993 Jun;194(2):838-42.
409. Lu CC, Jeng YY, Tsai CH, Liu MY, Yeh SW, Hsu TY, et al. Genome-wide transcription program and expression of the Rta responsive gene of Epstein-Barr virus. Virology. 2006 Feb 20;345(2):358-72.
410. Yuan J, Cahir-McFarland E, Zhao B, Kieff E. Virus and cell RNAs expressed during Epstein-Barr virus replication. J Virol. 2006 Mar;80(5):2548-65.
411. Angel P, Imagawa M, Chiu R, Stein B, Imbra RJ, Rahmsdorf HJ, et al. Phorbol ester-inducible genes contain a common cis element recognized by a TPA-modulated trans-acting factor. Cell. 1987 Jun 19;49(6):729-39.
412. Davies AH, Grand RJ, Evans FJ, Rickinson AB. Induction of Epstein-Barr virus lytic cycle by tumor-promoting and non-tumor-promoting phorbol esters requires active protein kinase C. J Virol. 1991 Dec;65(12):6838-44.
413. Flemington E, Speck SH. Identification of phorbol ester response elements in the promoter of Epstein-Barr virus putative lytic switch gene BZLF1. J Virol. 1990 Mar;64(3):1217-26.
414. Takada K. Cross-linking of cell surface immunoglobulins induces Epstein-Barr virus in Burkitt lymphoma lines. Int J Cancer. 1984 Jan 15;33(1):27-32.
415. Takada K, Ono Y. Synchronous and sequential activation of latently infected Epstein-Barr virus genomes. J Virol. 1989 Jan;63(1):445-9.
416. Wen W, Iwakiri D, Yamamoto K, Maruo S, Kanda T, Takada K. Epstein-Barr virus BZLF1 gene, a switch from latency to lytic infection, is expressed as an immediate-early gene after primary infection of B lymphocytes. J Virol. 2007 Jan;81(2):1037-42.
417. Bergbauer M, Kalla M, Schmeinck A, Gobel C, Rothbauer U, Eck S, et al. CpG-methylation regulates a class of Epstein-Barr virus promoters. PLoS Pathog. 2010;6(9):e1001114.
418. Kalla M, Schmeinck A, Bergbauer M, Pich D, Hammerschmidt W. AP-1 homolog BZLF1 of Epstein-Barr virus has two essential functions dependent on the epigenetic state of the viral genome. Proc Natl Acad Sci U S A. 2010 Jan 12;107(2):850-5.
419. Gerber P, Lucas S, Nonoyama M, Perlin E, Goldstein LI. Oral excretion of Epstein-Barr virus by healthy subjects and patients with infectious mononucleosis. Lancet. 1972 Nov 11;2(7785):988-9.
420. Hsu DH, de Waal Malefyt R, Fiorentino DF, Dang MN, Vieira P, de Vries J, et al. Expression of interleukin-10 activity by Epstein-Barr virus protein BCRF1. Science. 1990 Nov 9;250(4982):830-2.
421. Ding Y, Qin L, Kotenko SV, Pestka S, Bromberg JS. A single amino acid determines the immunostimulatory activity of interleukin 10. J Exp Med. 2000 Jan 17;191(2):213-24.
422. Ryon JJ, Hayward SD, MacMahon EM, Mann RB, Ling Y, Charache P, et al. In situ detection of lytic Epstein-Barr virus infection: expression of the NotI early gene and viral interleukin-10 late gene in clinical specimens. J Infect Dis. 1993 Aug;168(2):345-51.
423. Stuart AD, Stewart JP, Arrand JR, Mackett M. The Epstein-Barr virus encoded cytokine viral interleukin-10 enhances transformation of human B lymphocytes. Oncogene. 1995 Nov 2;11(9):1711-9.
424. Vieira P, de Waal-Malefyt R, Dang MN, Johnson KE, Kastelein R, Fiorentino DF, et al. Isolation and expression of human cytokine synthesis inhibitory factor cDNA clones: homology to Epstein-Barr virus open reading frame BCRFI. Proc Natl Acad Sci U S A. 1991 Feb 15;88(4):1172-6.
425. de Waal Malefyt R, Haanen J, Spits H, Roncarolo MG, te Velde A, Figdor C, et al. Interleukin 10 (IL-10) and viral IL-10 strongly reduce antigen-specific human T cell proliferation by diminishing

the antigen-presenting capacity of monocytes via downregulation of class II major histocompatibility complex expression. J Exp Med. 1991 Oct 1;174(4):915-24.
426. Fiorentino DF, Zlotnik A, Vieira P, Mosmann TR, Howard M, Moore KW, et al. IL-10 acts on the antigen-presenting cell to inhibit cytokine production by Th1 cells. J Immunol. 1991 May 15;146(10):3444-51.
427. Moore KW, O'Garra A, de Waal Malefyt R, Vieira P, Mosmann TR. Interleukin-10. Annu Rev Immunol. 1993;11:165-90.
428. Qin L, Ding Y, Tahara H, Bromberg JS. Viral IL-10-induced immunosuppression requires Th2 cytokines and impairs APC function within the allograft. J Immunol. 2001 Feb 15;166(4):2385-93.
429. Hislop AD, Ressing ME, van Leeuwen D, Pudney VA, Horst D, Koppers-Lalic D, et al. A CD8+ T cell immune evasion protein specific to Epstein-Barr virus and its close relatives in Old World primates. J Exp Med. 2007 Aug 6;204(8):1863-73.
430. Keating S, Prince S, Jones M, Rowe M. The lytic cycle of Epstein-Barr virus is associated with decreased expression of cell surface major histocompatibility complex class I and class II molecules. J Virol. 2002 Aug;76(16):8179-88.
431. Ressing ME, Horst D, Griffin BD, Tellam J, Zuo J, Khanna R, et al. Epstein-Barr virus evasion of CD8(+) and CD4(+) T cell immunity via concerted actions of multiple gene products. Semin Cancer Biol. 2008 Dec;18(6):397-408.
432. Hsu WL, Chung PJ, Tsai MH, Chang CL, Liang CL. A role for Epstein-Barr viral BALF1 in facilitating tumor formation and metastasis potential. Virus Res. 2012 Feb;163(2):617-27.
433. Nalesnik MA. Clinical and pathological features of post-transplant lymphoproliferative disorders (PTLD). Springer Semin Immunopathol. 1998;20(3-4):325-42.
434. Brunstein CG, Weisdorf DJ, DeFor T, Barker JN, Tolar J, van Burik JA, et al. Marked increased risk of Epstein-Barr virus-related complications with the addition of antithymocyte globulin to a nonmyeloablative conditioning prior to unrelated umbilical cord blood transplantation. Blood. 2006 Oct 15;108(8):2874-80.
435. Barker JN, Martin PL, Coad JE, DeFor T, Trigg ME, Kurtzberg J, et al. Low incidence of Epstein-Barr virus-associated posttransplantation lymphoproliferative disorders in 272 unrelated-donor umbilical cord blood transplant recipients. Biol Blood Marrow Transplant. 2001;7(7):395-9.
436. Curtis RE, Travis LB, Rowlings PA, Socie G, Kingma DW, Banks PM, et al. Risk of lymphoproliferative disorders after bone marrow transplantation: a multi-institutional study. Blood. 1999 Oct 1;94(7):2208-16.
437. Nalesnik MA, Makowka L, Starzl TE. The diagnosis and treatment of posttransplant lymphoproliferative disorders. Curr Probl Surg. 1988 Jun;25(6):367-472.
438. Ho M, Miller G, Atchison RW, Breinig MK, Dummer JS, Andiman W, et al. Epstein-Barr virus infections and DNA hybridization studies in posttransplantation lymphoma and lymphoproliferative lesions: the role of primary infection. J Infect Dis. 1985 Nov;152(5):876-86.
439. Savoie A, Perpete C, Carpentier L, Joncas J, Alfieri C. Direct correlation between the load of Epstein-Barr virus-infected lymphocytes in the peripheral blood of pediatric transplant patients and risk of lymphoproliferative disease. Blood. 1994 May 1;83(9):2715-22.
440. Brauninger A, Spieker T, Mottok A, Baur AS, Kuppers R, Hansmann ML. Epstein-Barr virus (EBV)-positive lymphoproliferations in post-transplant patients show immunoglobulin V gene mutation patterns suggesting interference of EBV with normal B cell differentiation processes. Eur J Immunol. 2003 Jun;33(6):1593-602.
441. Liebowitz D. Epstein-Barr virus and a cellular signaling pathway in lymphomas from immunosuppressed patients. N Engl J Med. 1998 May 14;338(20):1413-21.
442. Thomas JA, Hotchin NA, Allday MJ, Amlot P, Rose M, Yacoub M, et al. Immunohistology of Epstein-Barr virus-associated antigens in B cell disorders from immunocompromised individuals. Transplantation. 1990 May;49(5):944-53.

443. Young L, Alfieri C, Hennessy K, Evans H, O'Hara C, Anderson KC, et al. Expression of Epstein-Barr virus transformation-associated genes in tissues of patients with EBV lymphoproliferative disease. N Engl J Med. 1989 Oct 19;321(16):1080-5.
444. Perera SM, Thomas JA, Burke M, Crawford DH. Analysis of the T-cell micro-environment in Epstein-Barr virus-related post-transplantation B lymphoproliferative disease. J Pathol. 1998 Feb;184(2):177-84.
445. Shapiro RS, McClain K, Frizzera G, Gajl-Peczalska KJ, Kersey JH, Blazar BR, et al. Epstein-Barr virus associated B cell lymphoproliferative disorders following bone marrow transplantation. Blood. 1988 May;71(5):1234-43.
446. Paya CV, Fung JJ, Nalesnik MA, Kieff E, Green M, Gores G, et al. Epstein-Barr virus-induced posttransplant lymphoproliferative disorders. ASTS/ASTP EBV-PTLD Task Force and The Mayo Clinic Organized International Consensus Development Meeting. Transplantation. 1999 Nov 27;68(10):1517-25.
447. Starzl TE, Nalesnik MA, Porter KA, Ho M, Iwatsuki S, Griffith BP, et al. Reversibility of lymphomas and lymphoproliferative lesions developing under cyclosporin-steroid therapy. Lancet. 1984 Mar 17;1(8377):583-7.
448. Khatri VP, Baiocchi RA, Peng R, Oberkircher AR, Dolce JM, Ward PM, et al. Endogenous CD8+ T cell expansion during regression of monoclonal EBV-associated posttransplant lymphoproliferative disorder. J Immunol. 1999 Jul 1;163(1):500-6.
449. Beral V, Peterman T, Berkelman R, Jaffe H. AIDS-associated non-Hodgkin lymphoma. Lancet. 1991 Apr 6;337(8745):805-9.
450. Gaidano G, Carbone A, Dalla-Favera R. Pathogenesis of AIDS-related lymphomas: molecular and histogenetic heterogeneity. Am J Pathol. 1998 Mar;152(3):623-30.
451. MacMahon EM, Glass JD, Hayward SD, Mann RB, Becker PS, Charache P, et al. Epstein-Barr virus in AIDS-related primary central nervous system lymphoma. Lancet. 1991 Oct 19;338(8773):969-73.
452. Delecluse HJ, Hummel M, Marafioti T, Anagnostopoulos I, Stein H. Common and HIV-related diffuse large B-cell lymphomas differ in their immunoglobulin gene mutation pattern. J Pathol. 1999 Jun;188(2):133-8.
453. Hamilton-Dutoit SJ, Rea D, Raphael M, Sandvej K, Delecluse HJ, Gisselbrecht C, et al. Epstein-Barr virus-latent gene expression and tumor cell phenotype in acquired immunodeficiency syndrome-related non-Hodgkin's lymphoma. Correlation of lymphoma phenotype with three distinct patterns of viral latency. Am J Pathol. 1993 Oct;143(4):1072-85.
454. Hamilton-Dutoit SJ, Pallesen G, Franzmann MB, Karkov J, Black F, Skinhoj P, et al. AIDS-related lymphoma. Histopathology, immunophenotype, and association with Epstein-Barr virus as demonstrated by in situ nucleic acid hybridization. Am J Pathol. 1991 Jan;138(1):149-63.
455. Kersten MJ, Klein MR, Holwerda AM, Miedema F, van Oers MH. Epstein-Barr virus-specific cytotoxic T cell responses in HIV-1 infection: different kinetics in patients progressing to opportunistic infection or non-Hodgkin's lymphoma. J Clin Invest. 1997 Apr 1;99(7):1525-33.
456. Kuppers R. The biology of Hodgkin's lymphoma. Nat Rev Cancer. 2009 Jan;9(1):15-27.
457. Harris NL, Jaffe ES, Stein H, Banks PM, Chan JK, Cleary ML, et al. A revised European-American classification of lymphoid neoplasms: a proposal from the International Lymphoma Study Group. Blood. 1994 Sep 1;84(5):1361-92.
458. Glaser SL, Lin RJ, Stewart SL, Ambinder RF, Jarrett RF, Brousset P, et al. Epstein-Barr virus-associated Hodgkin's disease: epidemiologic characteristics in international data. Int J Cancer. 1997 Feb 7;70(4):375-82.
459. Glaser SL, Jarrett RF. The epidemiology of Hodgkin's disease. Baillieres Clin Haematol. 1996 Sep;9(3):401-16.
460. MacMahon B. Epidemiology of Hodgkin's disease. Cancer Res. 1966 Jun;26(6):1189-201.

461. Anagnostopoulos I, Herbst H, Niedobitek G, Stein H. Demonstration of monoclonal EBV genomes in Hodgkin's disease and Ki-1-positive anaplastic large cell lymphoma by combined Southern blot and in situ hybridization. Blood. 1989 Aug 1;74(2):810-6.
462. Weiss LM, Movahed LA, Warnke RA, Sklar J. Detection of Epstein-Barr viral genomes in Reed-Sternberg cells of Hodgkin's disease. N Engl J Med. 1989 Feb 23;320(8):502-6.
463. Weiss LM, Strickler JG, Warnke RA, Purtilo DT, Sklar J. Epstein-Barr viral DNA in tissues of Hodgkin's disease. Am J Pathol. 1987 Oct;129(1):86-91.
464. Boiocchi M, Dolcetti R, De Re V, Gloghini A, Carbone A. Demonstration of a unique Epstein-Barr virus-positive cellular clone in metachronous multiple localizations of Hodgkin's disease. Am J Pathol. 1993 Jan;142(1):33-8.
465. Grasser FA, Murray PG, Kremmer E, Klein K, Remberger K, Feiden W, et al. Monoclonal antibodies directed against the Epstein-Barr virus-encoded nuclear antigen 1 (EBNA1): immunohistologic detection of EBNA1 in the malignant cells of Hodgkin's disease. Blood. 1994 Dec 1;84(11):3792-8.
466. Herbst H, Dallenbach F, Hummel M, Niedobitek G, Pileri S, Muller-Lantzsch N, et al. Epstein-Barr virus latent membrane protein expression in Hodgkin and Reed-Sternberg cells. Proc Natl Acad Sci U S A. 1991 Jun 1;88(11):4766-70.
467. Pallesen G, Hamilton-Dutoit SJ, Rowe M, Young LS. Expression of Epstein-Barr virus latent gene products in tumour cells of Hodgkin's disease. Lancet. 1991 Feb 9;337(8737):320-2.
468. Deacon EM, Pallesen G, Niedobitek G, Crocker J, Brooks L, Rickinson AB, et al. Epstein-Barr virus and Hodgkin's disease: transcriptional analysis of virus latency in the malignant cells. J Exp Med. 1993 Feb 1;177(2):339-49.
469. Braeuninger A, Kuppers R, Strickler JG, Wacker HH, Rajewsky K, Hansmann ML. Hodgkin and Reed-Sternberg cells in lymphocyte predominant Hodgkin disease represent clonal populations of germinal center-derived tumor B cells. Proc Natl Acad Sci U S A. 1997 Aug 19;94(17):9337-42.
470. Kanzler H, Kuppers R, Hansmann ML, Rajewsky K. Hodgkin and Reed-Sternberg cells in Hodgkin's disease represent the outgrowth of a dominant tumor clone derived from (crippled) germinal center B cells. J Exp Med. 1996 Oct 1;184(4):1495-505.
471. Kuppers R, Rajewsky K. The origin of Hodgkin and Reed/Sternberg cells in Hodgkin's disease. Annu Rev Immunol. 1998;16:471-93.
472. Kuppers R, Rajewsky K, Zhao M, Simons G, Laumann R, Fischer R, et al. Hodgkin disease: Hodgkin and Reed-Sternberg cells picked from histological sections show clonal immunoglobulin gene rearrangements and appear to be derived from B cells at various stages of development. Proc Natl Acad Sci U S A. 1994 Nov 8;91(23):10962-6.
473. Rickinson AB, Kieff E. Epstein-Barr virus. In: Knipe DM, Howley PM, editors. Fields Virology. 5th ed. Philadelphia: Lippincott, Williams & Wilkins; 2007. p. 2655-700.
474. Booth K, Burkitt DP, Bassett DJ, Cooke RA, Biddulph J. Burkitt lymphoma in Papua, New Guinea. Br J Cancer. 1967 Dec;21(4):657-64.
475. Levine PH, Kamaraju LS, Connelly RR, Berard CW, Dorfman RF, Magrath I, et al. The American Burkitt's Lymphoma Registry: eight years' experience. Cancer. 1982 Mar 1;49(5):1016-22.
476. Philip T, Lenoir GM, Bryon PA, Gerard-Marchant R, Souillet G, Philippe N, et al. Burkitt-type lymphoma in France among non-Hodgkin malignant lymphomas in Caucasian children. Br J Cancer. 1982 May;45(5):670-8.
477. Magrath I. The pathogenesis of Burkitt's lymphoma. Adv Cancer Res. 1990;55:133-270.
478. Carbone A. Emerging pathways in the development of AIDS-related lymphomas. Lancet Oncol. 2003 Jan;4(1):22-9.
479. Carbone A, Gaidano G, Gloghini A, Larocca LM, Capello D, Canzonieri V, et al. Differential expression of BCL-6, CD138/syndecan-1, and Epstein-Barr virus-encoded latent membrane protein-

1 identifies distinct histogenetic subsets of acquired immunodeficiency syndrome-related non-Hodgkin's lymphomas. Blood. 1998 Feb 1;91(3):747-55.
480. Klein G. Dysregulation of lymphocyte proliferation by chromosomal translocations and sequential genetic changes. Bioessays. 2000 May;22(5):414-22.
481. Leder P. Translocations among antibody genes in human cancer. IARC Sci Publ. 1985(60):341-57.
482. Goossens T, Klein U, Kuppers R. Frequent occurrence of deletions and duplications during somatic hypermutation: implications for oncogene translocations and heavy chain disease. Proc Natl Acad Sci U S A. 1998 Mar 3;95(5):2463-8.
483. Bellan C, Lazzi S, Hummel M, Palummo N, de Santi M, Amato T, et al. Immunoglobulin gene analysis reveals 2 distinct cells of origin for EBV-positive and EBV-negative Burkitt lymphomas. Blood. 2005 Aug 1;106(3):1031-6.
484. Dang CV, O'Donnell KA, Zeller KI, Nguyen T, Osthus RC, Li F. The c-Myc target gene network. Semin Cancer Biol. 2006 Aug;16(4):253-64.
485. Barna M, Pusic A, Zollo O, Costa M, Kondrashov N, Rego E, et al. Suppression of Myc oncogenic activity by ribosomal protein haploinsufficiency. Nature. 2008 Dec 18;456(7224):971-5.
486. Gil J, Peters G. Regulation of the INK4b-ARF-INK4a tumour suppressor locus: all for one or one for all. Nat Rev Mol Cell Biol. 2006 Sep;7(9):667-77.
487. Hoffman B, Liebermann DA. Apoptotic signaling by c-MYC. Oncogene. 2008 Oct 27;27(50):6462-72.
488. Nilsson JA, Cleveland JL. Myc pathways provoking cell suicide and cancer. Oncogene. 2003 Dec 8;22(56):9007-21.
489. Schuhmacher M, Staege MS, Pajic A, Polack A, Weidle UH, Bornkamm GW, et al. Control of cell growth by c-Myc in the absence of cell division. Curr Biol. 1999 Nov 4;9(21):1255-8.
490. Askew DS, Ashmun RA, Simmons BC, Cleveland JL. Constitutive c-myc expression in an IL-3-dependent myeloid cell line suppresses cell cycle arrest and accelerates apoptosis. Oncogene. 1991 Oct;6(10):1915-22.
491. Evan GI, Wyllie AH, Gilbert CS, Littlewood TD, Land H, Brooks M, et al. Induction of apoptosis in fibroblasts by c-myc protein. Cell. 1992 Apr 3;69(1):119-28.
492. Neri A, Barriga F, Inghirami G, Knowles DM, Neequaye J, Magrath IT, et al. Epstein-Barr virus infection precedes clonal expansion in Burkitt's and acquired immunodeficiency syndrome-associated lymphoma. Blood. 1991 Mar 1;77(5):1092-5.
493. Kieff E, Rickinson AB. Epstein-Barr virus and its replication. Fields Virology. Philadelphia: Lippincott-Raven; 2007. p. 2511.
494. Schaefer BC, Strominger JL, Speck SH. Redefining the Epstein-Barr virus-encoded nuclear antigen EBNA-1 gene promoter and transcription initiation site in group I Burkitt lymphoma cell lines. Proc Natl Acad Sci U S A. 1995 Nov 7;92(23):10565-9.
495. Nonkwelo C, Skinner J, Bell A, Rickinson A, Sample J. Transcription start sites downstream of the Epstein-Barr virus (EBV) Fp promoter in early-passage Burkitt lymphoma cells define a fourth promoter for expression of the EBV EBNA-1 protein. J Virol. 1996 Jan;70(1):623-7.
496. Robertson KD, Manns A, Swinnen LJ, Zong JC, Gulley ML, Ambinder RF. CpG methylation of the major Epstein-Barr virus latency promoter in Burkitt's lymphoma and Hodgkin's disease. Blood. 1996 Oct 15;88(8):3129-36.
497. Sample J, Brooks L, Sample C, Young L, Rowe M, Gregory C, et al. Restricted Epstein-Barr virus protein expression in Burkitt lymphoma is due to a different Epstein-Barr nuclear antigen 1 transcriptional initiation site. Proc Natl Acad Sci U S A. 1991 Jul 15;88(14):6343-7.
498. Schaefer BC, Woisetschlaeger M, Strominger JL, Speck SH. Exclusive expression of Epstein-Barr virus nuclear antigen 1 in Burkitt lymphoma arises from a third promoter, distinct from the promoters used in latently infected lymphocytes. Proc Natl Acad Sci U S A. 1991 Aug 1;88(15):6550-4.

499. Kieff E, Rickinson A. Epstein-Barr Virus and Its Replication. In: DM K, PM H, editors. Fields Virology. 5th ed ed. Philadelphia: Lippincott Williams and Wilkins; 2007.
500. Komano J, Sugiura M, Takada K. Epstein-Barr virus contributes to the malignant phenotype and to apoptosis resistance in Burkitt's lymphoma cell line Akata. J Virol. 1998 Nov;72(11):9150-6.
501. Holowaty MN, Zeghouf M, Wu H, Tellam J, Athanasopoulos V, Greenblatt J, et al. Protein profiling with Epstein-Barr nuclear antigen-1 reveals an interaction with the herpesvirus-associated ubiquitin-specific protease HAUSP/USP7. J Biol Chem. 2003 Aug 8;278(32):29987-94.
502. Bhatia KG, Gutierrez MI, Huppi K, Siwarski D, Magrath IT. The pattern of p53 mutations in Burkitt's lymphoma differs from that of solid tumors. Cancer Res. 1992 Aug 1;52(15):4273-6.
503. Farrell PJ, Allan GJ, Shanahan F, Vousden KH, Crook T. p53 is frequently mutated in Burkitt's lymphoma cell lines. EMBO J. 1991 Oct;10(10):2879-87.
504. Komano J, Maruo S, Kurozumi K, Oda T, Takada K. Oncogenic role of Epstein-Barr virus-encoded RNAs in Burkitt's lymphoma cell line Akata. J Virol. 1999 Dec;73(12):9827-31.
505. Nanbo A, Yoshiyama H, Takada K. Epstein-Barr virus-encoded poly(A)- RNA confers resistance to apoptosis mediated through Fas by blocking the PKR pathway in human epithelial intestine 407 cells. J Virol. 2005 Oct;79(19):12280-5.
506. Ruf IK, Rhyne PW, Yang C, Cleveland JL, Sample JT. Epstein-Barr virus small RNAs potentiate tumorigenicity of Burkitt lymphoma cells independently of an effect on apoptosis. J Virol. 2000 Nov;74(21):10223-8.
507. Wong HL, Wang X, Chang RC, Jin DY, Feng H, Wang Q, et al. Stable expression of EBERs in immortalized nasopharyngeal epithelial cells confers resistance to apoptotic stress. Mol Carcinog. 2005 Oct;44(2):92-101.
508. Yamamoto N, Takizawa T, Iwanaga Y, Shimizu N. Malignant transformation of B lymphoma cell line BJAB by Epstein-Barr virus-encoded small RNAs. FEBS Lett. 2000 Nov 3;484(2):153-8.
509. Kelly G, Bell A, Rickinson A. Epstein-Barr virus-associated Burkitt lymphomagenesis selects for downregulation of the nuclear antigen EBNA2. Nat Med. 2002 Oct;8(10):1098-104.
510. Kelly GL, Milner AE, Tierney RJ, Croom-Carter DS, Altmann M, Hammerschmidt W, et al. Epstein-Barr virus nuclear antigen 2 (EBNA2) gene deletion is consistently linked with EBNA3A, -3B, and -3C expression in Burkitt's lymphoma cells and with increased resistance to apoptosis. J Virol. 2005 Aug;79(16):10709-17.
511. Anderton E, Yee J, Smith P, Crook T, White RE, Allday MJ. Two Epstein-Barr virus (EBV) oncoproteins cooperate to repress expression of the proapoptotic tumour-suppressor Bim: clues to the pathogenesis of Burkitt's lymphoma. Oncogene. 2008 Jan 17;27(4):421-33.
512. Garibal J, Hollville E, Bell AI, Kelly GL, Renouf B, Kawaguchi Y, et al. Truncated form of the Epstein-Barr virus protein EBNA-LP protects against caspase-dependent apoptosis by inhibiting protein phosphatase 2A. J Virol. 2007 Jul;81(14):7598-607.
513. Altmann M, Hammerschmidt W. Epstein-Barr virus provides a new paradigm: a requirement for the immediate inhibition of apoptosis. PLoS Biol. 2005 Dec;3(12):e404.
514. Paschos K, Smith P, Anderton E, Middeldorp JM, White RE, Allday MJ. Epstein-barr virus latency in B cells leads to epigenetic repression and CpG methylation of the tumour suppressor gene Bim. PLoS Pathog. 2009 Jun;5(6):e1000492.
515. Speck SH, Strominger JL. Analysis of the transcript encoding the latent Epstein-Barr virus nuclear antigen I: a potentially polycistronic message generated by long-range splicing of several exons. Proc Natl Acad Sci U S A. 1985 Dec;82(24):8305-9.
516. Schaefer BC, Strominger JL, Speck SH. Redefining the Epstein-Barr virus-encoded nuclear antigen EBNA-1 gene promoter and transcription initiation site in group I Burkitt lymphoma cell lines. Proc Natl Acad Sci U S A. 1995 Nov 7;92(23):10565-9.
517. Nonkwelo C, Skinner J, Bell A, Rickinson A, Sample J. Transcription start sites downstream of the Epstein-Barr virus (EBV) Fp promoter in early-passage Burkitt lymphoma cells define a fourth promoter for expression of the EBV EBNA-1 protein. J Virol. 1996 Jan;70(1):623-7.

518. Schaefer BC, Strominger JL, Speck SH. The Epstein-Barr virus BamHI F promoter is an early lytic promoter: lack of correlation with EBNA 1 gene transcription in group 1 Burkitt's lymphoma cell lines. J Virol. 1995 Aug;69(8):5039-47.

519. Tsai CN, Liu ST, Chang YS. Identification of a novel promoter located within the Bam HI Q region of the Epstein-Barr virus genome for the EBNA 1 gene. DNA Cell Biol. 1995 Sep;14(9):767-76.

520. Reisman D, Sugden B. trans activation of an Epstein-Barr viral transcriptional enhancer by the Epstein-Barr viral nuclear antigen 1. Mol Cell Biol. 1986 Nov;6(11):3838-46.

521. Rawlins DR, Milman G, Hayward SD, Hayward GS. Sequence-specific DNA binding of the Epstein-Barr virus nuclear antigen (EBNA-1) to clustered sites in the plasmid maintenance region. Cell. 1985 Oct;42(3):859-68.

522. Jones CH, Hayward SD, Rawlins DR. Interaction of the lymphocyte-derived Epstein-Barr virus nuclear antigen EBNA-1 with its DNA-binding sites. J Virol. 1989 Jan;63(1):101-10.

523. Ambinder RF, Shah WA, Rawlins DR, Hayward GS, Hayward SD. Definition of the sequence requirements for binding of the EBNA-1 protein to its palindromic target sites in Epstein-Barr virus DNA. J Virol. 1990 May;64(5):2369-79.

524. Ambinder RF, Mullen MA, Chang YN, Hayward GS, Hayward SD. Functional domains of Epstein-Barr virus nuclear antigen EBNA-1. J Virol. 1991 Mar;65(3):1466-78.

525. Yates JL, Camiolo SM, Bashaw JM. The minimal replicator of Epstein-Barr virus oriP. J Virol. 2000 May;74(10):4512-22.

526. Gahn TA, Schildkraut CL. The Epstein-Barr virus origin of plasmid replication, oriP, contains both the initiation and termination sites of DNA replication. Cell. 1989 Aug 11;58(3):527-35.

527. Wysokenski DA, Yates JL. Multiple EBNA1-binding sites are required to form an EBNA1-dependent enhancer and to activate a minimal replicative origin within oriP of Epstein-Barr virus. J Virol. 1989 Jun;63(6):2657-66.

528. Aiyar A, Tyree C, Sugden B. The plasmid replicon of EBV consists of multiple cis-acting elements that facilitate DNA synthesis by the cell and a viral maintenance element. EMBO J. 1998 Nov 2;17(21):6394-403.

529. Simpson K, McGuigan A, Huxley C. Stable episomal maintenance of yeast artificial chromosomes in human cells. Mol Cell Biol. 1996 Sep;16(9):5117-26.

530. Ohno S, Luka J, Lindahl T, Klein G. Identification of a purified complement-fixing antigen as the Epstein-Barr-virus determined nuclear antigen (EBNA) by its binding to metaphase chromosomes. Proc Natl Acad Sci U S A. 1977 Apr;74(4):1605-9.

531. Kapoor P, Lavoie BD, Frappier L. EBP2 plays a key role in Epstein-Barr virus mitotic segregation and is regulated by aurora family kinases. Mol Cell Biol. 2005 Jun;25(12):4934-45.

532. Shire K, Ceccarelli DF, Avolio-Hunter TM, Frappier L. EBP2, a human protein that interacts with sequences of the Epstein-Barr virus nuclear antigen 1 important for plasmid maintenance. J Virol. 1999 Apr;73(4):2587-95.

533. Wu H, Kapoor P, Frappier L. Separation of the DNA replication, segregation, and transcriptional activation functions of Epstein-Barr nuclear antigen 1. J Virol. 2002 Mar;76(5):2480-90.

534. Sears J, Ujihara M, Wong S, Ott C, Middeldorp J, Aiyar A. The amino terminus of Epstein-Barr Virus (EBV) nuclear antigen 1 contains AT hooks that facilitate the replication and partitioning of latent EBV genomes by tethering them to cellular chromosomes. J Virol. 2004 Nov;78(21):11487-505.

535. Norio P, Schildkraut CL, Yates JL. Initiation of DNA replication within oriP is dispensable for stable replication of the latent Epstein-Barr virus chromosome after infection of established cell lines. J Virol. 2000 Sep;74(18):8563-74.

536. Gahn TA, Sugden B. An EBNA-1-dependent enhancer acts from a distance of 10 kilobase pairs to increase expression of the Epstein-Barr virus LMP gene. J Virol. 1995 Apr;69(4):2633-6.

537. Davenport MG, Pagano JS. Expression of EBNA-1 mRNA is regulated by cell cycle during Epstein-Barr virus type I latency. J Virol. 1999 Apr;73(4):3154-61.
538. Sung NS, Wilson J, Davenport M, Sista ND, Pagano JS. Reciprocal regulation of the Epstein-Barr virus BamHI-F promoter by EBNA-1 and an E2F transcription factor. Mol Cell Biol. 1994 Nov;14(11):7144-52.
539. Canaan A, Haviv I, Urban AE, Schulz VP, Hartman S, Zhang Z, et al. EBNA1 regulates cellular gene expression by binding cellular promoters. Proc Natl Acad Sci U S A. 2009 Dec 29;106(52):22421-6.
540. O'Neil JD, Owen TJ, Wood VH, Date KL, Valentine R, Chukwuma MB, et al. Epstein-Barr virus-encoded EBNA1 modulates the AP-1 transcription factor pathway in nasopharyngeal carcinoma cells and enhances angiogenesis in vitro. J Gen Virol. 2008 Nov;89(Pt 11):2833-42.
541. Yin Y, Manoury B, Fahraeus R. Self-inhibition of synthesis and antigen presentation by Epstein-Barr virus-encoded EBNA1. Science. 2003 Sep 5;301(5638):1371-4.
542. Tellam J, Smith C, Rist M, Webb N, Cooper L, Vuocolo T, et al. Regulation of protein translation through mRNA structure influences MHC class I loading and T cell recognition. Proc Natl Acad Sci U S A. 2008 Jul 8;105(27):9319-24.
543. Kennedy G, Komano J, Sugden B. Epstein-Barr virus provides a survival factor to Burkitt's lymphomas. Proc Natl Acad Sci U S A. 2003 Nov 25;100(24):14269-74.
544. Cohen JI, Wang F, Mannick J, Kieff E. Epstein-Barr virus nuclear protein 2 is a key determinant of lymphocyte transformation. Proc Natl Acad Sci U S A. 1989 Dec;86(23):9558-62.
545. Hammerschmidt W, Sugden B. Genetic analysis of immortalizing functions of Epstein-Barr virus in human B lymphocytes. Nature. 1989 Aug 3;340(6232):393-7.
546. Miller G, Robinson J, Heston L, Lipman M. Differences between laboratory strains of Epstein-Barr virus based on immortalization, abortive infection, and interference. Proc Natl Acad Sci U S A. 1974 Oct;71(10):4006-10.
547. Rickinson AB, Gregory CD, Young LS. Viruses and cancer risks: outgrowth of Epstein-Barr virus-positive Burkitt's lymphoma in the immune host. Med Oncol Tumor Pharmacother. 1987;4(3-4):177-86.
548. Tomkinson B, Kieff E. Second-site homologous recombination in Epstein-Barr virus: insertion of type 1 EBNA 3 genes in place of type 2 has no effect on in vitro infection. J Virol. 1992 Feb;66(2):780-9.
549. Cancian L, Bosshard R, Lucchesi W, Karstegl CE, Farrell PJ. C-terminal region of EBNA-2 determines the superior transforming ability of type 1 Epstein-Barr virus by enhanced gene regulation of LMP-1 and CXCR7. PLoS Pathog. 2011 Jul;7(7):e1002164.
550. Harada S, Yalamanchili R, Kieff E. Epstein-Barr virus nuclear protein 2 has at least two N-terminal domains that mediate self-association. J Virol. 2001;75(5):2482-7.
551. Yalamanchili R, Harada S, Kieff E. The N-terminal half of EBNA2, except for seven prolines, is not essential for primary B-lymphocyte growth transformation. J Virol. 1996 Apr;70(4):2468-73.
552. Cohen JI, Wang F, Kieff E. Epstein-Barr virus nuclear protein 2 mutations define essential domains for transformation and transactivation. J Virol. 1991 May;65(5):2545-54.
553. Grossman SR, Johannsen E, Tong X, Yalamanchili R, Kieff E. The Epstein-Barr virus nuclear antigen 2 transactivator is directed to response elements by the J kappa recombination signal binding protein. Proc Natl Acad Sci U S A. 1994 Aug 2;91(16):7568-72.
554. Henkel T, Ling PD, Hayward SD, Peterson MG. Mediation of Epstein-Barr virus EBNA2 transactivation by recombination signal-binding protein J kappa. Science. 1994 Jul 1;265(5168):92-5.
555. Zimber-Strobl U, Strobl LJ, Meitinger C, Hinrichs R, Sakai T, Furukawa T, et al. Epstein-Barr virus nuclear antigen 2 exerts its transactivating function through interaction with recombination signal binding protein RBP-J kappa, the homologue of Drosophila Suppressor of Hairless. EMBO J. 1994 Oct 17;13(20):4973-82.

556. Cohen JI, Kieff E. An Epstein-Barr virus nuclear protein 2 domain essential for transformation is a direct transcriptional activator. J Virol. 1991;65(11):5880-5.
557. Tsui S, Schubach WH. Epstein-Barr virus nuclear protein 2A forms oligomers in vitro and in vivo through a region required for B-cell transformation. J Virol. 1994 Jul;68(7):4287-94.
558. Yalamanchili R, Tong X, Grossman S, Johannsen E, Mosialos G, Kieff E. Genetic and biochemical evidence that EBNA 2 interaction with a 63-kDa cellular GTG-binding protein is essential for B lymphocyte growth transformation by EBV. Virology. 1994 Nov 1;204(2):634-41.
559. Waltzer L, Logeat F, Brou C, Israel A, Sergeant A, Manet E. The human J kappa recombination signal sequence binding protein (RBP-J kappa) targets the Epstein-Barr virus EBNA2 protein to its DNA responsive elements. EMBO J. 1994 Dec 1;13(23):5633-8.
560. Furukawa T, Maruyama S, Kawaichi M, Honjo T. The Drosophila homolog of the immunoglobulin recombination signal-binding protein regulates peripheral nervous system development. Cell. 1992 Jun 26;69(7):1191-7.
561. Schweisguth F, Posakony JW. Suppressor of Hairless, the Drosophila homolog of the mouse recombination signal-binding protein gene, controls sensory organ cell fates. Cell. 1992 Jun 26;69(7):1199-212.
562. Seto ES, Bellen HJ, Lloyd TE. When cell biology meets development: endocytic regulation of signaling pathways. Genes Dev. 2002 Jun 1;16(11):1314-36.
563. Lai EC. Keeping a good pathway down: transcriptional repression of Notch pathway target genes by CSL proteins. EMBO Rep. 2002 Sep;3(9):840-5.
564. Kidd S, Lieber T, Young MW. Ligand-induced cleavage and regulation of nuclear entry of Notch in Drosophila melanogaster embryos. Genes Dev. 1998 Dec 1;12(23):3728-40.
565. Schroeter EH, Kisslinger JA, Kopan R. Notch-1 signalling requires ligand-induced proteolytic release of intracellular domain. Nature. 1998 May 28;393(6683):382-6.
566. Hsieh JJ, Hayward SD. Masking of the CBF1/RBPJ kappa transcriptional repression domain by Epstein-Barr virus EBNA2. Science. 1995 Apr 28;268(5210):560-3.
567. Jarriault S, Brou C, Logeat F, Schroeter EH, Kopan R, Israel A. Signalling downstream of activated mammalian Notch. Nature. 1995 Sep 28;377(6547):355-8.
568. Sakai T, Taniguchi Y, Tamura K, Minoguchi S, Fukuhara T, Strobl LJ, et al. Functional replacement of the intracellular region of the Notch1 receptor by Epstein-Barr virus nuclear antigen 2. J Virol. 1998 Jul;72(7):6034-9.
569. Hsieh JJ, Henkel T, Salmon P, Robey E, Peterson MG, Hayward SD. Truncated mammalian Notch1 activates CBF1/RBPJk-repressed genes by a mechanism resembling that of Epstein-Barr virus EBNA2. Mol Cell Biol. 1996 Mar;16(3):952-9.
570. Hofelmayr H, Strobl LJ, Marschall G, Bornkamm GW, Zimber-Strobl U. Activated Notch1 can transiently substitute for EBNA2 in the maintenance of proliferation of LMP1-expressing immortalized B cells. J Virol. 2001 Mar;75(5):2033-40.
571. Cohen JI. A region of herpes simplex virus VP16 can substitute for a transforming domain of Epstein-Barr virus nuclear protein 2. Proc Natl Acad Sci U S A. 1992;89(17):8030-4.
572. Tong X, Drapkin R, Yalamanchili R, Mosialos G, Kieff E. The Epstein-Barr virus nuclear protein 2 acidic domain forms a complex with a novel cellular coactivator that can interact with TFIIE. Mol Cell Biol. 1995 Sep;15(9):4735-44.
573. Tong X, Drapkin R, Reinberg D, Kieff E. The 62- and 80-kDa subunits of transcription factor IIH mediate the interaction with Epstein-Barr virus nuclear protein 2. Proc Natl Acad Sci U S A. 1995 Apr 11;92(8):3259-63.
574. Tong X, Wang F, Thut CJ, Kieff E. The Epstein-Barr virus nuclear protein 2 acidic domain can interact with TFIIB, TAF40, and RPA70 but not with TATA-binding protein. J Virol. 1995 Jan;69(1):585-8.

575. Wang L, Grossman SR, Kieff E. Epstein-Barr virus nuclear protein 2 interacts with p300, CBP, and PCAF histone acetyltransferases in activation of the LMP1 promoter. Proc Natl Acad Sci U S A. 2000 Jan 4;97(1):430-5.
576. Wu DY, Kalpana GV, Goff SP, Schubach WH. Epstein-Barr virus nuclear protein 2 (EBNA2) binds to a component of the human SNF-SWI complex, hSNF5/Ini1. J Virol. 1996 Sep;70(9):6020-8.
577. Zimber-Strobl U, Kremmer E, Grasser F, Marschall G, Laux G, Bornkamm GW. The Epstein-Barr virus nuclear antigen 2 interacts with an EBNA2 responsive cis-element of the terminal protein 1 gene promoter. EMBO J. 1993 Jan;12(1):167-75.
578. Ling PD, Rawlins DR, Hayward SD. The Epstein-Barr virus immortalizing protein EBNA-2 is targeted to DNA by a cellular enhancer-binding protein. Proc Natl Acad Sci U S A. 1993 Oct 15;90(20):9237-41.
579. Laux G, Dugrillon F, Eckert C, Adam B, Zimber-Strobl U, Bornkamm GW. Identification and characterization of an Epstein-Barr virus nuclear antigen 2-responsive cis element in the bidirectional promoter region of latent membrane protein and terminal protein 2 genes. J Virol. 1994 Nov;68(11):6947-58.
580. Kaiser C, Laux G, Eick D, Jochner N, Bornkamm GW, Kempkes B. The proto-oncogene c-myc is a direct target gene of Epstein-Barr virus nuclear antigen 2. J Virol. 1999 May;73(5):4481-4.
581. Lee JM, Lee KH, Weidner M, Osborne BA, Hayward SD. Epstein-Barr virus EBNA2 blocks Nur77- mediated apoptosis. Proc Natl Acad Sci U S A. 2002;99(18):11878-83. Epub 2002 Aug 23.
582. Li H, Kolluri SK, Gu J, Dawson MI, Cao X, Hobbs PD, et al. Cytochrome c release and apoptosis induced by mitochondrial targeting of nuclear orphan receptor TR3. Science. 2000 Aug 18;289(5482):1159-64.
583. Philips A, Lesage S, Gingras R, Maira MH, Gauthier Y, Hugo P, et al. Novel dimeric Nur77 signaling mechanism in endocrine and lymphoid cells. Mol Cell Biol. 1997 Oct;17(10):5946-51.
584. Sculley TB, Walker PJ, Moss DJ, Pope JH. Identification of multiple Epstein-Barr virus-induced nuclear antigens with sera from patients with rheumatoid arthritis. J Virol. 1984 Oct;52(1):88-93.
585. Dillner J, Kallin B, Ehlin-Henriksson B, Rymo L, Henle W, Henle G, et al. The Epstein-Barr virus determined nuclear antigen is composed of at least three different antigens. Int J Cancer. 1986 Feb 15;37(2):195-200.
586. Kallin B, Dillner J, Ernberg I, Ehlin-Henriksson B, Rosen A, Henle W, et al. Four virally determined nuclear antigens are expressed in Epstein-Barr virus-transformed cells. Proc Natl Acad Sci U S A. 1986 Mar;83(5):1499-503.
587. Sculley DG, Sculley TB, Pope JH. Reactions of sera from patients with rheumatoid arthritis, systemic lupus erythematosus and infectious mononucleosis to Epstein-Barr virus-induced polypeptides. J Gen Virol. 1986 Oct;67 (Pt 10):2253-8.
588. Rowe DT, Farrell PJ, Miller G. Novel nuclear antigens recognized by human sera in lymphocytes latently infected by Epstein-Barr virus. Virology. 1987 Jan;156(1):153-62.
589. Kienzle N, Young DB, Liaskou D, Buck M, Greco S, Sculley TB. Intron retention may regulate expression of Epstein-Barr virus nuclear antigen 3 family genes. J Virol. 1999 Feb;73(2):1195-204.
590. Allday MJ, Crawford DH, Griffin BE. Prediction and demonstration of a novel Epstein-Barr virus nuclear antigen. Nucleic Acids Res. 1988 May 25;16(10):4353-67.
591. Joab I, Rowe DT, Bodescot M, Nicolas JC, Farrell PJ, Perricaudet M. Mapping of the gene coding for Epstein-Barr virus-determined nuclear antigen EBNA3 and its transient overexpression in a human cell line by using an adenovirus expression vector. J Virol. 1987 Oct;61(10):3340-4.
592. Kerdiles B, Walls D, Triki H, Perricaudet M, Joab I. cDNA cloning and transient expression of the Epstein-Barr virus-determined nuclear antigen EBNA3B in human cells and identification of novel transcripts from its coding region. J Virol. 1990 Apr;64(4):1812-6.

593. Le Roux A, Kerdiles B, Walls D, Dedieu JF, Perricaudet M. The Epstein-Barr virus determined nuclear antigens EBNA-3A, -3B, and -3C repress EBNA-2-mediated transactivation of the viral terminal protein 1 gene promoter. Virology. 1994 Dec;205(2):596-602.
594. Marshall D, Sample C. Epstein-Barr virus nuclear antigen 3C is a transcriptional regulator. J Virol. 1995 Jun;69(6):3624-30.
595. Robertson ES, Grossman S, Johannsen E, Miller C, Lin J, Tomkinson B, et al. Epstein-Barr virus nuclear protein 3C modulates transcription through interaction with the sequence-specific DNA-binding protein J kappa. J Virol. 1995 May;69(5):3108-16.
596. Zhao B, Marshall DR, Sample CE. A conserved domain of the Epstein-Barr virus nuclear antigens 3A and 3C binds to a discrete domain of Jkappa. J Virol. 1996 Jul;70(7):4228-36.
597. Cooper A, Johannsen E, Maruo S, Cahir-McFarland E, Illanes D, Davidson D, et al. EBNA3A association with RBP-Jkappa down-regulates c-myc and Epstein-Barr virus-transformed lymphoblast growth. J Virol. 2003 Jan;77(2):999-1010.
598. Radkov SA, Bain M, Farrell PJ, West M, Rowe M, Allday MJ. Epstein-Barr virus EBNA3C represses Cp, the major promoter for EBNA expression, but has no effect on the promoter of the cell gene CD21. J Virol. 1997 Nov;71(11):8552-62.
599. Cludts I, Farrell PJ. Multiple functions within the Epstein-Barr virus EBNA-3A protein. J Virol. 1998 Mar;72(3):1862-9.
600. Zhao B, Sample CE. Epstein-barr virus nuclear antigen 3C activates the latent membrane protein 1 promoter in the presence of Epstein-Barr virus nuclear antigen 2 through sequences encompassing an spi-1/Spi-B binding site. J Virol. 2000 Jun;74(11):5151-60.
601. Johannsen E, Koh E, Mosialos G, Tong X, Kieff E, Grossman SR. Epstein-Barr virus nuclear protein 2 transactivation of the latent membrane protein 1 promoter is mediated by J kappa and PU.1. J Virol. 1995 Jan;69(1):253-62.
602. Kashuba E, Kashuba V, Pokrovskaja K, Klein G, Szekely L. Epstein-Barr virus encoded nuclear protein EBNA-3 binds XAP-2, a protein associated with Hepatitis B virus X antigen. Oncogene. 2000 Mar 30;19(14):1801-6.
603. Kashuba EV, Gradin K, Isaguliants M, Szekely L, Poellinger L, Klein G, et al. Regulation of transactivation function of the aryl hydrocarbon receptor by the Epstein-Barr virus-encoded EBNA-3 protein. J Biol Chem. 2006 Jan 13;281(2):1215-23.
604. Maruo S, Wu Y, Ishikawa S, Kanda T, Iwakiri D, Takada K. Epstein-Barr virus nuclear protein EBNA3C is required for cell cycle progression and growth maintenance of lymphoblastoid cells. Proc Natl Acad Sci U S A. 2006 Dec 19;103(51):19500-5.
605. Maruo S, Johannsen E, Illanes D, Cooper A, Kieff E. Epstein-Barr Virus nuclear protein EBNA3A is critical for maintaining lymphoblastoid cell line growth. J Virol. 2003 Oct;77(19):10437-47.
606. Krauer KG, Burgess A, Buck M, Flanagan J, Sculley TB, Gabrielli B. The EBNA-3 gene family proteins disrupt the G2/M checkpoint. Oncogene. 2004 Feb 19;23(7):1342-53.
607. Snopok B, Yurchenko M, Szekely L, Klein G, Kashuba E. SPR-based immunocapture approach to creating an interfacial sensing architecture: Mapping of the MRS18-2 binding site on retinoblastoma protein. Anal Bioanal Chem. 2006 Dec;386(7-8):2063-73.
608. Kashuba E, Yurchenko M, Yenamandra SP, Snopok B, Isaguliants M, Szekely L, et al. EBV-encoded EBNA-6 binds and targets MRS18-2 to the nucleus, resulting in the disruption of pRb-E2F1 complexes. Proc Natl Acad Sci U S A. 2008 Apr 8;105(14):5489-94.
609. Bajaj BG, Murakami M, Cai Q, Verma SC, Lan K, Robertson ES. Epstein-Barr virus nuclear antigen 3C interacts with and enhances the stability of the c-Myc oncoprotein. J Virol. 2008 Apr;82(8):4082-90.
610. Silins SL, Sculley TB. Burkitt's lymphoma cells are resistant to programmed cell death in the presence of the Epstein-Barr virus latent antigen EBNA-4. Int J Cancer. 1995 Jan 3;60(1):65-72.

611. McClellan MJ, Khasnis S, Wood CD, Palermo RD, Schlick SN, Kanhere AS, et al. Downregulation of integrin receptor-signaling genes by Epstein-Barr virus EBNA 3C via promoter-proximal and -distal binding elements. J Virol. 2012 May;86(9):5165-78.

612. White RE, Groves IJ, Turro E, Yee J, Kremmer E, Allday MJ. Extensive co-operation between the Epstein-Barr virus EBNA3 proteins in the manipulation of host gene expression and epigenetic chromatin modification. PLoS One. 2010;5(11):e13979.

613. Bodescot M, Chambraud B, Farrell P, Perricaudet M. Spliced RNA from the IR1-U2 region of Epstein-Barr virus: presence of an open reading frame for a repetitive polypeptide. EMBO J. 1984 Aug;3(8):1913-7.

614. Wang F, Petti L, Braun D, Seung S, Kieff E. A bicistronic Epstein-Barr virus mRNA encodes two nuclear proteins in latently infected, growth-transformed lymphocytes. J Virol. 1987 Apr;61(4):945-54.

615. Rowe DT. Epstein-Barr virus immortalization and latency. Front Biosci. 1999 Mar 15;4:D346-71.

616. Finke J, Rowe M, Kallin B, Ernberg I, Rosen A, Dillner J, et al. Monoclonal and polyclonal antibodies against Epstein-Barr virus nuclear antigen 5 (EBNA-5) detect multiple protein species in Burkitt's lymphoma and lymphoblastoid cell lines. J Virol. 1987 Dec;61(12):3870-8.

617. Rogers RP, Woisetschlaeger M, Speck SH. Alternative splicing dictates translational start in Epstein-Barr virus transcripts. EMBO J. 1990 Jul;9(7):2273-7.

618. Nitsche F, Bell A, Rickinson A. Epstein-Barr virus leader protein enhances EBNA-2-mediated transactivation of latent membrane protein 1 expression: a role for the W1W2 repeat domain. J Virol. 1997 Sep;71(9):6619-28.

619. Peng R, Tan J, Ling PD. Conserved regions in the Epstein-Barr virus leader protein define distinct domains required for nuclear localization and transcriptional cooperation with EBNA2. J Virol. 2000 Nov;74(21):9953-63.

620. Yokoyama A, Tanaka M, Matsuda G, Kato K, Kanamori M, Kawasaki H, et al. Identification of major phosphorylation sites of Epstein-Barr virus nuclear antigen leader protein (EBNA-LP): ability of EBNA-LP to induce latent membrane protein 1 cooperatively with EBNA-2 is regulated by phosphorylation. J Virol. 2001 Jun;75(11):5119-28.

621. Kitay MK, Rowe DT. Cell cycle stage-specific phosphorylation of the Epstein-Barr virus immortalization protein EBNA-LP. J Virol. 1996 Nov;70(11):7885-93.

622. Sinclair AJ, Palmero I, Peters G, Farrell PJ. EBNA-2 and EBNA-LP cooperate to cause G0 to G1 transition during immortalization of resting human B lymphocytes by Epstein-Barr virus. EMBO J. 1994 Jul 15;13(14):3321-8.

623. Kashuba E, Yurchenko M, Yenamandra SP, Snopok B, Szekely L, Bercovich B, et al. Epstein-Barr virus-encoded EBNA-5 forms trimolecular protein complexes with MDM2 and p53 and inhibits the transactivating function of p53. Int J Cancer. 2011 Feb 15;128(4):817-25.

624. Pokrovskaja K, Okan I, Kashuba E, Lowbeer M, Klein G, Szekely L. Epstein-Barr virus infection and mitogen stimulation of normal B cells induces wild-type p53 without subsequent growth arrest or apoptosis. J Gen Virol. 1999 Apr;80 (Pt 4):987-95.

625. Kelly G, Bell A, Rickinson A. Epstein-Barr virus-associated Burkitt lymphomagenesis selects for downregulation of the nuclear antigen EBNA2. Nat Med. 2002 Oct;8(10):1098-104.

626. Wang F, Tsang SF, Kurilla MG, Cohen JI, Kieff E. Epstein-Barr virus nuclear antigen 2 transactivates latent membrane protein LMP1. J Virol. 1990 Jul;64(7):3407-16.

627. Sadler RH, Raab-Traub N. The Epstein-Barr virus 3.5-kilobase latent membrane protein 1 mRNA initiates from a TATA-Less promoter within the first terminal repeat. J Virol. 1995;69(7):4577-81.

628. Fennewald S, van Santen V, Kieff E. Nucleotide sequence of an mRNA transcribed in latent growth- transforming virus infection indicates that it may encode a membrane protein. J Virol. 1984;51(2):411-9.

629. Coffin WF, 3rd, Erickson KD, Hoedt-Miller M, Martin JM. The cytoplasmic amino-terminus of the Latent Membrane Protein-1 of Epstein-Barr Virus: relationship between transmembrane orientation and effector functions of the carboxy-terminus and transmembrane domain. Oncogene. 2001 Aug 30;20(38):5313-30.
630. Uchida J, Yasui T, Takaoka-Shichijo Y, Muraoka M, Kulwichit W, Raab-Traub N, et al. Mimicry of CD40 signals by Epstein-Barr virus LMP1 in B lymphocyte responses. Science. 1999 Oct 8;286(5438):300-3.
631. Ardila-Osorio H, Clausse B, Mishal Z, Wiels J, Tursz T, Busson P. Evidence of LMP1-TRAF3 interactions in glycosphingolipid-rich complexes of lymphoblastoid and nasopharyngeal carcinoma cells. Int J Cancer. 1999;81(4):645-9.
632. Higuchi M, Izumi KM, Kieff E. Epstein-Barr virus latent-infection membrane proteins are palmitoylated and raft-associated: protein 1 binds to the cytoskeleton through TNF receptor cytoplasmic factors. Proc Natl Acad Sci U S A. 2001 Apr 10;98(8):4675-80.
633. Liebowitz D, Wang D, Kieff E. Orientation and patching of the latent infection membrane protein encoded by Epstein-Barr virus. J Virol. 1986 Apr;58(1):233-7.
634. Huen DS, Henderson SA, Croom-Carter D, Rowe M. The Epstein-Barr virus latent membrane protein-1 (LMP1) mediates activation of NF-kappa B and cell surface phenotype via two effector regions in its carboxy-terminal cytoplasmic domain. Oncogene. 1995 Feb 2;10(3):549-60.
635. Gires O, Kohlhuber F, Kilger E, Baumann M, Kieser A, Kaiser C, et al. Latent membrane protein 1 of Epstein-Barr virus interacts with JAK3 and activates STAT proteins. EMBO J. 1999 Jun 1;18(11):3064-73.
636. Kilger E, Kieser A, Baumann M, Hammerschmidt W. Epstein-Barr virus-mediated B-cell proliferation is dependent upon latent membrane protein 1, which simulates an activated CD40 receptor. EMBO J. 1998 Mar 16;17(6):1700-9.
637. Kondo S, Wakisaka N, Schell MJ, Horikawa T, Sheen TS, Sato H, et al. Epstein-Barr virus latent membrane protein 1 induces the matrix metalloproteinase-1 promoter via an Ets binding site formed by a single nucleotide polymorphism: enhanced susceptibility to nasopharyngeal carcinoma. Int J Cancer. 2005 Jun 20;115(3):368-76.
638. Yoshizaki T, Sato H, Furukawa M, Pagano JS. The expression of matrix metalloproteinase 9 is enhanced by Epstein-Barr virus latent membrane protein 1. Proc Natl Acad Sci U S A. 1998 Mar 31;95(7):3621-6.
639. Kim KR, Yoshizaki T, Miyamori H, Hasegawa K, Horikawa T, Furukawa M, et al. Transformation of Madin-Darby canine kidney (MDCK) epithelial cells by Epstein-Barr virus latent membrane protein 1 (LMP1) induces expression of Ets1 and invasive growth. Oncogene. 2000 Mar 30;19(14):1764-71.
640. Dawson CW, Rickinson AB, Young LS. Epstein-Barr virus latent membrane protein inhibits human epithelial cell differentiation. Nature. 1990 Apr 19;344(6268):777-80.
641. Wilson JB, Weinberg W, Johnson R, Yuspa S, Levine AJ. Expression of the BNLF-1 oncogene of Epstein-Barr virus in the skin of transgenic mice induces hyperplasia and aberrant expression of keratin 6. Cell. 1990 Jun 29;61(7):1315-27.
642. Eliopoulos AG, Young LS. LMP1 structure and signal transduction. Semin Cancer Biol. 2001 Dec;11(6):435-44.
643. Li HP, Chang YS. Epstein-Barr virus latent membrane protein 1: structure and functions. J Biomed Sci. 2003 Sep-Oct;10(5):490-504.
644. Song X, Tao YG, Zeng L, Deng XY, Lee LM, Gong JP, et al. Latent membrane protein 1 encoded by Epstein-Barr virus modulates directly and synchronously cyclin D1 and p16 by newly forming a c-Jun/Jun B heterodimer in nasopharyngeal carcinoma cell line. Virus Res. 2005 Nov;113(2):89-99.

645. Zhao XR, Gu HH, Weng XX, Yi W, Deng XY, Cao Y. The Primary Study on Expression and Function of D-Type Cyclins in Nasopharyngeal Carcinoma Cell Lines. Sheng Wu Hua Xue Yu Sheng Wu Wu Li Xue Bao (Shanghai). 2000;32(2):192-6.
646. Zhao XR, Deng L, Weng XX. [The effects of exogenous p16 expression on CDK4, Cyclin D1 and pRb in nasopharyngeal carcinoma cell lines]. Hunan Yi Ke Da Xue Xue Bao. 2000 Oct 28;25(5):428-30.
647. Ding L, Li L, Yang J, Zhou S, Li W, Tang M, et al. Latent membrane protein 1 encoded by Epstein-Barr virus induces telomerase activity via p16INK4A/Rb/E2F1 and JNK signaling pathways. J Med Virol. 2007 Aug;79(8):1153-63.
648. Ding L, Li LL, Yang J, Tao YG, Ye M, Shi Y, et al. Epstein-Barr virus encoded latent membrane protein 1 modulates nuclear translocation of telomerase reverse transcriptase protein by activating nuclear factor-kappaB p65 in human nasopharyngeal carcinoma cells. Int J Biochem Cell Biol. 2005 Sep;37(9):1881-9.
649. Horikawa I, Barrett JC. Transcriptional regulation of the telomerase hTERT gene as a target for cellular and viral oncogenic mechanisms. Carcinogenesis. 2003 Jul;24(7):1167-76.
650. Yang J, Deng X, Deng L, Gu H, Fan W, Cao Y. Telomerase activation by Epstein-Barr virus latent membrane protein 1 is associated with c-Myc expression in human nasopharyngeal epithelial cells. J Exp Clin Cancer Res. 2004 Sep;23(3):495-506.
651. Altieri DC. Validating survivin as a cancer therapeutic target. Nat Rev Cancer. 2003 Jan;3(1):46-54.
652. Dawson CW, Port RJ, Young LS. The role of the EBV-encoded latent membrane proteins LMP1 and LMP2 in the pathogenesis of nasopharyngeal carcinoma (NPC). Semin Cancer Biol. 2012 Apr;22(2):144-53.
653. Faqing T, Zhi H, Liqun Y, Min T, Huanhua G, Xiyun D, et al. Epstein-Barr virus LMP1 initiates cell proliferation and apoptosis inhibition via regulating expression of Survivin in nasopharyngeal carcinoma. Exp Oncol. 2005 Jun;27(2):96-101.
654. Hudson GS, Farrell PJ, Barrell BG. Two related but differentially expressed potential membrane proteins encoded by the EcoRI Dhet region of Epstein-Barr virus B95-8. J Virol. 1985 Feb;53(2):528-35.
655. Konishi K, Maruo S, Kato H, Takada K. Role of Epstein-Barr virus-encoded latent membrane protein 2A on virus-induced immortalization and virus activation. J Gen Virol. 2001 Jun;82(Pt 6):1451-6.
656. Laux G, Economou A, Farrell PJ. The terminal protein gene 2 of Epstein-Barr virus is transcribed from a bidirectional latent promoter region. J Gen Virol. 1989 Nov;70 (Pt 11):3079-84.
657. Laux G, Perricaudet M, Farrell PJ. A spliced Epstein-Barr virus gene expressed in immortalized lymphocytes is created by circularization of the linear viral genome. EMBO J. 1988 Mar;7(3):769-74.
658. Longnecker R, Miller CL, Miao XQ, Marchini A, Kieff E. The only domain which distinguishes Epstein-Barr virus latent membrane protein 2A (LMP2A) from LMP2B is dispensable for lymphocyte infection and growth transformation in vitro; LMP2A is therefore nonessential. J Virol. 1992 Nov;66(11):6461-9.
659. Longnecker R, Miller CL, Miao XQ, Tomkinson B, Kieff E. The last seven transmembrane and carboxy-terminal cytoplasmic domains of Epstein-Barr virus latent membrane protein 2 (LMP2) are dispensable for lymphocyte infection and growth transformation in vitro. J Virol. 1993 Apr;67(4):2006-13.
660. Longnecker R, Miller CL, Tomkinson B, Miao XQ, Kieff E. Deletion of DNA encoding the first five transmembrane domains of Epstein-Barr virus latent membrane proteins 2A and 2B. J Virol. 1993 Aug;67(8):5068-74.
661. Sample J, Liebowitz D, Kieff E. Two related Epstein-Barr virus membrane proteins are encoded by separate genes. J Virol. 1989 Feb;63(2):933-7.

662. Speck P, Kline KA, Cheresh P, Longnecker R. Epstein-Barr virus lacking latent membrane protein 2 immortalizes B cells with efficiency indistinguishable from that of wild-type virus. J Gen Virol. 1999 Aug;80 (Pt 8):2193-203.
663. Miller CL, Lee JH, Kieff E, Longnecker R. An integral membrane protein (LMP2) blocks reactivation of Epstein-Barr virus from latency following surface immunoglobulin crosslinking. Proc Natl Acad Sci U S A. 1994 Jan 18;91(2):772-6.
664. Miller CL, Longnecker R, Kieff E. Epstein-Barr virus latent membrane protein 2A blocks calcium mobilization in B lymphocytes. J Virol. 1993 Jun;67(6):3087-94.
665. Caldwell RG, Brown RC, Longnecker R. Epstein-Barr virus LMP2A-induced B-cell survival in two unique classes of EmuLMP2A transgenic mice. J Virol. 2000 Feb;74(3):1101-13.
666. Miller CL, Burkhardt AL, Lee JH, Stealey B, Longnecker R, Bolen JB, et al. Integral membrane protein 2 of Epstein-Barr virus regulates reactivation from latency through dominant negative effects on protein-tyrosine kinases. Immunity. 1995 Feb;2(2):155-66.
667. Miller CL, Lee JH, Kieff E, Burkhardt AL, Bolen JB, Longnecker R. Epstein-Barr virus protein LMP2A regulates reactivation from latency by negatively regulating tyrosine kinases involved in sIg-mediated signal transduction. Infect Agents Dis. 1994 Apr-Jun;3(2-3):128-36.
668. Longnecker R. Epstein-Barr virus latency: LMP2, a regulator or means for Epstein-Barr virus persistence? Adv Cancer Res. 2000;79:175-200.
669. Portis T, Longnecker R. Epstein-Barr virus (EBV) LMP2A mediates B-lymphocyte survival through constitutive activation of the Ras/PI3K/Akt pathway. Oncogene. 2004 Nov 11;23(53):8619-28.
670. Mancao C, Hammerschmidt W. Epstein-Barr virus latent membrane protein 2A is a B-cell receptor mimic and essential for B-cell survival. Blood. 2007 Nov 15;110(10):3715-21.
671. Portis T, Dyck P, Longnecker R. Epstein-Barr Virus (EBV) LMP2A induces alterations in gene transcription similar to those observed in Reed-Sternberg cells of Hodgkin lymphoma. Blood. 2003 Dec 1;102(12):4166-78.
672. Hino R, Uozaki H, Inoue Y, Shintani Y, Ushiku T, Sakatani T, et al. Survival advantage of EBV-associated gastric carcinoma: survivin up-regulation by viral latent membrane protein 2A. Cancer Res. 2008 Mar 1;68(5):1427-35.
673. Swanson-Mungerson M, Bultema R, Longnecker R. Epstein-Barr virus LMP2A imposes sensitivity to apoptosis. J Gen Virol. 2010 Sep;91(Pt 9):2197-202.
674. Bultema R, Longnecker R, Swanson-Mungerson M. Epstein-Barr virus LMP2A accelerates MYC-induced lymphomagenesis. Oncogene. 2009 Mar 19;28(11):1471-6.
675. Rovedo M, Longnecker R. Epstein-barr virus latent membrane protein 2B (LMP2B) modulates LMP2A activity. J Virol. 2007 Jan;81(1):84-94.
676. Rechsteiner MP, Berger C, Zauner L, Sigrist JA, Weber M, Longnecker R, et al. Latent membrane protein 2B regulates susceptibility to induction of lytic Epstein-Barr virus infection. J Virol. 2008 Feb;82(4):1739-47.
677. Rechsteiner MP, Berger C, Weber M, Sigrist JA, Nadal D, Bernasconi M. Silencing of latent membrane protein 2B reduces susceptibility to activation of lytic Epstein-Barr virus in Burkitt's lymphoma Akata cells. J Gen Virol. 2007 May;88(Pt 5):1454-9.
678. Shah KM, Stewart SE, Wei W, Woodman CB, O'Neil JD, Dawson CW, et al. The EBV-encoded latent membrane proteins, LMP2A and LMP2B, limit the actions of interferon by targeting interferon receptors for degradation. Oncogene. 2009 Nov 5;28(44):3903-14.
679. Henderson S, Huen D, Rowe M, Dawson C, Johnson G, Rickinson A. Epstein-Barr virus-coded BHRF1 protein, a viral homologue of Bcl-2, protects human B cells from programmed cell death. Proc Natl Acad Sci U S A. 1993 Sep 15;90(18):8479-83.
680. Cabras G, Decaussin G, Zeng Y, Djennaoui D, Melouli H, Broully P, et al. Epstein-Barr virus encoded BALF1 gene is transcribed in Burkitt's lymphoma cell lines and in nasopharyngeal carcinoma's biopsies. J Clin Virol. 2005 Sep;34(1):26-34.

681. Kelly GL, Milner AE, Tierney RJ, Croom-Carter DS, Altmann M, Hammerschmidt W, et al. Epstein-Barr virus nuclear antigen 2 (EBNA2) gene deletion is consistently linked with EBNA3A, -3B, and -3C expression in Burkitt's lymphoma cells and with increased resistance to apoptosis. J Virol. 2005 Aug;79(16):10709-17.
682. Hardwick JM, Bellows DS. Viral versus cellular BCL-2 proteins. Cell Death Differ. 2003 Jan;10 Suppl 1:S68-76.
683. Huang Q, Petros AM, Virgin HW, Fesik SW, Olejniczak ET. Solution structure of the BHRF1 protein from Epstein-Barr virus, a homolog of human Bcl-2. J Mol Biol. 2003 Oct 3;332(5):1123-30.
684. Desbien AL, Kappler JW, Marrack P. The Epstein-Barr virus Bcl-2 homolog, BHRF1, blocks apoptosis by binding to a limited amount of Bim. Proc Natl Acad Sci U S A. 2009 Apr 7;106(14):5663-8.
685. Lee MA, Yates JL. BHRF1 of Epstein-Barr virus, which is homologous to human proto-oncogene bcl2, is not essential for transformation of B cells or for virus replication in vitro. J Virol. 1992 Apr;66(4):1899-906.
686. Marchini A, Tomkinson B, Cohen JI, Kieff E. BHRF1, the Epstein-Barr virus gene with homology to Bc12, is dispensable for B-lymphocyte transformation and virus replication. J Virol. 1991 Nov;65(11):5991-6000.
687. Marshall WL, Yim C, Gustafson E, Graf T, Sage DR, Hanify K, et al. Epstein-Barr virus encodes a novel homolog of the bcl-2 oncogene that inhibits apoptosis and associates with Bax and Bak. J Virol. 1999 Jun;73(6):5181-5.
688. Bellows DS, Howell M, Pearson C, Hazlewood SA, Hardwick JM. Epstein-Barr virus BALF1 is a BCL-2-like antagonist of the herpesvirus antiapoptotic BCL-2 proteins. J Virol. 2002 Mar;76(5):2469-79.
689. Arrand JR, Rymo L. Characterization of the major Epstein-Barr virus-specific RNA in Burkitt lymphoma-derived cells. J Virol. 1982 Feb;41(2):376-89.
690. Arrand JR, Young LS, Tugwood JD. Two families of sequences in the small RNA-encoding region of Epstein-Barr virus (EBV) correlate with EBV types A and B. J Virol. 1989 Feb;63(2):983-6.
691. Howe JG, Shu MD. Epstein-Barr virus small RNA (EBER) genes: unique transcription units that combine RNA polymerase II and III promoter elements. Cell. 1989 Jun 2;57(5):825-34.
692. Glickman JN, Howe JG, Steitz JA. Structural analyses of EBER1 and EBER2 ribonucleoprotein particles present in Epstein-Barr virus-infected cells. J Virol. 1988 Mar;62(3):902-11.
693. Rosa MD, Gottlieb E, Lerner MR, Steitz JA. Striking similarities are exhibited by two small Epstein-Barr virus-encoded ribonucleic acids and the adenovirus-associated ribonucleic acids VAI and VAII. Mol Cell Biol. 1981 Sep;1(9):785-96.
694. Chang KL, Chen YY, Shibata D, Weiss LM. Description of an in situ hybridization methodology for detection of Epstein-Barr virus RNA in paraffin-embedded tissues, with a survey of normal and neoplastic tissues. Diagn Mol Pathol. 1992 Dec;1(4):246-55.
695. Howe JG, Steitz JA. Localization of Epstein-Barr virus-encoded small RNAs by in situ hybridization. Proc Natl Acad Sci U S A. 1986 Dec;83(23):9006-10.
696. Fok V, Friend K, Steitz JA. Epstein-Barr virus noncoding RNAs are confined to the nucleus, whereas their partner, the human La protein, undergoes nucleocytoplasmic shuttling. J Cell Biol. 2006 May 8;173(3):319-25.
697. Schwemmle M, Clemens MJ, Hilse K, Pfeifer K, Troster H, Muller WE, et al. Localization of Epstein-Barr virus-encoded RNAs EBER-1 and EBER-2 in interphase and mitotic Burkitt lymphoma cells. Proc Natl Acad Sci U S A. 1992 Nov 1;89(21):10292-6.
698. Barletta JM, Kingma DW, Ling Y, Charache P, Mann RB, Ambinder RF. Rapid in situ hybridization for the diagnosis of latent Epstein-Barr virus infection. Mol Cell Probes. 1993 Apr;7(2):105-9.
699. Rymo L. Identification of transcribed regions of Epstein-Barr virus DNA in Burkitt lymphoma-derived cells. J Virol. 1979 Oct;32(1):8-18.

700. Wu TC, Mann RB, Charache P, Hayward SD, Staal S, Lambe BC, et al. Detection of EBV gene expression in Reed-Sternberg cells of Hodgkin's disease. Int J Cancer. 1990 Nov 15;46(5):801-4.
701. Labrecque LG, Lampert I, Kazembe P, Philips J, Griffin BE. Correlation between cytopathological results and in situ hybridisation on needle aspiration biopsies of suspected African Burkitt's lymphomas. Int J Cancer. 1994 Dec 1;59(5):591-6.
702. Burke AP, Yen TS, Shekitka KM, Sobin LH. Lymphoepithelial carcinoma of the stomach with Epstein-Barr virus demonstrated by polymerase chain reaction. Mod Pathol. 1990 May;3(3):377-80.
703. Fina F, Romain S, Ouafik L, Palmari J, Ben Ayed F, Benharkat S, et al. Frequency and genome load of Epstein-Barr virus in 509 breast cancers from different geographical areas. Br J Cancer. 2001 Mar 23;84(6):783-90.
704. Lerner MR, Andrews NC, Miller G, Steitz JA. Two small RNAs encoded by Epstein-Barr virus and complexed with protein are precipitated by antibodies from patients with systemic lupus erythematosus. Proc Natl Acad Sci U S A. 1981 Feb;78(2):805-9.
705. Greifenegger N, Jager M, Kunz-Schughart LA, Wolf H, Schwarzmann F. Epstein-Barr virus small RNA (EBER) genes: differential regulation during lytic viral replication. J Virol. 1998 Nov;72(11):9323-8.
706. Rooney C, Howe JG, Speck SH, Miller G. Influence of Burkitt's lymphoma and primary B cells on latent gene expression by the nonimmortalizing P3J-HR-1 strain of Epstein-Barr virus. J Virol. 1989 Apr;63(4):1531-9.
707. Clemens MJ. The small RNAs of Epstein-Barr virus. Mol Biol Rep. 1993 Feb;17(2):81-92.
708. Clarke PA, Sharp NA, Clemens MJ. Expression of genes for the Epstein-Barr virus small RNAs EBER-1 and EBER-2 in Daudi Burkitt's lymphoma cells: effects of interferon treatment. J Gen Virol. 1992 Dec;73 (Pt 12):3169-75.
709. Sharp TV, Schwemmle M, Jeffrey I, Laing K, Mellor H, Proud CG, et al. Comparative analysis of the regulation of the interferon-inducible protein kinase PKR by Epstein-Barr virus RNAs EBER-1 and EBER-2 and adenovirus VAI RNA. Nucleic Acids Res. 1993 Sep 25;21(19):4483-90.
710. Nanbo A, Inoue K, Adachi-Takasawa K, Takada K. Epstein-Barr virus RNA confers resistance to interferon-alpha-induced apoptosis in Burkitt's lymphoma. EMBO J. 2002 Mar 1;21(5):954-65.
711. Samanta M, Iwakiri D, Takada K. Epstein-Barr virus-encoded small RNA induces IL-10 through RIG-I-mediated IRF-3 signaling. Oncogene. 2008 Jul 10;27(30):4150-60.
712. Kitagawa N, Goto M, Kurozumi K, Maruo S, Fukayama M, Naoe T, et al. Epstein-Barr virus-encoded poly(A)(-) RNA supports Burkitt's lymphoma growth through interleukin-10 induction. EMBO J. 2000 Dec 15;19(24):6742-50.
713. Iwakiri D, Eizuru Y, Tokunaga M, Takada K. Autocrine growth of Epstein-Barr virus-positive gastric carcinoma cells mediated by an Epstein-Barr virus-encoded small RNA. Cancer Res. 2003 Nov 1;63(21):7062-7.
714. Iwakiri D, Sheen TS, Chen JY, Huang DP, Takada K. Epstein-Barr virus-encoded small RNA induces insulin-like growth factor 1 and supports growth of nasopharyngeal carcinoma-derived cell lines. Oncogene. 2005 Mar 3;24(10):1767-73.
715. Yang L, Aozasa K, Oshimi K, Takada K. Epstein-Barr virus (EBV)-encoded RNA promotes growth of EBV-infected T cells through interleukin-9 induction. Cancer Res. 2004 Aug 1;64(15):5332-7.
716. Wu Y, Maruo S, Yajima M, Kanda T, Takada K. Epstein-Barr virus (EBV)-encoded RNA 2 (EBER2) but not EBER1 plays a critical role in EBV-induced B-cell growth transformation. J Virol. 2007 Oct;81(20):11236-45.
717. Ruf IK, Lackey KA, Warudkar S, Sample JT. Protection from interferon-induced apoptosis by Epstein-Barr virus small RNAs is not mediated by inhibition of PKR. J Virol. 2005 Dec;79(23):14562-9.

718. Henderson S, Rowe M, Gregory C, Croom-Carter D, Wang F, Longnecker R, et al. Induction of bcl-2 expression by Epstein-Barr virus latent membrane protein 1 protects infected B cells from programmed cell death. Cell. 1991 Jun 28;65(7):1107-15.
719. Gilligan K, Sato H, Rajadurai P, Busson P, Young L, Rickinson A, et al. Novel transcription from the Epstein-Barr virus terminal EcoRI fragment, DIJhet, in a nasopharyngeal carcinoma. J Virol. 1990 Oct;64(10):4948-56.
720. Hitt MM, Allday MJ, Hara T, Karran L, Jones MD, Busson P, et al. EBV gene expression in an NPC-related tumour. EMBO J. 1989 Sep;8(9):2639-51.
721. Gilligan KJ, Rajadurai P, Lin JC, Busson P, Abdel-Hamid M, Prasad U, et al. Expression of the Epstein-Barr virus BamHI A fragment in nasopharyngeal carcinoma: evidence for a viral protein expressed in vivo. J Virol. 1991 Nov;65(11):6252-9.
722. Chen HL, Lung MM, Sham JS, Choy DT, Griffin BE, Ng MH. Transcription of BamHI-A region of the EBV genome in NPC tissues and B cells. Virology. 1992 Nov;191(1):193-201.
723. Sugiura M, Imai S, Tokunaga M, Koizumi S, Uchizawa M, Okamoto K, et al. Transcriptional analysis of Epstein-Barr virus gene expression in EBV-positive gastric carcinoma: unique viral latency in the tumour cells. Br J Cancer. 1996 Aug;74(4):625-31.
724. Zhang J, Chen H, Weinmaster G, Hayward SD. Epstein-Barr virus BamHi-a rightward transcript-encoded RPMS protein interacts with the CBF1-associated corepressor CIR to negatively regulate the activity of EBNA2 and NotchIC. J Virol. 2001 Mar;75(6):2946-56.
725. Brooks LA, Lear AL, Young LS, Rickinson AB. Transcripts from the Epstein-Barr virus BamHI A fragment are detectable in all three forms of virus latency. J Virol. 1993 Jun;67(6):3182-90.
726. Chen H, Smith P, Ambinder RF, Hayward SD. Expression of Epstein-Barr virus BamHI-A rightward transcripts in latently infected B cells from peripheral blood. Blood. 1999 May 1;93(9):3026-32.
727. Sadler RH, Raab-Traub N. Structural analyses of the Epstein-Barr virus BamHI A transcripts. J Virol. 1995 Feb;69(2):1132-41.
728. Smith PR, Gao Y, Karran L, Jones MD, Snudden D, Griffin BE. Complex nature of the major viral polyadenylated transcripts in Epstein-Barr virus-associated tumors. J Virol. 1993 Jun;67(6):3217-25.
729. Chen H, Huang J, Wu FY, Liao G, Hutt-Fletcher L, Hayward SD. Regulation of expression of the Epstein-Barr virus BamHI-A rightward transcripts. J Virol. 2005 Feb;79(3):1724-33.
730. Kusano S, Raab-Traub N. An Epstein-Barr virus protein interacts with Notch. J Virol. 2001 Jan;75(1):384-95.
731. Smith PR, de Jesus O, Turner D, Hollyoake M, Karstegl CE, Griffin BE, et al. Structure and coding content of CST (BART) family RNAs of Epstein-Barr virus. J Virol. 2000 Apr;74(7):3082-92.
732. Fries KL, Sculley TB, Webster-Cyriaque J, Rajadurai P, Sadler RH, Raab-Traub N. Identification of a novel protein encoded by the BamHI A region of the Epstein-Barr virus. J Virol. 1997 Apr;71(4):2765-71.
733. Karran L, Gao Y, Smith PR, Griffin BE. Expression of a family of complementary-strand transcripts in Epstein-Barr virus-infected cells. Proc Natl Acad Sci U S A. 1992 Sep 1;89(17):8058-62.
734. Kienzle N, Buck M, Greco S, Krauer K, Sculley TB. Epstein-Barr virus-encoded RK-BARF0 protein expression. J Virol. 1999 Oct;73(10):8902-6.
735. Al-Mozaini M, Bodelon G, Karstegl CE, Jin B, Al-Ahdal M, Farrell PJ. Epstein-Barr virus BART gene expression. J Gen Virol. 2009 Feb;90(Pt 2):307-16.
736. Kienzle N, Sculley TB, Poulsen L, Buck M, Cross S, Raab-Traub N, et al. Identification of a cytotoxic T-lymphocyte response to the novel BARF0 protein of Epstein-Barr virus: a critical role for antigen expression. J Virol. 1998 Aug;72(8):6614-20.
737. van Beek J, Brink AA, Vervoort MB, van Zijp MJ, Meijer CJ, van den Brule AJ, et al. In vivo transcription of the Epstein-Barr virus (EBV) BamHI-A region without associated in vivo BARF0 protein expression in multiple EBV-associated disorders. J Gen Virol. 2003 Oct;84(Pt 10):2647-59.

738. Cai X, Schafer A, Lu S, Bilello JP, Desrosiers RC, Edwards R, et al. Epstein-Barr virus microRNAs are evolutionarily conserved and differentially expressed. PLoS Pathog. 2006 Mar;2(3):e23.
739. Cosmopoulos K, Pegtel M, Hawkins J, Moffett H, Novina C, Middeldorp J, et al. Comprehensive profiling of Epstein-Barr virus microRNAs in nasopharyngeal carcinoma. J Virol. 2009 Mar;83(5):2357-67.
740. Grundhoff A, Sullivan CS, Ganem D. A combined computational and microarray-based approach identifies novel microRNAs encoded by human gamma-herpesviruses. RNA. 2006 May;12(5):733-50.
741. Zhu JY, Pfuhl T, Motsch N, Barth S, Nicholls J, Grasser F, et al. Identification of novel Epstein-Barr virus microRNA genes from nasopharyngeal carcinomas. J Virol. 2009 Apr;83(7):3333-41.
742. Hutzinger R, Feederle R, Mrazek J, Schiefermeier N, Balwierz PJ, Zavolan M, et al. Expression and processing of a small nucleolar RNA from the Epstein-Barr virus genome. PLoS Pathog. 2009 Aug;5(8):e1000547.
743. Pratt ZL, Kuzembayeva M, Sengupta S, Sugden B. The microRNAs of Epstein-Barr Virus are expressed at dramatically differing levels among cell lines. Virology. 2009 Apr 10;386(2):387-97.
744. Xing L, Kieff E. Epstein-Barr virus BHRF1 micro- and stable RNAs during latency III and after induction of replication. J Virol. 2007 Sep;81(18):9967-75.
745. Cameron JE, Fewell C, Yin Q, McBride J, Wang X, Lin Z, et al. Epstein-Barr virus growth/latency III program alters cellular microRNA expression. Virology. 2008 Dec 20;382(2):257-66.
746. Austin PJ, Flemington E, Yandava CN, Strominger JL, Speck SH. Complex transcription of the Epstein-Barr virus BamHI fragment H rightward open reading frame 1 (BHRF1) in latently and lytically infected B lymphocytes. Proc Natl Acad Sci U S A. 1988 Jun;85(11):3678-82.
747. Pearson GR, Luka J, Petti L, Sample J, Birkenbach M, Braun D, et al. Identification of an Epstein-Barr virus early gene encoding a second component of the restricted early antigen complex. Virology. 1987 Sep;160(1):151-61.
748. Edwards RH, Marquitz AR, Raab-Traub N. Epstein-Barr virus BART microRNAs are produced from a large intron prior to splicing. J Virol. 2008 Sep;82(18):9094-106.
749. Kim do N, Chae HS, Oh ST, Kang JH, Park CH, Park WS, et al. Expression of viral microRNAs in Epstein-Barr virus-associated gastric carcinoma. J Virol. 2007 Jan;81(2):1033-6.
750. Feederle R, Linnstaedt SD, Bannert H, Lips H, Bencun M, Cullen BR, et al. A viral microRNA cluster strongly potentiates the transforming properties of a human herpesvirus. PLoS Pathog. 2011 Feb;7(2):e1001294.
751. Seto E, Moosmann A, Gromminger S, Walz N, Grundhoff A, Hammerschmidt W. Micro RNAs of Epstein-Barr virus promote cell cycle progression and prevent apoptosis of primary human B cells. PLoS Pathog. 2010 august 6(8).
752. Li Z, Chen X, Li L, Liu S, Yang L, Ma X, et al. EBV encoded miR-BHRF1-1 potentiates viral lytic replication by downregulating host p53 in nasopharyngeal carcinoma. Int J Biochem Cell Biol. 2012 Feb;44(2):275-9.
753. Xia T, O'Hara A, Araujo I, Barreto J, Carvalho E, Sapucaia JB, et al. EBV microRNAs in primary lymphomas and targeting of CXCL-11 by ebv-mir-BHRF1-3. Cancer Res. 2008 Mar 1;68(5):1436-42.
754. Marquitz AR, Mathur A, Nam CS, Raab-Traub N. The Epstein-Barr Virus BART microRNAs target the pro-apoptotic protein Bim. Virology. 2011 Apr 10;412(2):392-400.
755. Nachmani D, Stern-Ginossar N, Sarid R, Mandelboim O. Diverse herpesvirus microRNAs target the stress-induced immune ligand MICB to escape recognition by natural killer cells. Cell Host Microbe. 2009 Apr 23;5(4):376-85.

756. Choy EY, Siu KL, Kok KH, Lung RW, Tsang CM, To KF, et al. An Epstein-Barr virus-encoded microRNA targets PUMA to promote host cell survival. J Exp Med. 2008 Oct 27;205(11):2551-60.
757. Iizasa H, Wulff BE, Alla NR, Maragkakis M, Megraw M, Hatzigeorgiou A, et al. Editing of Epstein-Barr virus-encoded BART6 microRNAs controls their dicer targeting and consequently affects viral latency. J Biol Chem. 2010 Oct 22;285(43):33358-70.
758. Dolken L, Malterer G, Erhard F, Kothe S, Friedel CC, Suffert G, et al. Systematic analysis of viral and cellular microRNA targets in cells latently infected with human gamma-herpesviruses by RISC immunoprecipitation assay. Cell Host Microbe. 2010 Apr 22;7(4):324-34.
759. Barth S, Pfuhl T, Mamiani A, Ehses C, Roemer K, Kremmer E, et al. Epstein-Barr virus-encoded microRNA miR-BART2 down-regulates the viral DNA polymerase BALF5. Nucleic Acids Res. 2008 Feb;36(2):666-75.
760. Lo AK, To KF, Lo KW, Lung RW, Hui JW, Liao G, et al. Modulation of LMP1 protein expression by EBV-encoded microRNAs. Proc Natl Acad Sci U S A. 2007 Oct 9;104(41):16164-9.
761. Lung RW, Tong JH, Sung YM, Leung PS, Ng DC, Chau SL, et al. Modulation of LMP2A expression by a newly identified Epstein-Barr virus-encoded microRNA miR-BART22. Neoplasia. 2009 Nov;11(11):1174-84.
762. Ramakrishnan R, Donahue H, Garcia D, Tan J, Shimizu N, Rice AP, et al. Epstein-Barr virus BART9 miRNA modulates LMP1 levels and affects growth rate of nasal NK T cell lymphomas. PLoS One. 2011;6(11):e27271.
763. Skalsky RL, Corcoran DL, Gottwein E, Frank CL, Kang D, Hafner M, et al. The viral and cellular microRNA targetome in lymphoblastoid cell lines. PLoS Pathog. 2012 Jan;8(1):e1002484.
764. Riley KJ, Rabinowitz GS, Yario TA, Luna JM, Darnell RB, Steitz JA. EBV and human microRNAs co-target oncogenic and apoptotic viral and human genes during latency. EMBO J. 2012 May 2;31(9):2207-21.
765. Lagana A, Forte S, Russo F, Giugno R, Pulvirenti A, Ferro A. Prediction of human targets for viral-encoded microRNAs by thermodynamics and empirical constraints. J RNAi Gene Silencing. 2010;6(1):379-85.
766. Gregory CD, Rowe M, Rickinson AB. Different Epstein-Barr virus-B cell interactions in phenotypically distinct clones of a Burkitt's lymphoma cell line. J Gen Virol. 1990 Jul;71 (Pt 7):1481-95.
767. Kelly GL, Milner AE, Baldwin GS, Bell AI, Rickinson AB. Three restricted forms of Epstein-Barr virus latency counteracting apoptosis in c-myc-expressing Burkitt lymphoma cells. Proc Natl Acad Sci U S A. 2006 Oct 3;103(40):14935-40.
768. Schneider U, Schwenk HU, Bornkamm G. Characterization of EBV-genome negative "null" and "T" cell lines derived from children with acute lymphoblastic leukemia and leukemic transformed non-Hodgkin lymphoma. Int J Cancer. 1977 May 15;19(5):621-6.
769. Bell AI, Groves K, Kelly GL, Croom-Carter D, Hui E, Chan AT, et al. Analysis of Epstein-Barr virus latent gene expression in endemic Burkitt's lymphoma and nasopharyngeal carcinoma tumour cells by using quantitative real-time PCR assays. J Gen Virol. 2006 Oct;87(Pt 10):2885-90.
770. Delecluse HJ, Hilsendegen T, Pich D, Zeidler R, Hammerschmidt W. Propagation and recovery of intact, infectious Epstein-Barr virus from prokaryotic to human cells. Proc Natl Acad Sci U S A. 1998 Jul 7;95(14):8245-50.
771. Yandava CN, Speck SH. Characterization of the deletion and rearrangement in the BamHI C region of the X50-7 Epstein-Barr virus genome, a mutant viral strain which exhibits constitutive BamHI W promoter activity. J Virol. 1992 Sep;66(9):5646-50.
772. Robertson MJ, Cochran KJ, Cameron C, Le JM, Tantravahi R, Ritz J. Characterization of a cell line, NKL, derived from an aggressive human natural killer cell leukemia. Exp Hematol. 1996 Feb;24(3):406-15.

773. Ressing ME, Keating SE, van Leeuwen D, Koppers-Lalic D, Pappworth IY, Wiertz EJ, et al. Impaired transporter associated with antigen processing-dependent peptide transport during productive EBV infection. J Immunol. 2005 Jun 1;174(11):6829-38.
774. Junying J, Herrmann K, Davies G, Lissauer D, Bell A, Timms J, et al. Absence of Epstein-Barr virus DNA in the tumor cells of European hepatocellular carcinoma. Virology. 2003 Feb 15;306(2):236-43.
775. Neuhierl B, Feederle R, Hammerschmidt W, Delecluse HJ. Glycoprotein gp110 of Epstein-Barr virus determines viral tropism and efficiency of infection. Proc Natl Acad Sci U S A. 2002 Nov 12;99(23):15036-41.
776. Chen C, Ridzon DA, Broomer AJ, Zhou Z, Lee DH, Nguyen JT, et al. Real-time quantification of microRNAs by stem-loop RT-PCR. Nucleic Acids Res. 2005;33(20):e179.
777. Zuker M. Mfold web server for nucleic acid folding and hybridization prediction. Nucleic Acids Res. 2003 Jul 1;31(13):3406-15.
778. Hofacker IL. Vienna RNA secondary structure server. Nucleic Acids Res. 2003 Jul 1;31(13):3429-31.
779. Hofacker IL, Stadler PF. Memory efficient folding algorithms for circular RNA secondary structures. Bioinformatics. 2006 May 15;22(10):1172-6.
780. Emig D, Salomonis N, Baumbach J, Lengauer T, Conklin BR, Albrecht M. AltAnalyze and DomainGraph: analyzing and visualizing exon expression data. Nucleic Acids Res. 2010 Jul;38(Web Server issue):W755-62.
781. Rowe M, Rowe DT, Gregory CD, Young LS, Farrell PJ, Rupani H, et al. Differences in B cell growth phenotype reflect novel patterns of Epstein-Barr virus latent gene expression in Burkitt's lymphoma cells. EMBO J. 1987 Sep;6(9):2743-51.
782. Swartwout SG, Kinniburgh AJ. c-myc RNA degradation in growing and differentiating cells: possible alternate pathways. Mol Cell Biol. 1989 Jan;9(1):288-95.
783. Bissels U, Wild S, Tomiuk S, Holste A, Hafner M, Tuschl T, et al. Absolute quantification of microRNAs by using a universal reference. RNA. 2009 Dec;15(12):2375-84.
784. Imig J, Motsch N, Zhu JY, Barth S, Okoniewski M, Reineke T, et al. microRNA profiling in Epstein-Barr virus-associated B-cell lymphoma. Nucleic Acids Res. 2011 Mar;39(5):1880-93.
785. Cullum R, Alder O, Hoodless PA. The next generation: using new sequencing technologies to analyse gene regulation. Respirology. 2011 Feb;16(2):210-22.
786. Chen SJ, Chen GH, Chen YH, Liu CY, Chang KP, Chang YS, et al. Characterization of Epstein-Barr virus miRNAome in nasopharyngeal carcinoma by deep sequencing. PLoS One. 2010;5(9).
787. Gottwein E, Cai X, Cullen BR. A novel assay for viral microRNA function identifies a single nucleotide polymorphism that affects Drosha processing. J Virol. 2006 Jun;80(11):5321-6.
788. Fabian MR, Sonenberg N, Filipowicz W. Regulation of mRNA translation and stability by microRNAs. Annu Rev Biochem. 2010;79:351-79.
789. Kim do N, Lee SK. Biogenesis of Epstein-Barr virus microRNAs. Mol Cell Biochem. 2012 Jun;365(1-2):203-10.
790. Kim do N, Song YJ, Lee SK. The role of promoter methylation in Epstein-Barr virus (EBV) microRNA expression in EBV-infected B cell lines. Exp Mol Med. 2011 Jul 30;43(7):401-10.
791. Tierney RJ, Kirby HE, Nagra JK, Desmond J, Bell AI, Rickinson AB. Methylation of transcription factor binding sites in the Epstein-Barr virus latent cycle promoter Wp coincides with promoter down-regulation during virus-induced B-cell transformation. J Virol. 2000 Nov;74(22):10468-79.
792. Lennox KA, Behlke MA. Chemical modification and design of anti-miRNA oligonucleotides. Gene Ther. 2011 Dec;18(12):1111-20.
793. Torres AG, Fabani MM, Vigorito E, Gait MJ. MicroRNA fate upon targeting with anti-miRNA oligonucleotides as revealed by an improved Northern-blot-based method for miRNA detection. RNA. 2011 May;17(5):933-43.

794. Kloosterman WP, Lagendijk AK, Ketting RF, Moulton JD, Plasterk RH. Targeted inhibition of miRNA maturation with morpholinos reveals a role for miR-375 in pancreatic islet development. PLoS Biol. 2007 Aug;5(8):e203.
795. Zamecnik PC, Stephenson ML. Inhibition of Rous sarcoma virus replication and cell transformation by a specific oligodeoxynucleotide. Proc Natl Acad Sci U S A. 1978 Jan;75(1):280-4.
796. Kurreck J. Antisense technologies. Improvement through novel chemical modifications. Eur J Biochem. 2003 Apr;270(8):1628-44.
797. Boutla A, Delidakis C, Tabler M. Developmental defects by antisense-mediated inactivation of micro-RNAs 2 and 13 in Drosophila and the identification of putative target genes. Nucleic Acids Res. 2003 Sep 1;31(17):4973-80.
798. Esau C, Kang X, Peralta E, Hanson E, Marcusson EG, Ravichandran LV, et al. MicroRNA-143 regulates adipocyte differentiation. J Biol Chem. 2004 Dec 10;279(50):52361-5.
799. Hutvagner G, Simard MJ, Mello CC, Zamore PD. Sequence-specific inhibition of small RNA function. PLoS Biol. 2004 Apr;2(4):E98.
800. Meister G, Landthaler M, Dorsett Y, Tuschl T. Sequence-specific inhibition of microRNA- and siRNA-induced RNA silencing. RNA. 2004 Mar;10(3):544-50.
801. Krutzfeldt J, Kuwajima S, Braich R, Rajeev KG, Pena J, Tuschl T, et al. Specificity, duplex degradation and subcellular localization of antagomirs. Nucleic Acids Res. 2007;35(9):2885-92.
802. Krutzfeldt J, Rajewsky N, Braich R, Rajeev KG, Tuschl T, Manoharan M, et al. Silencing of microRNAs in vivo with 'antagomirs'. Nature. 2005 Dec 1;438(7068):685-9.
803. Orum H, Wengel J. Locked nucleic acids: a promising molecular family for gene-function analysis and antisense drug development. Curr Opin Mol Ther. 2001 Jun;3(3):239-43.
804. Braasch DA, Corey DR. Locked nucleic acid (LNA): fine-tuning the recognition of DNA and RNA. Chem Biol. 2001 Jan;8(1):1-7.
805. Elayadi AN, Corey DR. Application of PNA and LNA oligomers to chemotherapy. Curr Opin Investig Drugs. 2001 Apr;2(4):558-61.
806. Hansen A, Henderson S, Lagos D, Nikitenko L, Coulter E, Roberts S, et al. KSHV-encoded miRNAs target MAF to induce endothelial cell reprogramming. Genes Dev. 2010 Jan 15;24(2):195-205.
807. McLaughlin J, Cheng D, Singer O, Lukacs RU, Radu CG, Verma IM, et al. Sustained suppression of Bcr-Abl-driven lymphoid leukemia by microRNA mimics. Proc Natl Acad Sci U S A. 2007 Dec 18;104(51):20501-6.
808. Sun BS, Dong QZ, Ye QH, Sun HJ, Jia HL, Zhu XQ, et al. Lentiviral-mediated miRNA against osteopontin suppresses tumor growth and metastasis of human hepatocellular carcinoma. Hepatology. 2008 Dec;48(6):1834-42.
809. Amoroso R, Fitzsimmons L, Thomas WA, Kelly GL, Rowe M, Bell AI. Quantitative studies of Epstein-Barr virus-encoded microRNAs provide novel insights into their regulation. J Virol. 2011 Jan;85(2):996-1010.
810. Herold MJ, van den Brandt J, Seibler J, Reichardt HM. Inducible and reversible gene silencing by stable integration of an shRNA-encoding lentivirus in transgenic rats. Proc Natl Acad Sci U S A. 2008 Nov 25;105(47):18507-12.
811. Baer M, Nilsen TW, Costigan C, Altman S. Structure and transcription of a human gene for H1 RNA, the RNA component of human RNase P. Nucleic Acids Res. 1990 Jan 11;18(1):97-103.
812. Seibler J, Kleinridders A, Kuter-Luks B, Niehaves S, Bruning JC, Schwenk F. Reversible gene knockdown in mice using a tight, inducible shRNA expression system. Nucleic Acids Res. 2007;35(7):e54.
813. Smyth GK. Limma: linear models for microarray data. In: R. Gentleman, V. Carey, S. Dudoit, R. Irizarry, W. Huber (eds.), editor. Bioinformatics and Computational Biology Solutions Using R and Bioconductor. New York: Springer; 2005. p. 397-420.

814. Gottwein E, Corcoran DL, Mukherjee N, Skalsky RL, Hafner M, Nusbaum JD, et al. Viral microRNA targetome of KSHV-infected primary effusion lymphoma cell lines. Cell Host Microbe. 2011 Nov 17;10(5):515-26.
815. Gottwein E, Cullen BR. A human herpesvirus microRNA inhibits p21 expression and attenuates p21-mediated cell cycle arrest. J Virol. 2010 May;84(10):5229-37.
816. Gottwein E, Mukherjee N, Sachse C, Frenzel C, Majoros WH, Chi JT, et al. A viral microRNA functions as an orthologue of cellular miR-155. Nature. 2007 Dec 13;450(7172):1096-9.
817. Haecker I, Gay LA, Yang Y, Hu J, Morse AM, McIntyre LM, et al. Ago HITS-CLIP Expands Understanding of Kaposi's Sarcoma-associated Herpesvirus miRNA Function in Primary Effusion Lymphomas. PLoS Pathog. 2012 Aug;8(8):e1002884.
818. Gil-Parrado S, Fernandez-Montalvan A, Assfalg-Machleidt I, Popp O, Bestvater F, Holloschi A, et al. Ionomycin-activated calpain triggers apoptosis. A probable role for Bcl-2 family members. J Biol Chem. 2002 Jul 26;277(30):27217-26.
819. Hajnoczky G, Davies E, Madesh M. Calcium signaling and apoptosis. Biochem Biophys Res Commun. 2003 May 9;304(3):445-54.
820. Murgia M, Giorgi C, Pinton P, Rizzuto R. Controlling metabolism and cell death: at the heart of mitochondrial calcium signalling. J Mol Cell Cardiol. 2009 Jun;46(6):781-8.
821. Brown BD, Naldini L. Exploiting and antagonizing microRNA regulation for therapeutic and experimental applications. Nat Rev Genet. 2009 Aug;10(8):578-85.
822. Walker JC, Harland RM. microRNA-24a is required to repress apoptosis in the developing neural retina. Genes Dev. 2009 May 1;23(9):1046-51.
823. Le MT, Teh C, Shyh-Chang N, Xie H, Zhou B, Korzh V, et al. MicroRNA-125b is a novel negative regulator of p53. Genes Dev. 2009 Apr 1;23(7):862-76.
824. Susa T, Kato T, Kato Y. Reproducible transfection in the presence of carrier DNA using FuGENE6 and Lipofectamine2000. Mol Biol Rep. 2008 Sep;35(3):313-9.
825. Lepik D, Jaks V, Kadaja L, Varv S, Maimets T. Electroporation and carrier DNA cause p53 activation, cell cycle arrest, and apoptosis. Anal Biochem. 2003 Jul 1;318(1):52-9.
826. Obad S, dos Santos CO, Petri A, Heidenblad M, Broom O, Ruse C, et al. Silencing of microRNA families by seed-targeting tiny LNAs. Nat Genet. 2011 Apr;43(4):371-8.
827. Liu YP, Berkhout B. miRNA cassettes in viral vectors: problems and solutions. Biochim Biophys Acta. 2011 Nov-Dec;1809(11-12):732-45.
828. Hager S, Frame FM, Collins AT, Burns JE, Maitland NJ. An internal polyadenylation signal substantially increases expression levels of lentivirus-delivered transgenes but has the potential to reduce viral titer in a promoter-dependent manner. Hum Gene Ther. 2008 Aug;19(8):840-50.
829. Xing L, Kieff E. cis-Acting effects on RNA processing and Drosha cleavage prevent Epstein-Barr virus latency III BHRF1 expression. J Virol. 2011 Sep;85(17):8929-39.
830. Chakraborty S, Mehtab S, Patwardhan A, Krishnan Y. Pri-miR-17-92a transcript folds into a tertiary structure and autoregulates its processing. RNA. 2012 May;18(5):1014-28.
831. Millenaar FF, Okyere J, May ST, van Zanten M, Voesenek LA, Peeters AJ. How to decide? Different methods of calculating gene expression from short oligonucleotide array data will give different results. BMC Bioinformatics. 2006;7:137.
832. Allison DB, Cui X, Page GP, Sabripour M. Microarray data analysis: from disarray to consolidation and consensus. Nat Rev Genet. 2006 Jan;7(1):55-65.
833. Kawahara Y, Zinshteyn B, Sethupathy P, Iizasa H, Hatzigeorgiou AG, Nishikura K. Redirection of silencing targets by adenosine-to-inosine editing of miRNAs. Science. 2007 Feb 23;315(5815):1137-40.
834. Vereide DT, Sugden B. Lymphomas differ in their dependence on Epstein-Barr virus. Blood. 2011 Feb 10;117(6):1977-85.
835. Kirchmaier AL, Sugden B. Dominant-negative inhibitors of EBNA-1 of Epstein-Barr virus. J Virol. 1997 Mar;71(3):1766-75.

836. Schmitz R, Young RM, Ceribelli M, Jhavar S, Xiao W, Zhang M, et al. Burkitt lymphoma pathogenesis and therapeutic targets from structural and functional genomics. Nature. 2012 Aug 12.

837. Ebert MS, Neilson JR, Sharp PA. MicroRNA sponges: competitive inhibitors of small RNAs in mammalian cells. Nat Methods. 2007 Sep;4(9):721-6.

838. Elefant N, Berger A, Shein H, Hofree M, Margalit H, Altuvia Y. RepTar: a database of predicted cellular targets of host and viral miRNAs. Nucleic Acids Res. 2011 Jan;39(Database issue):D188-94.

839. Maragkakis M, Reczko M, Simossis VA, Alexiou P, Papadopoulos GL, Dalamagas T, et al. DIANA-microT web server: elucidating microRNA functions through target prediction. Nucleic Acids Res. 2009 Jul;37(Web Server issue):W273-6.